

University of Nevada, Reno

The Design and Synthesis of Monomers for use in Two-Dimensional Polymerizations

A dissertation submitted in partial fulfillment of the requirements for the degree of Doctor of Philosophy in Chemistry

by

Dustin Day Patterson

Dr. Benjamin T. King/Dissertation Advisor

August 2017

UNIVERSITY
OF NEVADA
RENO

THEGRADUATE SCHOOL

We recommend that the dissertation
prepared under our supervision by

DUSTIN DAY PATTERSON

Entitled

**The Design And Synthesis Of Monomers For Use in Two-Dimensional
Polymerizations**

be accepted in partial fulfillment of the
requirements for the degree of

DOCTOR OF PHILOSOPHY

Benjamin T. King, Ph.D., Advisor

Robert S. Sheridan, Ph.D., Committee Member

Christopher S. Jeffrey, Ph.D., Committee Member

Lora Richards, Ph.D., Committee Member

Glenn Miller, Ph.D., Graduate School Representative

David W. Zeh, Ph. D., Dean, Graduate School

August 2017

Abstract

The Design and Synthesis of Monomers for Two-Dimensional Polymerizations

Dustin Day Patterson

Ph.D. Advisor: Professor Benjamin T. King

The focus of this dissertation is the design and synthesis of monomers for use in the synthesis of two dimensional polymers (2DPs).

2DPs can be described as laterally connected repeat units which cover a plane with no gaps or overlaps. Monomers used for the synthesis of 2DPs must be designed with at least three reactive functional groups; this permits polymerization into a 2D sheet of repeat units.

A total of seven different monomer designs were synthetically sought out. Three of the seven monomers, **1-H**, **1-MeO**, and **1-F** are previously reported and their synthesis was improved upon. Synthesis of three novel monomers, **1-FOH**, **1-FPOH**, and **1-PZn** was attempted with the completion of two of the three targets **1-FOH**, **1-PZn** and a known derivative, **1-P**. The above monomers were designed with anthraceno functionalities intended to undergo [4+4] cycloadditions during solid state and air-water interface polymerizations. The monomers intended for polymerization at the air-water interface (**1-FOH**, **1-FPOH** and **1-PZn**) were designed with synthetic handles for attachment of a hydrophilic substituent. A pyridine-DEG ligand was synthesized to ligate **1-PZn** at the air-water interface.

Growth of single crystals of **1-P** and **1-H**:C₇₀ co-crystals were grown and irradiated at 365 nm, 400 nm, and 465 nm at 100 K-250 K. However, no polymerization occurred because a proper packing motif allowing a topochemical 2D polymerization was not achieved.

Monomer, **1-pyz**, was synthesized using a novel route which takes advantage of Suzuki coupling chemistry. **1-pyz** possesses three pyrazole functionalities intended to undergo

coordination with a metal center during polymerization. Monomer **1-pyz** relies on reversible coordinative bonding in solution to form a metal coordinated lamellar crystal that can be exfoliated into single 2DP sheets. The highly insoluble monomer was reacted with various Ag, Au, and Mn salts under high temperature and superheated high pressure conditions towards polymerization. A single crystal containing metal coordinated layers of **1-pyz** has yet to be realized.

This thesis is dedicated:

to my friends and family for their support and encouragement

to my lab mates, past and present

to my advisor, Professor Benjamin T. King

Acknowledgements

I would like to acknowledge all the people that have made this dissertation possible:

Professor Benjamin T. King, for being an excellent advisor and all of your training during these past five years. For brining me out of my comfort zone and making me a better chemist whether I knew it or not at the time. And showing me a different way of learning and approaching problems.

Professor Christopher Jeffrey, for your support and sharing of knowledge that has made me a more well-rounded chemist. And for serving as a doctoral committee member.

Professor Robert Sheridan, for your support, willingness to help, and teaching one of my favorite classes (photochemistry). And for serving as a doctoral committee member.

Professor Lora Richards and **Professor Glenn Miller** for serving as doctoral committee members.

Dr. Sarah A. Cummings, for mentoring me as a teaching assistant, and giving me the opportunity to teach CHEM 220.

Professor Vincent Catalano, for his invaluable help and training with the X-ray diffractometer, and help with solving crystal structures.

Dr. Stephen Spain, for training and helping with instrumentation.

Jennifer Heck, for being able to solve any problem you bring to her.

My parents, for their continuous support and encouragement.

My family, for their support, encouragement, and enthusiasm.

Dr. Johnson, Dr. Bergkamp, Dr. Bridgewater, Dr. Buttrick, Mike Leonard, Mike Walley, Tom Brown, Rob Gilley, Daniel Murray, and Allyissa Murray, for their friendship, support, encouragement, and help throughout my education.

William Thompson, for his friendship, support, motivation, and time spent helping with my OP and thesis.

King group members (past and present), for the camaraderie and all I have learned for you.

The Chemistry Department at the University of Nevada, Reno

All of my Friends

Table of Contents

	Page
Abstract	i
Dedication	iii
Acknowledgements	iv
Table of Contents	vi
List of Figures	x
List of Schemes	xiii
List of Tables	xvi
Chapter 1: Introduction.....	1
1.1. One-Dimensional Polymers	1
1.2. Two-Dimensional Polymers	3
1.3. Synthetic Approaches to Two-Dimensional Polymers.....	6
1.3.1. Ultra-High Vacuum Approach.....	6
1.3.2. Two-Dimensional Covalent Organic Framework	8
1.3.3. Single Crystal Approach	9
1.3.4. Air-Water Interface Approach	18
1.4. Applications of Two-Dimensional Polymers	21
1.4.1. Separation	21
1.4.2. Scaffolds	23
1.5. Aim of the Dissertation	25
1.6. Overview of Chapters	26
Summary of Chapter 2.	26
Summary of Chapter 3.	28
Summary of Chapter 4.	29

Summary of Chapter 5.	30
Summary of Chapter 6.	31
References	31
2. Synthetic Routes Towards Four Structurally Related Monomers	33
2.1. Overview	33
2.2. Previous Work	37
2.3. Results and Discussion	41
2.3.1. Aromatization with DARCO	42
2.3.2. X-ray Data of Regioisomer	44
2.3.3. One-Step Diels-Alder Approach	47
2.3.4. Two-Step Diels-Alder Approach	51
2.3.5. Bromination	53
2.3.6. Furan-Adduct	54
2.3.7. Sulfolene Reaction	55
2.3.8. Dehydration and Oxidation	56
2.3.9. Fluorinated One-Step Diels-Alder Approach	60
2.3.10 OH-Fantrip Synthesis	64
2.4. Conclusions	69
2.5. Materials and Methods	70
References	80
3. Synthetic Efforts Towards a Pentiptycene Based Monomer	81
3.1. Overview	81
3.2. Results and Discussion	83
3.3. Future	93
3.4. Conclusion	94

3.5. Experimental	94
References	96
4. Synthetic Development of Monomer 1-pyz and Efforts Towards its Polymerization	98
4.1. Overview	98
4.2. Background.....	98
4.3. Results and Discussion	100
4.4. Polymerization of 1-pyz	107
4.5. LB Trough Method.....	109
4.6. Conclusion	110
4.7. Experimental	111
References	112
5. Efforts Towards the 2D Polymerization of a Porphyrin Based Monomer	114
5.1. Overview	114
5.2. Results and Discussion	115
5.3. Crystallization Approach.....	117
5.5. LB Trough Approach.....	122
5.6. Control Reaction.....	128
5.7. Conclusion	130
5.8. Experimental	130
References	131
6. Antrip and Fantrip Co-crystallizations with Fullerenes Towards Single Crystal Polymerizations.....	132
6.1. Overview	132
6.2. Co-crystallization.....	135
6.3. Conclusion	139

References	140
Appendix 1: Supplemental Information for Chapter 2	141
Appendix 2: Supplemental Information for Chapter 3	154
Appendix 3: Supplemental Information for Chapter 4	159
Appendix 4: Supplemental Information for Chapter 4	163

List of Figures

Chapter 1

Figure 1.1. Three different architectures of 1D polymers	1
Figure 1.2. Illustration of a two-functional monomer and its 1D polymerization.....	1
Figure 1.3. Illustration of a three-functional monomer and its 2D polymerization	3
Figure 1.4. Example of a periodic tiling and a non-periodic tiling	4
Figure 1.5. Relation between a monomer/repeat unit and a respective tiling.....	5
Figure 1.6. A halogenated monomer and its 2D polymerization under UHV.....	7
Figure 1.7. COF reactants and SEM of product	9
Figure 1.8. Lamellar crystal being polymerized and exfoliated.....	12
Figure 1.9. Description of anthracene and an anthraceno group	13
Figure 1.10. Photoinduced dimerization of anthracene.....	13
Figure 1.11. Antrip monomer	15
Figure 1.12. Antrip π - π interactions driving a hexagonally packed lattice and its polymerization	15
Figure 1.13 Crystal structure of antrip benzene solvate	16
Figure 1.14. Fantrip and crystal structure of its monomer and polymer	18
Figure 1.15. Cartoon of monomer packing and polymerized at the air-water interface	19
Figure 1.16. Antrip-DEG monomer	20
Figure 1.17. STM image of Antrip-DEG polymer and a simulation.....	20
Figure 1.18. Cartoon comparing an inefficient and efficient membrane.....	22
Figure 1.19. Cartoon of a 2D polymer being used as a template for 2DP synthesis	24
Figure 1.20. Four structurally related monomers	27
Figure 1.21. Pentipitycene based monomer	29
Figure 1.22. Description of pentipitycene and pentipitycene quinone	29

Figure 1.23. 1-pyz monomer and its metal coordinated hexagonal unit.....	30
Figure 1.24. Porphyrin monomers 1-P and 1-PZn	30
Chapter 2	
Figure 2.1. different acenes and their general structural formula.....	34
Figure 2.2. Four target monomers.....	35
Figure 2.3. Breakdown of antrip monomer.....	36
Figure 2.4. Retrosynthetic breakdown of three routes towards parent framework.....	37
Figure 2.5. Bond rotation of tris-ketoacid intermediate.....	39
Figure 2.6. Antrip quinone crystal structure nitromethane solvate.....	45
Figure 2.7. Defining the proximal and distal sites of triptycene.....	45
Figure 2.8. Possible regioisomers of antrip (1-H) and methoxy antrip (1-MeO).....	46
Figure 2.9. N-methyl isoindole.....	48
Figure 2.10. Configurational isomers of the one-step Diels-Alder intermediate 7	50
Chapter 3	
Figure 3.1. Framework of pentiptycene based monomer.....	81
Figure 3.2. Square packing of pentiptycene based monomer 1-FP	82
Figure 3.3. Difference between triptycene and pentiptycene.....	82
Figure 3.4. Structures of pentiptycene and pentiptycene quinone.....	86
Figure 3.5. A new route towards octabromo pentiptycene.....	93
Chapter 4	
Figure 4.1. Monomer 1-pyz and its coordination into a hexagonal unit.....	99
Chapter 5	
Figure 5.1. Porphyrin framework.....	114
Figure 5.2. Structure of porphyrin monomer 1-P	115
Figure 5.3. Square packing of 1-P illustrating π - π interactions between monomers.....	116

Figure 5.4. Top down view of the square packing of 1-P	117
Figure 5.5. Crystal structures of 1-P , pyridine and toluene solvates.....	119
Figure 5.6. Toluene solvate of 1-P showing distance between anthracene blades	119
Figure 5.7. Image of benzene microcrystals in bromoform before and after irradiation	122
Figure 5.8. 1-P complexing a metal to which a hydrophilic ligand is attached	123
Figure 5.9. 1-PZn complexing isonicotinic acid.....	125
Figure 5.10. Absorption spectrum of 1-PZn and 1-PZn complexed with pyridine	126
Figure 5.11. 1-PZn complexing pyridyl DEG ligand 20	128
Figure 5.11. Porphyrin core distortion after anthraceno blade dimerization	129
Chapter 6	
Figure 6.1. Structures of antrip and fantrip and their polymer simulation.....	132
Figure 6.2. A proposed packing of the parent framework and a fullerene	133
Figure 6.3. Comparison of geometry of C_{60} and C_{70}	134
Figure 6.4. A C_{60} /corannulene crystal structure.....	135
Figure 6.5. Crystal structure of antrip/ C_{70} tetrachloroethylene solvate	138

List of Schemes

Chapter 1

Scheme 1.1. Retrosynthetic breakdown of three synthetic approaches towards the triptycene based monomer	28
--	-----------

Chapter 2

Scheme 2.1. Swaggers Friedel-Crafts protocol towards antrip (1-H)	38
Scheme 2.2. Modified Friedel-Crafts protocol towards antrip (1-H)	40
Scheme 2.3. Modified Friedel-Crafts protocol towards MeO-antrip (1-MeO).....	41
Scheme 2.4. Pd/C oxidation of hydrogenated iptycene	42
Scheme 2.5. Oxidation of hydrogenated anthracene with DARCO	43
Scheme 2.6. DARCO oxidation of hydrogenated intermediate 5-MeO	43
Scheme 2.7. Acene synthesis using a one-step Diels-Alder approach	47
Scheme 2.8. General scheme for the one-step Diels-Alder towards antrip (1-H).....	49
Scheme 2.9. Cheletropic elimination of a fluorinated PAH	50
Scheme 2.10. General scheme for the two-step Diels-Alder route.....	52
Scheme 2.11. Bromination of triptycene.....	53
Scheme 2.12. Diels-Alder cycloaddition between intermediate 2 furan	55
Scheme 2.13. Diels-Alder cycloaddition between intermediate 8 and 3-sulfolene	56
Scheme 2.14. Acid catalyzed dehydration of 9	57
Scheme 2.15. General oxidation of intermediate 10 to 1-H or 1-MeO	57
Scheme 2.16. One pot dehydration/oxidation of 9 to 1-H or 1-MeO	59
Scheme 2.17. Improved two-step Diels-Alder scheme towards 1-H or 1-MeO	60
Scheme 2.18. General One-step Diels-Alder for fantrip 1-F	61
Scheme 2.19. Diels-Alder between 2-Br and 12-F	62
Scheme 2.20. Deamination of 11-F using mCPBA	63

Scheme 2.21. Deamination of 11-F using H ₂ O ₂	64
Scheme 2.22. Synthetic route towards MeO-fantrip (1-FMeO).....	66
Scheme 2.23. Synthetic route towards hydroxy fantrip (1-FOH)	69
Chapter 3	
Scheme 3.1. General route to 1-FP	83
Scheme 3.2. Pentiptycene synthesis	84
Scheme 3.3. Bromination of pentiptycene.....	85
Scheme 3.4. General route towards pentiptycene quinone based monomer 1-FPQ	87
Scheme 3.5. Synthesis of pentiptycene quinone.....	88
Scheme 3.6. Bromination of pentiptycene quinone towards 14-Br	88
Scheme 3.7. General route towards protected monomer 1-Fpiv	89
Scheme 3.8. Reduction of pentiptycene quinone to 15-OH	90
Scheme 3.9. Pivaloyl protection of 15-OH giving 15-piv	91
Scheme 3.10. Bromination of 15-piv towards 16-Br	91
Scheme 3.11. Bromination of 15-piv using iodine catalyst towards 16-Br	92
Chapter 4	
Scheme 4.1. Willgerodt-Kindler route for the preparation of 1-pyz	100
Scheme 4.2. One-pot Willgerodt-Kindler reaction and hydrolysis	101
Scheme 4.3. Thioamide intermediate of the one-pot Willgerodt-Kindler reaction	101
Scheme 4.4. Microwave procedure for the Willgerodt-Kindler reaction.....	102
Scheme 4.5. General route for the Suzuki route towards 1-pyz	103
Scheme 4.6. Synthesis of boronic ester intermediate 18	104
Scheme 4.7. Suzuki cross coupling between 18 and 1,3,5-tribromobenzene giving 19	104
Scheme 4.8. Microscale deprotection of 19	105
Scheme 4.9. Macroscale deprotection of 19	105

Chapter 5

Scheme 5.1. Synthetic conditions for the synthesis of 1-P	116
Scheme 5.2. Insertion of Zn into 1-P	124
Scheme 5.3. Attachment of DEG chain to 4-hydroxypyridine	127

List of Tables**Chapter 5****Table 5.1** Examples of the solvents used for microcrystal screening of **1-P** **121****Chapter 6****Table 6.1.** Solvents used for cocrystallizations between monomers and fullerenes **137**

1. Introduction

1.1. One-Dimensional Polymers

A polymer is defined as a large molecule constructed from many smaller structural units, referred to as repeat units, that are bonded in any conceivable pattern.¹ Three main architectures of one-dimensional polymers (1DPs) are shown below in Figure 1.1. Referring to a polymer as 1D can be confusing due to the fact that the 1D polymers we use every day occupy three-dimensional (3D) space. When defining a polymer as 1D one looks at the



Figure 1.1. Three different architectures of 1DPs.

topology of the connected repeat units. The example architectures above show increasing complexity, but because each is comprised of topologically linear chains of repeat units, each example is classified as 1D.

A monomer to be used for a 1D polymerization must possess a functionality (number of reactive sites) of at least two, furthermore, employment of monomers with a functionality greater than two can lead to more complex architectures such as branched or crosslinked polymers seen above in Figure 1.1. Figure 1.2 illustrates a monomer with a functionality of

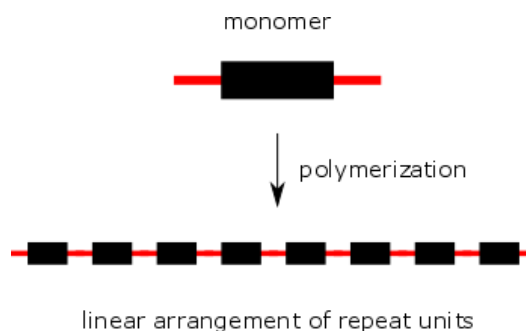


Figure 1.2. Illustration of a monomer with a functionality and its arrangement into a linear 1-D polymer. Red ends represent functional groups.

two polymerizing into a linear arrangement of repeat units. Depending on the chemical makeup of the repeat units, architecture of the final product, and length of the polymer chains, the final polymer will possess physical properties which can be exploited for a number of different uses.

The birth of polymer science started with Charles Goodyear's development of the rubber vulcanization process in the 1830s.² For decades after, the molecular make-up of polymers were highly misunderstood and believed to be colloidal in nature, *i.e.* large molecules held together by intermolecular forces. It was not until 1927 that German organic chemist Hermann Staudinger began to convince the scientific community of a new outlook towards polymers. He discovered that polymers were not colloidal in nature, but were in fact massive molecules comprised of linear arrangements of covalently linked repeat units.¹ Staudinger eventually persuaded the scientific community towards his more accurate description of a polymer. This provided better understanding of the physical nature of polymers and led to many breakthroughs over the following decades, such as the development of nylon by Wallace Carothers in 1930, the synthesis of Teflon by Roy Plunkett in 1938, and the synthesis of polyethylene in 1939. These are all polymers that continue to be widely used to this day.

Polymers are materials we continuously use in our daily lives, from polyester clothing to polycarbonate safety glasses. Polymers are an integral part of the modern world.³ Polymeric materials are so versatile and ubiquitous that it would be difficult to go throughout a day without using a product made from them. The massive range of applications and conveniences afforded by polymer products motivates the continuous evolution of polymer chemistry. Furthermore, innovations in the broader field of chemistry, such as novel

transformations and catalytic processes, continue to be eagerly applied to polymer science, giving rise to new and creative monomer designs and polymerization conditions.^{4,5} The evolution of polymer chemistry over the past century is evident by the world around us.

Synthetic 1D polymers are the most common; indeed, when the word polymer is used it is usually referring to a 1D polymer. What we typically think of when we hear the word “polymer”, are synthetic materials made from linear arrangements of repeat units. However, the recent characterization of graphene, a naturally occurring two-dimensional polymer (2DP), has provided motivation towards exploring polymers of higher dimension.⁶

1.2. Two-Dimensional Polymers

The field of two-dimensional polymers (2DPs) is a new and steadily growing field.⁷ A 2DP in its simplest form can be viewed as a polymer which possesses laterally connected repeat units that cover a two-dimensional plane to form a sheet.⁷ One quality required of a monomer for application in 2D polymerizations is the presence of at least three functionalities.⁸ Much like a functionality of two represents linear growth, a functionality of three, in this case, represents growth about a plane, Figure 1.3.

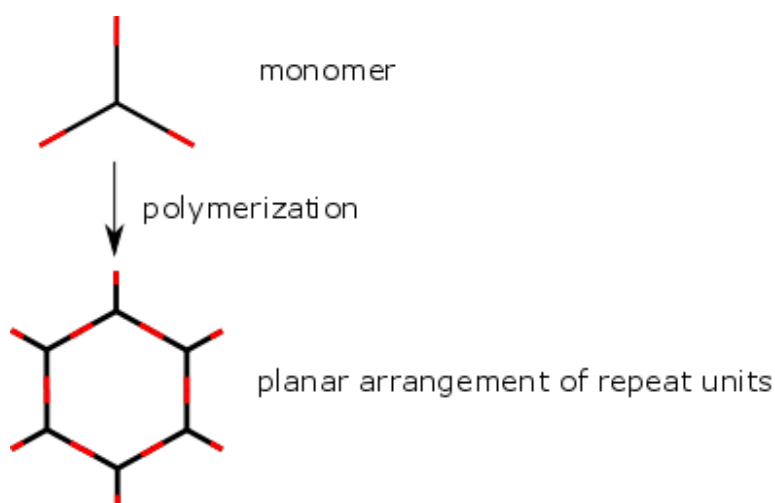


Figure 1.3. Illustration of a monomer used for 2DP synthesis and its polymerization into a 2DP. Red ends represent functional groups.

There are currently multiple ways to define a 2DP.^{8,7,9} The “loose” use of the term two-dimensional when defining extremely thin materials or layered materials, commonly leads to confusion with actual 2DPs.^{10,7} Using topology to define 2DPs allows one to employ tile theory, a mathematical concept which investigates ways to precisely cover 2D planes with geometric shapes.¹¹ Utilizing tile theory to define 2DPs allows periodic and non-periodic materials to be considered. This provides a comprehensive definition that satisfies the debate associated with defining a 2DP.^{7,8,9} Naturally occurring graphene is a perfect example of a 2DP.¹² Graphene consists of covalently bound sp^2 hybridized carbon repeat units which propagate in a hexagonal 2D lattice, as illustrated in Figure 1.4. One could use the fact that graphene is a single repeat unit thick and is periodic in two dimensions to define a 2DP. However, for a comprehensive definition, one must also consider non-periodic materials that are one monomer unit thick and propagate in two dimensions.⁸

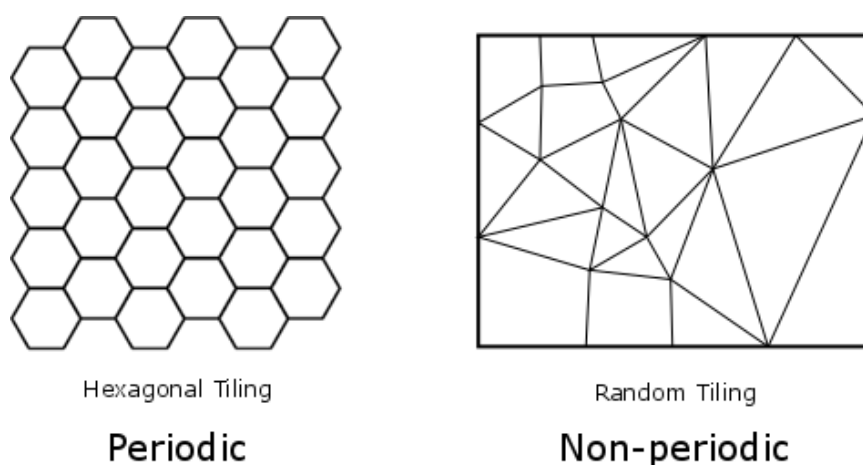
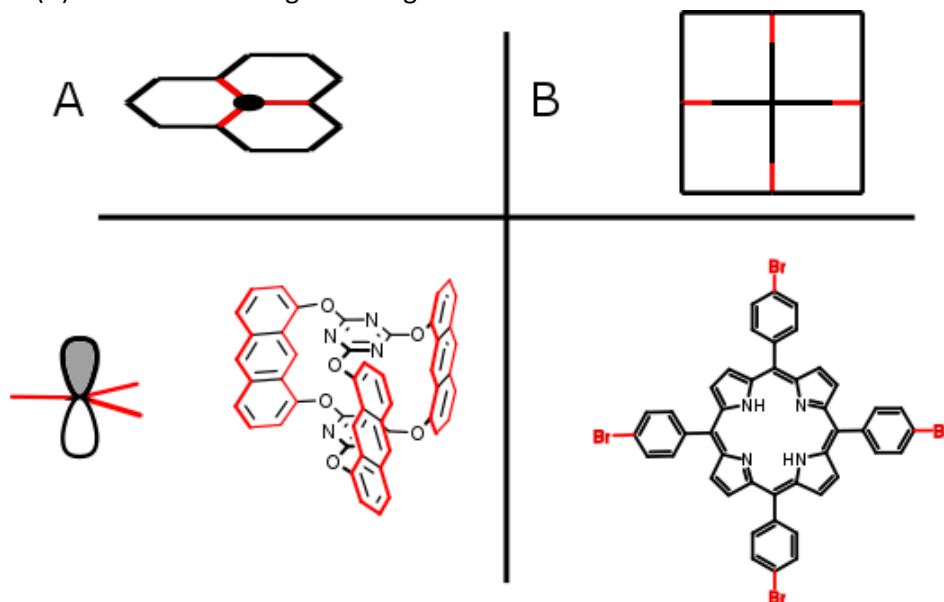


Figure 1.4. Example of a periodic hexagonal tiling, representative of graphene (left). A random non-periodic tiling (right).

Connectivity of tiles over a 2D plane with no gaps or overlaps directly relates to the connectivity of repeat units covering a plane, as with 2DPs. Seen above in Figure 1.4 are two examples of tilings, one periodic and one non-periodic, where the vertices and lines of the above graphs define a tile. When applied to defining a 2DP, each vertex is viewed as a repeat unit and the lines connecting them are viewed as chemical bonds. This allows for a solid understanding of how to topologically define a 2DP. A practical requirement of a 2DP is that the material can be isolated as a single sheet with the thickness of a repeat unit; this excludes layered materials that are incapable of being exfoliated into sheets.⁹ If the material is not isolated as an independent sheet, then it does not relate to a tiling. This definition not only includes covalently bound 2D materials, but also those where the repeat units are held together by

Figure 1.5. (A) Color coded hexagonal tiling section with a black circle at the vertex denoting



a repeat unit and red edges denoting bonds (top). An sp^2 hybridized carbon, the repeat unit for graphene with three red bonds (bottom, left). Next to it, a monomer with three anthracene functional groups (bottom, right). Each monomer is shape persistent and has three-fold symmetry between bonding sites, denoted in red, and map perfectly over the above tiling. (B) A square tiling showing a black cross to denote a repeat unit and red tips to

denote bonds (top). An analogous porphyrin monomer with four-fold functionality, colored in red, which maps over the above tiling (bottom).

coordinate, hydrogen, or other bonds. Seen below are two examples of how a monomer or repeat unit relates to an analogous tiling, Figure 1.5.

1.3. Synthetic Approaches to Two-Dimensional Polymers

Usually some type of organization process is imposed to facilitate planar growth during polymerization. A 2D polymerization requires the functional groups of the monomers to react within the same plane. Typically, entropy will oppose the organization of an ordered 2D arrangement of monomers if they are simply put in solution to react.¹³ This would likely result in a random network of repeat units that does not cover a plane, has multiple gaps, and overlaps; not qualifying it as a 2DP. Overcoming this obstacle was the key challenge in the preparation of 2DPs.

There are multiple methods of organizing monomers in preparation for 2D polymerizations. Some methods are useful as a proof of concept, because they enable easy characterization and verification of a monomers viability, and other techniques aspire to yield large polymer sheets for material applications.^{14,15} Each approach used in 2DP chemistry has its advantages and disadvantages. However, the field of 2D polymers is relatively new, and exploration of all prospective methods is a benefit to the field. Herein is a short list of the current conditions and methods used to pre-organize monomers and synthesize 2DPs.

1.3.1. Ultra-High Vacuum Approach

The ultra-high vacuum (UHV) approach relies on depositing monomers onto a flat coinage surface, via sublimation, under UHV conditions. The atomically flat coinage surface limits the monomers to the lateral movement needed to react.¹⁶ Typically the monomers used for this process are flat aromatic compounds. The compounds used are commonly halogenated, allowing them to undergo a surface catalyzed C-C coupling reaction. A common

coupling employed is the Ullman coupling, which utilizes halogenated polycyclic aromatic hydrocarbons (PAHs) as monomers. Seen below is an illustration of a monomer, simulated polymer, and an AFM of a porous graphene product from the Bieri group, Figure 1.6.¹⁴

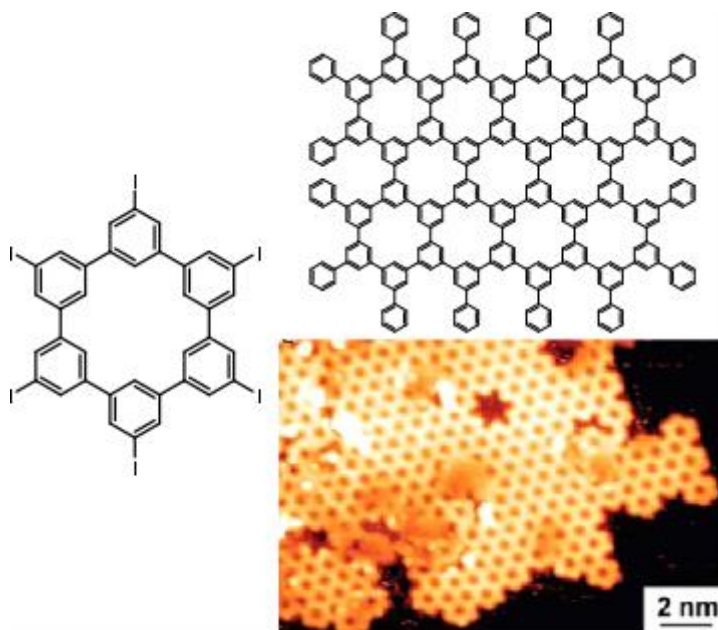


Figure 1.6. An iodinated cyclohexaphenylene monomer (left), polymerized via an Ullman coupling on a Cu(111) surface. To the right is the simulated polymer (top) and an AFM showing a large section of their porous graphene product(bottom).¹⁴

The domain size of the above product in Figure 1.6 is typical of polymers synthesized using the UHV approach. This approach typically results in domains on the nm scale with many imperfections, as seen in Figure 1.6. It is hypothesized that the halogenated byproducts formed during polymerization interfere with long range order.¹⁴ A considerable amount of research is being put toward polymerization conditions that result in less obstructing by-products towards obtaining larger ordered domains.¹⁷

With such small domains, the UHV approach seems to be limited to the high throughput testing of monomers for polymerizations and their characterization by microscopy. While the resulting 2DP domain sizes are small, utilizing surface catalyzed C-C coupling reactions allows the monomers to be simple halogenated aromatics. Developing the UHV approach towards increasing the domain sizes with fewer imperfections gives the

potential of utilizing simple aromatics such as 1,3,5-tribromobenzene, a commercially available molecule, as a possible monomer.

Further development of the UHV method has the potential to yield larger, more useful 2DPs. However, by-products from the polymerization process are thought to cause imperfections and lead to domains on the nm scale, currently making them unfit for application. Another limitation of the UHV approach is the expense of the process. The domain size of polymers synthesized by the UHV approach is ultimately limited by the size of the atomically flat surface on which the polymerization takes place. Not only are these surfaces extremely expensive, obtaining a UHV environment requires a specialized apparatus that necessitates expensive materials and conditions. Even with the above limitations of the UHV approach, finding a method of polymerization on a surface that prevents by-products from causing imperfections and yields large areas of periodic polymers would make the UHV approach beneficial beyond proof of concept and characterization.¹⁴

1.3.2. Two-Dimensional Covalent Organic Framework

Solution phase 2DP synthesis requires the reaction of an appropriate monomer under reversible bonding conditions.⁷ The initial organization comes from the monomers reacting with one another to form pseudo organized domains, and through dynamic reversible bonding the domains can re-organize into periodic, crystalline structures. If a crystalline, lamellar material is produced then it must survive exfoliation into single sheets. The exfoliation process involves breaking up the grain boundaries between the layers of the material. This can be accomplished by employing chemical methods, such as solvent and heat, and or mechanical methods such as sonication or slow rotation of a solution. However, there are currently no reports showing evidence of a successful exfoliation of crystals formed using the solution method into individual sheets. Typically the bulk crystals formed using the

solution method are referred to as covalent organic frameworks (COFs) and only once exfoliated into single sheets would they be considered 2DPs, Figure 1.7.¹⁸

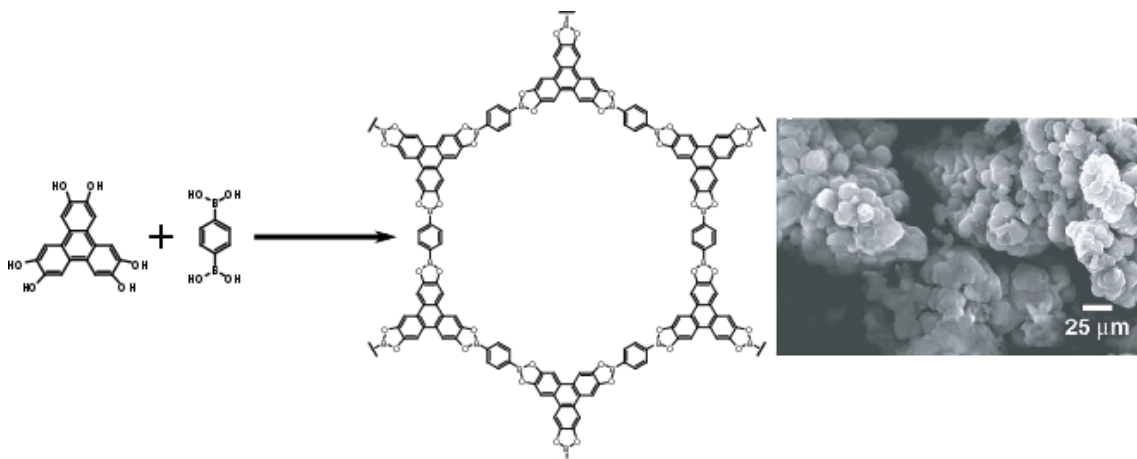


Figure 1.7. Condensation reaction between monomers giving a hexagonal lattice (hexagonal unit shown), and SEM image of bulk material.

The current methods of synthesizing 2DPs in solution commonly yield microcrystalline bulk material.⁷ Upon exfoliation of the microcrystalline material, the detection and characterization single 2DP sheets has yet to be realized. Obtaining large area sheets with this method is dependent on a monomers ability to remain in solution, and generate a large area sheet versus reacting to form an endless number of microcrystals.¹³ When considering entropy and the lack of pre-organization, the solution approach is intrinsically susceptible to defects. The solution phase method is poised for a battle between entropy and order, and the linchpin of successfully polymerizing large domains rests on monomer design and its ability to favor order over disorder under the imposed conditions. While this approach's simplicity is elegant and deserves continued research, currently the small domains and reversible nature of the bonds pose a potential problem for characterization and physical application.

1.3.3. Single Crystal Approach

In the King group, one of the main types of monomer preorganization utilized is single crystal growth followed by solid state polymerization.^{9,15} The first successful topochemical 2D polymerization was performed by Dr. Kissel of the Schluter group.¹⁹ This involved the synthesis of a complex monomer, with three-fold symmetry followed by its crystallization and irradiation. The reacting moieties of the monomer were anthraceno and alkyne substituents that were organized through crystallization to allow a Diels-Alder cycloaddition between the diene (anthraceno group) and dienophile (alkyne group), Figure 1.8.

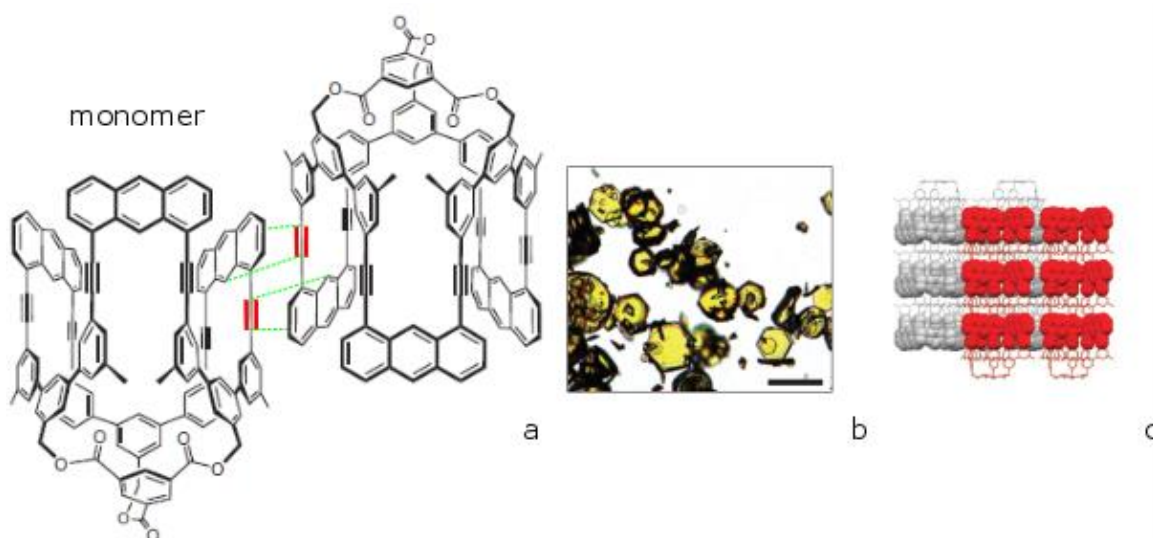


Figure 1.8. The monomer by Kissel *et al.* illustrating the up-down packing with dotted green lines, and red triple bonds denoting the carbon atoms participating in the Diels-Alder cycloaddition (a), image of hexagonal crystals, (b) and the monomers crystal structure showing its lamellar nature (c).

The unique lamellar packing of the monomers and their up-down orientation permitted polymerization via Diels-Alder cycloaddition and resulted in the first 2DP prepared by organic synthesis. Unfortunately, upon polymerization the crystals did not retain their integrity and were unsuitable for X-ray diffraction for characterization. However, the reacted crystals, consisting of 2DP layers, were exfoliated by heating in 1-methyl-2-pyrrolidone (NMP)

for three days at 150 °C leading to liberation of single 2DP sheets that were characterized by AFM and TEM, however molecular-resolution images were not obtained.¹⁹

A major benefit of the crystallization approach is that it has the potential for much larger ordered domains than deposition under UHV or the microcrystalline products of solution phase polymerizations. While the crystallization approach is capable of providing larger domains, the area of the polymeric sheets is ultimately limited by the size of the parent single crystal.

A major benefit of the crystallization approach is ease of characterization. Ideally the single crystal can be characterized by single crystal X-ray diffraction before and after polymerization. The lamellar crystal comprised of polymeric sheets can then be exfoliated for further characterization and analysis by microscopy.

Crystallization of the monomers would ideally result in a lamellar crystal with the monomers having the appropriate overlap of reactive groups and orientation within the crystal. Monomers within the crystal have minimal movement during polymerization, therefore, crystallization conditions must be found that not only result in a single crystal but one in which the desired packing of the monomers is obtained. The topochemical postulate states that in addition to proper alignment of functional groups, the distance between them must be at least 4.2 Å for a topochemical transformation to take place.²⁰ Once the functional groups are appropriately arranged they can undergo a solid state (topochemical) polymerization that is initiated by either heat or light. A generic example of a lamellar crystal and its polymerization followed by exfoliation is illustrated in Figure 1.8.

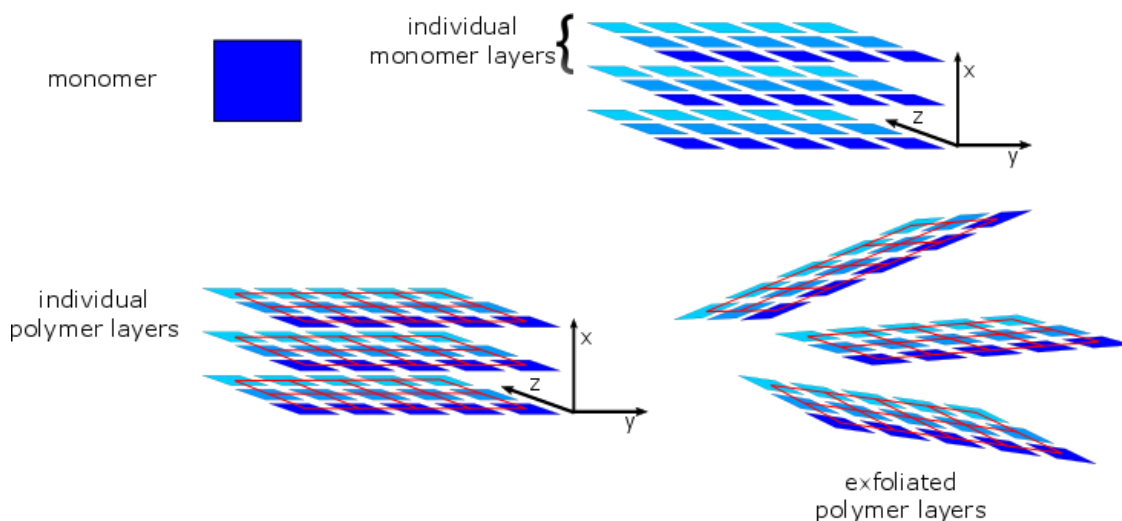


Figure 1.8. An illustration of a monomer with a functionality of four, in a lamellar crystal and its polymerization followed by exfoliation. Red lines denote bonding between monomers.

Recent progress in the field of 2D polymers has explored new and creative monomer designs, however, the transformations used for solid state polymerizations are limited.^{15,19} Cycloaddition transformations, such as [4+4] and Diels-Alder cycloadditions, are common for topochemical 2D polymerizations. Cycloaddition reactions result in no byproducts that would have to escape the lattice, giving them great atom economy; this attribute is why their application is so common in solid-state 2DP synthesis. If a topochemical transformation were to have a side product(s), the side products generation could potentially disrupt the delicate crystal lattice. Disrupting the packing between neighboring monomers could possibly result in loss of overlap between reactive moieties of those monomers. This loss of overlap would result in an incomplete polymerization or no polymerization at all.²¹ For the same reasons, minimal atomic movement during reaction is also desirable. Transformations that result in large movements have the potential to cause disorder within the lattice and lead to incomplete polymerizations.²⁰ Ideally, the volume occupied by the starting orientation of the reactive moieties and their product after reaction should be as close as possible. This prevents shrinking or expansion of the crystal and allows reactive moieties to retain their intended overlap.

The King group and the Schluter group from ETH Zurich are two leaders in the field of 2DPs. Both groups commonly employ anthraceno moieties as reactive functional groups in their 2DP monomers. The 2,3-anthraceno group is common in King group monomers, and substitutions of anthracene, such as at the 9 position are fairly common in Schluter group monomers. Seen below is picture of anthracene, showing its numbering system, and a 2,3-anthraceno moiety, Figure 1.9.

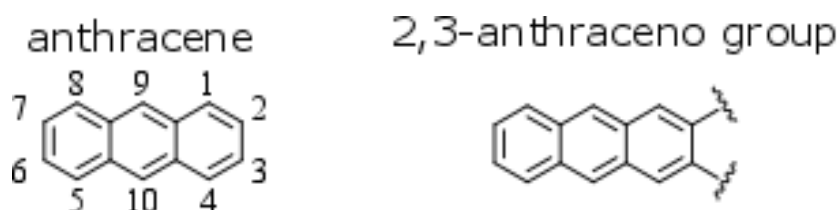


Figure 1.9. Description of anthracene and the anthraceno group referred to throughout.

Anthraceno moieties not only aid in preorganization through π - π interactions, they conveniently undergo photoinduced [4+4] cyclizations.²² A 2D polymerization utilizing anthraceno groups provides atom economical transformations that result in limited atomic movement. Use of anthraceno moieties have yielded both crystal to crystal transformations and polymerizations at the air water interface. Seen below is a basic description of two anthracene molecules undergoing a [4+4] cycloaddition between their 9 and 10 positions upon irradiation with 365 nm light, Figure 1.9.^{23,15}



Figure 1.10. The photoinduced [4+4] dimerization of anthracene using 365nm light.

Topochemical reactions using photoreactive molecules such as anthracene and derivatives thereof have been researched since the 1960s. Anthracene readily dimerizes between its medial 9,10 positions when irradiated at its absorbance maximum of 365 nm.²² It was found, during the topochemical dimerization of anthracene and derivatives, that the

integrity of the crystal was commonly destroyed during irradiation. This prevents characterization by X-ray diffraction. However, decades of topochemistry research have given insight towards how to retain crystal structure during irradiation. Using a lower energy, less effective, wavelength of radiation allows for a gentler and more even reaction. A uniform reaction throughout the crystal will promote retention of crystal integrity. The absorbance maximum of the anthraceno moiety is 365 nm. Wavelengths between 400-465 nm, which pertains to the fine structure of anthracene and have a much lower molar absorptivity, are typically used as less efficient, lower energy wavelengths.²⁰ As a photon's wavelength deviates from the absorbance maximum of a molecule it is less likely to be absorbed. And using a less efficient wavelength during a topochemical transformation has been found to allow the light to penetrate into the crystal a further distance before being absorbed; as opposed to an efficient wavelength that would be absorbed by one of the first molecules it hits. Irradiation at the absorbance maximum typically leads to a reacted crust on the outside of the crystal. As the crust propagates throughout the crystal it causes uneven molecular motion and inhomogeneity, this typically leads to defects and damage to crystal integrity. However, a less efficient wavelength can penetrate deep into the crystal and typically leads to an even, uniform transformation, which allows retention of crystal integrity. Therefore, ideal conditions are a low energy, even irradiation of the crystal causing molecular motions to work in a homogenous manner, leading to retention of crystal integrity.

The following is an example of the monomer antrip from the King group, which consists of a triptycene core with three anthraceno blades, Figure 1.11.⁹

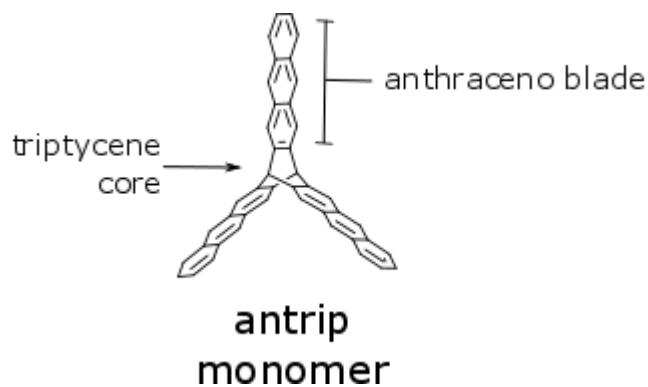


Figure 1.11. Antrip monomer.

The threefold symmetrical monomer antrip is designed to take advantage of π - π interactions between anthraceno blades promoting a hexagonal organization during crystallization. The ideal hexagonal packing of the monomer is seen in Figure 1.12. The π - π interactions between anthraceno blades are designed to promote overlap between their 9,10 positions which then undergo [4+4] cycloaddition upon irradiation.^{22,9}

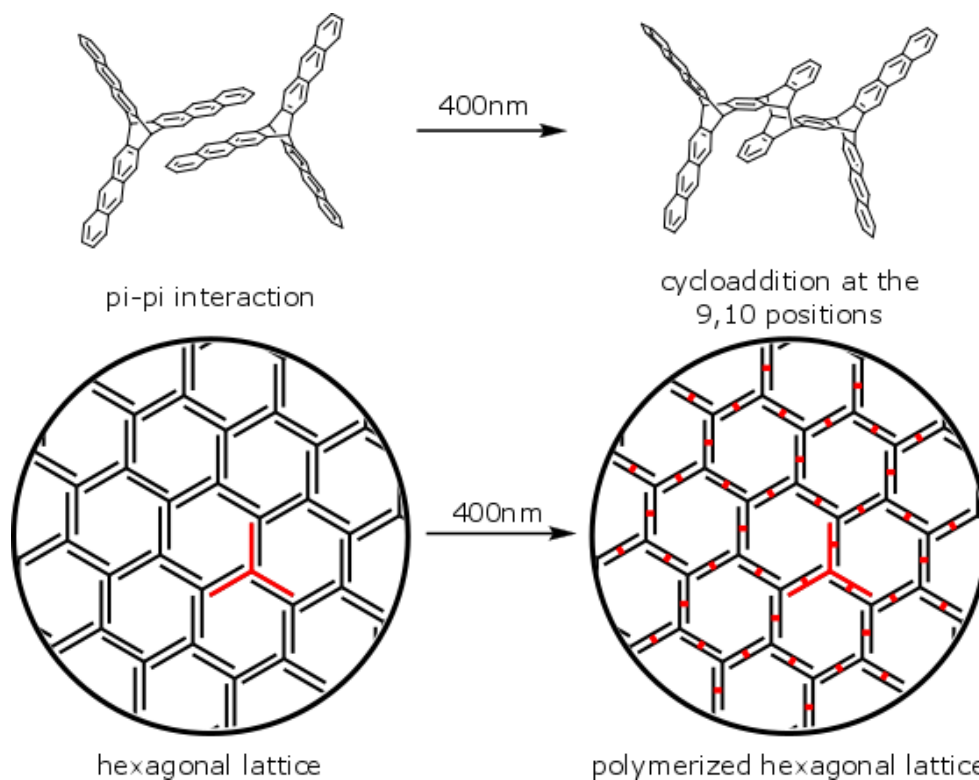


Figure 1.12. Illustration of the π - π interactions between the anthraceno blades of two monomers, followed by a [4+4] dimerization between anthraceno blades (for clarity, only one

pair of anthraceno blades are shown dimerizing) (top). A top down view of an ideal hexagonal packing of monomers followed by their photo initiated [4+4] dimerization to give a polymer, red lines denoting bonds between monomers (bottom).

Former King group member Dr. Bhola synthesized the antrip monomer and was able to crystallize it into a quasi-hexagonal packing. Seen below, Figure 1.13, is a crystal structure of the antrip monomer prior to polymerization. It can be seen that the monomers are packed into hexagonal units, however, when looking perpendicular to a single hexagonal unit, the green half is offset to the other by 35.3° .⁹ After acquiring a crystal structure she polymerized the sample, via irradiation at 365 nm, which yielded the group's first 2DP. My initial contributions to this specific project were minimal, however, after its completion I took on the task of optimizing the synthesis of antrip.

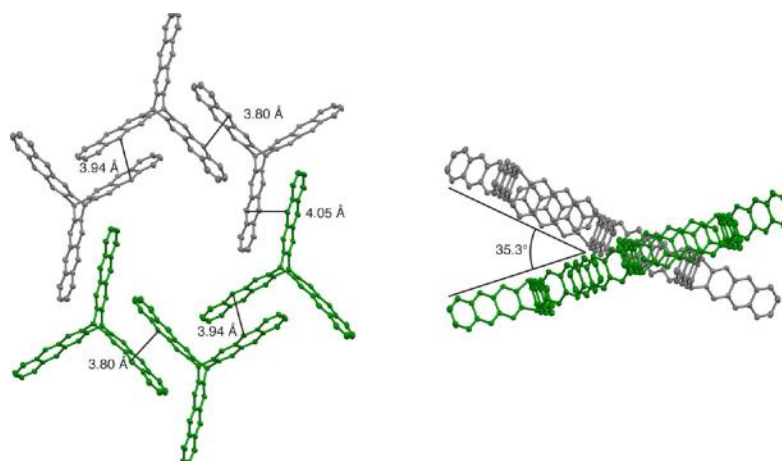


Figure 1.13. Crystal structure of antrip benzene solvate looking down hexagonal channel (left). Viewing perpendicular to hexagonal channel showing the two halves offset by 35.3° (right).⁹ Green and silver colors are to facilitate visualization.

Following irradiation of the antrip crystal, a crystal structure could not be obtained. It is believed the molecular movement during polymerization is what damaged the crystal integrity. For polymerization to occur in the above crystal structure, each half of the hexagonal unit, which are offset by 35.3° , must shift towards coplanarity. While imperative

for polymerization to occur, this drastic movement most likely damaged crystal integrity and prevented characterization by X-ray diffraction. While final polymer was unable to be characterized by X-ray diffraction, the product was exfoliated, and single polymerized sheets were confirmed by AFM and other forms of microscopy, indicating the presence of a 2DP.⁹

The ultimate form of characterization for a 2DP is single crystal X-ray diffraction. This gives undeniable evidence of bonding between repeat units as well as confirmation of 2D connectivity between them. Failure to characterize the polymerization of antrip by single crystal X-ray diffraction was due to the 35.3° offset between the halves of the hexagonal units; the initial lack of co-planarity between monomers necessitated too much movement during polymerization causing crystal degradation. A different crystal with all monomers packed in a hexagonal manner, but with all monomers coplanar to one another could potentially allow a crystal to crystal polymerization of antrip. A crystal to crystal polymerization is defined as a topochemical polymerization in which the unreacted and reacted crystals can be characterized by single crystal X-ray diffraction. Discovering conditions for the crystallization of antrip that resulted in co-planarity between every monomer could potentially allow a crystal to crystal polymerization. However, during my time in the King group efforts were made towards growing such a crystal with antrip, but the proper conditions have yet to be found.

While conditions for the crystal to crystal polymerization of antrip were not found, a fluorinated derivative of the antrip framework was sought out by former post-doc, Dr. Patrick Kissel.²³ The fluorinated blades were incorporated to take advantage of their increased ability for π - π interactions. This was designed to promote co-facial packing between the anthraceno blades of all monomers. Building a monomer which avoids the 35.3° offset that antrip adopted during crystallization would bring us that much closer to obtaining a crystal to crystal polymerization.

Fantrip was crystallized by slow evaporation in chloroform at room temperature. Single crystal X-ray diffraction of the fantrip crystals confirmed a cofacial packing of hexagonal units. With an ideal hexagonal packing, a gentle, low energy, polymerization was performed by irradiating a single crystal in two steps. Irradiations at 465 nm for 1 hr at 225 K and 400 nm for 1 hr at 225 K were carried out in order to preservation crystal integrity. Shown below is the fantrip monomer, its crystal structure, and its polymerized crystal structure, Figure 1.14.



Figure 1.14. Fantrip monomer and the crystal structure of its chloroform solvate before and after polymerization. Polymerization was performed in two stages. Irradiation with 465 nm giving a partial polymerization (crystal structure not shown), followed by irradiation at 400 nm, to complete the polymerization.²³

1.3.4. Air-Water Interface Approach

Another method of preorganization is preorganization at the air-water interface using a Langmuir-Blodgett trough (LB trough). Use of a LB trough can provide an efficient method of acquiring large area two-dimensional polymer sheets. The technology for preorganization and polymerizing using UHV, solution, and crystallization methods are currently limited to very small domains that would be very limited for application in commercial use. Theoretically the area of a 2DP synthesized using an LB trough is only limited to the area of the trough. Furthermore, this method of preorganization limits the monomers movements to a 2D surface. One can engineer a monomer that not only floats at the air water interface but has attributes that promotes the desired packing of functionalities. Confinement to 2D removes

a variable and avoids some of the uncertainty associated with the crystallization or solution approach. Considering all other forms of 2DP synthesis, this approach holds the most promise for real world applications simply due to the large area of polymer possible and its inherent isolation to two-dimensions during pre-organization.

For organization at the air water interface to occur, a specific type of monomer must be used. An amphiphilic monomer must be “floated” at the air water interface. Use of a hydrophilic anchor attached to the monomer will keep orientation of the monomers consistent with respect to one another by forcing them to float flat on the surface of a water sub-phase. As seen in Figure 1.14, square monomers with anchors to represent amphiphilic tails, are shown floating at an air water interface. Compressing the barriers of the LB trough, shown in black, allows for packing of the monomers and formation of a monolayer. If the monomer is designed properly, a compression can be achieved that results in overlap of functional groups, thus allowing polymerization. Once the proper conditions are met, the monomers are polymerized by chemical, thermal, or photo-induced means to yield a single large area 2DP, Figure 1.15. The layers can then be transferred to various surfaces for characterization and application.



Figure 1.15. Polymerization using an LB trough. Monomers depicted by squares are compressed into a monolayer by the black barriers. Anchors represent hydrophilic groups which keep the monomers consistent in orientation with respect to each other. Polymerization indicated by red lines between monomers.²⁴

The King group was able to take advantage of its familiarity with antrip synthesis and synthesize the antrip-DEG monomer, which consists of an antrip body bound to a diethylene glycol amphiphile at the bridgehead position, Figure 1.16.¹⁵ My contribution to this project

was synthesis of the antrip monomer with a methoxy group at the bridgehead, referred to as methoxy antrip. DEG chain attachment was performed by former group member Dr. Bhola.

Amphiphilic Monomer Antrip-DEG

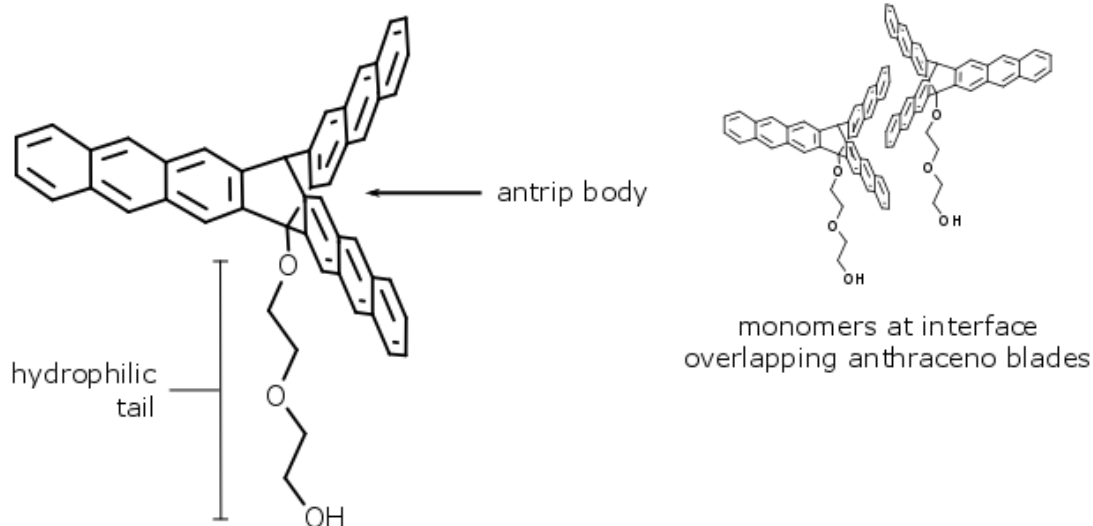


Figure 1.16. Antrip-DEG monomer. Antrip body bound to an amphiphilic diethylene glycol tail at the bridgehead position(left). Two monomers with the hydrophilic tails pointed downward causing them to have the same orientation with overlapping anthraceno blades (right).

Antrip-DEG was deposited to the air-water interface on the LB trough, by former group member Dr. Daniel Murray, and compressed to give monolayers with hexagonal packing. The monolayer was irradiated with 365 nm light to yield a large area 2DP. The polymer was conveniently transferred to a number of substrates for analysis by microscopy. Seen below is an STM image of a polymerized sheet that was transferred to highly oriented pyrolytic graphite (HOPG) alongside a simulated polymer for comparison, Figure 1.17.¹⁵

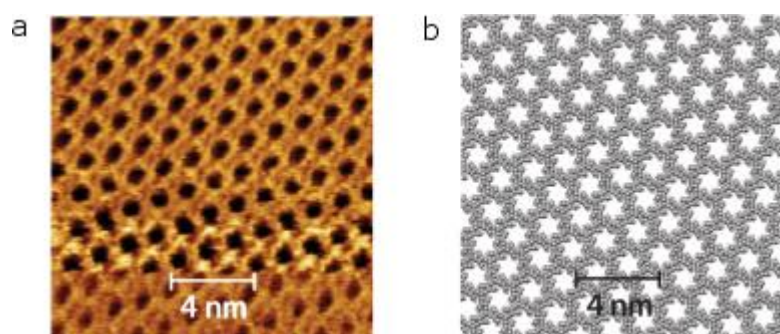


Figure 1.17. An STM image of polymerized antrip-DEG on HOPG (a), and simulated image of the polymer (b).

The synthesis of monomers used for 2D polymerizations is by no means trivial. To our knowledge there is no commercially available monomer for the sole purpose of synthesizing 2DPs. However, this does not imply that such a compound could not be found. Typically, monomers used for 2DP synthesis are inherently complex due to the necessity for the proper functional groups, geometry, and ability to float at the air water interface (in the case of the LB trough method). That being said, creative design of new monomers will likely result in complex molecules which are not easily accessible by synthetic means.

1.4. Applications of Two-Dimensional Polymers

1.4.1. Separation

The advancement of membrane technology will assist countless scientific fields, from biological separations to industrial applications, and thus membrane technology is relevant.²⁵ Currently, a vital part of membrane science focuses on the increasingly important area of desalination.²⁶ Periodic 2DPs have the potential to be engineered with specific pore sizes, giving access to a “perfect membrane”. While non-periodic 2DPs are an important category of 2DP chemistry, they are not suited for membrane applications which demand a specific and consistent porosity. Uniform pore size is possible because 2DPs can be synthesized from the ground up, and methods to acquire long-range periodic packing have been and continue to be developed.⁸ With the proper monomer design, a seemingly endless number of membranes can be envisioned.

Lack of access to clean drinking water affects over 2.5 billion people worldwide.²⁷ With population growing at a rate of 80 million a year, the water strained areas will only become more desperate.²⁶ One potential solution to this worldwide issue is the desalination

of sea water. Engineering an efficient membrane that requires low energy and is capable of easily converting salt water to consumable water would change the lives of billions of people.

Currently, state of the art membrane technology for water purification employs reverse osmosis membranes (RO) membranes.²⁸ These membranes consist of thin film crosslinked polymers, such as polyamides or cellulose acetate reinforced by a porous support layer. While these materials represent cutting edge membranes, there remains room for improvement. Flux through a membrane is the rate at which a filtrate permeates through a membrane. The units of flux are expressed as volume per area per unit of time.²⁷ From a qualitative viewpoint, this means that the thinner the membrane and the higher the pore density (number of pores per unit area), the higher the flux and therefore the more efficient membrane, Figure 1.18.

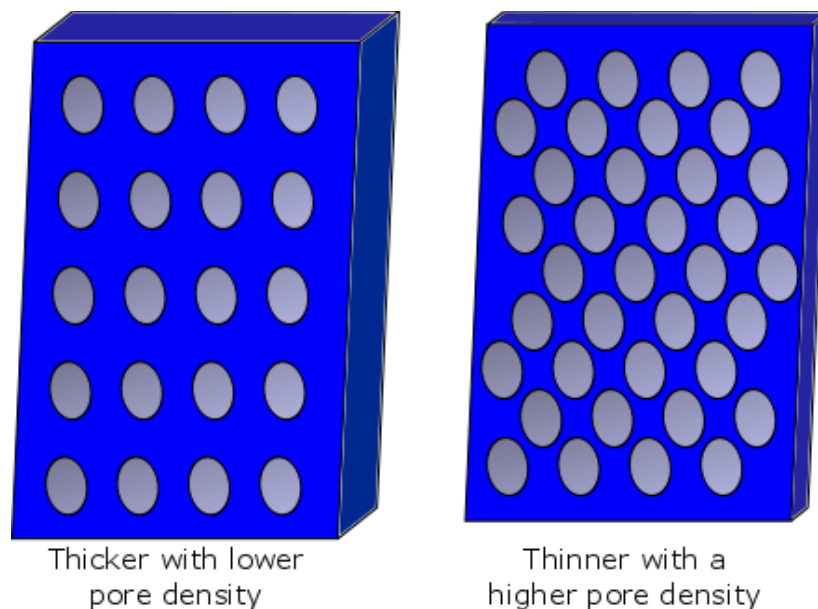


Figure 1.18. Illustration showing the difference between a thicker and less porous membrane versus a more efficient thinner, more porous membrane.

It is impossible to obtain defined pores with a crosslinking polymerization, therefore one must have a sufficiently thick crosslinked polymer to allow for enough overlap and entanglement to create a semipermeable membrane capable of blocking out ions.²⁸ This

means that the filtrate molecules (water) must adsorb to the membrane and then navigate their way through its random channels; and diffusion kinetics limit flux.

While thin film composites are extensively used throughout the world and research continues to improve their technology, 2DP membranes utilize a more elegant approach to membrane technology. The use of a 2DP for a membrane has the advantage of being engineered from the ground up. 2DPs are inherently ultra-thin (one monomer unit thick) and can be designed to have a specific pore size and pore density. This means that a 2DP can be engineered to provide a flux orders of magnitude higher than leading RO membranes available. This presents the advantage of requiring less energy for flux across the membrane, and having pores of a specified size for near quantitative purification.

Once 2DP membrane technology is perfected, devices that require limited energy and yield high purity drinking water will be available to the masses. The potential of 2DP materials to positively impact so many lives will most definitely help drive forward 2DP technology.

1.4.2. Scaffolds

Being able to design a monomer that after polymerization yields a periodic 2DP where each repeat unit possesses a functional handle would be extremely useful in many areas of science. A periodic, functionalized surface would make available attachment of a catalyst, giving rise to new and unique catalytic surfaces, and attachment of biosensors.²⁹ A 2DP scaffold could be specifically designed to be used for any application that requires or benefits from molecular organization.⁷

A periodic 2D scaffold could be used in advancing 2DP chemistry by serving as a template for the synthesis of other 2DPs. One of the most important and challenging aspects of 2DP synthesis is organization of the monomers before polymerization. Synthesis of a 2DP scaffold that possesses a periodic array of synthetic handles, available for further chemistry, could serve as a tool to expand upon 2DP synthesis. A periodic arrangement of functional

groups could covalently hold in place other monomers possessing a compatible functionality. The monomers would be held in array by reversible bonds and then polymerized, followed by reversal of the initial bonds releasing the newly formed 2DP. Seen below is a cartoon illustrating the process of monomers being templated and polymerized into a 2DP, Figure 1.19.

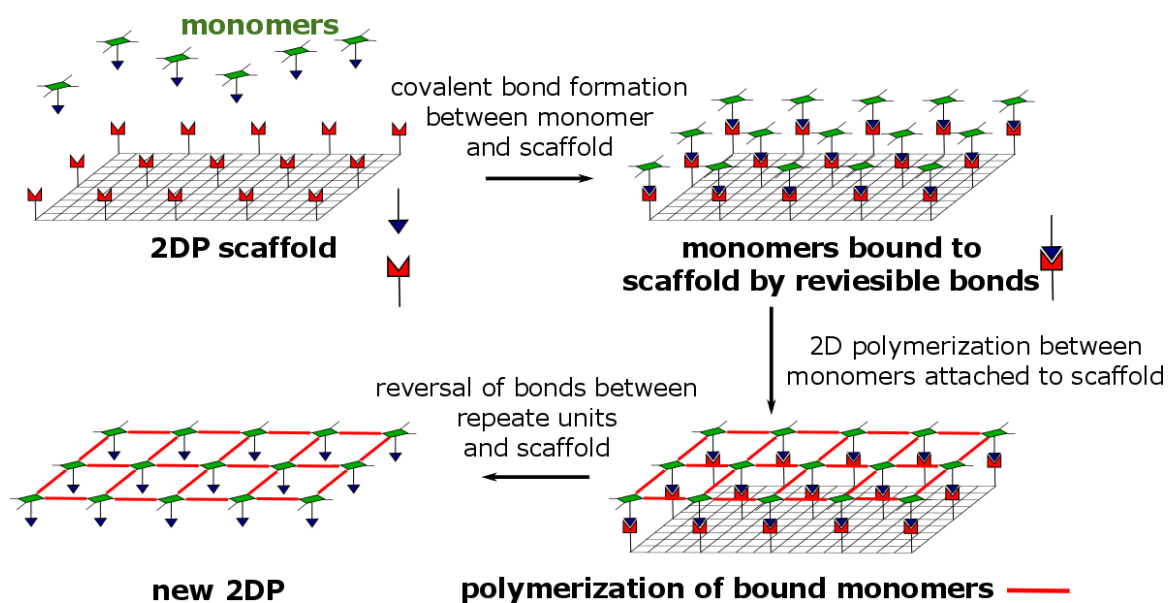


Figure 1.19. Clockwise from top left; introduction of monomers to the 2DP scaffold, followed by an ordered covalent bonding, polymerization of the bound monomers, and finally liberation of a 2DP sheet by reversal of the initial bonds between the 2DP and scaffold. The red shape and blue triangle represent functional groups which undergo reversible bonding.

With monomers held in place by a scaffold, one could potentially employ transformations that are either unlikely or impossible using the crystallization or LB trough methods. For example, C-C coupling reactions typically require a metal catalyst, or a coinage surface in the case of the UHV approach.³⁰ Due to the robust strength of aryl-aryl C-C bonds, for example, and the high atom economy of C-C coupling reactions make them ideal transformations for 2D polymerizations. However, the requirement of a metal catalyst makes their execution very unlikely when attempting to polymerize using the solution, crystallization, or LB trough approaches to 2D polymerizations.

Incorporating a catalyst into the crystal or LB trough approaches seems improbable. However, if monomers are organized by being bound to a periodic scaffold, one might be able to use conventional solution phase chemistry conditions to carry out a 2D polymerization. This would allow one to expand on the transformations possible for 2D polymerizations, such as C-C coupling reactions, rather than relying on the currently small library of possible transformations such as cycloadditions. After the 2D polymerization has taken place, reversible bonds to the newly made polymer could be selectively cleaved from the scaffold. No such experiment has been explored thus far, however, has the potential to expand greatly upon the field of 2DPs.

Perhaps, in the future, pre-organizational approaches, such as the LB trough, will be solely applied to the synthesis of scaffolds. Learning and developing monomer pre-organization and polymerization at the air-water interface towards scaffold synthesis could be what early 2DP research gives to the world. A specifically designed 2DP template could be used for further 2DP chemistry and potentially lead to countless numbers of interesting 2D polymers using transformations that would otherwise be impossible by other means of polymerization.

1.5. Aim of the Dissertation

All chapters of this dissertation focus on the creative design and synthetic development of monomers to be used in the synthesis of 2DPs. Unlike the field of 1DPs, the field of 2DPs is still in its infancy. This means that one cannot order monomers from a chemical supplier for synthesis of a 2DP, whereas this is common practice for 1DP synthesis. That being said, guidelines for monomer design are much more stringent and require a great deal of forethought when considering packing, preorganization, and functionality. Working within these limitations can require a significant amount of synthetic effort. Much of this

dissertation will emphasize the synthetic evolution towards monomer construction and will touch on efforts towards polymerization.

1.6. Overview of Chapters

Summary of Chapter 2: Synthetic routes towards Four Structurally Related Monomers.

Chapter two of this dissertation focuses on my efforts towards developing the synthesis of antrip(**1-H**), fantrip(**1-F**), methoxy antrip (**1-MeO**), and hydroxyl fantrip (**1-FOH**). Antrip (**1-H**) and fantrip (**1-F**) had been previously synthesized in small quantities and their synthetic improvement was applied to two novel monomers **1-MeO** and **1-FOH**. The main goal of this chapter was synthetic development of the below monomers to afford preparative scale yields of each, Figure 1.20. Research towards the polymerization of the below monomers using the crystal and LB trough approaches involves continuous consumption of monomer. Having access to large quantities of monomer aids in developing polymerization techniques and prevents having to constantly replenish monomer supply due to a low yielding synthetic route.

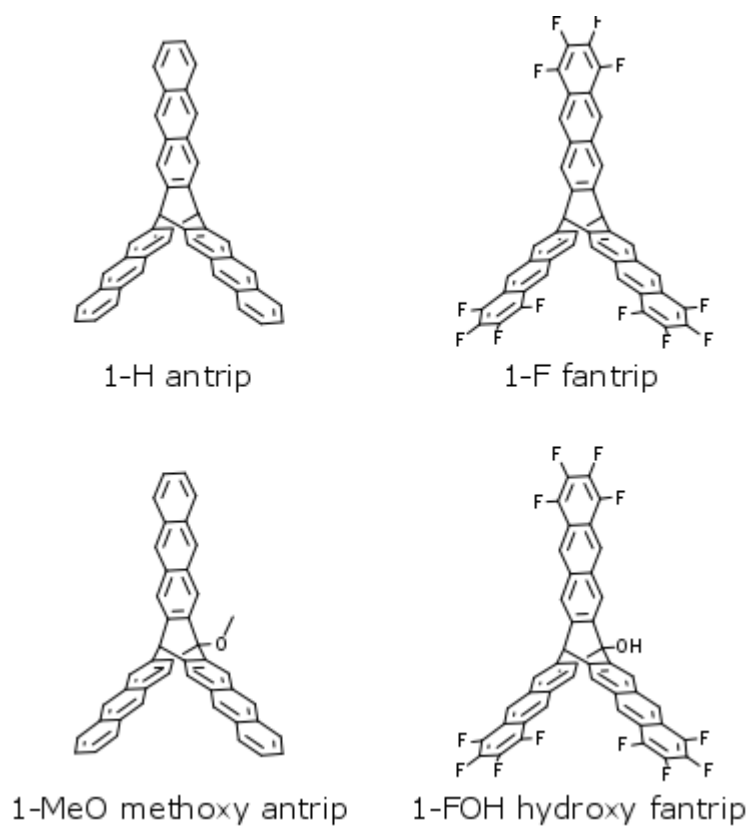
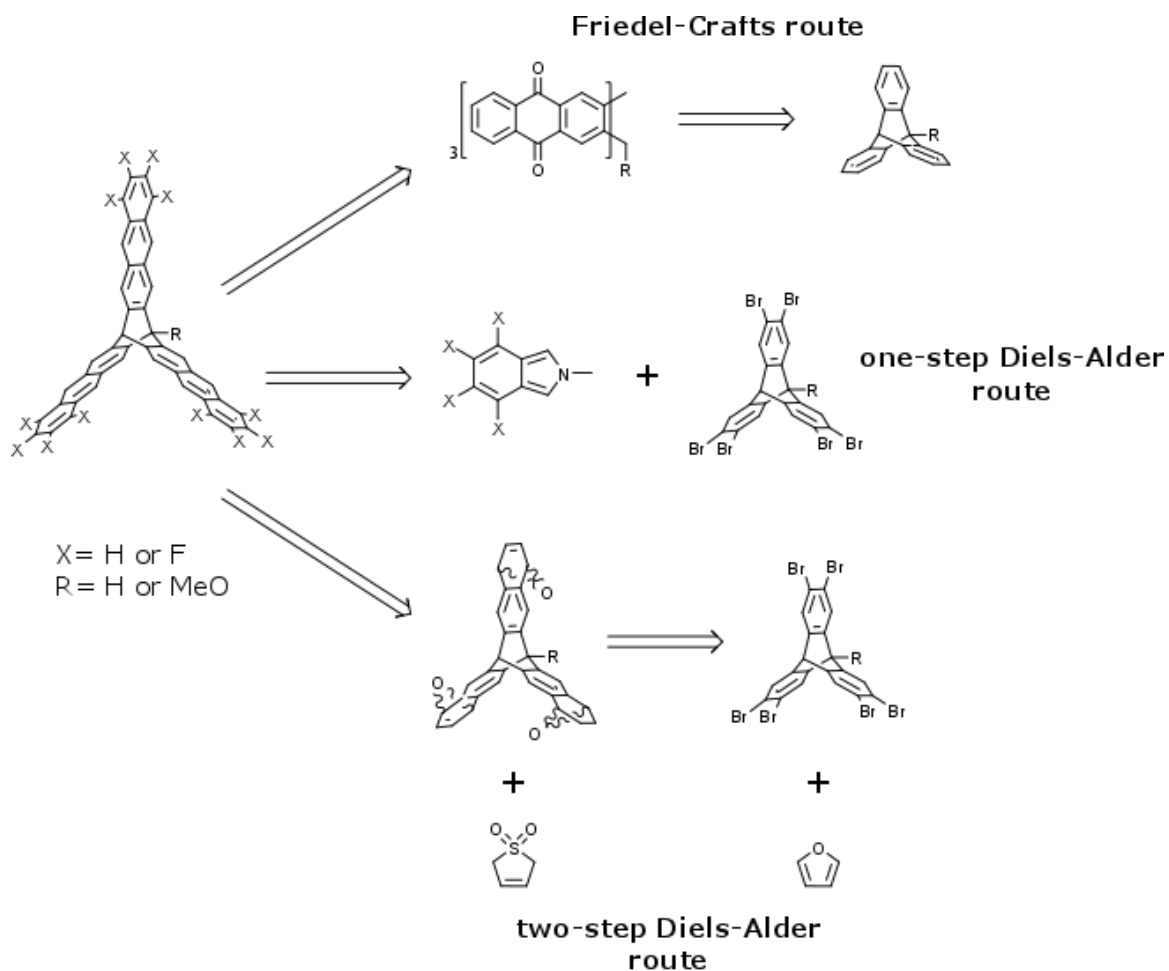


Figure 1.20. Four structurally related monomers.

Synthesis of the above monomers consisted of acene homologation from a triptycene core. Below is a retrosynthetic breakdown of the three different approaches taken towards the preparative scale synthesis of the monomers, Scheme 1.1.



Scheme 1.1. Retrosynthetic breakdown of the three synthetic routes taken towards the four monomers.

Summary of Chapter 3: Synthetic Efforts Towards Pentiptycene based monomer.

Chapter three focuses on my efforts towards synthesis of a pentiptycene based monomer for use in crystallization and LB trough polymerizations, Figure 1.21.

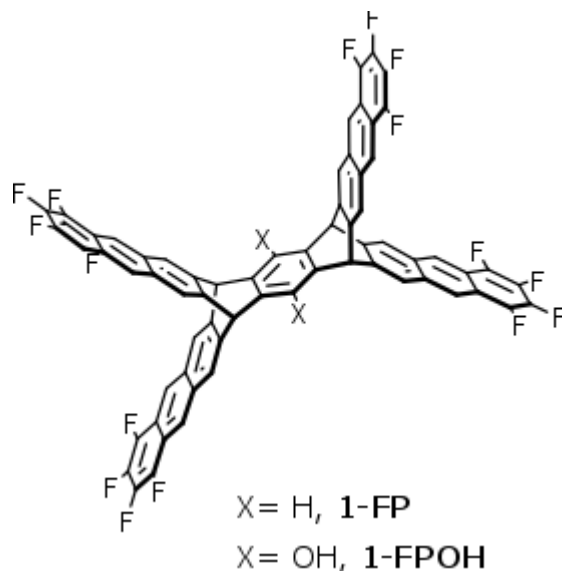


Figure 1.21. Pentiptycene based monomer.

Two separate routes were taken towards the synthesis of the above pentiptycene based framework. One that started with pentiptycene and one that started with the more easily accessible pentiptycene quinone. The one-step Diels-Alder approach, from Scheme 1.1, was the intended route with the pentiptycene moiety serving as a core, Figure 1.22.

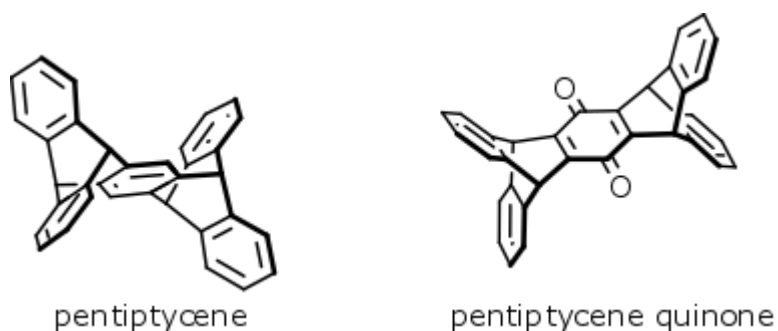


Figure 1.22. Two cores used in the synthesis of the above fluorinated monomer framework.

Summary of Chapter 4: Synthetic Development of a 1,3,5-tripyrzole Benzene Monomer (1-pyz) and Efforts Towards its 2D Polymerization

Chapter four focuses on the synthetic development of a 1,3,5-tripyrzole benzene monomer and its polymerization with various metals, Figure 1.23.

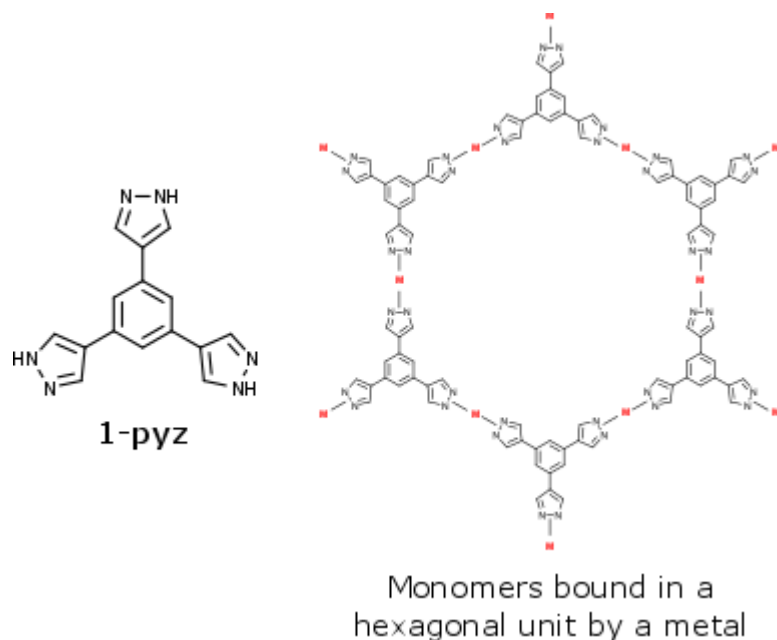


Figure 1.23. Tri-pyrazole monomer **1-pyz**, and a simulation of a polymerized hexagonal unit coordinated by a metal labeled M.

Solution phase and crystallization approaches were taken using various metal salts and conditions for polymerization.

Summary of Chapter 5: Efforts Towards the 2D Polymerization of a Porphyrin Based Monomer.

Chapter five focuses on the synthesis of a porphyrin monomer which has anthracene functional groups and is meant for crystallization and LB trough polymerizations, Figure 1.24.

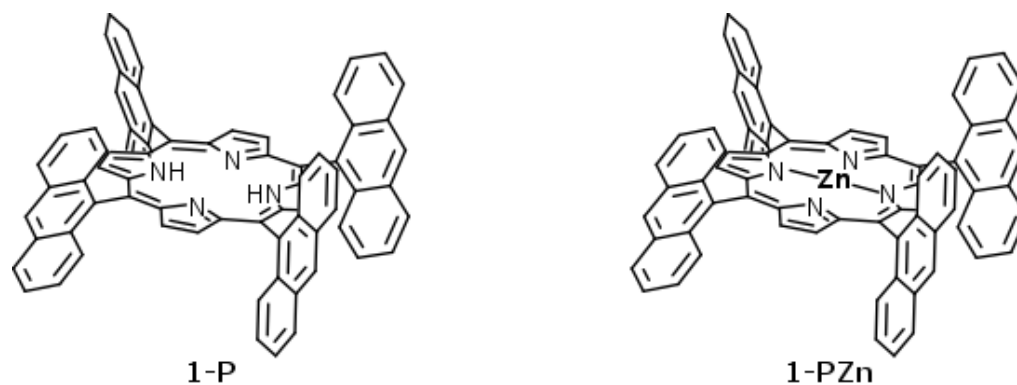


Figure 1.24. Porphyrin monomer meant for crystallization approach (**1-P**) and porphyrin monomer intended for polymerization at the air-water interface (**1-PZn**).

Monomer **1-PZn** is ligating zinc which is meant to serve as a synthetic handle for a hydrophilic tail for polymerization at the air water interface.

Summary of Chapter 6: Antrip and Fantrip Co-crystallizations with Fullerenes Towards Single Crystal Polymerizations.

Chapter 6 focuses on efforts towards growth of an antrip (**1-H**) single-crystal suitable for a single-crystal to single-crystal polymerization, and growth of C₆₀ and C₇₀ fantrip (**1-F**) or antrip (**1-H**) co-crystals that are suitable for polymerization.

References.

- (1) Cowie, J. M. G.; Arrighi, V. *Polymers: chemistry and physics of modern materials*, 3rd ed.; CRC Press: Boca Raton, 2008.
- (2) Fried, J. R. *Polymer science and technology*, Third edition.; Prentice Hall: Upper Saddle River, NJ, 2014.
- (3) Pibarot, P.; Dumesnil, J. G. *Circulation* **2009**, *119* (7), 1034.
- (4) Sutthasupa, S.; Shiotsuki, M.; Sanda, F. *Polym. J.* **2010**, *42* (12), 905.
- (5) Roy, R. K.; Meszynska, A.; Laure, C.; Charles, L.; Verchin, C.; Lutz, J.-F. *Nat. Commun.* **2015**, *6*, 7237.
- (6) Defino, Juliet L. **2012**.
- (7) Colson, J. W.; Dichtel, W. R. *Nat. Chem.* **2013**, *5* (6), 453.
- (8) Sakamoto, J.; van Heijst, J.; Lukin, O.; Schlüter, A. D. *Angew. Chem. Int. Ed.* **2009**, *48* (6), 1030.
- (9) Bhola, R.; Payamyar, P.; Murray, D. J.; Kumar, B.; Teator, A. J.; Schmidt, M. U.; Hammer, S. M.; Saha, A.; Sakamoto, J.; Schlüter, A. D.; King, B. T. *J. Am. Chem. Soc.* **2013**, *135* (38), 14134.
- (10) Asakuma, S.; Kunitake, T. *Chem. Lett.* **1989**, No. 11, 2059.
- (11) Kumar, N. A.; Dar, M. A.; Gul, R.; Baek, J.-B. *Mater. Today* **2015**, *18* (5), 286.
- (12) Akiyama, S.; Thuswaldner, J. M. *Geom. Dedicata* **2004**, *109* (1), 89.
- (13) Evans, A. M. *Ore geology and industrial minerals: an introduction*, 3. ed., reprinted.; Geoscience texts; Blackwell Science: Oxford, 2001.
- (14) Fan, Q.; Gottfried, J. M.; Zhu, J. *Acc. Chem. Res.* **2015**, *48* (8), 2484.
- (15) Murray, D. J.; Patterson, D. D.; Payamyar, P.; Bhola, R.; Song, W.; Lackinger, M.; Schlüter, A. D.; King, B. T. *J. Am. Chem. Soc.* **2015**, *137* (10), 3450.
- (16) Bieri, M.; Treier, M.; Cai, J.; Ait-Mansour, K.; Ruffieux, P.; Gröning, O.; Gröning, P.; Kastler, M.; Rieger, R.; Feng, X.; Müllen, K.; Fasel, R. *Chem. Commun.* **2009**, No. 45, 6919.
- (17) Fan, Q.; Wang, C.; Liu, L.; Han, Y.; Zhao, J.; Zhu, J.; Kuttner, J.; Hilt, G.; Gottfried, J. M. *J. Phys. Chem. C* **2014**, *118* (24), 13018.
- (18) Cote, A. P. *Science* **2005**, *310* (5751), 1166.
- (19) Kissel, P.; Erni, R.; Schweizer, W. B.; Rossell, M. D.; King, B. T.; Bauer, T.; Götzinger, S.; Schlüter, A. D.; Sakamoto, J. *Nat. Chem.* **2012**, *4* (4), 287.
- (20) Biradha, K.; Santra, R. *Chem Soc Rev* **2013**, *42* (3), 950.
- (21) Lauher, J. W.; Fowler, F. W.; Goroff, N. S. *Acc. Chem. Res.* **2008**, *41* (9), 1215.
- (22) Breton, G. W.; Vang, X. *J. Chem. Educ.* **1998**, *75* (1), 81.

- (23) Kissel, P.; Murray, D. J.; Wulftange, W. J.; Catalano, V. J.; King, B. T. *Nat. Chem.* **2014**, *6* (9), 774.
- (24) Langmuir, I. *J. Am. Chem. Soc.* **1917**, *39* (9), 1848.
- (25) Subramanian, S.; Seeram, R. *Desalination* **2013**, *308*, 198.
- (26) Service, R. F. *Science* **2006**, *313* (5790), 1088.
- (27) Shannon, M. A.; Bohn, P. W.; Elimelech, M.; Georgiadis, J. G.; Mariñas, B. J.; Mayes, A. M. *Nature* **2008**, *452* (7185), 301.
- (28) Zou, H.; Jin, Y.; Yang, J.; Dai, H.; Yu, X.; Xu, J. *Sep. Purif. Technol.* **2010**, *72* (3), 256.
- (29) Peplow, M. *Nature* **2015**, *520* (7546), 148.
- (30) *New trends in cross-coupling: theory and applications*; Colacot, T. J., Ed.; RSC catalysis series; The Royal Society of Chemistry: Cambridge, 2015.

2. Synthetic Routes Towards Four Structurally Related Monomers

2.1. Overview

When fabricating a monomer used for 2D polymer synthesis, shape persistence and characteristics that promote organization are ideal qualities. Incorporating moieties that can accomplish organization as well as reactivity into a monomer is the main challenge when designing a monomer. Below is a description of our efforts towards the design and synthesis of four structurally related monomers which use polycyclic aromatic hydrocarbons (PAHs) as an organizational tool and as the reactive moieties.

One can take advantage of PAHs reactive abilities through cycloaddition reactions as well as their willingness to organize through π - π interactions. PAHs tend to be rigid, flat, and commonly organize by stacking with one another to increase van der Waals contact (π - π interactions). Not only can PAH moieties be used as an organizational tool, but, acenes, a family of PAHs, have the potential to react via a photo initiated [4+4] cycloaddition after being stacked with one another. Relying on PAH chemistry, more specifically acene chemistry, for monomer design and synthesis is not a requirement, however, the properties listed above make them quite common in the field of 2DPs.³¹

Acenes are a family of PAHs that are defined as linearly fused benzene rings.³² The use of acene moieties in 2D monomers are by far the most common compared to other PAHs.^{15,19,33} Acenes and their derivatives are used for a variety of electronic applications, such as organic light emitting diodes and molecular wires. Their popularity in electronics has inspired a substantial library of acene synthesis chemistry which we have employed during the synthesis of our monomers.^{34,35} Seen below are some common acenes and their general formula, Figure 2.1.

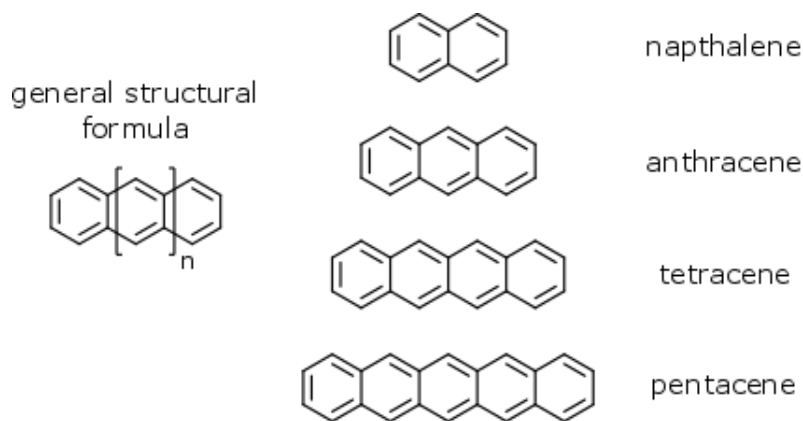


Figure 2.1. Examples of different acenes and their general structural formula.

Using acene moieties within the framework of the monomer and as the reactive groups takes advantage of their favorable packing behavior as well as their reactivity. [4+4] Cycloadditions between acenes have the advantage of being photo initiated. This is less invasive than using heat to induce a polymerization in a crystal to crystal or air-water interface polymerization. The heat involved in a thermal reaction has the potential to disrupt a crystal lattice or monolayer at the air-water interface, preventing a 2D polymerization.

Presented herein is the synthetic development of four different structurally related monomers, Figure 2.2, all of which possess triptycene cores with three fused anthraceno blades. The purely carbon hydrogen framework (antrip, **1-H**) will be referred to as the parent framework throughout this chapter. Our parent monomer, antrip (**1-H**), is a simple, non-functionalized compound on which three other monomers are based. MeO-antrip (**1-MeO**) is the parent framework that is functionalized at the bridgehead with a methoxy group. Fantrip (**1-F**) is the parent framework that is decorated with fluorines at the tips of each anthraceno blade, and OH-fantrip (**1-FOH**) is a fluorinated parent framework with a hydroxyl functionality at the bridgehead.

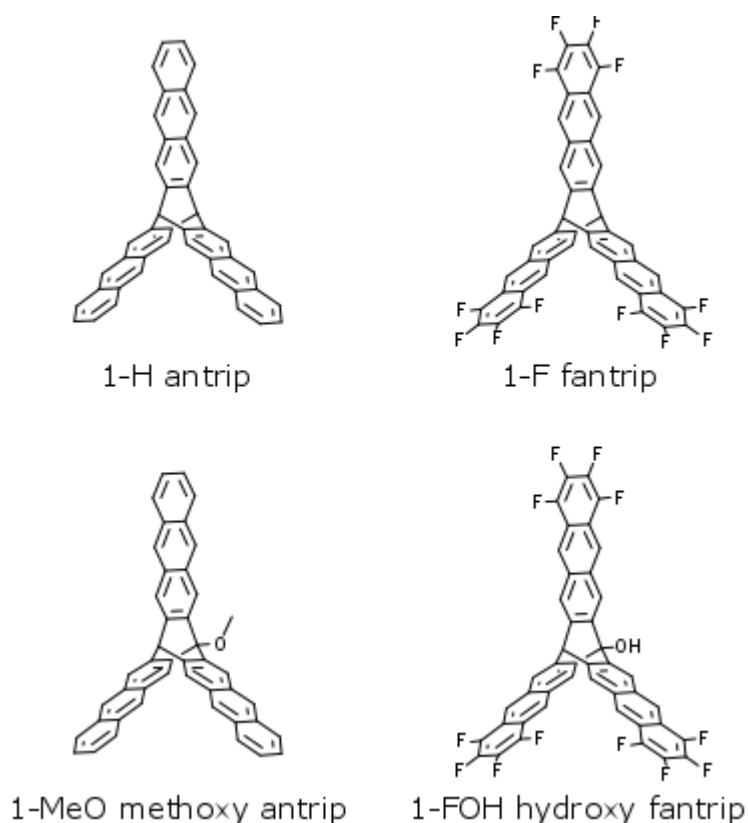


Figure 2.2. Monomers built for crystal to crystal polymerizations (left) and monomers built for polymerization at the air water interface (right).

Antrip (**1-H**) was previously synthesized by the Swager group, however, their synthesis resulted in low yields.³⁶ A previous postdoc from the King group, Pat Kissel, previously synthesized fantrip (**1-F**), which also resulted in low yields. This chapter describes my contributions to the synthetic improvement of the antrip (**1-H**) and fantrip (**1-F**) synthesis and how that synthetic knowledge was applied to the development and synthesis of MeO-antrip (**1-MeO**) and OH-fantrip (**1-FOH**). The objective for all four monomers is the three-fold unidirectional acene elongation from a triptycene core to yield the carbon skeleton of the monomers, Figure 2.3.

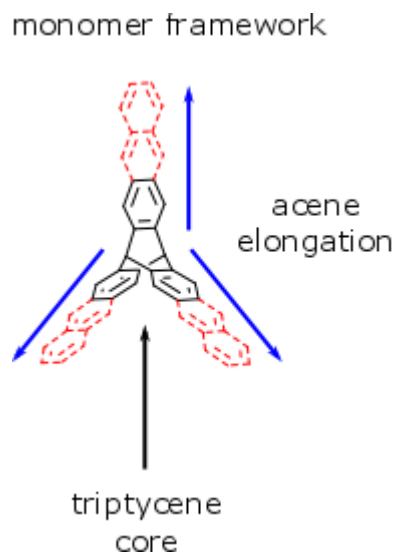


Figure 2.3. Illustration of monomer framework showing the triptycene core. Red dashed bonds denote the acene section synthesized and blue arrows show direction of acene elongation.

Herein I elaborate on three different approaches of acene elongation taken towards monomer synthesis: Friedel-Crafts acylation, a one-step Diels-Alder approach and a two-step Diels-Alder approach. Seen in Figure 2.4 is a retrosynthetic breakdown of the three strategies taken during synthesis and development of all derivatives of the monomer.

Some of the schemes for monomer synthesis are closely related to previous work, however, it is important to show the pitfalls and advances made during monomer design in order to give a global picture of synthetic development.^{9,15,36} I took a small part in using the Friedel-Crafts approach towards novel monomer methoxy antrip (**1-MeO**), however, most of my synthetic efforts focused on development of the Diels-Alder approaches towards the synthesis of all monomers listed above in Figure 2.2.

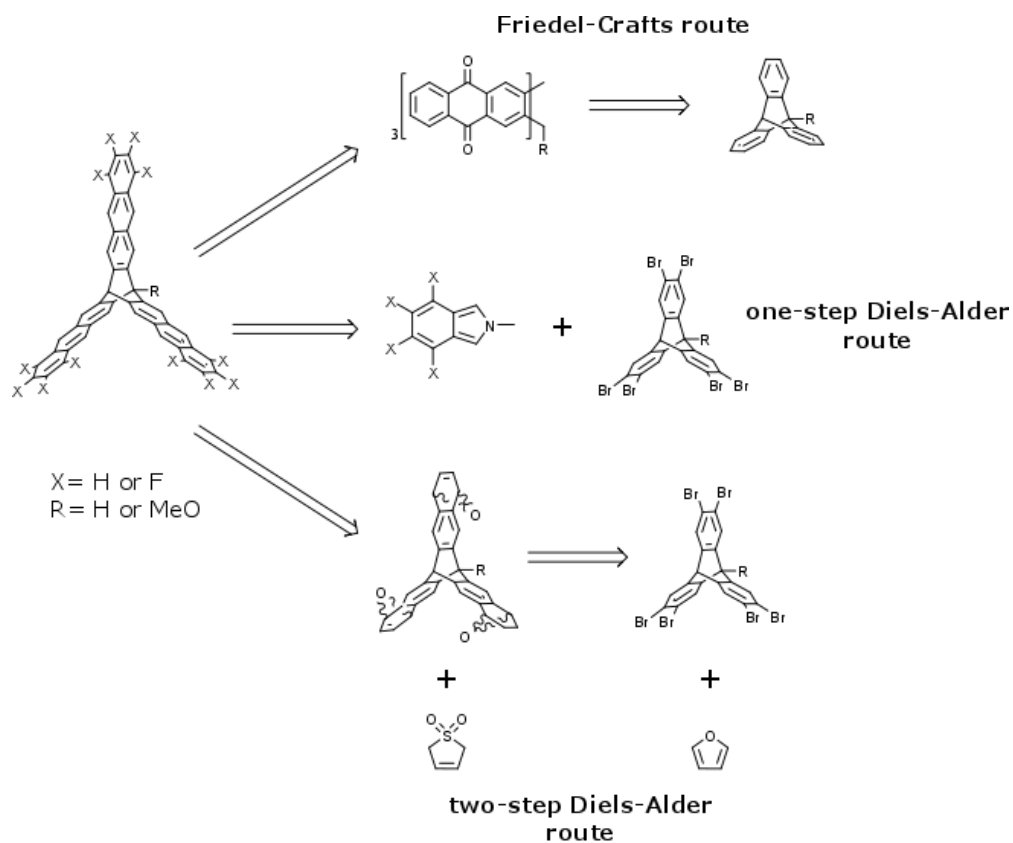
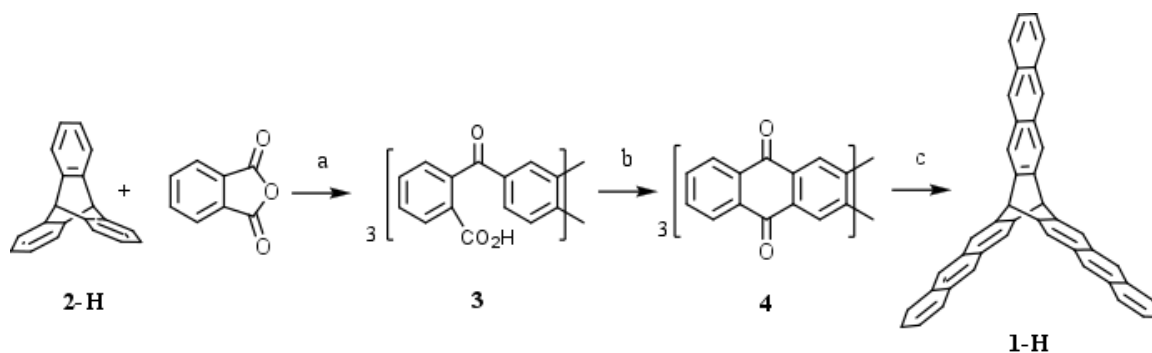


Figure 2.4. A retrosynthetic breakdown of the three strategies taken towards monomer synthesis.

2.2. Previous Work

Antrip (**1-H**) was synthesized by the Swager group in 2001 using a Friedel-Crafts approach to build the acene blades of the monomer.³⁶ Their synthesis starts with a Friedel-Crafts acylation of triptycene (**2-H**) with phthalic anhydride, giving tris-ketoacid (**3**). Tris-ketoacid (**3**) is then cyclized using harsh, high temperature sulfuric acid at 100 °C to give quinone intermediate (**4**), which is then reduced using a mercury-aluminum amalgam (Al-HgCl₂) to give final product antrip (**1-H**) with an overall yield of 1.8%, Scheme 2.1.³⁷



Scheme 2.1. Swager's protocol. Conditions: a) phthalic anhydride, AlCl_3 , tetrachloroethylene, $120\text{ }^\circ\text{C}$; b) sulfuric acid, $100\text{ }^\circ\text{C}$; c) Al-HgCl_2 , cyclohexanol, reflux.³⁷

Swager's approach is capable of making final product antrip (**1-H**), however, requires harsh conditions, toxic reagents, and results in poor yields. However, we were unable to reproduce the synthesis in our laboratories.³⁶

Dr. Bhola, a former King group member, devised a modified version of Swager's approach. Her closely related route also gave poor yields and suffered from troublesome purification.

It was considered that formation of unwanted regioisomers during the Friedel-Crafts steps were responsible for the low yields and difficult purification of Dr. Bhola's initial modified synthesis. This hypothesis was supported by ^1H NMR and later confirmed by X-ray diffraction (which will be later discussed in this chapter). The regioisomeric problem of the route began with the initial Friedel-Crafts product of the route, intermediate (**3**). The intermediate shown below, Figure 2.5, illustrates the free bond rotation about the blue bond which gives the carboxylic acid moiety two different sites at which it can react during the next high temperature cyclization step with sulfuric acid. The two different sites of reactivity on the arene moiety are represented by red asterisks. While this cyclization completes the carbon framework of the monomer, the free bond rotation can lead to product **4** (all blades in plane) or a number of regioisomers represented by **4'** (one or more blades out of plane),

Figure 2.5. With bond rotation being possible on all three blades of intermediate **3**, a total of six different regioisomers are possible and are denoted by **4'**. As identified by NMR, four regioisomers are present in the crude mixture, distinguishing the cyclization as a very inefficient step. Intensive purification was necessary to isolate the desired regioisomer **4** which led to low yields. Poor solubility and similar R_f values between regioisomers made this difficult. Therefore, unwanted regioisomers were typically carried over and reduced as a mixture of **4** and **4'** giving regioisomerically impure final product **1-H**. This was allowed because a regioisomerically impure mixture of **1-H** was easier to purify than the poorly soluble, precursor quinone intermediate **4**. Nonetheless, this further complicated the next purification step of the crude **1-H** product. These obstacles in the synthetic route motivated further alteration of the Friedel-Crafts route. Modifications were made that could avoid regioisomeric issues and give final product on the preparative scale.

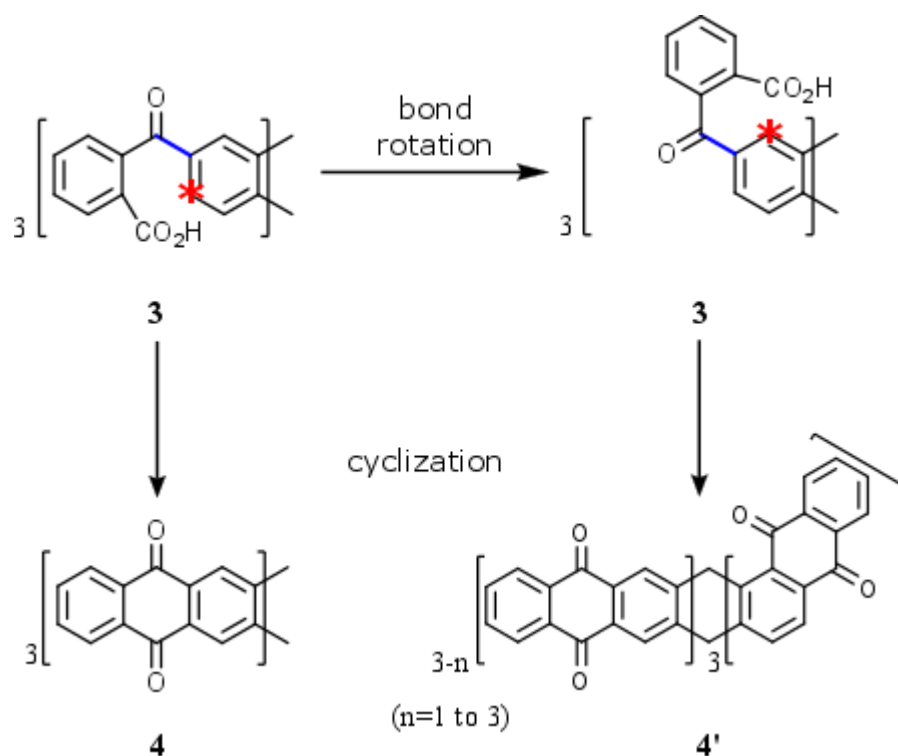
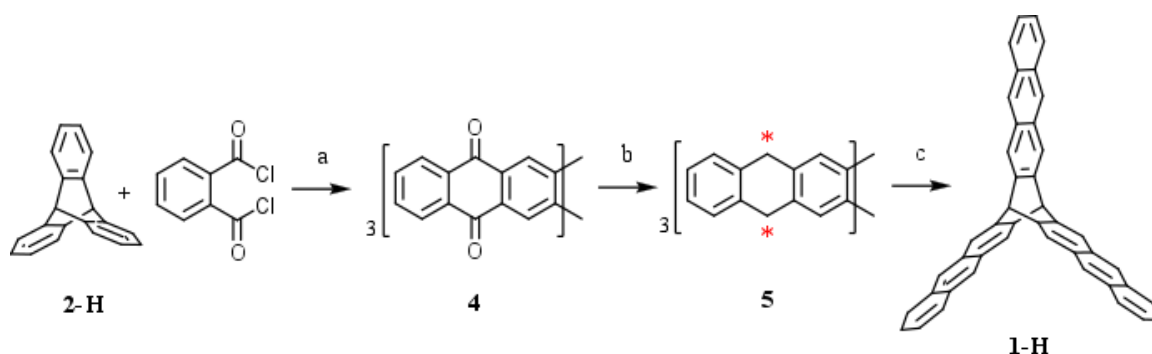


Figure 2.5. Illustration of the free bond rotation about blue bond in intermediate **3** and the desired cyclization product, **4**, and undesired regioisomers, **4'**.

In an attempt to avoid regioisomers, the Friedel-Crafts route was modified, by Dr. Bhola, again in a way that avoided tris-ketoacid, **3**, as an intermediate. This was accomplished by reacting triptycene, **2-H**, with phthalic chloride instead of phthalic anhydride. Phthalic chloride is more reactive towards triptycene and directly leads to quinone intermediate **4** in a one pot process, this avoided the harsh sulfuric acid cyclization step, seen above in Figure 2.5, which lead to regioisomers. While this modification avoided tris-ketoacid intermediate **3** and was a shorter route, it still suffered from regioisomeric problems, which will be discussed in a later section.

This one pot process using phthalic chloride was intended to eliminate the regioisomeric problems associated with the bond rotation of intermediate **3** and avoid the low yielding, harsh cyclization to quinone **4** with sulfuric acid at 100 °C. Once quinone intermediate **4** was obtained, a milder two-step reduction approach was taken where **4** is partially reduced followed by oxidation to antrip, **1-H**, Scheme 2.2. Use of HI/AcOH to reduce intermediate **4** to **5** was intended to partially reduce the carbonyls to the fully aromatic final product **1-H**. However,

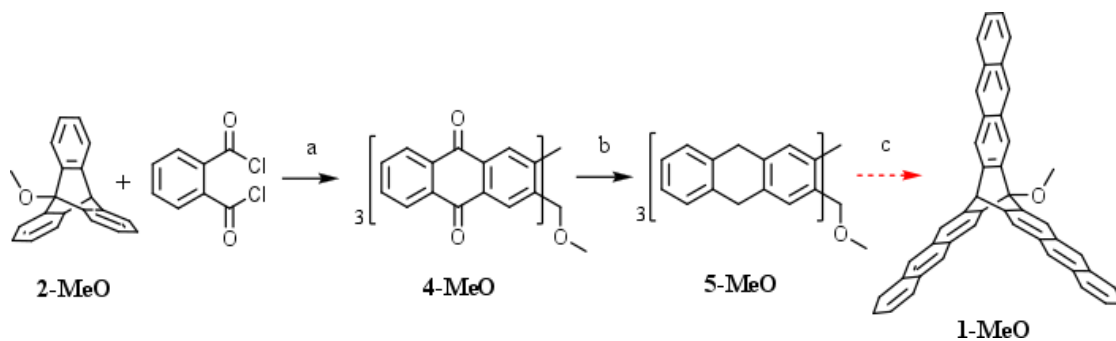


Scheme 2.2. a). Nitrobenzene, AlCl_3 , 90 °C b). HI/AcOH, reflux c). Pd/C, xylenes, reflux. Red asterisks in intermediate **5** denote a hybridization of either sp^3 or sp^2 .

during the HI/AcOH reduction an uncertain number of blades are over reduced to sp^3 hybridized carbons instead of the desired sp^2 hybridization. The red asterisks in Scheme 2.2 are used to denote the uncertainty of the adjacent carbons hybridization. And after the partial reduction with HI/AcOH, intermediate **5** is oxidized to final product **1-H** using Pd/C.

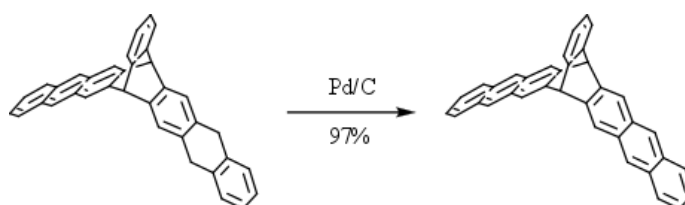
2.3. Results and Discussion

My synthetic efforts towards monomer synthesis started with the synthesis of novel monomer methoxy antrip (**1-MeO**) using a Friedel-Crafts route. Synthesis began by applying Dr. Bhola's modified Friedel-Crafts route, using phthalic chloride, and applying those steps towards the synthesis of a novel monomer, methoxy antrip (**1-MeO**). Her improved Friedel-Crafts procedure gave better results than Swagers previous parent antrip (**1-H**) route, but the overall yield for the methoxy derivative (**1-MeO**) was still less than 5%. While monomer **1-MeO** was obtained, a preparative scale synthesis was still desired. In both the parent and methoxy derivatives, the lowest yielding step was the Pd/C oxidation of the hydrogenated intermediates **5** and **5-MeO** to final products **1-H** and **1-MeO**. While adapting Dr. Bhola's modified Friedel-Crafts route towards MeO-antrip (**1-MeO**), new methods of oxidation, outside of Pd/C, were attempted to increase the yield of the low yielding oxidation step. Fortunately, leading up to the final oxidation step, all the transformations of Dr. Bhola's modified Friedel-Crafts route translated identically to the methoxylated intermediates, leaving improvement of the final oxidation yield as my sole interest, Scheme 2.3.



Scheme 2.3. a). Nitrobenzene, AlCl_3 , $90\text{ }^\circ\text{C}$, 11% b). (microwave) HI/AcOH , $150\text{ }^\circ\text{C}$, 200W, 65% c). oxidation development.

Palladium on carbon (Pd/C, 10% wt. % loading) was the initial choice for the retro-hydrogenation of **5-MeO** to final product **1-MeO** and gave yields between 7% and 12%. Pd/C is a very common reagent for the oxidation of a hydrogenated acene to its aromatic counterpart; Pd/C consists of palladium supported on activated carbon. The high surface area of the activated carbon serves to increase the activity of the catalyst. Below is an example of an oxidative dehydrogenation employing Pd/C under thermal conditions, Scheme 2.4. The oxidation of **5-MeO** using Pd/C was initially performed on the benchtop by refluxing in xylenes for 3 days and gave inconsistent yields, Scheme 2.3. The same reaction conditions were expedited by reacting under high pressure microwave conditions which took reaction times from 3 days to 4 hours. While the reaction times were shorter the yields did

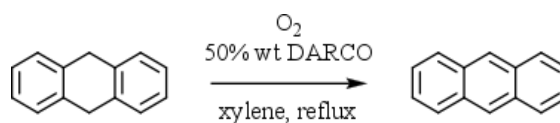


Scheme 2.4. Oxidation of a hydrogenated iptycene; conditions: mesitylene, Pd/C, reflux, 60hr, 97%.³⁸

not change. It was suspected that during aromatization of **5-MeO** the monomers were polymerizing on the surface of the Pd/C. Evidence of this was shown by Dr. Bhola on an adjacent project; heating her used Pd/C in d_6 -DMSO at $200\text{ }^\circ\text{C}$ followed by an NMR showed the presence of her antrip (**1-H**) monomer. To avoid the low yield and high cost of Pd/C, other oxidation conditions were explored.

2.3.1. Aromatization with DARCO®

Hayashi and co-workers discovered that high surface area activated carbon (DARCO KB-G) could oxidize 9,10-dihydroanthracenes and derivatives to their respective anthracenes using atmospheric oxygen as an oxidant, Scheme 2.5.³⁹ In their work with anthracene and its derivatives, the Hayashi group were able to obtain yields comparable to that of Pd/C oxidations using DARCO as a catalyst, which is significantly cheaper. Oxidations of **5-MeO** using DARCO were first explored thermally on the bench top and compared to Pd/C gave slightly improved yields of **1-MeO**, 35%. While the DARCO reactions improved the yields, the reactions took twice as long as oxidation using Pd/C and still required careful chromatography, Scheme 2.6.



Scheme 2.5. Oxidation of 9,10-dihydroxyanthracene using DARCO and atmospheric O₂, 93% yield.



Scheme 2.6. Oxidation of hydrogenated intermediate **5-MeO** giving **1-MeO**, with yields reaching 35%.

Chromatography of the oxidation product proved to be difficult and inconsistent. Unfortunately, **1-MeO** had poor solubility in the solvent systems that provided the best resolution, therefore, dry packing of the column was necessary. In an attempt to get a cleaner

oxidation with fewer side products, the use of a microwave reactor with DARCO as a catalyst was sought out.

Some studies have shown that reactions using a microwave reactor result in much shorter reaction times as well cleaner reactions (fewer unwanted side products).⁴⁰ Use of the microwave reactor for the DARCO oxidation of **5-MeO** to **1-MeO** gave significantly shorter reaction times, going from 4 days to 6 hours. Compared to the thermal reaction, the microwave reactor showed significantly shorter reaction times, but there was no difference in the product purity. Furthermore, the microwave reactor limited the reaction to 100 mg scale which was a bottleneck on the throughput of monomer.

2.3.2. X-Ray Data of Regioisomer

Parallel to my synthesis of **1-MeO** using the Friedel-Crafts route, an undergraduate, Aaron Teator, was synthesizing parent antrip (**1-H**) with the same modified Friedel-Crafts approach. Performing column chromatography of his crude parent quinone intermediate **4**, he was able to isolate a major and minor band. An NMR spectrum taken of the major band of his column showed no presence of parent quinone intermediate **4**. I grew a single crystal from the major band by slow evaporation of a nitromethane/chloroform solution and analyzed by single crystal X-ray diffraction. The crystal was found in the monoclinic system with a C2/c space group with: $a=37.6\text{ \AA}$, $b=15.8\text{ \AA}$, $c=29.1\text{ \AA}$, $\alpha=90^\circ$, $\beta=118.8^\circ$ and a volume of $15,272\text{ \AA}^3$ and $Z=16$. The crystal structure unfortunately indicated that the major product of the modified Friedel-Crafts route is the regioisomer where one blade is out of plane, **4***, Figure 2.6.

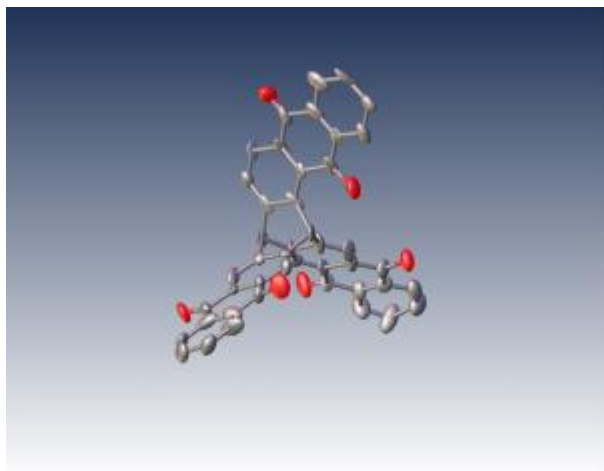


Figure 2.6. Nitromethane solvate of antrip quinone (**4***) regioisomer. The asterisk denotes a regioisomer of the desired intermediate (**4**).

The modified Friedel-Crafts route using phthalic chloride was meant to avoid the regioisomers caused by cyclization of tris-ketoacid intermediate **3**, and give quinone intermediates **4** and **4-MeO** in one pot. However, direct synthesis of quinone intermediate **4** also suffers from regiochemistry issues. As seen in Figure 2.7, acylation with phthalic chloride can occur at two different sites which are defined as distal and proximal.

The major product of the modified Friedel-Crafts route of parent antrip (**1-H**) was an unwanted regioisomer, which resulted in low yields and difficult separation. While not investigated, it is likely the same regioisomeric complications occur when using identical

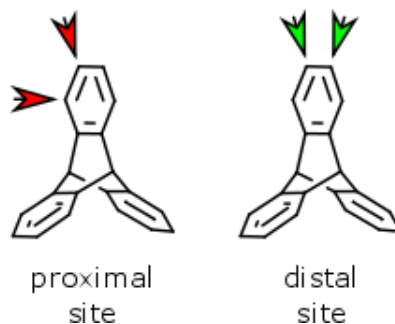


Figure 2.7. Illustration of the two possible sites for acylation between triptycene and phthalic chloride. Reaction at proximal site leads to undesired regioisomer and distal site leads to target.

conditions to synthesize methoxy antrip (**1-MeO**). However, the yields for the methoxy derivative were consistently lower than those for parent antrip. Methoxy antrip (**1-MeO**) has

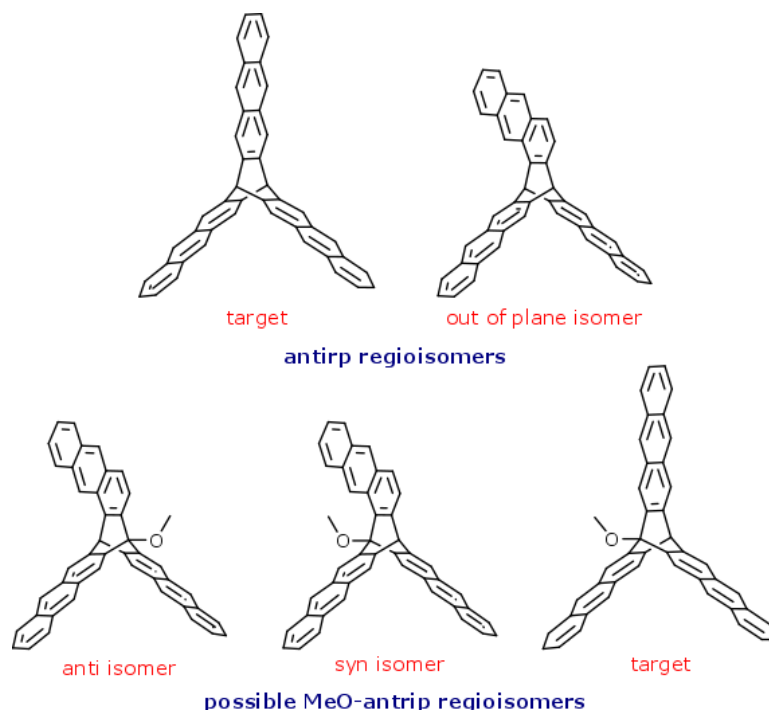


Figure 2.8. The minor (**1-H**) and major (regioisomer) products of the parent antrip synthesis using the modified Friedel-Crafts route (top). Analogous regioisomers with the MeO-antrip route (**1-MeO**) (bottom); use of the term analogous refers to the isomer side products of MeO-antrip (**1-MeO**) being limited to only one out of plane blade as with the antrip (**1-H**) route.

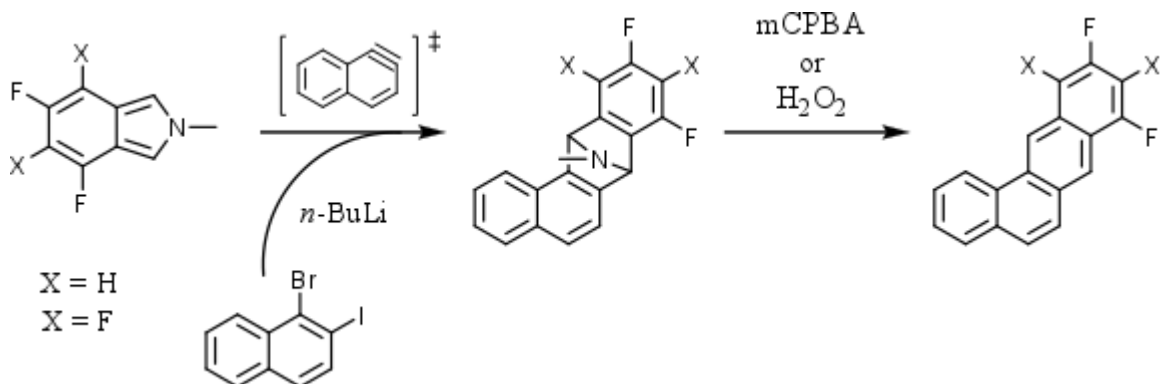
a lower symmetry than parent antrip (**1-H**) due to the methoxy group at the bridgehead. With the major product of the Friedel-Crafts route resulting in one out of plane blade, the presence of the methoxy group in **1-MeO** now gives the possibility of three different regioisomers instead of two, Figure 2.8. Having 3 regioisomers or more present, each with very similar R_f ,

values, adds another level of difficulty when resolving bands during chromatography. This is likely the cause of the difficult and inconsistent chromatography of **1-MeO**.

After determining Swager's Friedel-Crafts route, and its modified versions, towards the synthesis of antrip (**1-H**) and methoxy antrip (**1MeO**) were inherently plagued by regioisomeric problems, other routes were sought out that would allow regioisomeric control over the monomer framework.

2.3.3. One-Step Diels-Alder Approach

After discovering the poor regioselectivity of the previous routes we decided to take an approach that "locks in" the regiochemistry using a one-step Diels-Alder route to the parent framework. Gribble and Swager have reported the use of isoindole moieties reacted with an aryne intermediate, generated from a dihalogenated species, through a Diels-Alder reaction to build acenes.^{41,42} The dihalogenated arenes undergo lithium halogen exchange upon reaction with *n*-BuLi to create an aryne intermediate that undergoes a regioselective Diels-Alder with the isoindole species in solution. This is followed by cheletropic elimination of the N-methyl bridge to afford a section of acene growth, Scheme 2.7.



Scheme 2.7. Acene synthesis using a one-step Diels-Alder approach.^{42,43}

This approach to acene synthesis has been shown to work quite well, especially with fluorinated isoindole moieties as seen above. The fluoro substituents provide stability to the isoindole reagents making them more stable than their non-fluorinated counterparts. This is why most accounts using this one-step Diels-Alder method of acene synthesis employ fluorinated isoindole moieties. Without any fluoro groups to provide stability, N-methyl-isoindole, seen below Figure 2.9, has poor thermal stability making it easily prone to reactions which grant it aromatization, effectively destroying its diene character.⁴⁴ Fortunately, literature precedent exists for the synthesis of N-methyl-isoindole and its use towards the synthesis of **1-H** was eagerly applied.⁴⁵

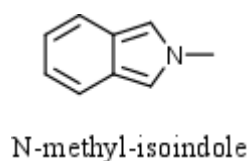
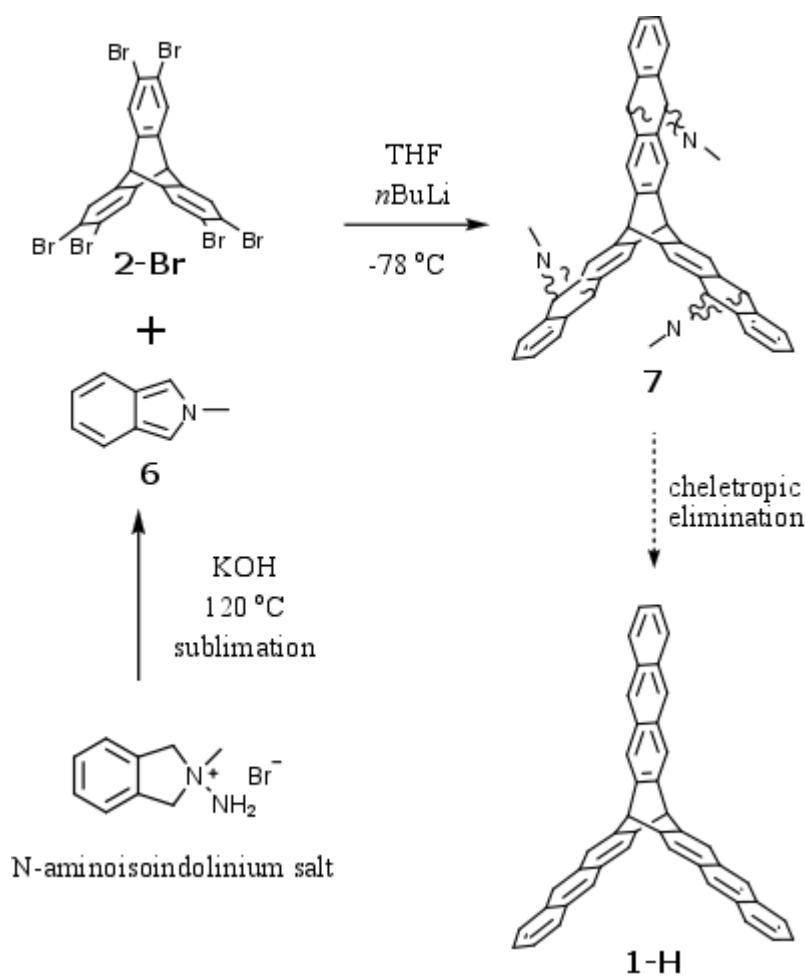


Figure 2.9. N-methyl-isoindole.

The one-step Diels-Alder approach towards **1-H** uses the three-fold generation of benzyne intermediates from **2-Br** followed by trapping with N-methyl-isoindole (**6**), giving construction to the carbon skeleton of **1-H**. The benzyne intermediate is generated from a reaction between easily prepared hexabromotriptycene (**2-Br**) and *n*-BuLi.¹⁵ The loss of bromines from **2-Br**, when reacted with *n*-BuLi, allow for the benzyne to only be generated between the distal carbons of the triptycene core, and trapped by excess N-methyl-isoindole (**6**) through a Diels-Alder cycloaddition. After trapping the benzyne intermediate the carbon framework of the monomer is given with intermediate **7**. In a subsequent step the N-methyl bridge is then cheletropically eliminated to give the final product **1-H**, Scheme 2.8.



Scheme 2.8. Overview and synthetic details of the one-step Diels-Alder route towards **1-H**.

Using the one-step Diels-Alder route to synthesize **1-H** was first attempted by Professor King while on sabbatical at ETH Zurich. A synthetic approach with such straightforward access to acene growth deserved further investigation, and was revisited towards synthesis of monomer **1-H**, Scheme 2.8.

N-Methylisindole was synthesized using an N-aminoisindolinium salt precursor that was suspended in oil, Scheme 2.7. The oil suspension is mixed with powdered KOH and sublimed at 120 °C under reduced pressure and resulted in pure, dry N-methylisindole on the cold finger of the sublimation apparatus and needed no further purification. Due to the poor thermal stability of N-methylisindole, the product was immediately transferred to a

reaction vessel containing hexabromotriptycene (**2-Br**) in tetrahydrofuran at $-78\text{ }^{\circ}\text{C}$. *n*-BuLi was added to the solution and was let to stir under N_2 for 30 mins followed by quenching with 5% methanol/toluene. The resulting mixture was run through a short plug of silica and two polar bands were collected. Two bands were expected due to the two configurational isomers resulting from the arrangement of the three N-methyl bridges of intermediate **7**, Figure 2.10.

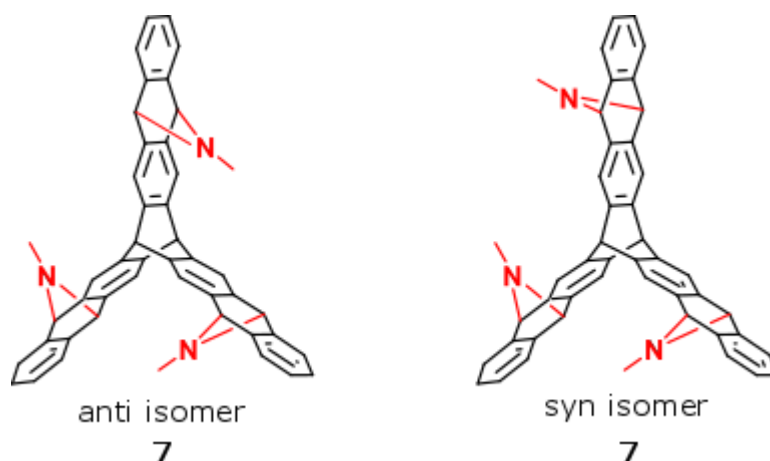
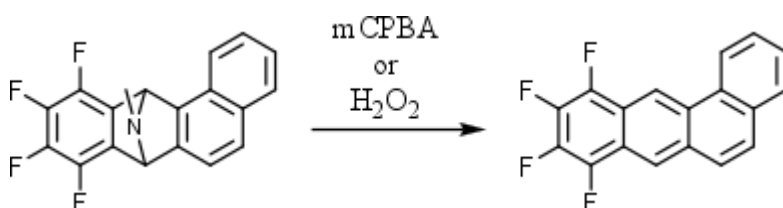


Figure 2.10. Two configurational isomers of **7**, anti and syn with respect to the orientation of the N-methyl bridges.

Further purification of intermediate **7** did not lead to clean intermediate, however, elimination of the N-methyl bridges was attempted on the impure material using mCPBA, which is a common reagent used for deamination of similar compounds, Scheme 2.9.⁴¹ The cheletropic elimination of the N-methyl bridge can be performed with a peracid or peroxide and involves an initial oxidation of the nitrogen to create an amine oxide, followed by cheletropic elimination yielding the aromatic hydrocarbon and a nitrosoalkane.



Scheme 2.9. Cheletropic elimination of an N-methyl bridge using mCPBA or H₂O₂.⁴¹

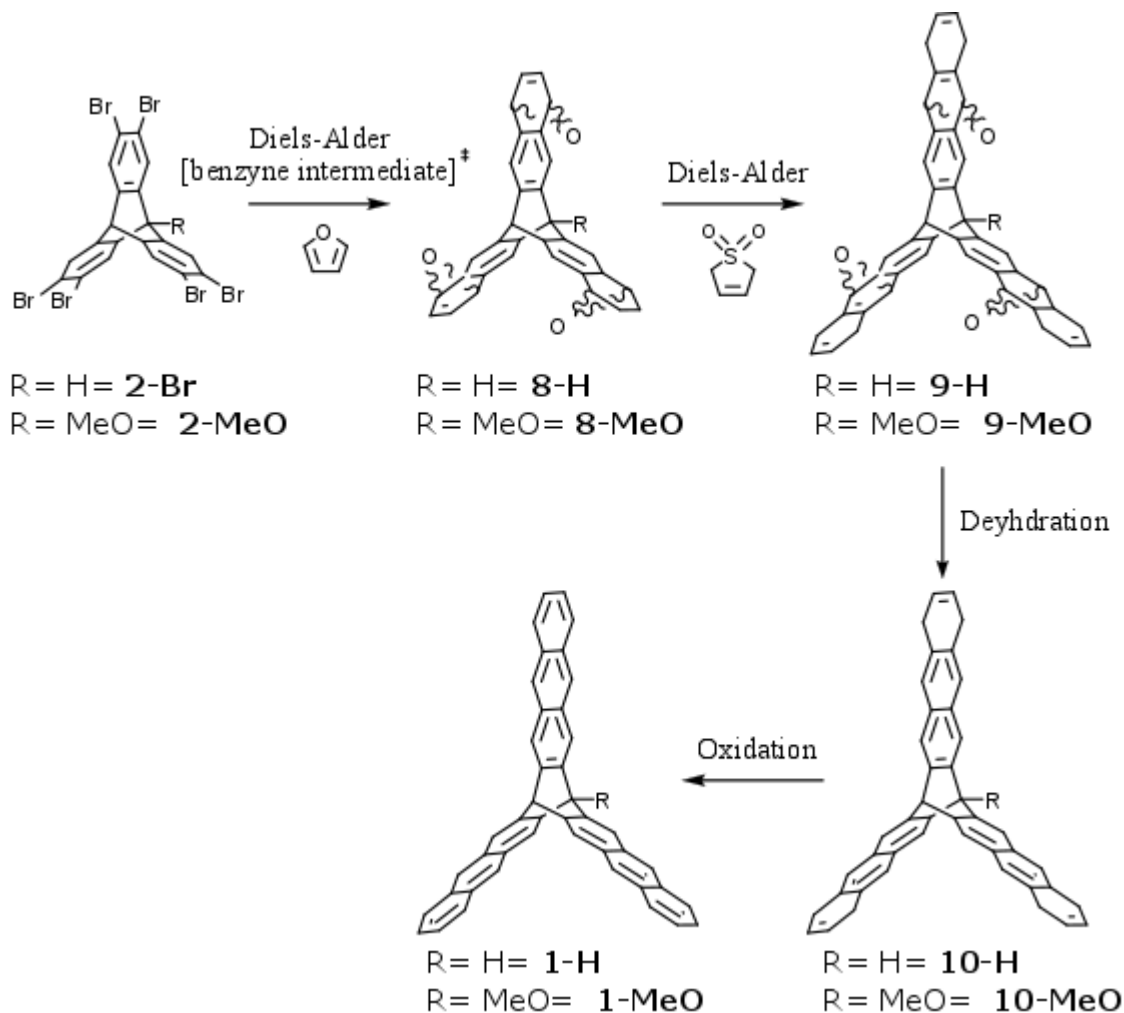
No antrip (**1-H**) was isolated from cheletropic elimination of impure **7**. One of the main issues with the one-step Diels-Alder approach is the reaction of two unstable species. Benzyne, which is generated from hexabromotriptycene (**2-Br**), is extremely reactive and short lived even at the low temperature of -78 °C.⁴⁶ N-Methylisindole (**6**) is highly unstable to heat and light and after isolation must be used quickly before degradation.⁴⁷ Bringing two highly reactive species such as these together and obtaining a specific transformation with limited side-product formation is rare. However, fluorinated isindole moieties are much more stable and can be stored over months when out of the light and at low temperatures. Employment of a more stable fluorinated isindole moiety for the one-step Diels-Alder reaction will be discussed in a later section of this chapter

2.3.4. Two-Step Diels-Alder Approach

The two-step Diels-Alder route aims to build the parent framework of the monomers by taking advantage of reagents and intermediates that are more stable compared to the one-step Diels-Alder route. While the previous one-step approach completes the carbon framework of the monomer in one step, the two-step approach trades off this brevity for a more predictable yet longer synthetic route. Most importantly, the regiochemistry of the framework forming transformations are still locked in with consecutive Diels-Alder cycloadditions.

The general transformations in the two-step Diels-Alder approach are shown in Scheme 2.10. The synthetic route was applied in parallel towards the synthesis of antrip (**1-H**) and MeO-antrip (**1-MeO**). One concern was that the presence of a methoxy group throughout the synthesis of **1-MeO** would require us to develop different conditions for **1-H** and **1-MeO**. Fortunately, the presence of a methoxy group did not require modification of

the steps, allowing for **1-H** and **1-MeO** to be prepared using the same reaction conditions. Therefore, the following describes the identical synthetic steps taken towards synthetic development and improvement of both monomers using the two-step Diels-Alder approach.



Scheme 2.10. General Scheme for the two-step Diels-Alder route.

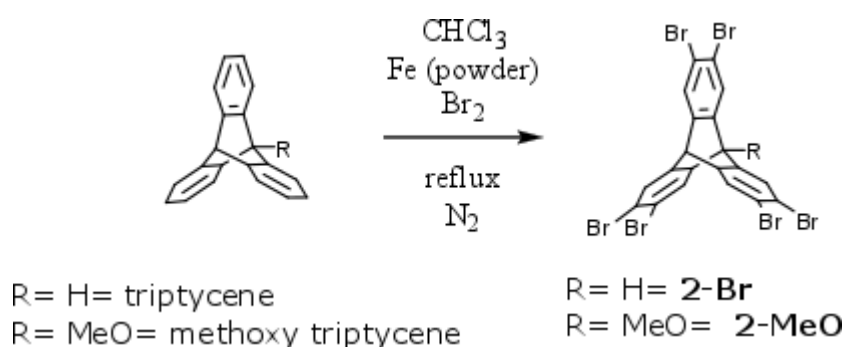
The first reaction is the *in situ* generation of a benzyne intermediate from hexabromotriptycene (**2**), that is trapped by excess furan via a Diels-Alder cycloaddition giving intermediates **8-H** and **8-MeO**. A second Diels-Alder cycloaddition between **8-H** and **8-MeO** with 3-sulfolene (a 1,3-butadiene equivalent) in a high pressure reactor gives the oxo-bridged intermediates **9-H** and **9-MeO**, completing the carbon framework of the monomer.

Intermediates **9-H** and **9-MeO** are dehydrated using an acid catalyst followed by oxidation of the hydrogenated intermediates **10-H** and **10-MeO** giving final products **1-H** and **1-MeO**. The development of each reaction is outlined below.

Since synthetic conditions and numerical prefixes for the intermediates towards **1-H** and **1-MeO** are identical, throughout this chapter the intermediates of both schemes will be referred to by only their numerical values.

2.3.4.1. Bromination

The first step in the two-step Diels-Alder synthesis is the bromination of triptycene and methoxy triptycene. Six-fold bromination of the triptycene starting material is perhaps the most important step of the two-step Diels-Alder synthesis. The regiochemistry of the entire route depends on the proper bromination of the triptycene starting material. Bromination of the distal carbons of triptycene has previously been worked out by a former member of the King group.⁴⁸ Fortunately, the bridgehead methoxy group of methoxy triptycene did not drastically affect its bromination, Scheme 2.11.



Scheme 2.11. Bromination of triptycene and methoxy triptycene using Br_2 and an Fe catalyst in refluxing chloroform, 65% yield.

The bromination of either triptycene starts with the use of dry chloroform. One must make sure to use chloroform that is stabilized by amylene. Ethanol stabilized chloroform will react with the bromine and alter the stoichiometry resulting in an incomplete bromination. The reaction mixture of chloroform, triptycene, and iron powder is stirred at room temperature and 6.1 equivalents of bromine are added. The solution is brought to reflux for 3 hours under a nitrogen atmosphere. The cooled solution is run through a short pad of silica followed by crystallizing product **2** from chloroform/methanol followed by chloroform/hexanes. Conveniently, target **2** preferentially crystallizes while leaving under brominated material in solution, with a yield of 65%.

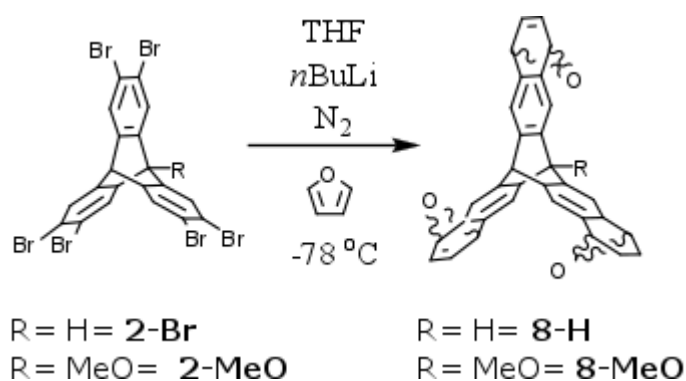
The internal free volume of the brominated triptycenes (**2**) readily allows for incorporation of solvents upon evaporation to dryness. This requires one to take precaution prior to using this reagent in the next lithiation step. If target **2** was previously dissolved in chloroform, for example, it will react with *n*-BuLi forming highly reactive carbenes resulting in unpredictable byproducts and inconsistent, low yields of **8**. A crystallization of **2** with hexanes or THF before use proved to be efficient in keeping **2** free of reactive solvents.

The above conditions effectively brominate methoxy triptycene, however, the HBr by-product of the reaction will deprotect the methoxy group of **2-MeO** to a hydroxy group. A gentle bubble of N₂ helps blow off HBr gas and reduce the percentage of hydroxyl side product formed. However, a simple methylation of the crude material, using dimethyl sulfate, easily converts any hydroxy triptycene to back to methoxy triptycene.⁴⁹

2.3.4.2. Furan-Adduct

The first framework forming step of monomer synthesis is a Diels-Alder between a benzyne intermediate and furan. The benzyne intermediate is generated by reacting **2** with

n-BuLi and is trapped via Diels-Alder cycloaddition by excess furan to give furan adduct intermediate **8**, Scheme 2.12.



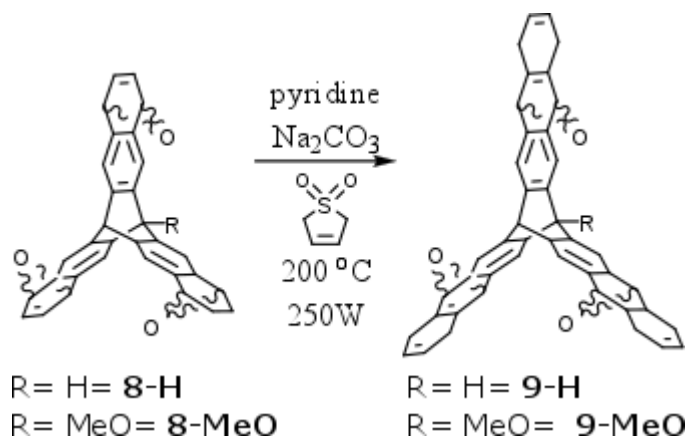
Scheme 2.12. Diels-Alder cycloaddition between furan and a benzyne intermediate generated from **2** and *n*-BuLi, 90% yield.

To ensure completion of reaction an excess of dry, freshly distilled furan (8 eqv.) followed by an excess of *n*-BuLi (3.5 eqv.) are added to the -78°C reaction mixture. Due to the extremely short lifetime of the benzyne intermediate, the reaction is completed shortly after addition of *n*-BuLi. The reaction is quenched at -78°C , 30 mins after addition on *n*-BuLi, with a 5% methanol/toluene mixture.

The crude mixture is dissolved in dichloromethane and passed through a pad of silica using a 20% hexane dichloromethane solution. The frontier bands are disposed of and the brown target bands are pushed through with ethyl acetate to give a yield of ~90% for **8**.

2.3.4.3. 3-Sulfolene Reaction

The following transformation is the second Diels-Alder and completes the carbon framework of the monomer with a cycloaddition between the terminal olefins on intermediate **8** and 3-sulfolene (a 1,3-butadiene equivalent), Scheme 2.13.



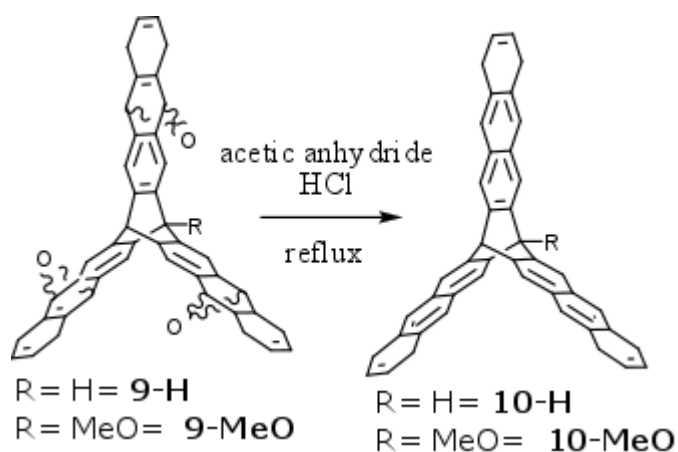
Scheme 2.13. Diels-Alder cycloaddition between **8** and 3-sulfolene, microwave conditions.

Upon heating to >60 °C, 3-sulfolene undergoes a cheletropic elimination yielding sulfur dioxide and 1,3-butadiene, which participates in the second Diels-Alder reaction. The gaseous state of 1,3-butadiene requires the reaction to be performed in a closed system. To serve as a high pressure reaction vessel a microwave reactor was used. With an excess of 3-sulfolene the reaction took 3hr in the sealed reactor at 200 °C, 200W. The microwave reactor allowed easy access to sealed reaction conditions, however, we were limited to 100 mg loadings of **8** which created a bottleneck in the throughput of monomer. Purchase of a 500 ml high pressure reaction vessel allowed for 0.5-1g loadings, using identical reagent equivalents. The benchtop procedure could be performed using thermal conditions over the weekend (~3 days) with 80% yields.

2.3.4.5. Dehydration and Oxidation

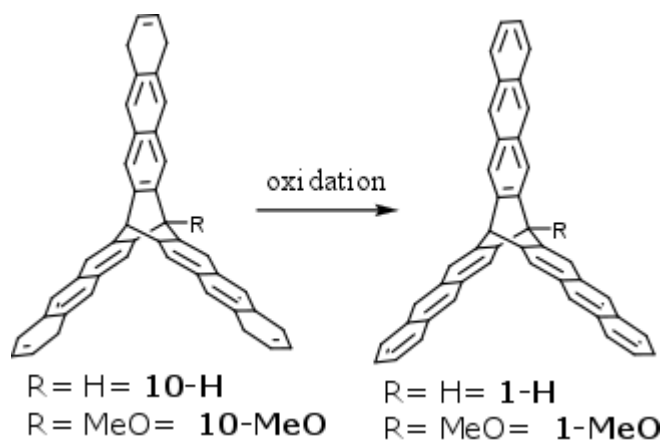
Dehydration of **8** is the next step towards the synthesis of the target monomers. Literature reports the use of ethanol and HCl for the dehydration of compounds similar to that of **9**.⁵⁰ Refluxing **9** in an HCl/ethanol solution at various ratios gave incomplete and impure products, which was most likely a solubility issue. The use of acetic anhydride and

HCl, however, resulted in complete dehydration of **9** giving hydrogenated intermediate **10** at 70% yield, Scheme 2.14.



Scheme 2.14. Acid catalyzed dehydration of **9** in acetic anhydride.

Oxidation of intermediate **10**, Scheme 2.15, proved to be difficult. All of the oxidation conditions that were used for the Friedel-Crafts approach were employed for the two-step Diels-Alder approach but gave inconsistent results.



Scheme 2.15. Oxidation of intermediate **10** to final product **1-H** and **1-MeO**.

Palladium on carbon (Pd/C 10% wt loading) was used under microwave conditions and no material was recovered upon work up. Due to the expense of Pd/C and the

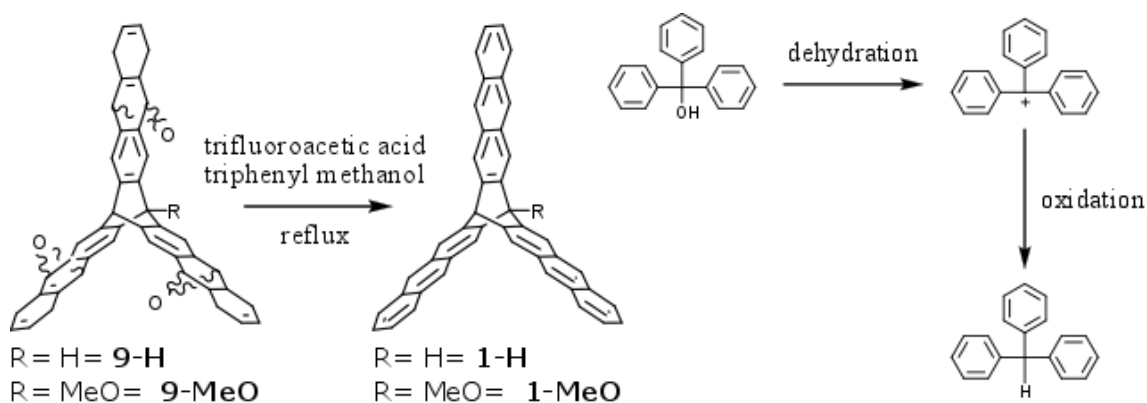
polymerization issues experienced with the Friedel-Crafts routes we did not spend much time exploring this transformation.

We had previously shown DARCO to be an inexpensive and efficient way of oxidizing the partially hydrogenated intermediate **5-MeO** from the Friedel-Crafts route. For this oxidation we chose to reflux, in toluene or xylenes, a stirring solution of **10** and DARCO under an O₂ atmosphere, rather than open air, for 24hr. This procedure gave both monomers antrip (**1-H**) and MeO-antrip (**1-MeO**) with inconsistent yields and multiple side products. A time consuming column was required to obtain target products. With intermediate **10**, DARCO gave results that did not react analogously to the Friedel-Crafts intermediate **5-MeO**. While product was obtained, the yields were inconsistent and difficulty isolating the target product lead us to explore different oxidation options.

Our next attempt at the oxidation of **10** was the use of DDQ. Partially hydrogenated acenes reacted with excess DDQ in refluxing benzene or toluene is a common method of oxidation. However, with intermediate **10**, the yields were low, and multiple side products were formed. Removal of excess DDQ from the reaction mixture via chromatography proved to be difficult. During chromatography, the excess DDQ would streak and co-elute with the target band making isolation extremely difficult, resulting in unreliable yields. Furthermore, acenes and DDQ have the potential to undergo a Diels-Alder cyclization, which would add to the potential side products and difficulties in purification.⁵¹ Due to the purification issues, more mild methods of oxidation were explored.

The use of triphenylmethanol and trifluoroacetic acid to dehydrogenate **10** was investigated in an attempt to find a more efficient and higher yielding oxidation. Compared to the above oxidations this room temperature reaction was hoped to be a milder approach with fewer side products. The reaction with intermediate **10** at room temperature gave **1-H**

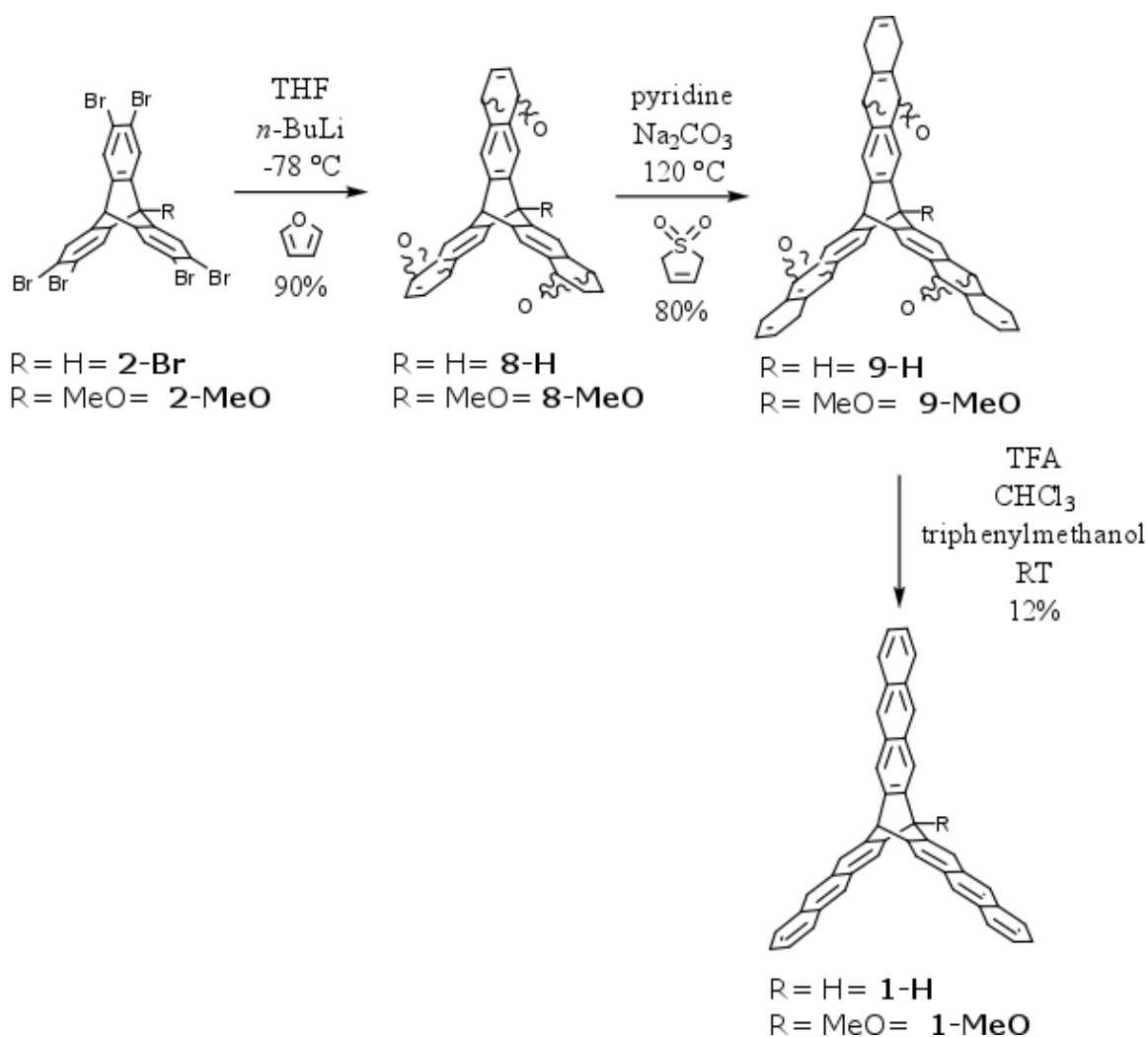
and **1-MeO** in ~17% yields. After discovering these promising results it was realized that the trifluoroacetic acid in the reaction mixture could also catalyze the dehydration of **9**, allowing us to perform two synthetic steps in one pot. Indeed, the one pot dehydration-oxidation reaction with trifluoroacetic acid and triphenylmethanol dehydrated and oxidized intermediate **9** to give final products **1-H** and **1-MeO**. The excess triphenylmethanol and the triphenylmethane byproducts were conveniently removed by a simple trituration of the crude reaction mixture with hot hexanes and hot methanol. Due to solubility issues, an unconventional approach was taken towards chromatography of **1-H** and **1-MeO**. After trituration, the crude mixture was suspended in a hot 20% hexanes/chloroform solvent system and poured directly onto a pad of silica and run through with the hot solvent system as the mobile phase. This allowed for good resolution and avoided dry loading or settling for an inferior solvent system with better solubility but worse resolution. This approach was by far the most successful and over both steps gave yields of ~12% for antrip (**1-H**) and MeO-antrip (**1-MeO**), Scheme 2.16.



Scheme 2.16. The one pot dehydration/oxidation of **9** to final products **1-H** and **1-MeO** (left).

The acid catalyzed dehydration of triphenyl methanol forming a stable carbocation which acts as an oxidant (right).

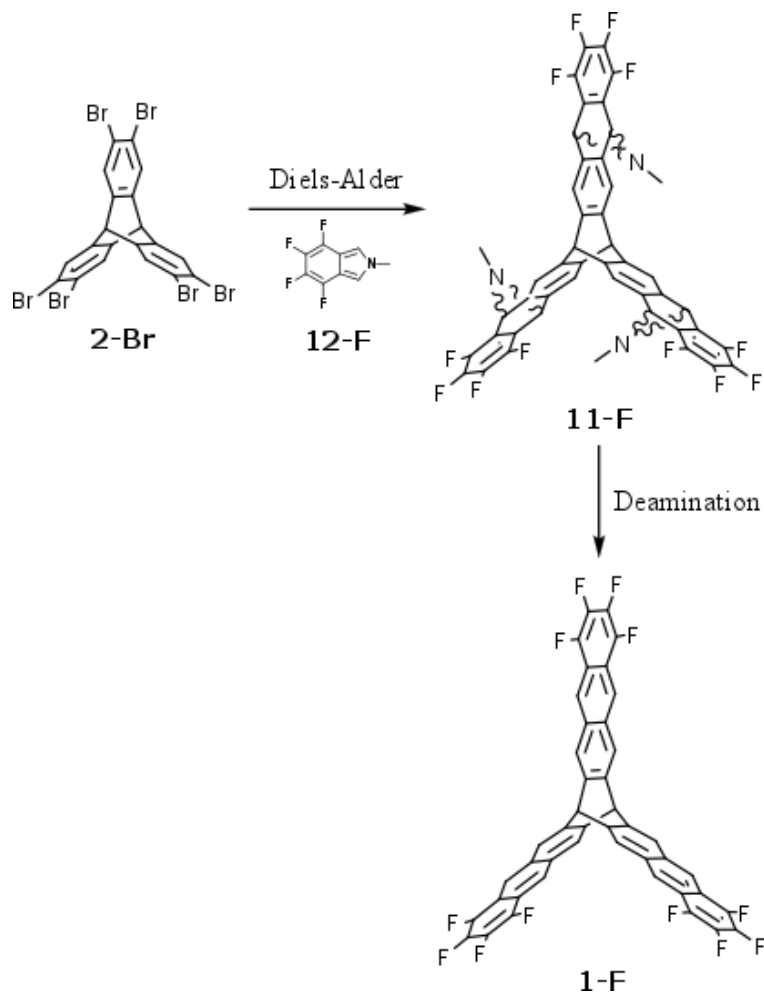
The improved synthetic scheme used towards **1-H** and **1-MeO** is described below, Scheme 2.17. Improvements in yields were made when compared to the original two-step Diels-Alder approach and Friedel-Crafts approaches. After the two framework forming Diels-Alder reactions a one-pot dehydration-oxidation was used to access the target compounds. Fortunately, all transformations used towards both targets employed identical conditions and gave comparable results.



Scheme 2.17. Improved two-step Diels-Alder synthetic scheme for **1-H** and **1-MeO** targets.

2.4. Fluorinated One-Step Diels-Alder Approach

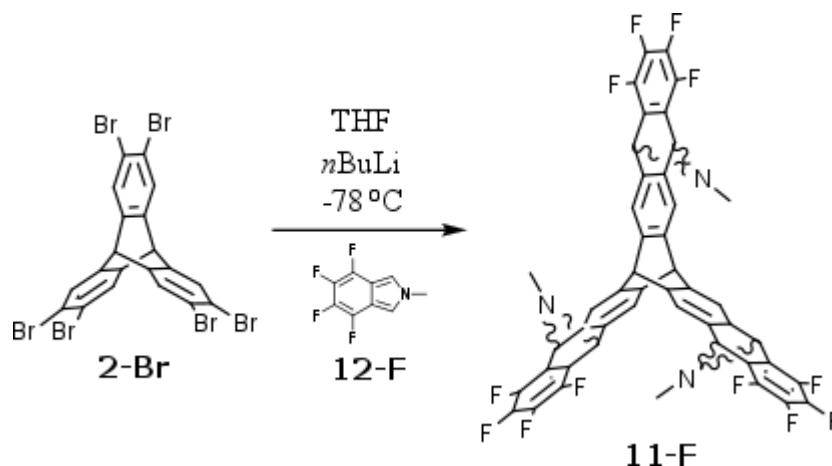
Fantrip **1-F** is built using a convergent synthesis and relies on a one-step Diels-Alder cycloaddition for construction of the carbon skeleton. The convergent nature of this approach and unique stability of tetrafluoroisindole (**12-F**) allows for the preparative scale synthesis of Fantrip **1-F**, Scheme 2.18.



Scheme 2.18. One-step Diels-Alder scheme for the synthesis of fantrip **1-F**.

The synthesis of **1-F** begins with generating a benzyne intermediate by reacting **2-Br** with *n*-BuLi at $-78\text{ }^{\circ}\text{C}$, followed by trapping with excess tetrafluoroisindole (**12-F**), via a Diels-Alder cycloaddition, to give the trifold adduct **11-F**. The product of the adduct results in a mixture of the mono, bis, and trifold adducts, with the trifold being the majority as indicated by mass spectra and NMR. Higher temperatures were attempted, however, no increase in tri-

fold adduct percentage was observed. Following the lithiation, the crude mixture is run through a pad of silica to isolate the trifold adduct (**11-F**) isomers. Due to the similar R_f values, a small amount of the bis-adduct co-elutes during chromatography. The eluent is precipitated with dichloromethane/methanol which effectively removes the majority of the bis-adduct, giving a 85% yield of **11-F**, Scheme 2.19.

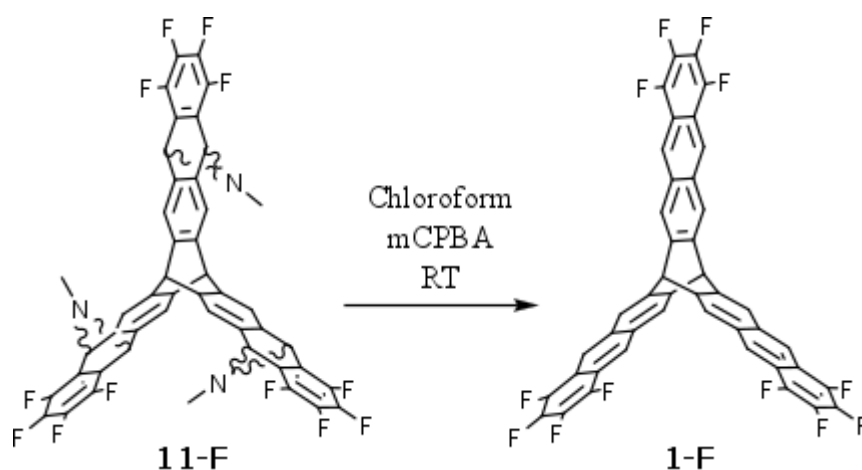


Scheme 2.19. Diels-Alder between **2-Br** and **12-F** to give trifold adduct intermediate **11-F**.

Following completion of the carbon framework, **11-F** is deaminated to give target monomer **1-F**. Initially, Dr. Kissel deaminated the trifold adduct using Gribbles method which involved the *in situ* generation of dichlorocarbene from chloroform by using a phase transfer catalyst and an aqueous sodium hydroxide solution.²³ While this method of oxidation has literature precedence, the yields were low and other methods of oxidative deamination were explored.⁵²

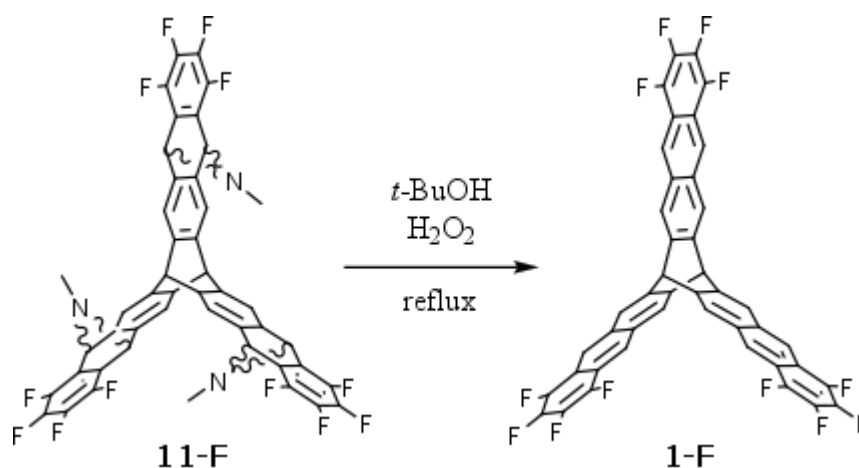
Gribble has also shown that use of mCPBA for the oxidative deamination of similar systems works quite efficiently and under mild conditions.⁴¹ The use of excess mCPBA, for the oxidative deamination of **11-F**, resulted in final compound **1-F**, however involved problematic separations between final product and the excess mCPBA during chromatography. A trend with the chromatography of this framework is that products and by-products tend to co-elute

with one another other making chromatography extremely challenging. While product was obtained with mCPBA, the inconsistent yields and problematic chromatography motivated the use other methods of deamination, Scheme 2.20.



Scheme 2.20. Deamination of **11-F** using mCPBA.

Gribble has used hydrogen peroxide as an oxidant in refluxing methanol with a similar naphthalene system.⁴¹ This approach was appealing due to the suggested yields of greater than 90%, and the ease of removing excess peroxide through a simple precipitation with water followed by filtration. Unfortunately, the first attempts using these conditions were unsuccessful and resulted in starting material. It was speculated that the failure of this approach was due to the low solubility of **11-F** in methanol and/or the lack of activation energy provided by the boiling point of methanol. We decided to use a higher boiling point solvent, *tert*-butanol, that would not be affected by the oxidative nature of the peroxide. Refluxing **11-F** at a higher temperature allowed the deamination to proceed as predicted, over a 12 hr period, giving a 35% yield, Scheme 2.21.



Scheme 2.21. Deamination of **11-F** using H_2O_2 in refluxing *tert*-butanol 35% yield.

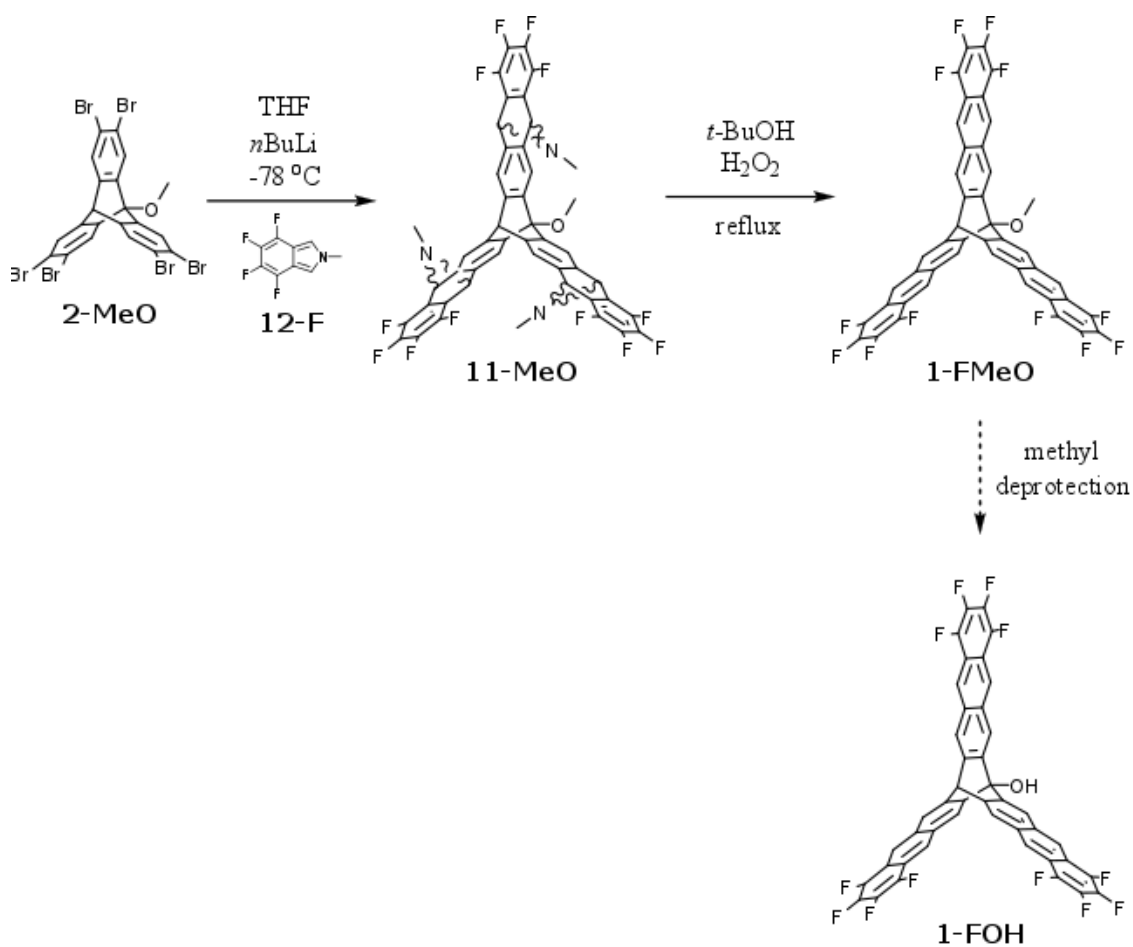
The crude product of the oxidative deamination is thought to be a mixture of fantrip and a small amount of single and double bladed product, as detected by MALDI-TOF. These partially bladed side products either carry through the chromatography process undetected or are possibly a result of fragmentation. Nevertheless, the R_f values of the target and the side products are very similar, resulting in a mixture that is very difficult to resolve through column chromatography. The ideal solvent systems capable of ideal resolution are unable to completely dissolve the crude mixture. After multiple attempts at dry loaded columns resulting in inconsistent yields, a more straightforward approach was taken. It was noticed that the target product **1-F** was noticeably less soluble than the side products. Therefore, the crude mixture is fully dissolved in tetrahydrofuran followed by evaporation under reduced pressure until a precipitate forms. This precipitate is placed in the freezer, followed by filtration. Repeating this process multiple times allows for removal of the side products and avoids column chromatography. While the overall yields of **1-F** are modest at 25%, its convergent nature and simple isolation allows for a high throughput gram scale preparation.

2.3.10. Hydroxy Fantrip Synthesis

The success of the fantrip (**1-F**) synthesis motivated the synthesis of hydroxy fantrip (**1-FOH**) which used similar conditions. Hydroxy fantrip (**1-FOH**) has a polar hydroxy group at the bridgehead which is intended to serve as a hydrophilic anchor at the air water interface or a synthetic handle. The initially proposed route to the synthesis of **1-FOH** began with the synthesis of methoxy fantrip, (**1-FMeO**) followed by the deprotection of its methoxy bridgehead to give target **1-FOH**, Scheme 2.20. The methoxy group was intended to serve as a protected hydroxyl throughout the synthesis. Fortunately, the presence of a methoxy group did not have a negative effect on any of the transformations and the same synthetic conditions for parent fantrip (**1-F**) were used.

As shown in Scheme 2.22 synthesis of methoxy fantrip, **1-FMeO**, went smoothly, however problems arose when attempting the methyl ether deprotection. Numerous reaction conditions were attempted, as discussed below.

Reaction conditions for the demethylation of methoxy triptycene and methoxy antrip (**1-MeO**) had been previously developed, by a former group member Dr. Bholá, using HBr in refluxing acetic acid.³⁷ These conditions were initially applied to the deprotection of methoxy fantrip (**1-FMeO**). Unfortunately, **1-FMeO** showed no signs of deprotection after 3 days in



Scheme 2.22. Synthetic route towards MeO-fantrip, **1-FMeO**, followed by methoxy deprotection to hydroxy fantrip target, **1-FOH**.

refluxing 38% HBr/Acetic under an N₂ atmosphere. Not only did **1-FMeO** have poor solubility in the above conditions, the relatively high reaction temperature and acidic environment seemed to decompose **1-FMeO** leading to multiple side products as determined by TLC and NMR.

With solubility and high temperatures being a possible issue with the above conditions, other means of methyl deprotection were sought out. BBr₃ is common reagent used to cleave ethers under mild conditions, and allows for the use of more suitable reaction solvents such as chloroform and dichloromethane.⁵³ Using *d*-chloroform and *d*-

dichloromethane allowed the convenience of monitoring the reactions by ^1H NMR. All conditions used were attempted with both *d*-chloroform and d_2 -dichloromethane separately.

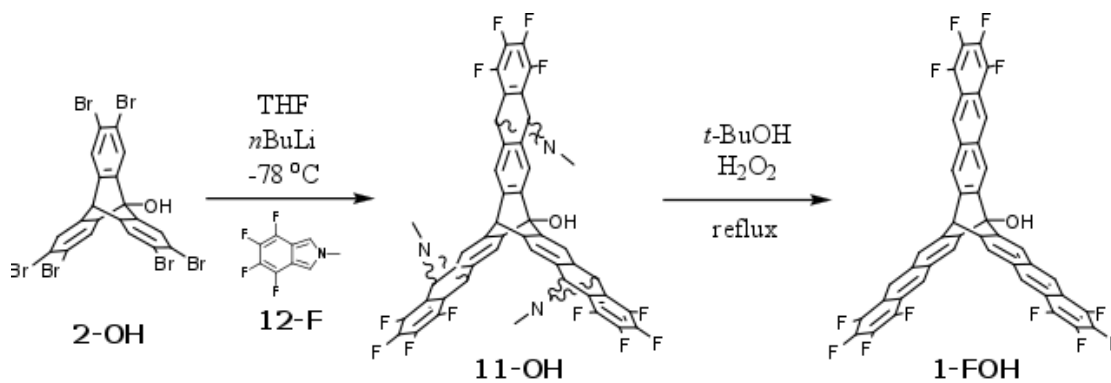
The first reaction conditions consisted of stirring a solution of **1-FMeO** with BBr_3 at $-78\text{ }^\circ\text{C}$, followed by room temperature, and finally at reflux. These conditions showed no sign of deprotection by NMR. To the above reaction conditions, NaH was added to act as a nucleophile in an attempt to help facilitate cleavage. This was performed at $-78\text{ }^\circ\text{C}$, room temperature, and reflux with no signs of cleavage. 15-Crown-5 was added to the reaction mixture to help further encourage the effectiveness of the NaH by complexing Na^+ . The reactions were performed at $-78\text{ }^\circ\text{C}$, room temperature, and reflux and showed no signs of deprotection. Next we tried a slightly different approach using *d*-chloroform, NaI and 15-crown-5 added to assist BBr_3 during ether cleavage. The reaction was performed at $0\text{ }^\circ\text{C}$ and reflux, both showed no signs of reactivity by TLC or NMR. None of the above conditions resulted in a reaction of any kind and **1-FMeO** starting material was recovered.

Iodotrimethylsilane (TMSI) is a common reagent for dealkylation reactions. Typical conditions for ether cleavage using TMSI are mild and effective towards methyl ether cleavage.⁵⁴ The following reactions were performed using microscale quantities and monitored by NMR. A solution of **1-FMeO** and TMSI in *d*-chloroform was stirred at room temperature overnight. NMR and TLC showed signs of reaction, however, the presence of **1-FOH** was not detected. A second reaction was performed in *d*-chloroform with the addition of NaI. This also resulted in undesirable side product formation. When changing the solvent to d_3 -acetonitrile, identical results of byproduct formation were observed. The above series of reaction conditions were applied to **1-FMeO** employing a similar reagent chlorotrimethylsilane (TMSCl) instead of TMSI, and showed very similar unwanted reactivity.

The deprotection of **1-FMeO** using FeCl_3 in AcO_2 at $80\text{ }^\circ\text{C}$ was explored.⁵⁵ While heat and acidity were thought to be the cause of unwanted byproducts in the case of HBr/AcOH , these conditions resulted in only starting material.⁵⁵ Deprotecting **1-FMeO** using AcCl and NaI in acetonitrile at room temperature was attempted and also resulted in starting material.⁵⁵ Hydroiodic acid (HI), much like HBr , is a common acid used for ether cleavage reactions via an $\text{S}_{\text{N}}2$ mechanism. A mixture HI and AcOH along with KI at reflux for 4 days was used to deprotect **1-FMeO**. After 4 days, the presence of **1-FOH** was detected by NMR and mass spec. However, most of the mixture consisted of starting material and by-products. The presence of **1-FOH** was promising, but the relatively harsh reaction conditions led to unwanted side-products, making chromatography extremely difficult and low yielding. In search for cleaner and more mild reaction conditions, demethylation using BF_3 and KI in *d*-chloroform at reflux was attempted. Much like the other Lewis acids employed for the deprotection of **1-FMeO** the conditions resulted in no reaction.

Attempts at deprotecting **1-FMeO** resulted in no isolable target **1-FOH**. The only reaction conditions to show any reactivity were harsh and acidic, resulting in reaction mixtures containing multiple side products. The difficulty in deprotecting **1-FMeO** and isolating pure **1-FOH** motivated another route to final product.

Starting out the synthetic route with hydroxytryptycene instead of methoxytryptycene had been considered but not attempted due to the potential incompatibility of the hydroxy group with the first lithiation step using *n*-BuLi. As previously stated, the deprotection of methoxy tryptycene to hydroxy tryptycene with 38% HBr in acetic acid proceeds smoothly with 90% yields.³⁷ Out of desperation, the route was attempted starting with hexabromo hydroxytryptycene and seemed to have no negative effects on reactivity, Scheme 2.23.



Scheme 2.23. Synthesis of hydroxy fantrip, **1-FOH**, starting with hydroxy hexabromotriptycene, **2-OH**.

Synthesis of **1-FOH** starting with **2-OH** proceeded with similar results to parent fantrip (**1-F**) synthesis. The presence of a hydroxy group did not interfere with any of the steps. **1-FOH** was able to be synthesized, isolated, and characterized with no modification to the one-step Diels-Alder protocol. Unfortunately lack of solubility and steric encumbrance of the final product hindered further modification to the bridgehead hydroxyl group. The fluorinated parent framework, fantrip (**1-F**), has been shown to have great packing capabilities, and modification of the bridgehead would open up potential towards polymerization via the LB trough as well as modification after polymerization towards a scaffold.²³ While the **1-FOH** monomer presents solubility issues, further research towards its bridgehead functionalization and polymerization is merited.

2.4. Conclusions

A two-step Diels-Alder synthesis has been developed for antrip (**1-H**) and MeO-antrip (**1-MeO**) and avoids the regiochemical issues that plagued the Friedel-Crafts routes. Use of Diels-Alder reactions via trapping of a benzyne generated from **2** allows one to dictate the regiochemistry of the reaction. The improved regiochemistry and yields of the individual

transformations increases the overall yield of **1-H** and **1-MeO** from 1.7% overall to 12% overall, allowing a higher throughput to pure final monomer.

The synthesis of fantrip (**1-F**) relies on a one-step Diels-Alder to build its framework. This is followed by an oxidative deamination to give final product. Previously this deamination step relied on a highly reactive carbene, generated *in situ*, which resulted in low yields. The use of H₂O₂ in refluxing *t*-BuOH provided gentler oxidative deamination conditions and resulted in a crude product that could be easily purified by precipitation in THF, allowing for a high throughput of monomer **1-F**. Improvement of the one-step Diels-Alder for fantrip (**1-F**) synthesis allowed for it to be applied towards hydroxy functionalized derivative **1-FOH** using the same conditions.

The above improvements give easier access to monomers, which can be applied towards furthering the development of novel 2DP chemistry.

2.5. Materials and Methods

General. All reactions were run under nitrogen atmosphere unless otherwise specified. Triptycene starting material was purchased and used as received from AKsci, Union City, CA. IR spectra were recorded using a total internal reflectance module having a spectral range 4000–600 cm⁻¹. Mass spectra were recorded using an atmospheric pressure photoionization (APPI) source on a time-of-flight (TOF) instrument in the positive mode. All NMR measurements were taken on either a 400 or 500 MHz VWR instrument.

Hexabromotriptycene (2-Br): Triptycene (1.0 g, 3.9 mmol) is dissolved in chloroform (250 mL). Then iron powder (0.03 g, 0.50 mmol) was added, followed by addition of bromine (1.2 mL, 23 mmol) to the stirring room temperature solution. The reaction mixture is heated to reflux for 3 h under a nitrogen atmosphere. The reaction mixture is cooled to room temperature and is eluted through a pad of silica to remove iron. The solute is evaporated under reduced

pressure, resulting in a mixture composed primarily of **2-Br** and partially brominated product. The remaining solid is then recrystallized twice using a binary solvent system of CHCl₃/MeOH then CHCl₃/hexanes. The resulting crystallizations yields clean **2-Br** 1.41 g (50%). The proton NMR and mass spectrum match previously reported results.⁴⁸ ¹H NMR (500 MHz, CDCl₃) δ 7.63 (s, 6H), 5.24 (s, 2H). 229 (4.95), 285 (3.49), 295 (3.83). MALDI-TOF: (2,3-dichloro-5,6-dicyano-1,4-benzoquinone (DDQ) matrix) calcd. for C₂₀H₈Br₆ 33.01, 1.11, 65.88. found 33.17, 1.19, 65.68.

Furan Adduct (8-H): A Schlenk flask is charged with hexabromotriptycene (**2-Br**) (5.0 g, 6.5 mmol) which has been previously dissolved in THF and evaporated multiple times.* The flask is then charged with freshly distilled THF (250 mL) under a nitrogen atmosphere. Dry, distilled furan (10 mL) is then added via syringe under a nitrogen atmosphere to the stirring mixture. The mixture is then brought down to -78 °C in a dry ice acetone bath followed by three evacuation purge cycles with N₂. A 3.5 eq of 1.6 M *n*-BuLi (14 mL) is added slowly via syringe pump to the vigorously stirring, atmospherically inert, solution over the span of 2 h. The solution is stirred under nitrogen for an additional 30 m at -78 °C. The reaction mixture is then quenched with 5% isopropyl alcohol/toluene solution then evaporated under reduced pressure. The mixture is dissolved in CHCl₃ followed by filtration through Whatman 1 filter paper to remove salts. The reaction mixture is then precipitated using CHCl₃/EtOH solvent system followed by filtration to give 90% of off white/grey material. ¹H NMR (500 MHz, CDCl₃) δ 7.21- 7.183 (m, 6H), δ 6.89-6.87 (m, 6H), δ 5.54-5.53 (m, 6H), δ 5.12 (s, 2H). ¹³C NMR (500 MHz, CDCl₃) δ 54.48, 54.75, 76.80, 77.05, 77.31, 82.18, 82.31, 116.45, 116.51, 116.54, 116.57, 116.74, 116.80, 116.82, 116.86, 143.08, 143.13, 143.22, 143.34, 143.40, 143.48, 143.56, 143.69, 143.73, 146.68, 146.70. UV-Vis λ_{max}/ nm (CHCl₃) (log ε): 235, 264, 296. IR (ATR) [cm⁻¹] 3045, 2945, 2854, 2776, 1687, 1609, 1436, 1375, 1318, 1262, 1219, 1089, 885, 811, 733, 689. HRMS (APPI-TOF) calcd. for C₃₂H₂₀O₃ 452.14, found 452.1537

* The internal free volume of **2-Br** allows for undesirable solvents such as chloroform to become trapped in its solid phase; solvents such as chloroform and dichloromethane will form reactive carbenes in the presence of *n*-BuLi which lead to undesired side products and yields for this reaction. Therefore, the **2-Br** substrate is dissolved in THF and evaporated multiple times to allow for solvents such as chloroform to be removed from the substrate.

** The furan adduct (**8-H**) is believed to degrade upon interaction with silica, therefore, the crude material is purified only by crystallization.

Sulfolene Product (9-H): A 500 mL high pressure reaction vessel is charged with sodium bicarbonate (1.1 g, 13.0 mmol), 3-sulfolene (2.2 g, 18.6 mmol), furan adduct (**8-H**) (973 mg, 2.0 mmol), and pyridine (70 mL). The vial is then sealed and allowed to react, under pressure, 120 °C for 4 days. After cooling to room temperature, the vessel is opened and the reaction mixture is evaporated to dryness under reduced pressure. The mixture is then dissolved in CH₂Cl₂ and ran through a Whatman 1 filter to remove salts. The filtered solution is precipitated with a CH₂Cl₂/EtOH solution to yield an off white yellowish product 1.76 g, (83%). ¹H NMR (500 MHz, CDCl₃) δ 7.25- 7.14 (m, 6H), δ 5.88-5.85 (m, 6H), 5.26-5.25 (d, J = 1.02Hz, 2H), 4.87-4.81 (m, 6H), 2.42-2.38 (m, 6H), 2.04-1.94 (m, 6H), 1.83-1.74 (m, 12H). ¹³C NMR (500 MHz, CDCl₃): 27.4, 42.2, 54.7, 76.7, 77.0, 77.2, 84.8, 114.7, 129.0, 142.9, 144.4. UV-Vis λ_{max} / nm (CHCl₃) (log ε): 234, 296. IR (ATR) [cm⁻¹]: 3045, 2950, 2854, 2781, 2117, 1987, 1687, 1436, 1379, 1318, 1297, 1262, 1214, 1089, 885, 815, 737, 698. HRMS (APPI-TOF) calcd. for C₄₄H₃₈O₃ 614.28, found 452.1537

Antrip (1-H): A round bottom flask was charged with sulfolene product (**9-H**) (1.76 mg, 2.8 mmol), 3.5 eq. triphenylmethanol (2.6 g, 8.4 mmol), and trifluoroacetic acid (80 mL) and stirred at room temperature overnight under N₂. The green solution is quenched with methanol and evaporated under reduced pressure. The material is triturated with hot hexanes three times followed by hot MeOH three times to remove excess triphenylmethanol and

triphenylmethane byproduct. The material is suspended in a mixture of hot 30% CHCl_3 /hexanes, sonicated, and eluted through a pad of silica using a 30% CHCl_3 /hexanes as the mobile phase; 250 mL fractions were taken and monitored by NMR. The semi-pure fractions were combined and precipitated using CH_2Cl_2 and cyclohexane to yield 170 mg of a yellow solid (11%). The proton NMR and mass spectrum match previously reported results.⁹ ^1H NMR (500 MHz, CDCl_3) δ 8.28 (s, 6H), δ 7.91 (s, 6H), δ 7.90-7.89 (m, 7H), δ 7.37-7.35 (m, 7H). (APPI-TOF) calcd. for $\text{C}_{44}\text{H}_{26}$ 554.2034, found 554.2027.

Methoxy triptycene: 9-Methoxyanthracene (8.52 g, 0.03 mmol) and isoamyl nitrite (6.0 mL, 0.04 mmol) are dissolved in 1,2-dimethoxyethane (DME) (60 mL) in a three-neck round bottom flask. The solution is brought to reflux at 96 °C. Anthranilic acid (15.6 g, 0.113 mmol) is dissolved in DME (70 mL) in a separate flask. The first half of the anthranilic acid solution is added dropwise to the refluxing solution, via syringe pump, over 3 h. After the first addition of the anthranilic acid solution, the reaction mixture is refluxed for additional 15 min to ensure full consumption of anthranilic acid, followed by cooling the reaction mixture to 40 °C. A second portion of isoamyl nitrite (6 mL) is slowly added to the cooled reaction mixture and brought back to reflux. Once at reflux, the remaining anthranilic acid solution is added dropwise to the refluxing reaction mixture over 3h. After complete addition of the anthranilic acid solution, the reaction mixture is cooled to room temperature. Ethanol (60 mL, 95%) is added to the cooled mixture, followed by a solution of sodium hydroxide (9.0 g in 120 mL water). The precipitated solids are filtered and washed with a cold 4:1 methanol:water solution (100 mL). The crude filtrate is dried and dissolved in xylenes (60 mL) followed by the addition of maleic anhydride (3.0 g). The mixture is refluxed for 30 min and cooled to 100 °C, followed by addition of 95% ethanol (29 mL) and a sodium hydroxide solution (8.8 g in 118 mL water) and stirred overnight. The resulting precipitate is filtered and the crude product is recrystallized from CH_2Cl_2 /methanol to give clean 9-methoxytriptycene 75% (5.5 g, 19.3

mmol). The proton NMR and mass spectrum match previously reported results.⁴⁹ ¹H NMR (500 MHz, CDCl₃) δ 7.56 – 7.51 (d, J = 7.4 Hz, 1H), 7.32 – 7.26 (d, J = 8.4 Hz, 1H), 7.01 – 6.89 (dtd, J = 25.2, 7.5, 1.3 Hz, 3H), 5.31 (s, 1H), 4.35 (s, 3H). HRMS calcd for C₂₁O₁H₁₆ 284.1201, found 284.1216. m.p. 204 – 205 °C.

Hexabromo-methoxytriptycene (2-MeO): Methoxy triptycene (1.0 g, 3.9 mmol) is dissolved in dry chloroform (stabilized with amylene) (250 mL), dried over 4 Å mol sieves, followed by the addition of fine mesh iron powder (0.03 g, 0.50 mmol). Via syringe, 6 eq of bromine (1.19 ml, 23.4 mmol) is added to the stirring room temperature solution. The reaction mixture is brought to reflux under a light flow of N₂ for 3 h. The mixture ran through a pad of silica to remove iron salts followed by evaporation under reduced pressure. The remaining solid tends to be a mixture of target MeO-HBT (**2-MeO**) and methyl deprotected OH-HBT (**2-OH**). The crude product solution is dissolved in a 30% toluene 70% hexanes mixture and ran through a pad of silica. The first band, MeO-HBT (**2-MeO**), is collected (*r.f.* of ~0.7) and dried under reduced pressure evaporation. The target product is then recrystallized twice, once from a THF/MeOH solution followed by a THF/hexanes solution to give a white to yellowish solid MeO-HBT (**2-MeO**) (1.59 g, 2.09 mmol), 60%. The remaining OH-HBT (**2-OH**) ~35%, can be isolated and re-methylated using a well-established literature method.⁴⁹ The proton NMR and mass spectrum match previously reported results.⁹ ¹H NMR (500 MHz, CDCl₃) δ 7.78 (s, 1H), 7.58 (s, 1H), 5.11 (s, 1H), 4.26 (s, 3H). HRMS calcd for C₂₁Br₆O₁H₁₀ 751.5832, found 751.5862. m.p. 354 – 355 °C.

MeO-Furan Adduct (8-MeO): The title compound is prepared following a modified literature method.⁵⁶ A sample of MeO-HBT (**2-MeO**) that is free of reactive solvents (5.0 g, 6.5 mmol) is added to a flame dried Schlenk flask followed by the addition of freshly distilled tetrahydrofuran (250 mL). Dry, freshly distilled furan (10 mL) is added via syringe under a N₂ atmosphere to the stirring mixture of **2-MeO**. The mixture is cooled to –78 °C in a dry ice

acetone bath and is evacuated and purged 3x with N₂ followed by the addition of 1.6 M *n*-BuLi (15 mL), added slowly, over one hour, via syringe pump to the vigorously stirring atmospherically inert solution. The solution is stirred under nitrogen at -78 °C for 30 mn after addition of *n*-BuLi. The reaction is quenched at -78 °C with a 5%isopropanol/toluene solution and is evaporated under reduced pressure. The remaining solid is dissolved in chloroform and filtered using Whatman 1 filter paper to remove salts. The resulting solution is precipitated from a chloroform/methanol solution followed by filtration yielding an off white solid MeO-Furan adduct (**8-MeO**) (2.3 g, 4.8 mmol), 75% yield.** The proton NMR and mass spectrum match previously reported results.¹⁵ ¹H NMR (500 MHz, CDCl₃) δ 7.47 (m, 3H), 7.25 (m, 3H), 6.94 (m, 6H), 5.58 (m, 6H), 5.04 (s, 1H), 4.29 (s, 3H). HRMS calcd for C₃₃H₂₈O₄ 482.1518, found 482.1527.

* The internal free volume of MeO-HBT (**2-MeO**) allows for undesirable solvents such as chloroform to become trapped in its solid phase; solvents such as chloroform and dichloromethane will form reactive carbenes in the presence of *n*-BuLi which lead to undesired side products and yields for this reaction. Therefore, the MeO-HBT (**2-MeO**) substrate is dissolved in THF and evaporated multiple times to allow for solvents such as chloroform to be removed from the solid.

** MeO-Furan adduct (**8-MeO**) is believed to degrade upon interaction with silica, therefore, the crude material is purified only by crystallization.

MeO-Sulfolene Product (9-MeO): The title compound was prepared following a modified literature method.¹⁵ A 500 mL pressure vessel is charged with sodium bicarbonate (500 mg, 5.95 mmol), 3-sulfolene (2.2 g, 18.61 mmol), MeO-Furan adduct (**8-MeO**) (1 g, 1.54 mmol), and pyridine (80 mL). The vial is capped and heated to 120 °C for 4 days. The reaction mixture is cooled and evaporated to dryness under reduced pressure. The remaining solid is dissolved in dichloromethane and filtered using a Whatman 1 filter paper to remove insoluble salts. The

resulting crude solution is purified by precipitation using a CH₂Cl₂/methanol solution followed by filtration to give (1.2 g) of an off white solid, quantitative yield*. The proton NMR and mass spectrum match previously reported results.¹⁵ ¹H NMR (500 MHz, CDCl₃) δ 7.42 (m, 3H), 7.17 (m, 3H), 5.87 (m, 6H), 5.16 (s, 1H), 4.86 (m, 6H), 4.33 (s, 3H), 2.41 (m, 6H), 1.97 (m, 6H), 1.8 (m, 6H). HRMS calcd for C₄₅H₄₀O₄ 644.2926, found 644.2903.

* MeO-Sulfolene Product (**9-MeO**) is believed to degrade upon interaction with silica, therefore, the crude material is purified only by crystallization.

MeO-Antrip (1-MeO): A flask is charged with the MeO-sulfolene Product (**9-MeO**) (1.2 g, 1.8 mmol) and 3.5eq triphenylmethanol (1.69 g, 6.5 mmol) followed by the slow addition of trifluoroacetic acid (80 mL). The reaction is stirred at room temperature under N₂ and stirring for 18h. The resulting green mixture is evaporated under reduced pressure. The excess triphenylmethanol and triphenylmethane byproduct are removed by trituration using hot hexanes followed by hot methanol. The resulting green solid was then suspended with a hot 30% CH₂Cl₂ 70% hexanes mixture and sonicated. The suspension is eluted through a pad of silica using a 30% CH₂Cl₂ 70% hexanes mobile phase. Fractions of 250 mL were collected and monitored by NMR. The resulting semi-pure white solid is precipitated using CH₂Cl₂ and cyclohexane to yield (64 mg, 0.10 mmol) 6% (1-H). The proton NMR and mass spectrum match previously reported results.¹⁵ ¹H NMR (500 MHz, CDCl₃) δ 8.34 (s, 3H), 8.28 (s, 3H), 8.24 (s, 3H), 8.00 (s, 3H), 7.92 (m, 6H), 7.40 (m, 6H), 5.67 (s, 1H), 4.69 (s, 3H). HRMS calcd for C₄₅H₃₄O 584.2140, found 584.2143. IR (ATR) [cm⁻¹] 3630, 3043, 2951, 2921, 2850, 2157, 2025, 1943, 1778, 1717, 1625, 1536, 1420, 1295, 1258, 1218, 1163, 1136, 1056, 1004, 977, 949, 891, 855, 787, 735, 699, 638. UV-Vis λ_{max}/nm (CH₂Cl₂): 279, 329, 344, 362, 380.

OH-Antrip (1-OH): A flask is charged with **1-MeO** (45 mg, 0.017 mmol) and acetic acid (1 mL) followed by the slow addition (5 to 10 mn) of 48% HBr/acetic acid (1 mL). The mixture is stirred at reflux overnight under N₂. The reaction mixture is quenched with ice and the

resulting precipitate is filtered. The precipitate is dissolved in 30% CH₂Cl₂ 70% hexanes and loaded on a pad of silica to elute any unreacted starting material then the mobile phase is switched to CH₂Cl₂ to elute **1-OH**. The target band is collected and evaporated under reduced pressure to yield a yellow solid (99%). The proton NMR and mass spectrum matched previously reported results.¹⁵ ¹H NMR (500 MHz, CDCl₃) δ 8.32 (s, 1H), 8.29 (s, 1H), 8.17 (s, 1H), 8.01 (s, 1H), 7.94-7.91 (m, 6H), 7.43-7.37 (m, 6H), 5.78 (s, 1H), 3.80 (s, 1H). HRMS calcd for C₄₄O₁H₂₆ 570.1984, found 570.1972. m.p. > 243 °C (decomposes).

Isoindole precursor. A 500 mL Schlenk flask is charged with chloropentafluorobenzene (9.0 mL, 14.12 g, 69.72 mmol) and freshly distilled diethyl ether and cooled to -78 °C under an inert atmosphere. After three evacuation and N₂ purge cycles, 1.6 M in hexanes *n*-BuLi (48.0 mL, 76.8 mmol) is slowly added over a period of 80 mn using a syringe pump. The reaction is let to react at -78 °C for 60 mn after *n*-BuLi addition. Freshly distilled N-methylpyrrole (25.0 mL, 22.9 g, 281.7 mmol) is added to the -78 °C solution over the span of 25 mn. The reaction is left under N₂ to warm to room temperature overnight. The crude reaction mixture is quenched with isopropanol and evaporated under reduced pressure followed by sublimation using a U-tube connected to the reaction mixture at 130 °C and a clean round bottom under reduced pressure. The resulting condensate is a mixture of isoindole precursor and excess N-methylpyrrole which is purified by crystallization with THF and hexanes. The resulting white needles are filtered and washed with cold hexanes yielding 7.8 g isoindole precursor. The proton NMR and mass spectrum match previously reported results.²³ ¹H NMR (500 MHz, CDCl₃) δ: 6.98 (s, broad, 2H), 4.86 (s, very broad, 2H), 2.14 (s, broad, 3H). Mp: 74 – 77.5 °C, Gribble⁵² Mp: 74.5 - 76 °C).

Isoindole (12-F). A round bottom is charged with (7.8 g, 34.04 mmol) of isoindole precursor and (150 mL) of CH₂Cl₂. Bis(2-pyridyl)-1,2,4,5-tetrazine²³ (8.5 g, 36.02 mmol) is added to the stirring, room temperature solution and is brought to reflux under N₂ for 18 h. The mixture is

cooled to room temperature and filtered through a pad of silica gel using CH₂Cl₂ as a mobile phase. A second pad using CH₂Cl₂ as a mobile phase is employed to isolate the isoindole from the excess tetrazine. The solution is evaporated under reduced pressure at < 45 °C to yield a clean orangish-yellow solid 4.7 g, 69% yield. The proton NMR and mass spectrum match previously reported results.²³ ¹H NMR (500 MHz, CDCl₃) δ: 7.16 (s, 2H), 4.00 (s, 3H). Mp: 168.5 – 170 °C (Lit. 172 – 174 °C).

Fantrip precursor, tri-fold adduct (11-F). A 500 mL oven dried Schlenk flask is charged with dry **2-Br** (4.93 g, 6.7 mmol) and isoindole (5.5 g, 27 mmol). Freshly distilled THF (250 mL) is added to the flask and the solution is brought down to -78 °C using a dry ice acetone bath. The solution is evacuated and purged with N₂ three times. 1.6 M *n*-BuLi (16 mL) is slowly added to the stirred mixture over 1 h. The reaction mixture is quenched with a 5% isopropanol/toluene solution and evaporated under reduced pressure. The crude solid is then dissolved in CH₂Cl₂ and ran through a pad using CH₂Cl₂ as the mobile phase. With a CH₂Cl₂ mobile phase, the first band contains excess isoindole. The mobile phase is then switched to EtOAc to elute the brown, more polar, target trifold adduct band. The EtOAc fraction is evaporated under reduced pressure to give a semi pure brown solid 4.4 g, that is precipitated with CH₂Cl₂ and methanol and filtered. The proton NMR and mass spectrum match previously reported results.²³ ¹H NMR (500 MHz, CDCl₃) δ: 7.42 – 7.22 (m, 6H), 5.24 – 4.97 (m, 8H), 2.27 – 2.02 (m, 9H).

Fantrip (1-F). A round bottom flask is charged with Fantrip precursor (**11-F**) (13.2 g) followed by the addition of *t*-BuOH (250 mL). To the stirring room temperature solution, 60 eq of H₂O₂ (92 mL) is added and the mixture is brought to reflux under N₂ for 18 h. The reaction mixture is diluted with 200 mL of CH₂Cl₂ and washed with H₂O. The organic layer is collected and evaporated under reduced pressure. The crude solid is dissolved in 250 mL of THF and evaporated down to ~90 mL to obtain a precipitate that is filtered and washed with cold THF.

This process is repeated three times to give a pure orangish-yellow solid (1.1 g, 1.4 mmol) 11%. The proton NMR and mass spectrum match previously reported results.²³ ¹H NMR (500 MHz, CDCl₃) δ: 8.55 (s, 6H), 8.15 (s, 6H), 5.94 (s, 2H).

Hydroxy fantrip (1-FOH). A 500 mL Schlenk flask was charged with (2.77 g, 0.0037 mol) **2-OH**, taken from the synthesis of hexabromo-methoxytryptcene (**2-MeO**), and 4 eq of tetrafluoroisindole (3.03 g, 0.0149 mol) **12-F**. Under a nitrogen atmosphere, 200 mL of freshly distilled THF is added to the flask and is brought down to -78 °C. *n*-BuLi, 4.5 eq, is added to the stirring solution under a nitrogen atmosphere over 15 min using a syringe pump. The reaction mixture was left to stir for 30 min at -78 °C after the addition of *n*-BuLi followed by quenching with 5% MeO/toluene solution. The reaction mixture was then evaporated under reduced pressure. The crude mixture is then eluted through a plug of silica initially using CH₂Cl₂ to collect excess **12-F** and non-polar impurities. The polar, brown target bands are pushed through using ethyl acetate. These bands are collected and evaporated under reduced pressure, followed by precipitation with CH₂Cl₂/methanol solvent system to acquire semi-pure **11-OH** (0.98 g). Due to the inability to fully isolate **11-OH**, deamination to target **1-FOH** was carried through with semi-pure **11-OH**. The same deamination conditions above towards target **1-F** were used for **1-FOH**. A 100 mL round bottom was charged with 0.98 g of semi-pure **11-OH** followed by the addition of 50 mL of *t*-BuOH and brought to 100 °C. To the stirring solution 60 eq of 70% H₂O₂/water was added to the solution and left to react overnight, in the dark, under a nitrogen atmosphere. Overnight an orange precipitate forms which is filtered using a Whatman 1 filter paper and rinsed with methanol, giving 120 mg of **1-FOH**, overall yield of 4%. ¹H NMR (500 MHz, CDCl₃) δ 8.34 (s, 3H), 8.28 (s, 3H), 8.24 (s, 3H), 8.00 (s, 3H), 7.92 (m, 6H), 7.40 (m, 6H), 5.67 (s, 1H), 4.69 (s, 3H). ¹³C NMR (500 MHz, CDCl₃): 51.6, 78.8, 118.5, 118.9, 119.1, 121.8, 131.1, 131.2, 139.6, 140.5, 142.6, 142.8. ¹⁹F NMR (500 MHz, CDCl₃): -132.8 (s), -139.7(s), -147.4(m), -156.5(dd, J=10.5, 6.5Hz). HRMS calcd for

C₄₄H₁₄F₁₂O 786.09, found 786.01. IR (ATR) [cm⁻¹] 3051, 2961, 2925, 2849, 1716, 1676, 1591, 1487, 1456, 1348, 1312, 1267, 1213, 1164, 1123, 993, 880, 822, 660, 629. UV-Vis λ_{max}/nm (CH₂Cl₂): 272, 325, 340, 357, 377.

References.

- (31) Wang, Z.; Randazzo, K.; Hou, X.; Simpson, J.; Struppe, J.; Ugrinov, A.; Kastern, B.; Wysocki, E.; Chu, Q. R. *Macromolecules* **2015**, *48* (9), 2894.
- (32) Kory, M. J.; Wörle, M.; Weber, T.; Payamyar, P.; van de Poll, S. W.; Dshemuchadse, J.; Trapp, N.; Schlüter, A. D. *Nat. Chem.* **2014**, *6* (9), 779.
- (33) Clar, E. *The aromatic sextet*; J. Wiley: London, New York, 1972.
- (34) Lin, C.-H.; Lin, K.-H.; Pal, B.; Tsou, L.-D. *Chem Commun* **2009**, No. 7, 803.
- (35) Anthony, J. E. *Chem. Rev.* **2006**, *106* (12), 5028.
- (36) Long, T. M.; Swager, T. M. *Adv. Mater.* **2001**, *13* (8), 601.
- (37) Bholra, R.; University of Nevada, R.; Department of Chemistry. *From flat to curved: two-dimensional polymers and [8] circulene*; 2012.
- (38) Luo, J.; Hart, H. J. *J. Org. Chem.* **1987**, *52* (22), 4833.
- (39) Nakamichi, N.; Kawabata, H.; Hayashi, M. *J. Org. Chem.* **2003**, *68* (21), 8272.
- (40) de la Hoz, A.; Díaz-Ortiz, Á.; Moreno, A. *Chem Soc Rev* **2005**, *34* (2), 164.
- (41) Gribble, G. W.; LeHoullier, C. S.; Sibi, M. P.; Allen, R. W. *J. Org. Chem.* **1985**, *50* (10), 1611.
- (42) Hilton, C. L.; Jamison, C. R.; Zane, H. K.; King, B. T. *J. Org. Chem.* **2009**, *74* (1), 405.
- (43) Willner, I.; Halpern, M. *Synthesis* **1979**, *1979* (3), 177.
- (44) Dehaen, W.; Corens, D.; L'abbé, G. *Synthesis* **1996**, *1996* (2), 201.
- (45) Gribble, G. W.; Allen, R. W.; LeHoullier, C. S.; Eaton, J. T.; Easton, N. R.; Slayton, R. I.; Sibi, M. P. *J. Org. Chem.* **1981**, *46* (5), 1025.
- (46) Suzuki, A.; Hara, S.; Huang, X. In *Encyclopedia of Reagents for Organic Synthesis*; John Wiley & Sons, Ltd, Ed.; John Wiley & Sons, Ltd: Chichester, UK, 2006.
- (47) Jung, M. E.; Martinelli, M. J.; Olah, G. A.; Surya Prakash, G. K.; Hu, J. In *Encyclopedia of Reagents for Organic Synthesis*; John Wiley & Sons, Ltd, Ed.; John Wiley & Sons, Ltd: Chichester, UK, 2005.
- (48) Wuts, P. G. M.; Greene, T. W. *Greene's Protective Groups in Organic Synthesis*; John Wiley & Sons, Inc.: Hoboken, NJ, USA, 2006.

3. Synthetic Efforts Towards Pentiptycene Based Monomer

3.1. Overview

This chapter focuses on working towards the synthesis of a monomer consisting of a pentiptycene core with four tetrafluoro anthraceno blades, Figure 3.1. The pentiptycene based monomer is hoped to

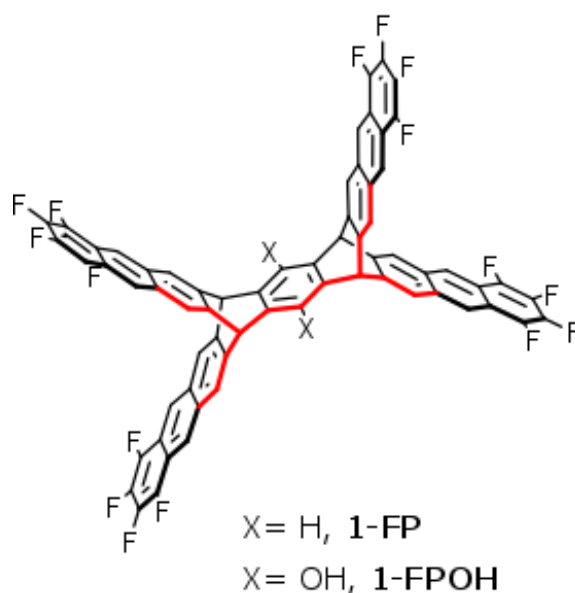


Figure 3.1. Framework of monomer with pentiptycene core shown in red.

have similar π - π interactions and reactivity as its fantrip counterpart from Chapter 2. However, instead of hexagonal packing the geometry of the above monomer will allow for topologically square packed units, Figure 3.2. The King group has yet to synthesize a 2DP with square packing using the crystal or LB trough methods of polymerization. The above monomer would be a novel addition to the field of 2DPs.

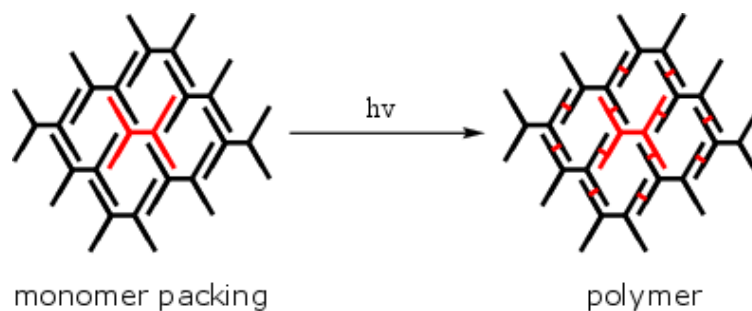


Figure 3.2. Square packing of pentiptycene based monomer, one in red for clarity, and their photo polymerization. Red lines represent bonds between repeat units.

Triptycene and pentiptycene are a class of aromatic compounds called iptycenes that are made up of arene units fused to a bicyclo[2.2.2]octatriene bridgehead system.⁵⁷ The naming of iptycenes is based on the number of arene planes separated by bicyclic bridgehead systems; the number of arene blades is denoted by a numeral prefix followed by the word iptycene. Triptycene has three arene planes separated by a bridgehead, hence the “tri” in triptycene, and pentiptycene has five arene planes separated by two bridgehead systems, hence the “pent” in pentiptycene, Figure 3.3.

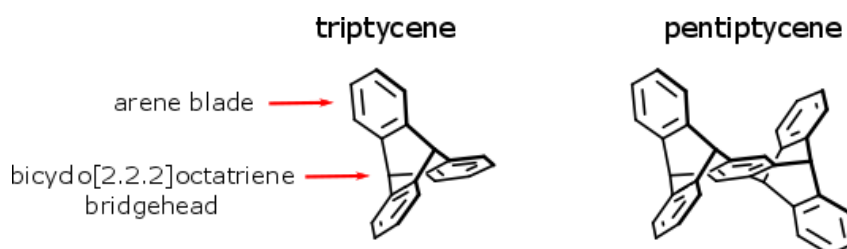
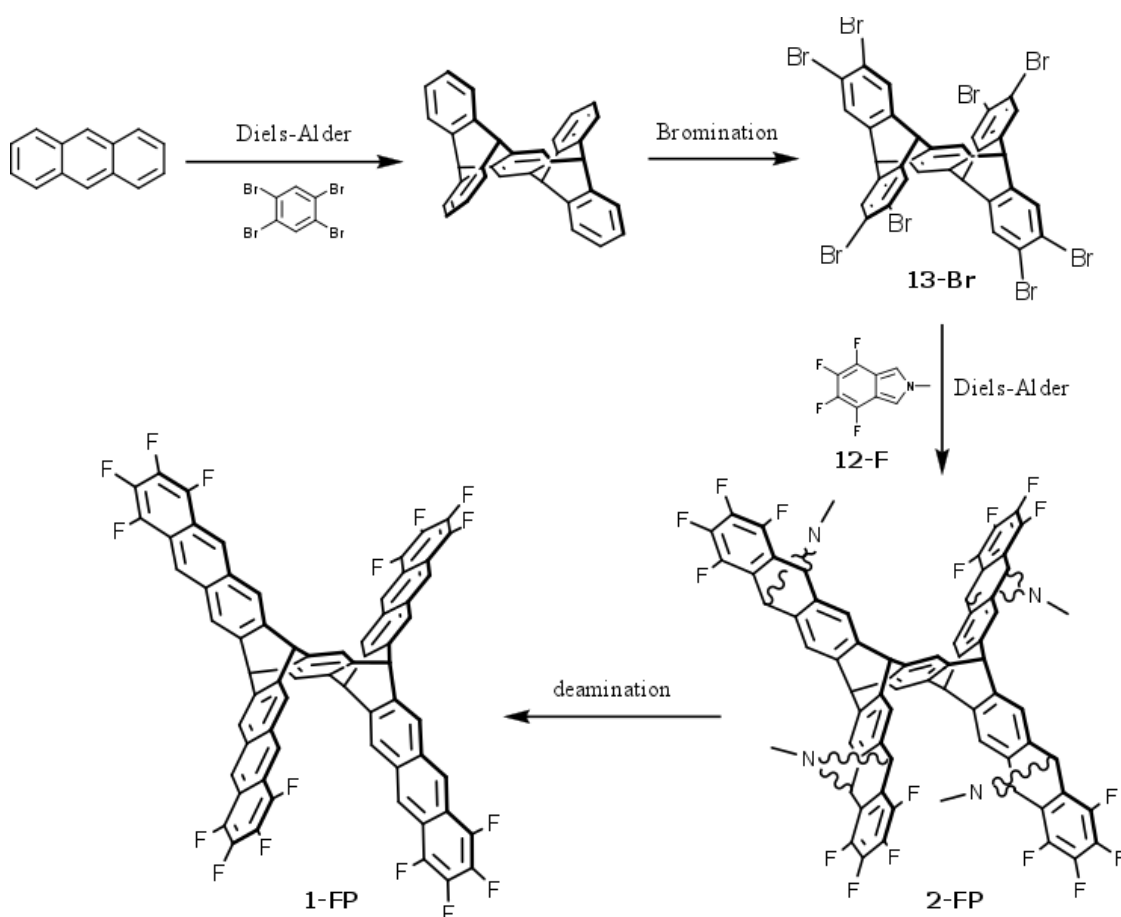


Figure 3.3. Examples of triptycene and pentiptycene illustrating the arene blades and bridgeheads.

Much like the synthesis of the monomers in Chapter 2, the synthesis of a pentiptycene based monomer consists of unidirectional acene homologation from the pentiptycene core. Fortunately, development of the monomers from chapter 2 has provided an understanding of acene synthesis that works for these types of systems.

3.2. Results and Discussion

Due to the success of the fantrip (**1-F**) synthesis, a similar synthetic route was designed for the pentiptycene based monomer, **1-FP**, using a one-step Diels-Alder route. Building the carbon framework of monomer **1-FP** starts with the synthesis of pentiptycene, followed by its bromination giving **13-Br** followed by a Diels-Alder with tetrafluoroisindole giving **12-F** and finally deamination to give target **1-FP**, Scheme 3.1.



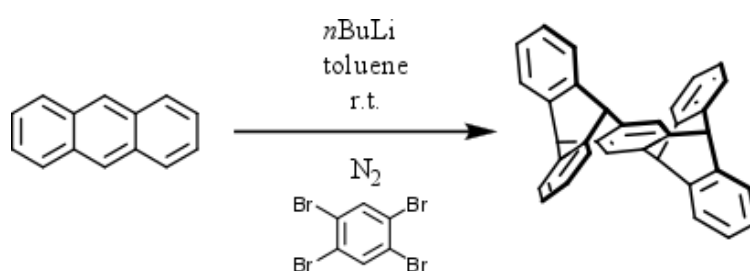
Scheme 3.1. General synthetic route towards monomer **1-FP**.

Hart *et. al.* previously made pentiptycene by lithiating a mixture of tetrabromobenzene and anthracene in room temperature toluene claiming a 97% yield.⁵⁸ Hart's yield, however, is deceiving because it is based on consumption of anthracene, not

isolated pentiptycene. Harts true yield of pentiptycene was actually 22%. In our hands, Harts conditions resulted in a 12% yield of pentiptycene, Scheme 3.2.

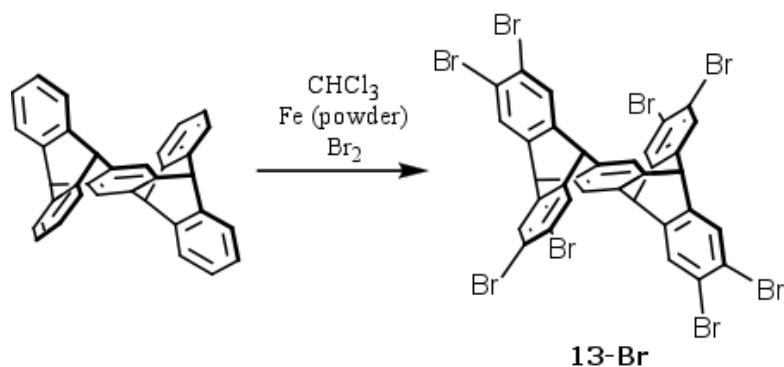
Room temperature conditions for the lithiation are used due to the limited solubility of anthracene and tetrabromobenzene in toluene. However, even in room temperature toluene solubility was minimal, which is likely responsible for the incomplete reaction and low yields of the transformation.

The crude reaction mixture consisted of unreacted anthracene, triptycene and pentiptycene. All have very similar R_f values making resolution by chromatography difficult. To assist in isolation via column chromatography, the crude mixture was reacted with maleic anhydride in refluxing xylenes. The maleic anhydride and anthracene in the crude mixture react to form a maleic anhydride-anthracene adduct which effectively increases the polarity of the left-over anthracene. This step kept the large excess of anthracene from co-eluting with the target pentiptycene during chromatography. Nevertheless, pentiptycene isolation was still difficult due to other side products and required a long column followed by trituration with hot hexanes.



Scheme 3.2. Pentiptycene synthesis using Harts conditions, 12% yield.⁵⁸

After obtaining clean pentiptycene, it was brominated using similar conditions to the bromination of triptycene with 8.1 equivalents of Br_2 , iron powder, and dry chloroform, Scheme 3.3.



Scheme 3.3. Bromination of pentiptycene using Br_2 , Fe (powder), in chloroform, semi-pure yields of 20%.

The eight-fold bromination of pentiptycene was accomplished, however, purification was problematic and column chromatography resulted in material that was slightly impure.

Bromination of iptycenes can be quite difficult. As observed with the six-fold bromination of triptycene, solubility drastically decreases as the number of carbon-bromine bonds increases. A lack of solubility was the main issue with the bromination of pentiptycene. Resolving a solubility issue is typically approached by using longer reaction times and higher temperatures. Unfortunately, longer reaction times and higher temperatures seemed to promote the evaporation of bromine, thus altering the reaction mixtures stoichiometry, leading to only small quantities eight-fold brominated product and randomly brominated material, as indicated by mass spectra and NMR. Higher boiling point solvents such as carbon tetrachloride and tetrachloroethane were employed but did not result in a solubility increase or a change in product. Unfortunately, ideal conditions for the eight-fold bromination were not found, resulting in randomly brominated products all with similar R_f values. The isolation of pure eight-fold brominated pentiptycene (**13-Br**) was impractical.

The small quantities of semi-pure **13-Br** obtained were reacted with $n\text{-BuLi}$ and excess of *N*-methyltetrafluoro isoindole (**12-F**) in THF at $-78\text{ }^\circ\text{C}$. Unfortunately, NMR or mass spectra

showed no signs of target **2-FP**, Scheme 3.1. This was likely due to the low solubility of **13-Br** in THF at cryogenic temperatures as well as its impure nature. The failure of this lithiation and difficulty in obtaining practical quantities of clean **13-Br** motivated exploration of other routes towards a pentiptycene based monomer.

Pentiptycene quinone has the same carbon framework as parent pentiptycene, and gram scale quantities of the quinone can be easily obtained through a simple Diels-Alder cycloaddition, Figure 3.4. This made pentiptycene quinone an ideal candidate as the starting core of the monomer.

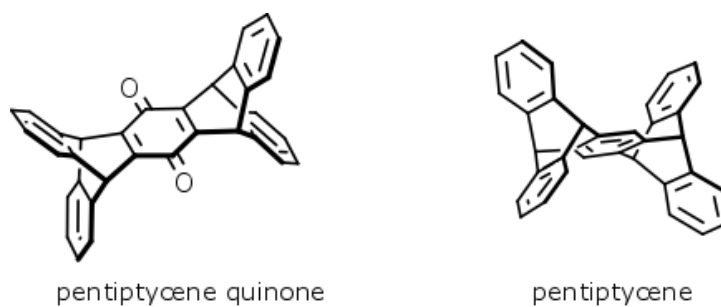
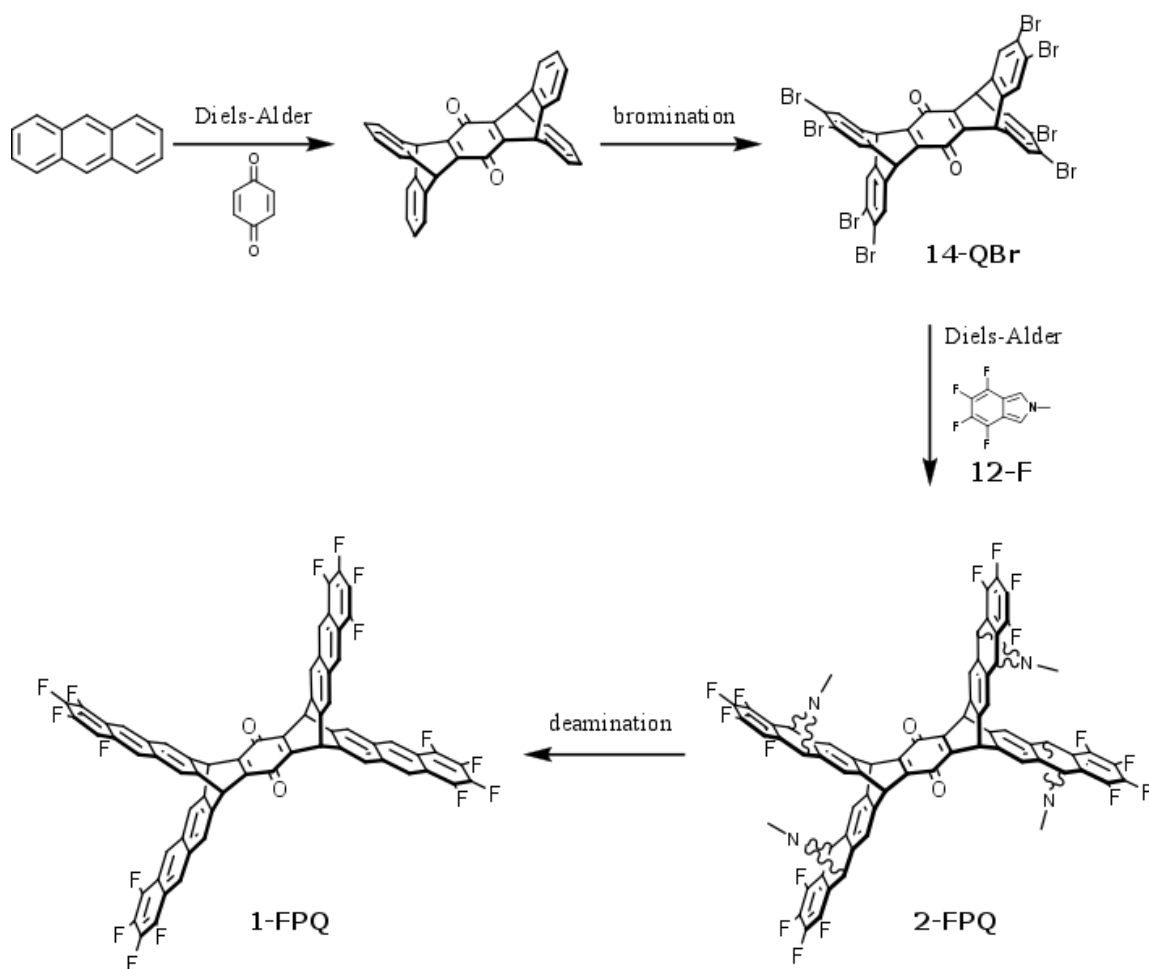


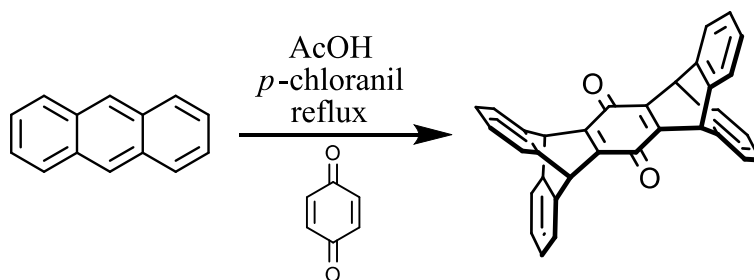
Figure 3.4. Structures of pentiptycene quinone and parent pentiptycene.

Seen below, Scheme 3.3, presents an alternative synthetic route that uses pentiptycene quinone as the core instead of pentiptycene, and a final product that results in the same carbon framework as **1-FP**. Once pentiptycene quinone is obtained, the same series of transformations for the **1-FP** route, Scheme 3.1, can be applied to the new core. It was believed that the presence of a quinone moiety would not directly interfere with the routes transformations or affect the final monomers ability to polymerize, therefore, we proceeded with the below route, Scheme 3.4.



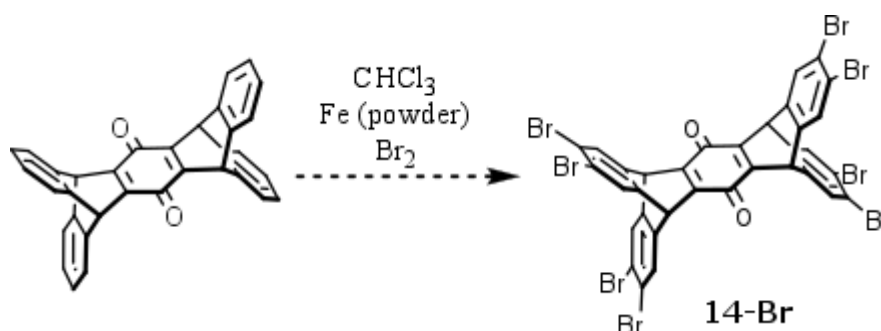
Scheme 3.4. New synthetic route utilizing the more synthetically accessible pentiptycene quinone as the starting core. This is followed by its bromination, Diels-Alder with **12-F**, and deamination to give final product **1-FPQ**.

Scheme 3.5 shows the one pot synthesis of pentiptycene quinone which was developed by the Chen group to yield product on the gram scale.⁵⁹ Synthesis involves a Diels-Alder between anthracene and benzoquinone in the presence of chloranil in refluxing acetic acid. A short pad of silica results in 85% yield, giving access to grams of the monomer core.



Scheme 3.5. Synthesis of pentiptycene quinone core, 85% yields.

After obtaining pure pentiptycene quinone the next step was its eight-fold bromination. As with parent pentiptycene, pentiptycene quinone suffered from perhaps even more severe solubility issues. Pentiptycene quinone would not fully go into solution in refluxing chloroform, and its solubility worsened as bromination proceeded as indicated by an orange precipitate. Monitoring the bromination by NMR and mass spectra gave conformation of bromination, however, no definitive evidence was found of an eight-fold bromination, **14-Br**, by mass spectra or NMR, Scheme 3.6.

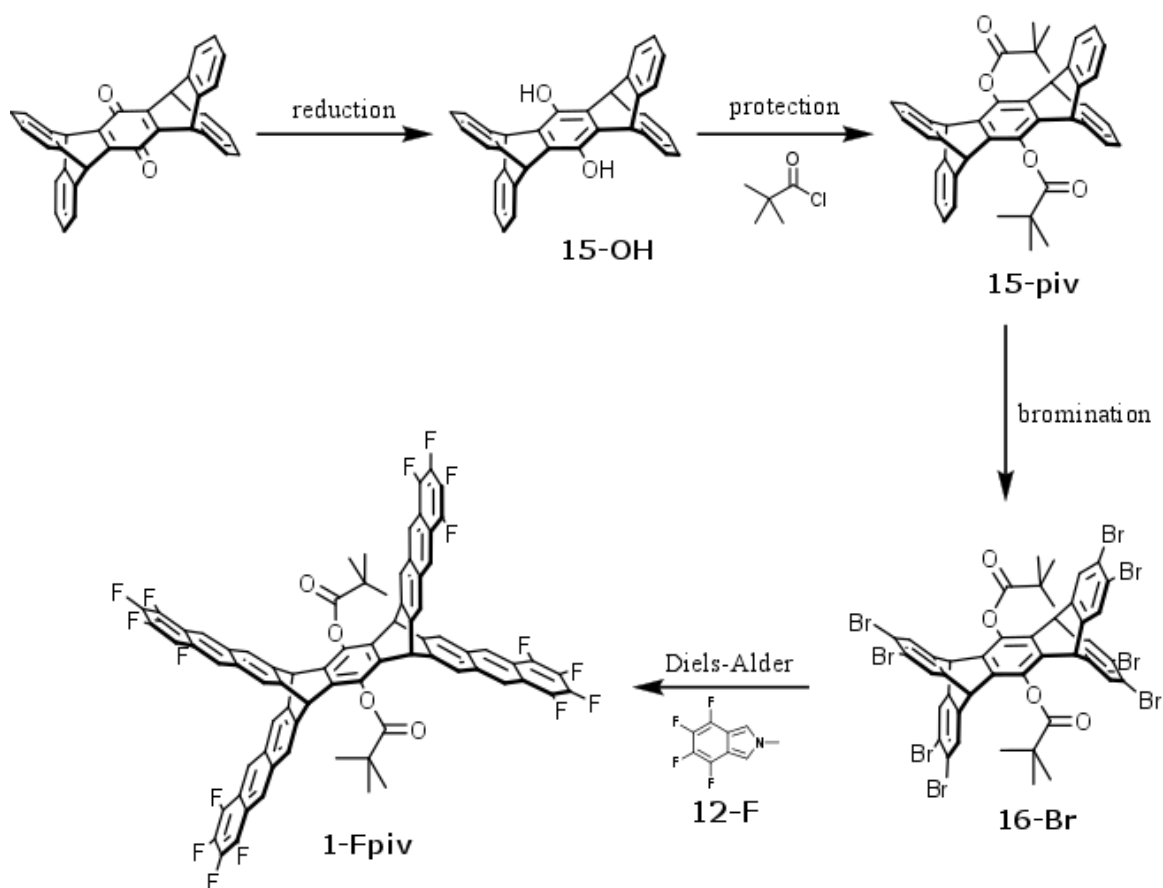


Scheme 3.6. Reaction towards the eight-fold bromination of pentiptycene quinone, **14-Br**, synthesis.

While pentiptycene quinone is much more accessible compared to pentiptycene, its lack of solubility during bromination prevented full conversion to **14-Br**. Fortunately, the quinone moiety provides synthetic handles which can be modified to help with solubility. Therefore, the synthetic route was modified by attachment of bulky substituents to increase

the solubility of the core. Reduction of the quinone carbonyls to hydroxyl groups provide convenient synthetic handles and is a known transformation.⁶⁰ Subsequent protection of the hydroxyl groups with bulky substituents would increase solubility and ideally allow the bromination to proceed to the final eight-fold brominated core before crashing out of solution.

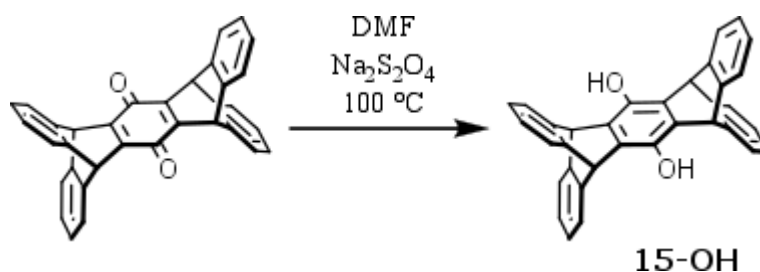
A pivaloyl substituent was chosen as the bulky hydroxyl protecting group due to its lack of reactivity with bromine and literature precedent showing a simple protection procedure of aryl hydroxides.⁶¹ A general outline of the synthetic route to the pivaloyl protected monomer **1-Fpiv** can be seen below, Scheme 3.7.



Scheme 3.7. Modified route to pentiptycene based monomer utilizing a pivaloyl protecting group.

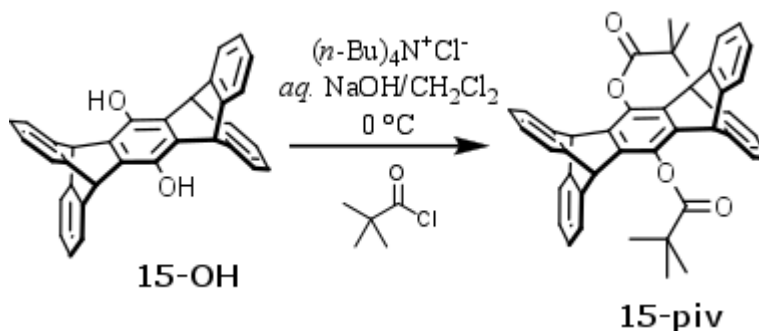
The above monomer **1-Fpiv** was initially designed for polymerization via the single crystal method. However, the deprotection of one hydroxy group would allow for attachment of a hydrophilic anchor. This would allow it to be deposited at the air-water interface and polymerized via the LB trough method. A monomer that can be polymerized via two different methods increases its chances for successful organization, which is the most difficult part in a 2D polymerization. This potential versatility makes the above monomer **1-Fpiv** very appealing.

The first transformation in the modified route towards **1-Fpiv** is the reduction of the carbonyls of pentiptycene quinone with sodium dithionite in DMF at 100 °C, a transformation that has been previously reported by the Leu group, Scheme 3.8.⁶⁰



Scheme 3.8. Reduction of pentiptycene quinone using sodium dithionite in DMF at 100 °C, 98% yield.

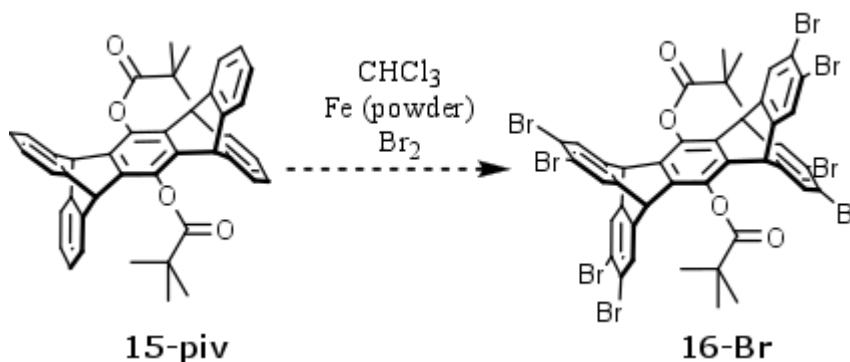
Intermediate **15-OH** was acylated with bulky pivaloyl groups under mild conditions using a biphasic mixture and the aid of a phase transfer catalyst, Scheme 3.9.⁶¹ The protection of **15-OH** involved its suspension in a 10% NaOH solution at 0 °C, this was followed by the simultaneous addition of a 0 °C dichloromethane/*tert*-butyl ammoniumchloride solution and 0 °C dichloromethane/pivaloyl chloride solution to the **15-OH** mixture and stirring for 30 minutes. Unfortunately, even with a large excess of pivaloyl chloride and extended reaction



Scheme 3.9. Protection of **15-OH** in a mixture of *aq.* NaOH/CH₂Cl₂, excess pivaloyl chloride, and phase transfer catalyst (*tert*-butylammoniumchloride) at 0 °C stirring for 30 mn, 75%.

times a small portion of mono and non-protected **15-OH** was present and required chromatography. After isolation of the target via column chromatography it was immediately evident that **15-piv** was substantially more soluble in chloroform than pentiptycene quinone or **15-OH**, Scheme 3.9.

Bromination of **15-piv** was attempted using our standard bromination conditions using dry chloroform, bromine, and iron powder, Scheme 3.10.

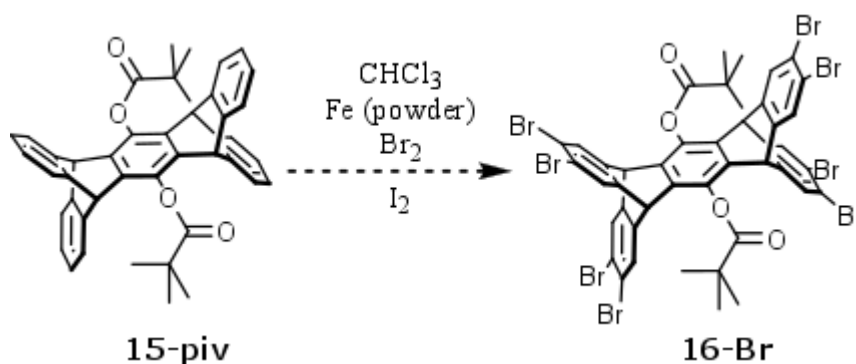


Scheme 3.10. Bromination of **15-piv**, with iron powder, bromine, in refluxing chloroform.

Unfortunately, the increased solubility of **15-piv** was not a silver bullet for the eight-fold bromination. During bromination an orange/brown precipitate formed which suggested a decrease in solubility upon bromination, and resulted in incomplete reactions. Multiple

brominations were attempted with modifications to the reaction time, temperature, and stoichiometry. Reaction times were varied from 3 h to 4 days, with catalyst loadings varying from 5 mol% to 1000 mol%. For solubility, the quantity of chloroform was increased by triple and gave no increase in solubility or reactivity. Higher boiling solvents such as carbon tetrachloride and tetrachloroethane were employed and gave no evidence of the eight-fold brominated product **16-Br**. While bromination did occur, none of the modifications produced the fully brominated **16-Br** as indicated by NMR or mass spectra.

Iodine will commonly be added to bromination reactions as a co-catalyst along with iron powder. It was hoped that by employing iodine the bromination rate towards **15-piv** would increase as well as allow a lower energy barrier towards final product **16-Br**. It was anticipated that an increased rate of bromination would out-compete bromine evaporation, thus leading to an eight-fold bromination. Seen below in Scheme 3.11 are the general conditions for the modified bromination.



Scheme 3.11. Bromination of **15-piv** using iodine as a co-catalyst with iron powder and bromine in refluxing chloroform. Reaction was monitored after 3 hours and over 4 days by NMR.

Unfortunately, the addition of iodine had no change on the bromination of **15-piv** and its eight-fold bromination was not isolated. The products, as indicated by NMR and mass spectra, were a random mixture of partially brominated material.

For a control reaction, an excess of bromine was used with an iron/iodine catalyst. This was attempted to see if it was even possible to for an eight-fold bromination. Unfortunately, refluxing in chloroform with multiple bromine additions, over 2 days, gave similar results to conditions using a stoichiometric amount of bromine. This suggested that an eight-fold bromination is not feasible with the current solubility of **15-piv**. Attempts using higher boiling solvents such as carbon tetrachloride and tetrachloroethane gave no changes in final product.

3.3. Future

The crux of the synthesis is the bromination of the pentiptycene core. Achieving an eight-fold bromination of **15-piv**, or some other pentiptycene derivative, deserves further consideration. Perhaps synthesis of a larger protecting group to promote increased solubility could lead to an eight-fold bromination. Or maybe a different route is required, one which starts with a tetrabrominated anthracene and avoids a bromination all together, Figure 3.5.

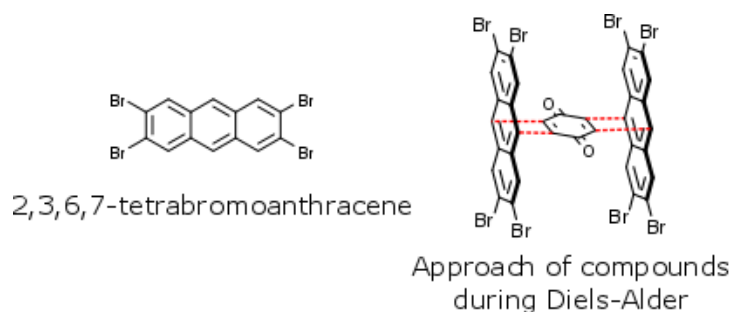


Figure 3.5. Showing 2,3,6,7-tetrabromobenzene and its approach with benzoquinone during a Diels-Alder. Red dotted lines connect bonding carbons during Diels-Alder cyclization.

A protecting group for intermediate **15-OH** that is much larger than a pivaloyl group would be a logical choice to gain increased solubility. Hydroxyl protections are well understood and access to an appropriate protecting group should be relatively straightforward. Using tetrabromoanthracene, Figure 3.5, would be an ideal reagent, however, it is extremely expensive and difficult to synthesize. Facilitating the synthesis of 2,3,6,7-tetrabromoanthracene is a worthwhile research project on its own.

3.4. Conclusion

Theoretically, monomers **1-FP** and **1-Fpiv** show promise. **1-Fpiv** has the potential to polymerize into 2DP sheets using the crystal and LB trough methods of polymerization. The main issue with both synthetic routes are the solubility issues during the eight-fold bromination. The eight-fold bromination of the pentiptycene core is the main roadblock in an otherwise understood series of transformations. If a way to increase solubility during the bromination can be achieved or the bromination step can be avoided, an interesting iptycene based monomer can be attained. There are many potential ways to acquire the final monomer framework and its synthesis deserves continued exploration.

3.5. Experimental

Synthesis of pentiptycene: To a room temperature dry toluene (250 mL) was added 1,2,4,5-tetrabromobenzene (2 g, 5 mmol), anthracene (1.78 g, 1 mol). To the stirring solution, under nitrogen, was added 1.6 M n-BuLi in hexanes (7.8 mL) over 3 h and stirred at room temperature under nitrogen for an additional 5 h. The solution was quenched using 5% methanol/toluene and evaporated under reduced pressure. The material was dissolved in xylenes and an excess of maleic anhydride was added. The solution was brought to reflux for 3 h followed by evaporation under reduced pressure. The solution was dissolved in hot chloroform and ran through a pad of silica. The first band was collected and precipitated with

hexanes giving a 12% yield. Spectral data matches previously reported results.⁶⁰ ¹H NMR (500 MHz, CDCl₃) δ 3.47 – 3.56 (s, 5H), 4.63 – 4.71 (s, 2H), 5.60 – 5.68 (s, 4H), 6.90 – 6.97 (dd, *J* = 5.4, 3.1 Hz, 8H), 7.30 – 7.36 (dd, *J* = 5.2, 3.2 Hz, 8H).

Synthesis of pentiptycene quinone: A 250 mL round bottom was charged with AcOH (120 mL), anthracene (3.65 g, 20 mmol), benzoquinone (1.08 g, 20 mmol), and an equivalent of chloranil (4.92 g, 20 mmol) and refluxed for 16 h under a nitrogen atmosphere. The solution was cooled to room temperature the resulting precipitate was filtrated and washed with cold ether giving 8.74 g of a yellow solid, 95% yield. Spectral data matches previously reported results.⁵⁹ ¹H NMR (500 MHz, CDCl₃) δ 5.73 – 5.80 (s, 4H), 6.93 – 7.03 (dd, *J* = 5.4, 3.1 Hz, 8H), 7.33 – 7.41 (dd, *J* = 5.3, 3.2 Hz, 8H).

Synthesis of pentiptycene di-hydroxide (15-OH): Pentiptycene quinone (5 g, 0.011 mol) was added to a stirring solution of NaHCO₃ (6.5 g, 0.078 mol) and Na₂S₂O₄ (6.5 g, 0.37 mol) in DMF (100 mL). The solution was heated under nitrogen at 100 °C. Over the period of 18 h three additional 6.5 g portions of Na₂S₂O₄ were added. The solution was cooled and poured into 100 mL of water and the precipitate was collected followed by reduced pressure evaporation to give **15-OH** in 97% yield. Spectral data matches previously reported results.⁵⁹ ¹H NMR (500 MHz, CDCl₃) δ 7.33 (ddd, *J* = 5.3, 3.2, 0.7 Hz, 8H), 6.94 (ddd, *J* = 5.4, 3.1, 0.8 Hz, 8H), 5.64 (s, 4H), 4.72 – 4.58 (m, 2H).

Synthesis of pivaloyl protection pentiptycene quinone (15-piv): A 100 mL round bottom was charged with **15-OH** (1.01 g, 2.1 mmol), a 10% aqueous NaOH solution (10 mL), dichloromethane (30 mL), and brought to 0 °C. In one flask a catalytic amount of tetrabutylammonium chloride (TBAC) (0.21 mmol) was dissolved in 5 mL of CH₂Cl₂ and in another flask pivaloyl chloride (6 eq) was mixed with CH₂Cl₂ (5 mL) and both were brought down to 0 °C. To the stirring, 0 °C, solution of **15-OH** was added both solutions of pivaloyl

chloride and TBAC. The solution was let to stir at 0 °C for 2 h. As the reaction proceeds it will go from a suspended precipitate to a fully dissolved yellow transparent solution. The solution is then quenched with 50 mL of ice water and the organic phase is worked up with a brine solution three times and with water three times. The organic phase is collected and dried with magnesium sulfate followed by evaporated under reduced pressure. The solution was dissolved and eluted through a silica plug using 20% hexane/ CH₂Cl₂ solution. Yellow target band was collected and evaporated under reduced pressure. The material was precipitated from a CH₂Cl₂/methanol solution and filtered giving **15-piv** at a 75% yield. ¹H NMR (500 MHz, CDCl₃) δ 1.67 – 1.72 (s, 18H), 5.26 – 5.29 (s, 4H), 6.92 – 6.96 (dd, *J* = 5.4, 3.1 Hz, 8H), 7.22 – 7.26 (dd, *J* = 5.3, 3.2 Hz, 8H). ¹³C NMR 500 MHz, CDCl₃): 27.7, 39.6, 48.8, 123.8, 125.3, 136.1, 138.6, 144.5. UV-Vis λ_{max} / nm (chloroform) (log ε): 233, 260, 270.5, 277. IR (ATR) [cm⁻¹]: 3065, 3038, 3020, 2975, 2930, 2867, 2238, 1743, 1635, 1456, 1393, 1366, 1298, 1271, 1235, 1200, 1177, 1092, 1024, 903, 723, 647. HRMS (APPI-TOF) calcd. for C₄₄H₃₈O₄ 630.28 found 630.89.

References.

- (49) Willner, I.; Halpern, M. *Synthesis* **1979**, 1979 (3), 177.
- (50) Dehaen, W.; Corens, D.; L'abbé, G. *Synthesis* **1996**, 1996 (2), 201.
- (51) Takahashi, T.; Kashima, K.; Li, S.; Nakajima, K.; Kanno, K. *J. Am. Chem. Soc.* **2007**, 129 (51), 15752.
- (52) Gribble, G. W.; Allen, R. W.; LeHoullier, C. S.; Eaton, J. T.; Easton, N. R.; Slayton, R. I.; Sibi, M. P. *J. Org. Chem.* **1981**, 46 (5), 1025.
- (53) Suzuki, A.; Hara, S.; Huang, X. In *Encyclopedia of Reagents for Organic Synthesis*; John Wiley & Sons, Ltd, Ed.; John Wiley & Sons, Ltd: Chichester, UK, 2006.
- (54) Jung, M. E.; Martinelli, M. J.; Olah, G. A.; Surya Prakash, G. K.; Hu, J. In *Encyclopedia of Reagents for Organic Synthesis*; John Wiley & Sons, Ltd, Ed.; John Wiley & Sons, Ltd: Chichester, UK, 2005.
- (55) Wuts, P. G. M.; Greene, T. W. *Greene's Protective Groups in Organic Synthesis*; John Wiley & Sons, Inc.: Hoboken, NJ, USA, 2006.
- (56) Filatov, M. A.; Balushev, S.; Ilieva, I. Z.; Enkelmann, V.; Miteva, T.; Landfester, K.; Aleshchenkov, S. E.; Cheprakov, A. V. *J. Org. Chem.* **2012**, 77 (24), 11119.
- (57) Chen, C.-F.; Ma, Y.-X. *Iptycenes chemistry: from synthesis to applications*; Springer: Heidelberg ; New York, 2013.
- (58) Hart, H.; Shamouilian, S.; Takehira, Y. *J. Org. Chem.* **1981**, 46 (22), 4427.
- (59) Cao, J.; Lu, H.-Y.; Chen, C.-F. *Tetrahedron* **2009**, 65 (39), 8104.

- (60) Yang, J.-S.; Lee, C.-C.; Yau, S.-L.; Chang, C.-C.; Lee, C.-C.; Leu, J.-M. *J. Org. Chem.* **2000**, *65* (3), 871.

4. Synthetic Development of Monomer **1-pyz** and Efforts Towards its Polymerization

4.1. Overview

In an attempt to explore other methods of polymerization outside of utilizing anthraceno functional groups, we synthesized monomer **1-pyz**, which is capable of polymerizing via coordinative bonding. While anthraceno groups are great organizational tools and undergo photopolymerization via [4+4] cycloadditions, other polymerization techniques need to be considered to expand our understanding of 2D polymerizations. Designing a 2DP which is held together by coordinative bonding broadens the scope of potential monomer design. When compared to covalent bond chemistry, ligand-metal bonding is much more flexible from a geometrical and bonding point of view. For example, metals can accommodate ligands from multiple directions and a ligand can be as simple as a Lewis base. Synthesis of a monomer possessing three or more ligands in the same plane will be capable of a 2D polymerization via coordinative bonding with a metal. Unlike a monomer whose functional groups polymerize through covalent bonding, one which polymerizes through coordinative bonding is far less restricted in terms of monomer design.

4.2. Background

Metal organic frameworks (MOFs) represent a huge field of chemistry. MOFs consist of organic ligands bound by coordinative bonds to a metal forming a crystalline lattice.⁶² Recently there have been examples of 2D coordination polymers being acquired by exfoliation of bulk MOF material and an example of a bottom up approach to synthesis.^{63,64} There are examples of 2DP coordination chemistry at the air water interface, however, the literature is sparse and deserves more attention.⁶⁵

The majority of coordination 2DPs are synthesized using the solution approach for polymerization. This relies on little to no pre-organization, but depends on reversible dynamic bonding; the goal being reversible bonding between monomer ligands and a metal until the system “self-heals” into an ordered crystal. Unfortunately, this approach commonly results in microcrystalline material making characterization by single crystal X-ray diffraction impossible. However, we hope to find conditions which allow us a quality single crystal.

Seen below is monomer **1-pyz** which consists of a benzene group with three pyrazole functionalities at the 1, 3, and 5 positions (**1-pyz**). Next to it is a simulation of **1-pyz** in an ideal topological packing showing the repeat units linked together via metal pyrazolate trimers with a metal labeled M, Figure 4.1. The proposed packing, seen below, stems from the well documented coordination behavior between pyrazolates and group 11 elements.⁶⁶

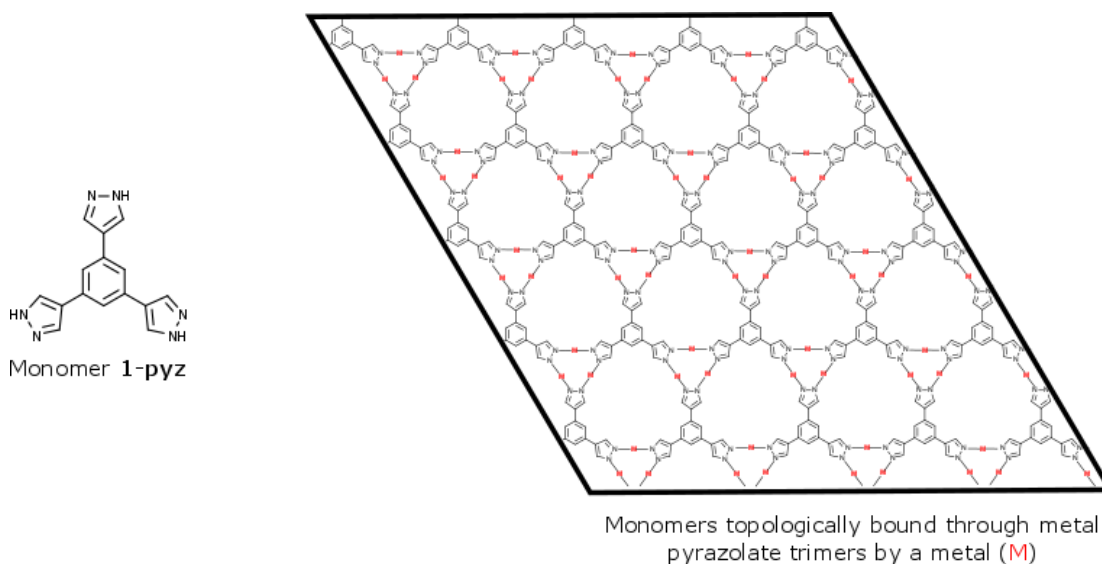


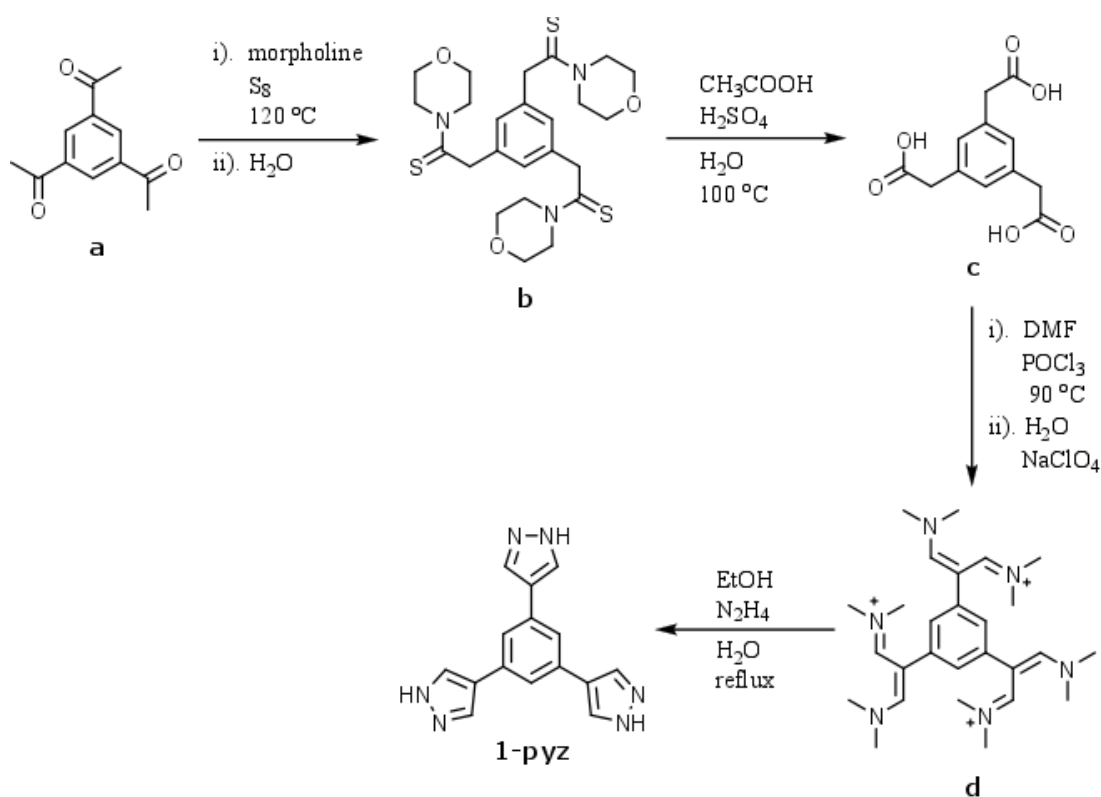
Figure 4.1. Monomer **1-pyz** with three pyrazole functionalities and its simulated packing upon a coordinative polymerization with a metal.

The solution approach, towards polymerization, was used for the polymerization of **1-pyz** and a group 11 element such as silver or gold; the main goal was to find conditions

which resulted in X-ray quality single crystals rather than microcrystals. The resulting lamellar crystalline material, would be comprised of two-dimensional coordination polymer layers, and would ideally be analyzed by single crystal X-ray diffraction followed by exfoliation into single sheets for further analysis. Accomplishing this goal first requires synthesis of the monomer and finding a metal that can undergo a polymerization resulting in metal ligand bonds robust enough to allow further characterization after exfoliation.⁶⁷

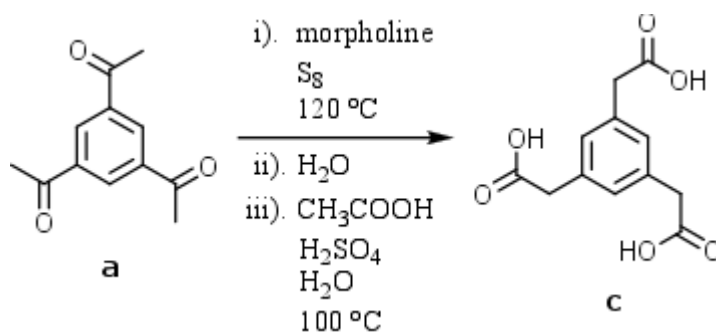
4.3. Results and Discussion

The target monomer, **1-pyz**, is a known compound and was first synthesized by Long *et al.* for use in a 3D metal organic framework (MOF).⁶⁸ Long's approach to synthesis of **1-pyz** was based on modification of the Willgerodt-Kindler Reaction seen below, Scheme 4.1.



Scheme 4.1. Willgerodt-Kindler route taken by Long and co-workers for the preparation of **1-pyz**.

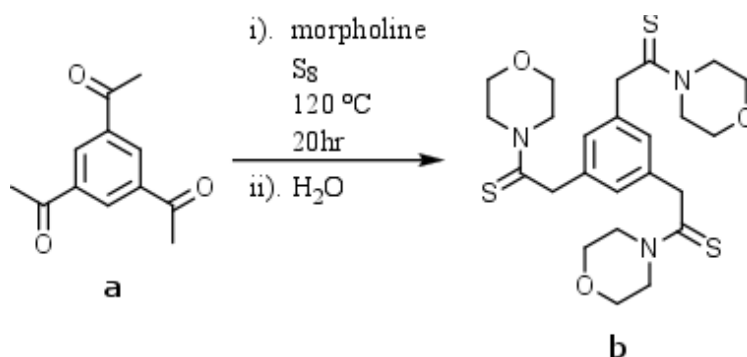
Having benzene triacetate (**a**) readily available, Longs route was attempted.⁶⁶ As reported, starting with **a**, intermediate **c** is synthesized in one-pot, Scheme 4.2.



Scheme 4.2. One-pot Willgerodt-Kindler Reaction and its hydrolysis in one pot to give benzene triacetic acid intermediate **c**.⁶⁸

The initial Willgerodt-Kindler Reaction and its hydrolysis to give **c** resulted in no product. Every attempt to make intermediate **c** resulted in brown polar material and no product by as detected by NMR or mass spectra.

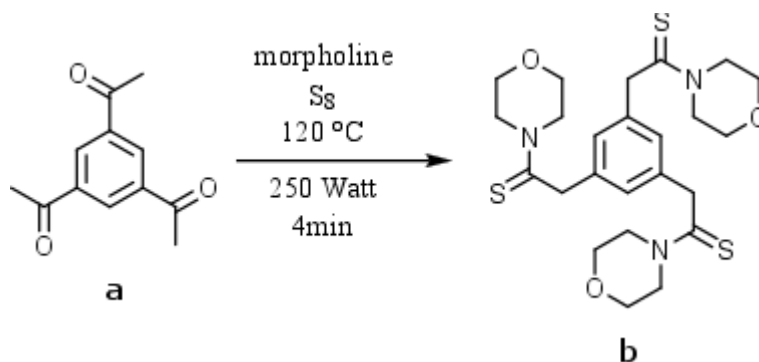
In order to gain a better understanding of the transformation, it was broken down into two separate steps to confirm that the initial bond forming reaction was taking place, Scheme 4.3.



Scheme 4.3. Synthesis of the thioamide product of the Willgerodt-Kindler Reaction.

The above transformation was attempted using Long's procedure, with the exclusion of the hydrolysis step, and gave no signs of thioamide intermediate **b**.⁶⁸

Further examination of the literature provided a procedure of the Willgerdt-Kindler reaction using microwave conditions, and reported shorter reaction times (4 mins opposed to 20 hr) with higher yields, Scheme 4.4.⁶⁹



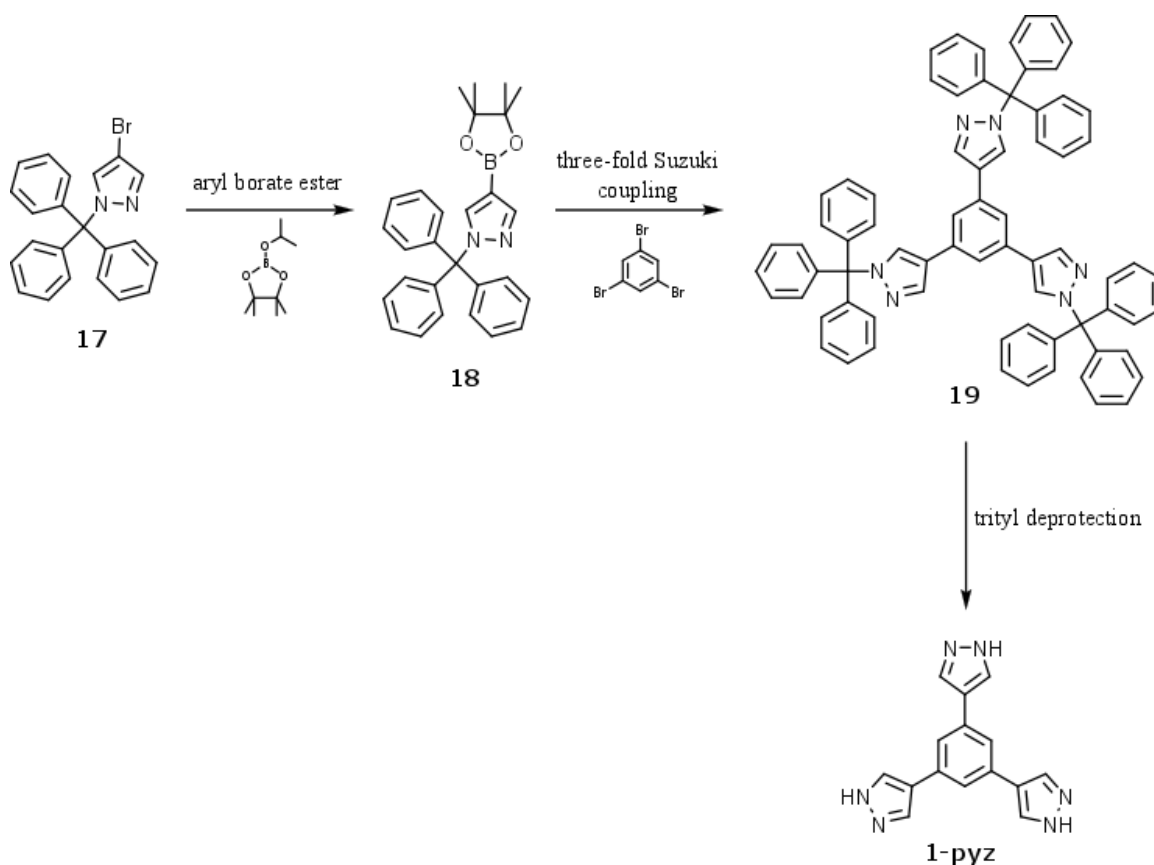
Scheme 4.4. Microwave procedure for the Willgerdt-Kindler reaction.

Attempts at the microwave synthesis also resulted in polar brown tar. Starting materials were double-checked for purity and different samples of sulfur were used to eliminate starting material inconsistencies as the problem, however, literature results were not reproduced. Not being able to replicate Long and co-workers synthesis motivated designing a new route to monomer synthesis.

Use of a metal catalyzed carbon-carbon coupling would grant straightforward access to the target monomer **1-pyz**. Unfortunately, no such reports in the literature existed for **1-pyz** using this approach and had to be developed.

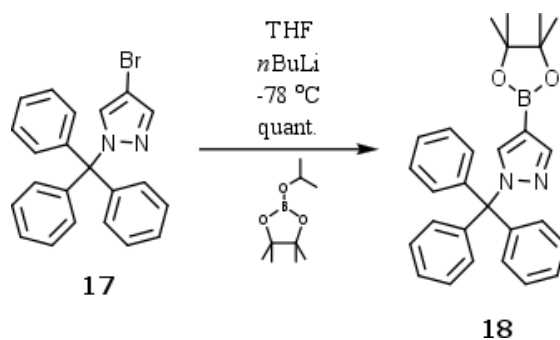
A former group member, Carey Johnson, had previously made a related compound to **1-pyz**. He had successfully performed a Suzuki cross coupling between a trityl protected 4-bromopyrazole (**17**) and a benzyl boronic pinicole ester which gave insight when investigating

a coupling transformation towards **1-pyz**.⁶⁶ With **17** and 1,3,5-tribromobenzene accessible, use of a Suzuki cross coupling was the first logical route towards synthesis of monomer **1-pyz**. Seen below are the general steps of the Suzuki route towards **1-pyz**, Scheme 4.5.



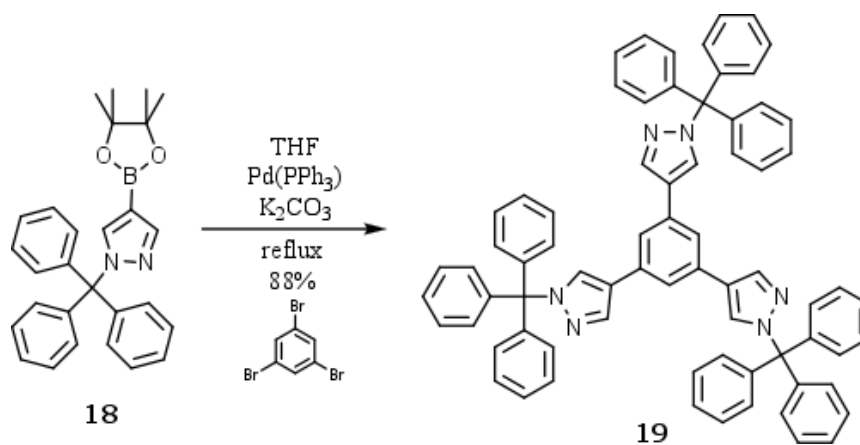
Scheme 4.5. General synthetic scheme for the Suzuki route towards monomer **1-pyz**.

Compound **17** had been previously synthesized by former group member Dr. Johnson from starting materials 4-bromopyrazole and tritylchloride.⁶⁶ There was the choice of converting 1,3,5-tribromobenzene to a three-fold boronic ester or converting **17** to boronic ester **18**, the latter was chosen. Either choice had the potential to undergo a Suzuki coupling. However, when considering chromatography, the polarity of a one-fold boronic ester is easier to deal with than a more polar three-fold boronic ester. Seen below is the quantitative synthesis of **18**, Scheme 4.6.



Scheme 4.6. Synthesis of boronic ester intermediate **18**.

Conversion of **17** to the boronic ester intermediate **18** in THF at $-78\text{ }^\circ\text{C}$ gave quantitative yields. This is followed by the three-fold Suzuki coupling of **18** with 1,3,5-tribromobenzene. After developing the Suzuki coupling reaction conditions and its purification by column chromatography, yields of 88% were achieved for **19**, Scheme 4.7.

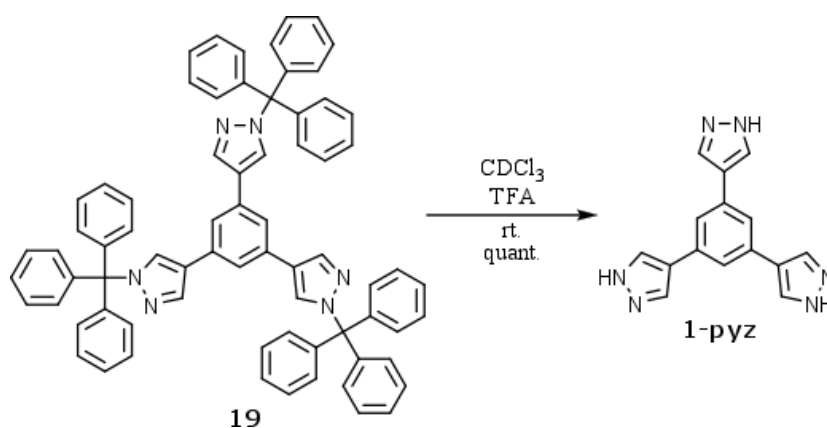


Scheme 4.7. Suzuki cross coupling between **18** and 1,3,5-tribromobenzene giving **19**.

$\text{Pd(PPh}_3)_4$ catalyst, 2M K_2CO_3 in refluxing THF for 2 days.

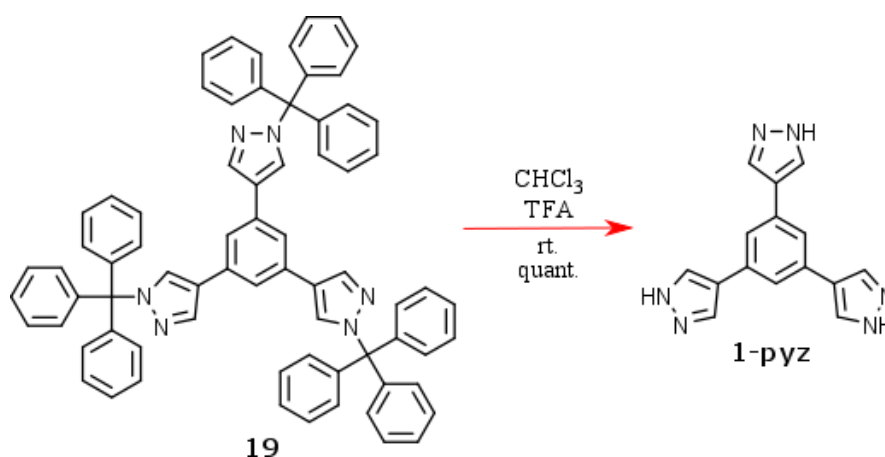
After obtaining the framework of the monomer with intermediate **19**, the deprotection of the trityl (Tr) groups gives final product **1-pyz**. Acidic conditions are common for the deprotection of trityl protecting groups. Stirring in a 5% TFA/ CHCl_3 solution followed by transfer through a pad of silica is a method of deprotection that has been reliable for similar Tr groups in the past.⁷⁰ This method of deprotection also makes monitoring by NMR

convenient if performed in *d*-chloroform. Below are the conditions for the microscale deprotection of **19**, ran in *d*-chloroform, Scheme 4.8.



Scheme 4.8. Microscale deprotection of **19** using *d*-chloroform.

After stirring in a 5% TFA/*d*-chloroform solution for 5mins the mixture was ran through a small pad of silica, directly into an NMR tube. Upon taking an NMR, the presence of **1-pyz** and trityl byproducts were evident with no sign of **19**, indicating quantitative deprotection. The success of the microscale deprotection motivated scaling up the reaction to ~100mg loadings, Scheme 4.9.



Scheme 4.9. Macroscale deprotection of **19** followed by purification. Red arrow indicates uncertainty in initial deprotections, however, solubility issues were resolved.

A 100mg scale up of the deprotection was performed using the same acidic conditions as above but with chloroform instead of *d*-chloroform. After running the reaction mixture through a pad of silica, it was dried down and triturated with hot methanol and hot hexanes to remove the trityl by-products from the mixture. The resulting grey/brown solid was dried under vacuum and an NMR sample was prepared. The NMR sample in *d*-chloroform resulted in grey/brown insoluble material at the bottom of the NMR tube. The NMR spectrum showed no peaks other than the chloroform and TMS peaks. This inconsistency motivated the use of other common deuterated solvents such as *d*₈-toluene, *d*₆-DMSO, *d*₃-MeOH, and *d*₃-acetonitrile for solubility. None of these solvents were able to dissolve the material. Scaling up of the reaction and a possible over concentration of acid were considered to be the cause of the insoluble material.

Inconsistency between microscale and macroscale deprotections motivated trying other conditions of deprotecting the Tr group. Firstly, the concentration of TFA was varied from 3 equivalents to 100%. These reactions were performed at the microscale, and the mixtures were run through small pads of silica directly into NMR tubes. Each spectrum showed target **1-pyz** and the expected trityl byproducts with no presence of **19**. However, upon purification of the reactions via trituration, the following NMR spectra showed no target **1-pyz**. These odd results caused further confusion and motivated the use of different acids for deprotection. Deprotections using HCl/MeOH, Ac₂O/AcOH, and AcOH under various temperatures were employed, and all yielded the same insoluble grey/brown material after purification via trituration with methanol and hexanes.

After a considerable amount of investigation, it was found that this insoluble grey/brown material was in fact target **1-pyz**. It turned out that the product is extremely insoluble and the presence of an acid, such as TFA, promotes its solubility in common organic

solvents. To date, the only common solvent that will solubilize the material without the aid of TFA is DMF. On the positive side, the extreme insolubility of **1-pyz** allows for its easy purification by triturating with hot solvents such as DCM giving high yields of pure **1-pyz**, 90%.

4.4. Polymerization of **1-pyz**

The polymerization of **1-pyz** with a metal relies on the solution phase approach with the primary goal of acquiring X-ray quality single crystals. However, the insolubility of **1-pyz** presents a problem that limits the number of solvents to experiment with for the polymerization. The lack of solubility of **1-pyz** is most likely due to stacking of the molecules. To increase van der Waals contact, large flat molecules commonly stack upon each other and in this case, creates an insoluble brick. Typically, one would start with at least 20 different solvents and screen conditions for this type of process.⁷¹ This becomes difficult if the number of solvents found with the ability to fully solvate the material are less than three.

It was hoped that the tendency of **1-pyz** to stack would impart some order during crystallization and facilitate single crystal growth, however, the few solvents available and the many conditions tried resulted in no success. All results of the crystallization attempts resulted in microcrystalline product. And unfortunately, microcrystalline material is difficult to fully characterize with the intent of proving the presence of a 2DP.

Literature precedent motivated the use of gold(I) and silver(I) as the metals used for the polymerization of **1-pyz**. It has been shown that gold(I) and silver(I) will make relatively strong polar covalent bonds with pyrazolate ligands which have the potential to yield a periodic 2D material such as that in Figure 4.1.

Silver and gold are commonly used to complex pyrazolate ligands which are extremely common and well understood.^{67,72} Therefore, the first attempts at polymerizing **1-pyz**

involved the common reagent, gold-THT-chloride, but resulted in the pyrazolate ligands reducing gold(I) to colloidal gold instead of the desired ligand complex. To avoid rapid reduction of gold, literature has shown that one can first react **1-pyz** with a silver salt to make a silver pyrazolate moiety, followed by its metathesis with gold. Examples of this metathesis approach are performed while the silver pyrazolate is in solution. However, our monomer is set up to undergo a 2D polymerization into an ordered crystal upon ligation with a metal, this makes the metathesis approach with gold unlikely when considering **1-pyz** would be crystalline after it initially reacts with silver. Therefore, efforts were shifted towards using silver in the polymerization of **1-pyz**.

For solubility, DMF and a mixed solvent system of 50:50 ethanol/water showed promise in their ability to dissolve **1-pyz**. DMF will completely solvate **1-pyz** and a 10% NaOH 50:50 water/ethanol solution can partially solvate **1-pyz**. Outside of the above conditions, other organic solvents and conditions were experimented with, however, all gave very limited or no solubility.

Use of a high-pressure reaction vessel was employed in hopes to achieve superheated temperatures of various solvents towards solvation and polymerization of **1-pyz** using various silver salts. This however, did not lead to the growth of X-ray quality single crystals. Furthermore, employing the microwave reactor as a convenient high pressure reaction vessel caused destruction of the apparatus. During irradiation, the silver in solution plated on the glass surface of the reaction vial and reflected the microwaves back into the reaction chamber causing melting and damage. A Teflon sleeve for the microwave vial was manufactured to avoid plating of the metal, however, damage to the microwave reactor continued and the Teflon sleeve melted. This was most likely due to the reaction mixture boiling over, allowing the silver solution to come into contact with the glass. Therefore, most experimentation with

high pressure reactions were performed thermally. Typical solvents used were DMF or a basic 50:50 ethanol:water. Use of metal salts such as AgTFA, AgOAc, Ag₂O, AgNO₃ with stoichiometry ranging from 1 to 3 equivalents and excess were employed. However, none of the conditions produced quality single crystals, only microcrystalline material. Superheated solvents such as pyridine, tetrachloroethane, toluene, and xylenes were used, however, even at extreme temperatures they did not seem to solvate **1-pyz** or give single crystals. Multiple reactions employing slow evaporation at room temperature or heating of the solution were attempted with the same conditions as above, however, gave similar microcrystalline results as the high-pressure experiments.

Unfortunately, the addition of TFA, which aids in solubilizing **1-pyz**, is not compatible with the polymerization reaction. The pyrazole groups must be deprotonated to function as a ligand, which is not possible with an acid present. Attempts at using a basic solvent, such as pyridine, in conjunction with a TFA solution were attempted. The idea was that an equilibrium would be established that would allow the pyridine solvent to deprotonate the solvated pyrazole long enough to facilitate its bonding with silver. Ideally, as crystallization progressed TFA would evaporate followed by the higher boiling pyridine, leaving behind X-ray quality single crystals. Multiple attempts employing a mixed TFA/pyridine solvent system using silver or manganese salts were attempted under atmospheric and high pressure reaction conditions but gave no single crystals.

4.5. LB Trough Method

A 2D polymerization of **1-pyz** with a metal salt, using the crystallization method, was unsuccessful and motivated the pursuit of the LB trough method of polymerization. The use of the LB trough would involve deposition of **1-pyz** to the air-water interface followed by its compression into a monolayer. A metal salt would be introduced into the sub-phase to allow

the ligands of **1-pyz** access the metal centers through diffusion, forming a 2D coordination polymer.

DMF is the only solvent found to fully solvate **1-pyz** and unfortunately is water soluble. Depositing **1-pyz**, or any molecule, to the air-water interface using a water-soluble solvent and acquiring a monolayer is difficult. Typically, a water immiscible solvent such as chloroform or dichloromethane is used when applying a solution to the interface. However, a DMF solution of **1-pyz** was made and applied to the air water interface, and gave no evidence of monolayer formation. Most likely, the DMF solution immediately immersed into the sub-phase upon application leaving behind aggregated islands of **1-pyz**. Recent literature has shown the use of an electrospray apparatus for deposition of water soluble solutions to the air-water interface and has given great results, unfortunately, we currently have no access to an electrospray apparatus.⁷³

An attempt to use a minimal amount of DMF, to solvate **1-pyz**, along with chloroform was used to apply **1-pyz** to the air-water interface and unfortunately did not result in a monolayer after compression of the barriers. A chloroform solution of **1-pyz** with the minimal amount of TFA needed for solubility was also used for deposition. The acidic solution gave no evidence of monolayer formation after compression.

Depositing **1-pyz** to the air-water interface was difficult due to its limited solubility in organic solvents. A continued search for a water immiscible solvent that can solvate **1-pyz** would allow further experimentation using the LB trough. However, this will likely necessitate modification of the benzene core of **1-pyz** with bulky groups to gain enhanced solubility.

4.6. Conclusion

A new and improved synthesis of **1-pyz** was developed using a tri-fold Suzuki coupling reaction. Making target **1-pyz** more accessible than previously reported due to its convergent synthesis and higher yields.

Solution and LB trough polymerization approaches were taken with **1-pyz**. Unfortunately, **1-pyz** is sparingly soluble in most common solvents. The proper solvent system and conditions towards a 2DP single crystal of **1-pyz** were not found, however, finding conditions for its polymerization merits further research.

Modifying 1,3,5-tribromobenzene with bulky or greasy substituents would allow alteration of the core while still retaining the convergent Suzuki coupling approach towards the synthesis of **1-pyz**. Modifications to **1-pyz** could lead to its increased solubility making its polymerization via crystallization or the LB trough methods more achievable. The main downfall of this project was undoubtedly the limited solubility of **1-pyz**. The preliminary synthesis and polymerization trials of **1-pyz** will likely motivate further research towards its derivatization and eventually its 2D polymerization.

4.7. Experimental

Synthesis of pyrazole boronic acid (18): To a 250 mL Schlenk flask was added trityl protected 4-bromopyrazole (1 g, 2.5 mmol), 2-Isopropoxy-4,4,5,5-tetramethyl-1,3,2-dioxaborolane (2.1 mL, 2.5 eq), and THF (120 mL). To the stirring solution under nitrogen at -78 °C *n*-BuLi (3 mL, 2.5 eq) was slowly added over 10 mn. The reaction was quenched with a 5% methanol/toluene solution and evaporated under reduced pressure. The material was dissolved in chloroform and eluted through a pad of silica with chloroform to remove salts, giving 1.12 g of **18**, quantitative yield. Spectral data matches previously reported results. ¹H NMR (400 MHz, CDCl₃) δ 1.26 – 1.30 (s, 12H), 7.09 – 7.15 (dd, *J* = 6.1, 3.7 Hz, 6H), 7.25 – 7.31 (m, 10H), 7.70 – 7.74 (s, 1H), 7.90 – 7.94 (s, 1H).

Synthesis of (19): A 250 mL round bottom was charged with (18) (2.03 g, 4.6 mmol), 1,3,5-tribromobenzene (0.39 g, 1.2 mmol) and Pd(PPh₃)₄ (220 mg, 0.19 mmol) while under a nitrogen atmosphere. A 2 M solution of K₂CO₃ (26 mL) and 70 mL of THF were added to the flask and was let to stir at 80 °C for 24 h under a nitrogen atmosphere. The reaction was monitored by TLC. The reaction mixture was cooled to room temperature and extracted three times with water. The organic phase was collected and evaporated to dryness under reduced pressure. The dried material was dissolved and eluted through a plug of silica with a 20% hexanes/CH₂Cl₂ solution followed by evaporation under reduced pressure. The resulting grey material was triturated with methanol followed by hexanes three times each yielding 1.1 g of (19), 87%. ¹H NMR (500 MHz, CDCl₃) δ 7.18 – 7.23 (dd, *J* = 6.8, 3.0 Hz, 7H), 7.28 – 7.29 (s, 1H), 7.30 – 7.37 (m, 10H), 7.61 – 7.63 (s, 1H), 7.93 – 7.95 (s, 1H). ¹³C NMR (500 MHz, CDCl₃): 25.5, 68.0, 79.4, 92.5, 27.8, 127.9, 130.1, 132.3, 140.2, 142.6. UV-Vis λ_{max} / nm (CHCl₃) (log ε): 226.6, 253.5. IR (ATR) [cm⁻¹]: 3150, 3087, 3056, 3029, 2957, 2921, 2849, 2233, 1955, 1806, 1716, 1600, 1487, 1438, 1384, 1321, 1298, 1182, 1155, 1078, 1029, 984, 898, 871, 844, 804, 741, 723, 692, 633. HRMS (APPI-TOF) calcd. for C₇₂H₅₄N₆ 1002.44 found 1001.89

Synthesis of (1-pyz): A sample of (19) (100 mg, 0.09 mmol) was dissolved in a 20% TFA/ CHCl₃ solution (20 mL) and let to stir at room temperature for 30 mn. The reaction mixture is eluted through a pad of silica using a 20% TFA/ CHCl₃ mobile phase, collected and evaporated to dryness under reduced pressure. The resulting gray material is triturated with hot methanol followed by hot hexanes to remove trityl byproducts, giving 24 mg of 1-pyz, 90% yield. Spectral data matches previously reported results.⁶⁸ ¹H NMR (400 MHz, CDCl₃) δ 7.91 – 8.04 (s, 2H), 8.58 – 8.72 (s, 3H). HRMS (APPI-TOF) calcd. for C₁₅H₁₂N₆ 276.11 found 275.3

References

- (61) Simion, A. M.; Hashimoto, I.; Mitoma, Y.; Egashira, N.; Simion, C. *Synth. Commun.* **2012**, *42* (6), 921.
(62) Zhou, H.-C.; Long, J. R.; Yaghi, O. M. *Chem. Rev.* **2012**, *112* (2), 673.

- (63) Peng, Y.; Li, Y.; Ban, Y.; Jin, H.; Jiao, W.; Liu, X.; Yang, W. *Science* **2014**, *346* (6215), 1356.
- (64) Rodenas, T.; Luz, I.; Prieto, G.; Seoane, B.; Miro, H.; Corma, A.; Kapteijn, F.; Llabrés i Xamena, F. X.; Gascon, J. *Nat. Mater.* **2014**, *14* (1), 48.
- (65) Bauer, T.; Zheng, Z.; Renn, A.; Enning, R.; Stemmer, A.; Sakamoto, J.; Schlüter, A. D. *Angew. Chem. Int. Ed.* **2011**, *50* (34), 7879.
- (66) Monica, G. L.; Ardizzoia, G. A. In *Progress in Inorganic Chemistry*; Karlin, K. D., Ed.; John Wiley & Sons, Inc.: Hoboken, NJ, USA, 1997; Vol. 46, pp 151–238.
- (67) Colombo, V.; Galli, S.; Choi, H. J.; Han, G. D.; Maspero, A.; Palmisano, G.; Masciocchi, N.; Long, J. R. *Chem. Sci.* **2011**, *2* (7), 1311.
- (68) Johnson, C. J.; University of Nevada, R.; Department of Chemistry. From gold-containing liquid crystals to homodesmotic reaction analysis, 2014.
- (69) Moghaddam, F. M.; Ghaffarzadeh, M. *Synth. Commun.* **2001**, *31* (2), 317.
- (70) Pathak, A. K.; Pathak, V.; Seitz, L. E.; Tiwari, K. N.; Akhtar, M. S.; Reynolds, R. C. *Tetrahedron Lett.* **2001**, *42* (44), 7755.
- (71) Long, J. R.; Yaghi, O. M. *Chem. Soc. Rev.* **2009**, *38* (5), 1213.
- (72) Woodall, C. H.; Fuertes, S.; Beavers, C. M.; Hatcher, L. E.; Parlett, A.; Shepherd, H. J.; Christensen, J.; Teat, S. J.; Intissar, M.; Rodrigue-Witchel, A.; Suffren, Y.; Reber, C.; Hendon, C. H.; Tiana, D.; Walsh, A.; Raithby, P. R. *Chem. - Eur. J.* **2014**, *20* (51), 16933.
- (73) *Chem. Eng. News Arch.* **2015**, *93* (34), 3.

5. Efforts Towards the 2D Polymerization of a Porphyrin Based Monomer.

5.1. Overview

Porphyrins are molecules imperative to biology and have been researched for over a century.⁷⁴ They are flat, rigid aromatic compounds that have been synthesized and customized to take advantage of their unique optical and aromatic properties.⁷⁵ Due to their large conjugated structure and ability to absorb light, porphyrins are commonly used to study aromaticity and photo-induced electron transfer.^{76,77} Seen below is a basic porphyrin framework, Figure 5.1.

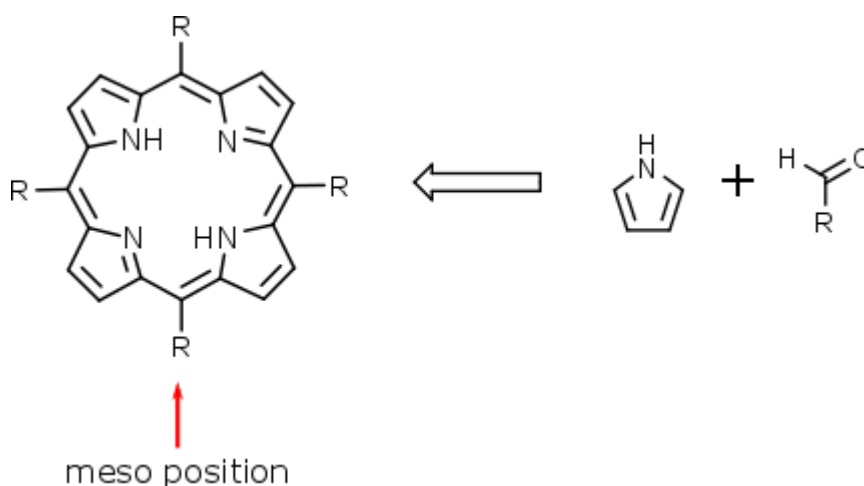


Figure 5.1. Porphyrin framework with the easily modified meso positions labeled.

A porphyrin's rigid nature, ease of synthesis, and four-fold symmetry makes a candidate framework for a monomer to be used in 2D polymerizations. Porphyrin synthesis often allows easy condensation of an aryl aldehyde with pyrrole in the presence of an acid catalyst. One is able to synthesize a porphyrin having a substituent of their choosing at the meso positions if the desired aryl aldehyde is available. Keeping in line with the use of anthraceno moieties as the polymerizable functional groups, the synthesis of a porphyrin using anthraldehyde was investigated, Figure 5.2.

When exploring the synthesis of the tetra-anthraceno porphyrin monomer **1-P**, it was no surprise that the synthetic protocol for the exact molecule had already been extensively worked out.^{78,79} The previous synthesis of **1-P** had been synthesized for its absorption qualities and to demonstrate the effect bulky anthraceno groups had on the yields of porphyrin condensation. We on the other hand, recognized the molecule for its potential as a monomer for 2DP synthesis. Seen below is monomer **1-P**, a porphyrin with anthraceno groups at its meso positions.

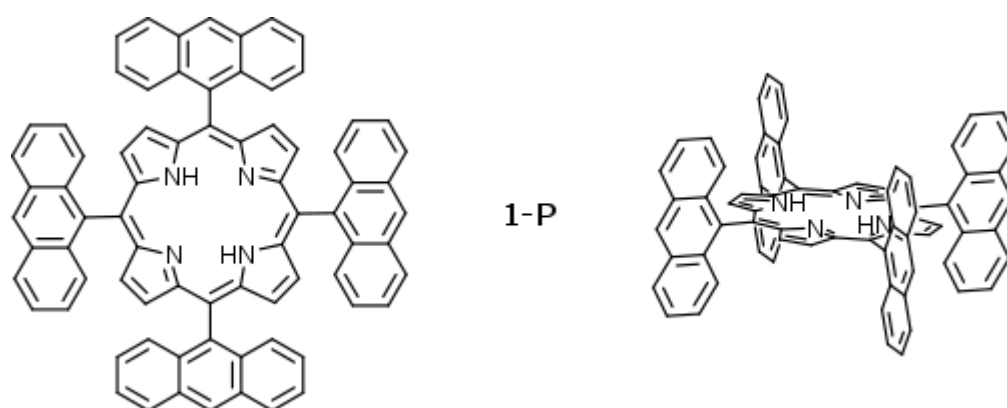
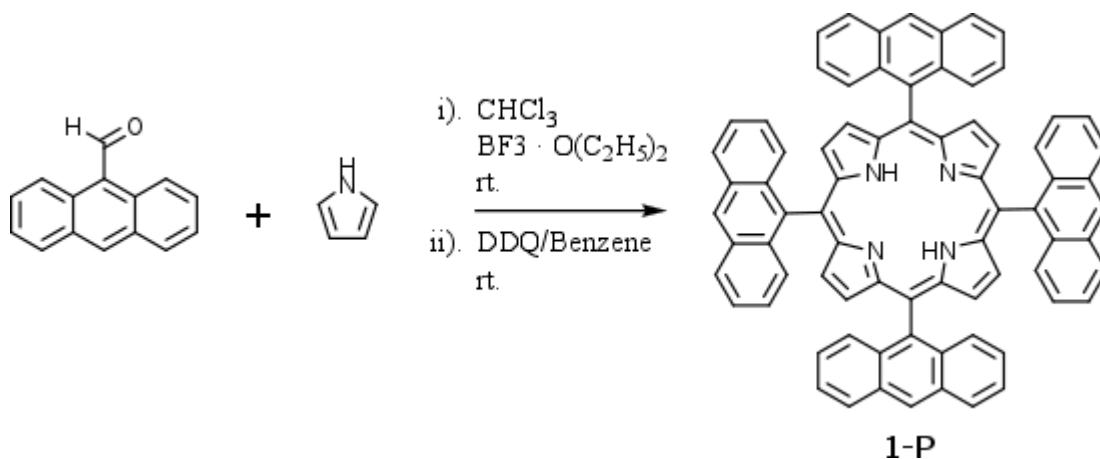


Figure 5.2. Structure of porphyrin monomer **1-P**. Figure shows a flattened top down view (left), and a geometrically realistic edge-on conformation (right).

5.2. Results and Discussion

Synthesis of **1-P** utilizes the Lindsay conditions of porphyrin synthesis.⁷⁹ A mixture of ethanol-stabilized chloroform, pyrrole, and anthraldehyde is stirred at room temperature in the dark, followed by the addition of boron trifluoride diethyletherate ($\text{BF}_3 \cdot \text{OEt}_2$) which catalyzes framework forming reactions of the porphyrin. A benzene slurry of DDQ is added to the reaction mixture 1 min after the addition of $\text{BF}_3 \cdot \text{OEt}_2$, which oxidizes the macrocycle to final product **1-P**, Scheme 5.1.⁷⁹



Scheme 5.1. Synthetic conditions for the synthesis of **1-P**. A room temperature solution of anthraldehyde, pyrrole and chloroform followed by the addition of BF_3OEt_2 . 1 min later a slurry of DDQ is added to oxidize the mixture to target **1-P**, 3% yield.⁷⁹

Due to the bulky anthraceno groups, the synthesis of **1-P** (*meso*-tetraanthrylporphyrin) is sterically demanding and results in low yields of 3%. While sterics cause low yields, they also cause the anthraceno functional groups to be perpendicular to the porphyrin

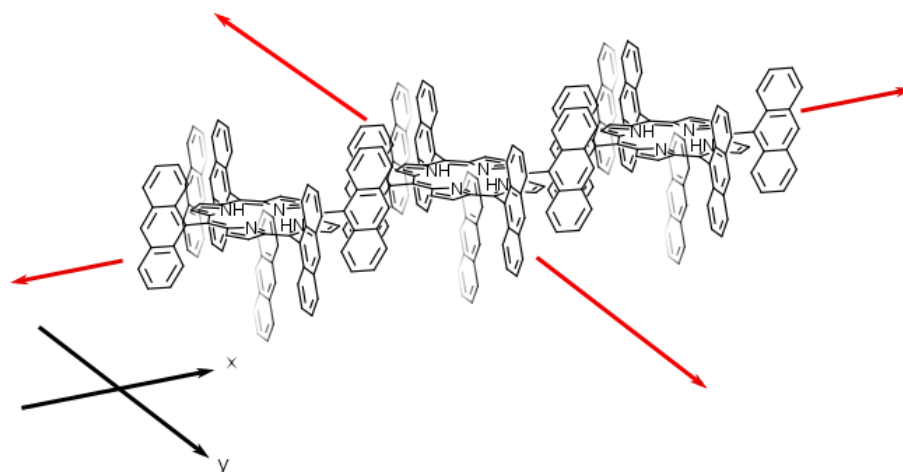


Figure 5.3. Illustration of the geometry of **1-P** and how the potential packing of the anthraceno moieties translates to lamellar packing. Red lines indicate direction of packing along the x,y plane. Porphyrin cores are omitted along the y axis for clarity.

core, as depicted in Figure 5.2. This perpendicular arrangement between the anthraceno groups and porphyrin core poises the functional groups in such a way that if organized properly, a 2D lamellar packing with overlap between anthraceno moieties is possible. As explained in previous chapters, the overlapping anthraceno moieties will dimerize via a photo induced [4+4] cycloaddition. Figure 5.3 demonstrates an ideal packing of the **1-P** monomer and illustrates an overlap of anthraceno blades poised for cycloaddition. Two different pre-organization approaches were taken: crystallization approach and LB trough approach.

5.3. Crystallization Approach

Crystallizing **1-P** into a properly packed lamellar network was the first approach to pre-organizing **1-P**. An ideal crystal packing would have a square packing with overlap of the anthraceno blades. A top down view of the packing can be seen in Figure 5.4.

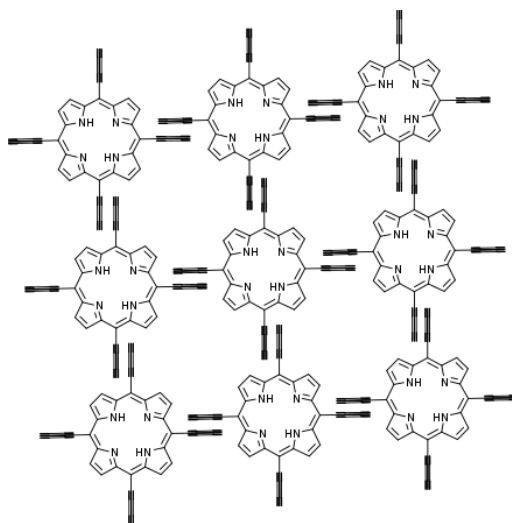


Figure 5.4. A top down view of an ideal lamellar packing of **1-P**.

The properly packed crystal of **1-P** would then be irradiated and undergo a crystal to crystal 2D polymerization. A variety of crystallization solvents and conditions were screened in an attempt to grow quality single crystals of **1-P**.

To learn how **1-P** crystallizes and discover any possible trends in crystallization, a variety of solvents were chosen and crystals were monitored via single crystal X-ray diffraction. Preliminary solvents ranged from aliphatic to aromatic: chloroform, nitromethane, and tetrahydrofuran; and aromatic solvents, benzene, toluene, fluorobenzene, dichlorobenzene, and pyridine. Due to the limited solubility of **1-P**, it was initially dissolved in hot chloroform and one of the above co-solvents was added and was let to crystallize through liquid-liquid diffusion at room temperature. Crystallizations were also performed in the neat solvents through slow evaporation at room temperature when solubility permitted. The single crystals grown from these solvents were examined and their preliminary diffractions gave important insight into **1-Ps** different crystal systems.

The single crystals that were obtained from the above crystallizations resulted in two main crystal systems. Depending on the solvent used, **1-P** crystallized in either the tetragonal P form or the monoclinic P form. Initially this was very exciting because the tetragonal P crystal form has the square packing of **1-P** that we are looking for.

The dichlorobenzene, toluene, and benzene solvates of **1-P** all had tetragonal P crystal systems, with only slight differences in their lattice parameters. The fluorobenzene, pyridine, chloroform solvates of **1-P** each possessed a less symmetrical monoclinic P crystal system. Seen below are examples of the monoclinic P form and tetragonal P form, Figure 5.5. The crystal structure on the left is of the monoclinic P form with a $P2_1/n$ space group, $a=15.50 \text{ \AA}$, $b=15.12 \text{ \AA}$, $c=15.84 \text{ \AA}$, $\alpha=90^\circ$, $\beta=105.88^\circ$, $\gamma=90^\circ$, and a unit cell volume of 3574.1 \AA^3 . And the crystal structure on the right is of the tetragonal P form with a $P4/n$ space group, $a=b=18.96 \text{ \AA}$, $c=10.34 \text{ \AA}$, $\alpha=\beta=\gamma=90^\circ$, and a unit cell volume of 3723.0 \AA^3 .

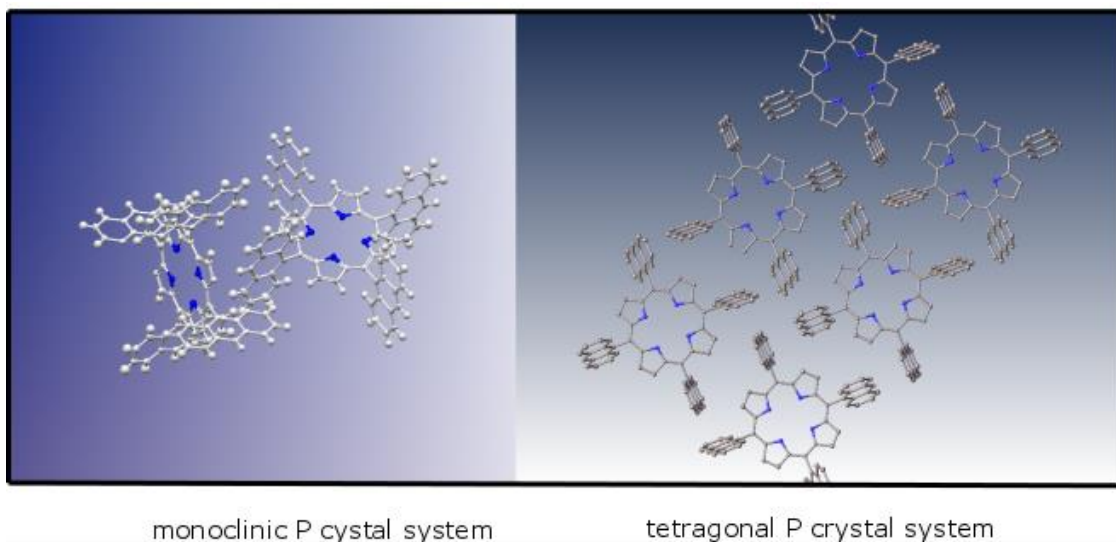


Figure 5.5. Monoclinic P pyridine solvate of **P-1** showing the orthogonal arrangement of adjacent porphyrins. Tetragonal P toluene solvate of **P-1** showing the lamellar, square packing system.

Seen below is a close up of the tetragonal P packing of **1-P** showing the 7.38 Å distance between the anthraceno blades of the porphyrin monomers and an edge on view, Figure 5.6.

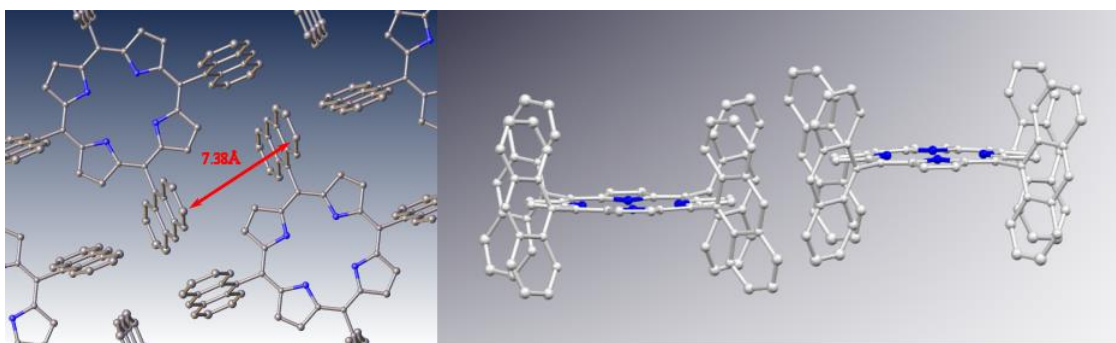


Figure 5.6. Close up of the tetragonal P packing of the toluene solvate, showing a distance of 7.38 Å between anthraceno blades (left). An edge on view of the same solvate showing two **1-P** monomers with their anthraceno blades only slightly off-set (right).

As seen above, the tetragonal P form is lamellar and the anthraceno blades are very close to cofacial. According to the topochemical postulate a solid-state reaction has the ability

to proceed if the reactive groups are within a distance 4.2 Å and have proper overlap. The blades of **1-P** being nearly cofacial to one another is very promising, unfortunately, a distance of 7.38 Å is too large for a topochemical reaction. The large distance forbids the orbital overlap necessary for the [4+4] cycloaddition to proceed within the constrained environment of the crystal lattice.

While the above tetragonal P crystal system did not adhere to the topochemical postulate, literature provides a few examples showing functional groups at a distance greater than 4.2 Å reacting in the solid state.²¹ This gives evidence that the mobility of molecules within a crystal can undergo significantly more movement than one is lead to believe. With this in mind, each crystal having a tetragonal P crystal system, regardless of the distance between anthraceno blades, was irradiated with a series of wavelengths at various temperatures.

A matrix was run on all crystal solvates and each tetragonal P crystal form found was irradiated with wavelengths of 465 nm and 365 nm at temperatures of 100 K and 250 K. To allow maximum mobility for a cycloaddition between the anthraceno blades to occur, higher temperatures were used to allow more movement of the monomers within the lattice. The post-irradiated crystals were monitored by X-ray diffraction and comparing the post and pre-unit cell parameters. Different unit cell parameters would indicate a reaction.

Unfortunately, none of the tetragonal P crystal forms that were irradiated displayed a significant change in unit cell parameters. While this was unfortunate, the tetragonal P forms of the crystal motivated further screening. Screening solvents by growing single crystals has the advantage of knowing the exact structure of the crystal, but the approach is time consuming and does not lend itself well to a high throughput screening, whereas, growing microcrystals is much faster. Microcrystals can be irradiated and screened for polymerization

using the solubility of the irradiated sample. If a sample did polymerize, its solubility should decrease, if not become completely insoluble.

To screen a large amount of solvents over a short period of time, microcrystals were grown in microscope well slides. **1-P** was dissolved in a chosen solvent and placed in the depression and left to evaporate, Table 5.1

Solvent	365nm irradiation	Solvation with CHBr ₃
chlorobenzene	1hr, argon, room temp	soluble
trichlorobenzene	1hr, argon, room temp	soluble
tetrachloroethane	1hr, argon, room temp	soluble
tetrachloroethylene	1hr, argon, room temp	soluble
1-bromo-4- <i>tert</i> -butylbenzene	1hr, argon, room temp	soluble
<i>tert</i> -butylbenzene	1hr, argon, room temp	soluble
nitrobenzene	1hr, argon, room temp	soluble
benzene	1hr, argon, room temp	soluble
tetrahydrofuran	1hr, argon, room temp	soluble
pentafluorochlorobenzene	1hr, argon, room temp	soluble
<i>o</i> -xylene	1hr, argon, room temp	soluble

Table 5.1. Example of the solvents used for microcrystal screening of **1-P**, with a microscope well slide, followed by their irradiation and solvation with CHBr₃.

The microcrystals were imaged under the microscope followed by irradiation using 365 nm at room temperature under a stream of Argon for 1hr. Afterwards the depression of the slide was filled with bromoform and placed back under the microscope. The microcrystals were imaged every 15 minutes to monitor evidence of dissolving. Bromoform was used because it was the solvent found to best dissolve monomer **1-P**. A polymerized microcrystal is expected to be close to completely insoluble. Therefore, any microcrystal that does not dissolve or show signs of exfoliation would be evidence of a reaction. Unfortunately, none of the irradiated microcrystals showed signs of polymerization. The image below is

representative of most solvents used; microcrystals on the left and evidence of their solvation in CHBr_3 on the right, Figure 5.7.

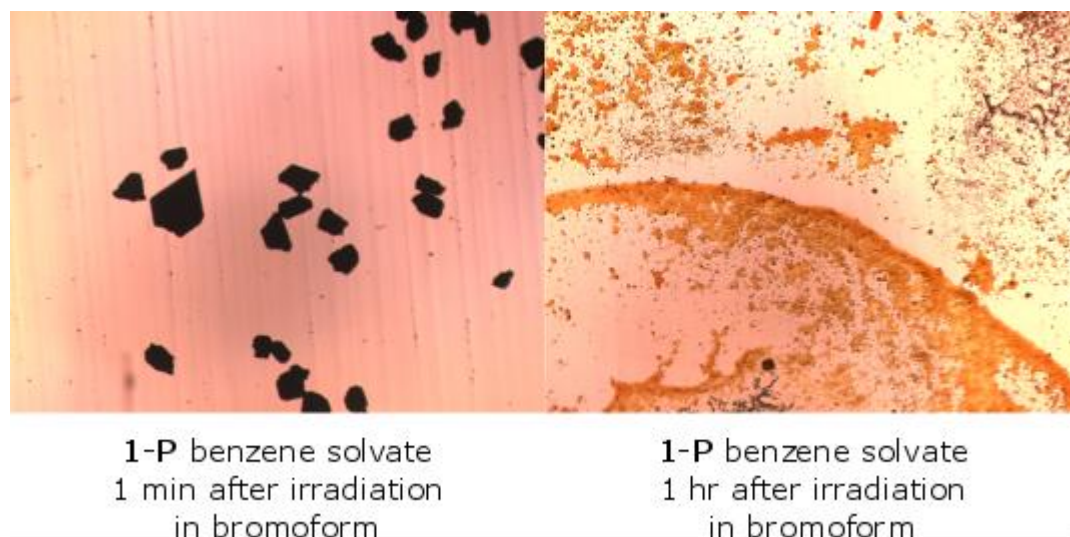


Figure 5.7. Benzene microcrystals before irradiation (left) and after irradiation, dissolved in CHBr_3 after 1 hour (right).

Without the use of crystal engineering, preorganization of monomers using crystallization takes excessive experimentation and quite a bit of luck. During crystallization, monomers will orient themselves to maximize van der Waals contact within 3D space. This gives the opportunity for a countless number of orientations. The π - π interactions from the anthraceno blades of **1-P** can help promote a desired orientation, however, conditions must be found in which these π - π interactions from the anthraceno blades are significant enough to overcome entropy and drive the orientation. Finding these conditions can be quite difficult.

None of the single crystals or microcrystals of **1-P** resulted in a polymer after irradiation. However, preliminary results of lamellar tetragonal P crystal forms suggest that a desired packing of **1-P** is possible and merits continued investigation.

5.5. LB Trough Approach

Opposed to the crystallization approach, the LB trough confines the monomers to two dimensions. By removing a dimension during pre-organization there is a higher likelihood for the monomer's to properly pack in 2D space and be polymerized. Attachment of a hydrophilic tail to the monomer will allow them to float flat and coplanar at the air water interface. This lower dimensional approach removes some of the uncertainty associated with the crystallization approach. With all monomers confined to the same orientation, one is more likely to acquire a packing with the desired overlap of anthraceno blades which can undergo a 2D polymerization.

Attaching a hydrophilic tail to **1-P** allows for the monomers use at the air-water interface. Exploiting the porphyrin's ability to complex metals was the obvious choice when designing an amphiphilic derivative. Inserting a metal into the porphyrin core would allow further attachment of an amphiphilic ligand to the central metal, allowing the tail to project perpendicular to the porphyrin core into the sub phase (water), Figure 5.8.

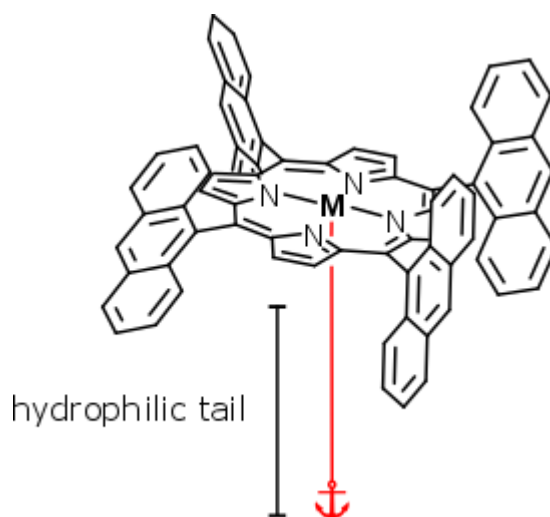
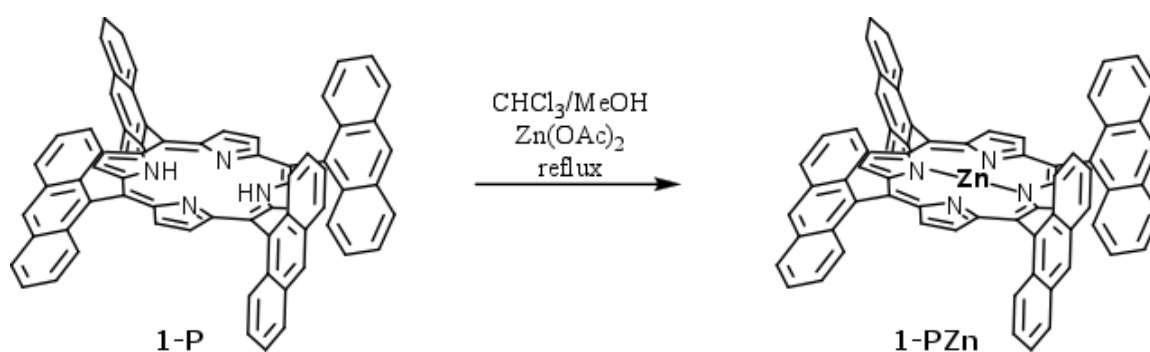


Figure 5.8. A metal (M) being complexed by **1-P** and its coordination to a hydrophilic ligand, illustrated by a red line connected to an anchor.

We first looked for a metal that could be complexed by the porphyrin as well as accommodate a hydrophilic ligand. The decision to use zinc was made simply for characterization purposes. Once inserted into the porphyrin, zinc will be in a diamagnetic state. This leaves characterization by NMR an available resource throughout synthesis of the monomer. Not to mention the insertion of zinc into a porphyrin framework is extremely well known and literature precedents show many examples of a zinc porphyrins complexing axial ligands.^{78,80,81} The zinc insertion synthesis towards **1-PZn** is seen below, Scheme 5.2.



Scheme 5.2. Insertion of Zn into **1-P** by refluxing in a 4:1 mixture of chloroform:methanol in the presence of zinc acetate giving **1-PZn** in 74% yield.

After reacting **1-P** with zinc acetate and zinc derivative **1-PZn** was obtained, a search for a suitable hydrophilic ligand that could act as an anchor was explored. Literature precedent shows many examples of pyridyl groups complexing zinc containing porphyrins.^{80,82,81} The Jin group had previously used isonicotinic acid to link zinc porphyrins and TiO_2 nanoparticles.⁸³ Its solubility in water and size made it a perfect candidate for a hydrophilic anchor. Seen below in Figure 5.9, is an illustration of **1-PZn** complexed with isonicotinic acid showing the carboxylic acid moiety extending past the anthraceno blades of the porphyrin and reaching into the sub phase, acting as an anchor.

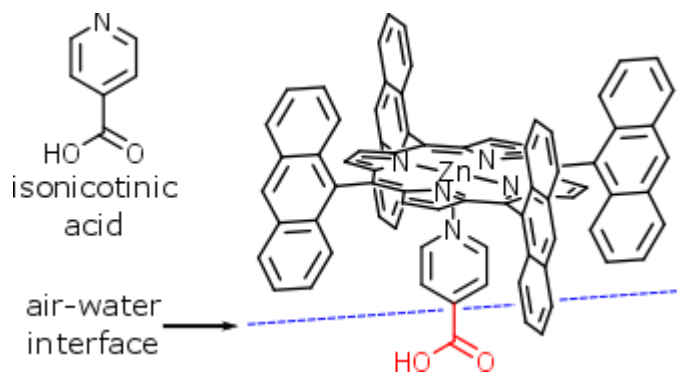


Figure 5.9. Illustration of axially coordinated isonicotinic acid acting as a hydrophilic anchor. Dashed blue line represents the air-water interface and the red carboxylic acid represents it being submerged.

When a zinc porphyrin is complexed by a pyridyl moiety its Soret band (absorbance maximum) is shifted to a lower energy absorbance (red shift).⁸³ To confirm that **1-PZn** was complexing isonicotinic acid, an absorption spectra was taken of **1-PZn** in chloroform followed by the addition of isonicotinic acid. Addition of isonicotinic acid did not result in a red shift of the spectrum. The bulky anthraceno blades were thought to be a source of steric encumbrance, preventing isonicotinic acid from complexing the zinc. To overcome this possible steric problem a solution of isonicotinic acid and **1-PZn** were heated to reflux in 1:1 chloroform:ethanol for 6 h. This was hoped to lead to an increase in the solubility of isonicotinic acid as well as adding the energy needed to overcome any possible steric issues. However, heating the mixture resulted in no red shifts by UV-vis.

The pK_a of isonicotinic acid is such that it will readily protonate its basic nitrogen. It was expected that the equilibrium established between the carboxylic acid and basic nitrogen moieties of isonicotinic acid would permit ligation of **1-PZn**. As a control, pyridine was added to a chloroform solution of **1-PZn** and the color instantly changed from red to yellow. An absorption spectrum of the mixture confirmed a red shift in the Soret band of the porphyrin.

Seen below is an absorption spectrum of **1-PZn** in chloroform and **1-PZn** in a chloroform/pyridine mixture, Figure 5.10.

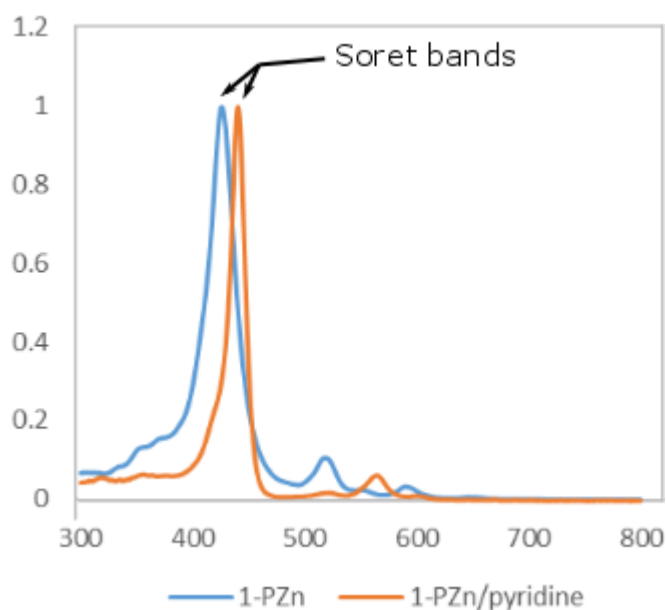
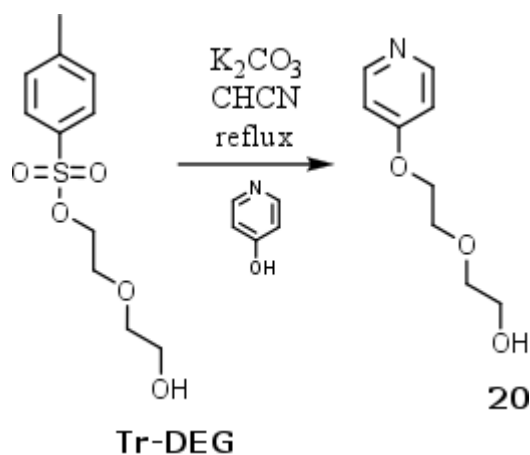


Figure 5.10. Absorption spectrum of **1-PZn** (blue) and **1-PZn** complexed with pyridine (orange).

With isonicotinic acid being useless as a ligand for **1-PZn**, another hydrophilic ligand was sought out. The main requirements for the ligand are a pyridyl moiety that has a hydrophilic substituent in the para position that reaches past the anthraceno blades of **1-PZn**. Unfortunately, no such ligands were commercially available and one had to be synthesized.

Various para substituted pyridines were contemplated when designing the hydrophilic ligand. Use of 4-hydroxypyridine as the starting material for the ligand was considered due to its hydroxyl functionality being a convenient synthetic handle. Performing a Williamson ether synthesis between 4-hydroxypyridine and a protected diethylene glycol (**Tr-DEG**) is a simple transformation. Furthermore, the increased length of a DEG chain could potentially serve as a better hydrophilic anchor than the short carboxylic substituent of

isonicotinic acid. Fortunately, the synthesis for ligand in question (**20**) has already been worked out, Scheme 5.3.⁸⁴



Scheme 5.3. Williamson ether synthesis between 4-hydroxypyridine and trityl protected diethylene glycol (**Tr-DEG**) in dry acetonitrile and potassium carbonate base, 75% yield.

To this point, ligand **20** has been made and **1-PZn** has been synthesized and characterized. The next step is to mix the two components together and verify an axial coordination of **20** and **1-PZn** by UV-vis. Then its deposition to the air-water interface will be developed followed by irradiation of the monolayer towards a 2DP. Figure 5.11, below, shows the axial coordination of **20** to **1-PZn**, and illustrates the hydrophilic substituent of **20** reaching past the anthraceno blades, into a hypothetical aqueous sub-phase.

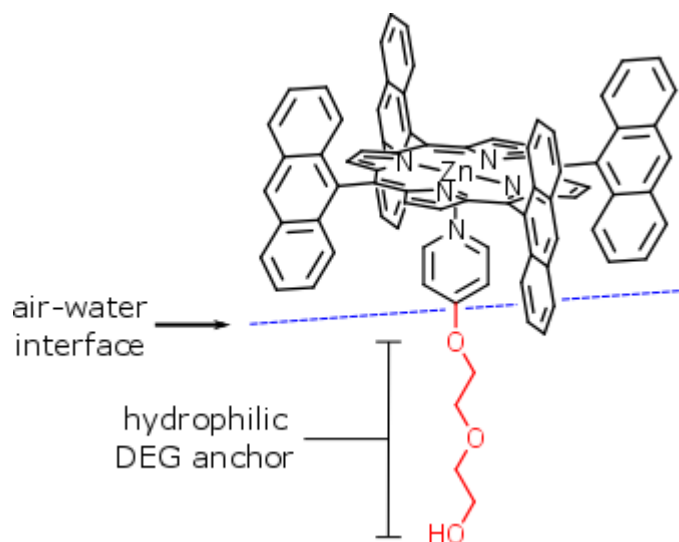


Figure 5.11. Monomer **1-PZn** being ligated by **20**, illustrating the distance at which the hydrophilic anchor goes into the hypothetical sub-phase.

5.6. Control Reaction

To make sure the reaction between the anthraceno blades of **1-P** is possible, a solution of **1-P** and anthracene in *d*-chloroform was made, and irradiated at 365nm for 6hrs under argon. The reaction was monitored by NMR and no sign of anthraceno group dimerization between monomers was observed.

One potential problem with this reaction is the high extinction coefficient of the porphyrin core. Porphyrins are notorious for their high extinction coefficients ranging from 40,000 to 50,000, and their absorbance maximum is typically in the 420 nm range. The wavelength needed for the [4+4] cycloaddition between anthraceno groups is in a similar range between 365 nm to 465 nm. This presents a potential problem because the porphyrin could be absorbing all the photons in the 365 to 465 region thus preventing excitation of the anthraceno groups and inhibiting their cycloaddition.

Another potential problem for why the control reaction failed could be explained by the resulting steric crowding of the [4+4] cyclization between **1-P** and anthracene. An energy minimization of the cyclization product between **1-P** and anthracene, using Avogadro, shows that a significant amount of distortion occurs to the porphyrin core after cyclization Figure 5.12.

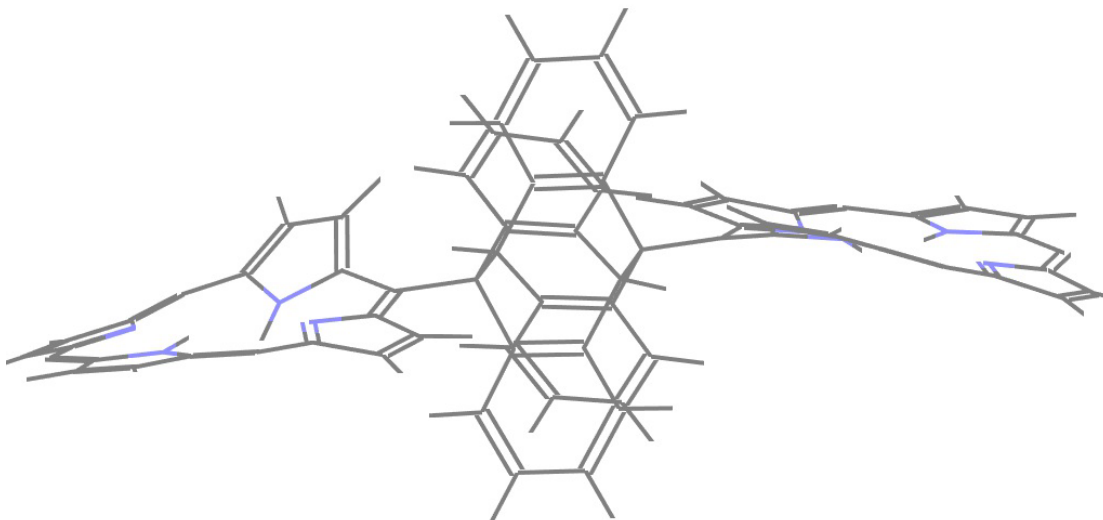


Figure 5.12. Energy minimization of the [4+4] cycloaddition product between one blade on each porphyrin monomer. Simulation shows the level of distortion of the porphyrin core caused from anthracene blade dimerization. Unreacted blades have been left out for clarity.

Overcoming the energy requirements needed produce such a sterically hindered product could potentially be what is preventing the control reaction from occurring in solution.

Crystal structures have shown that a porphyrin framework is capable of a significant amount of distortion.^{85,86} Therefore, perhaps the confinement of the solid state and monolayer conditions might be necessary for the reaction to proceed through such a sterically unfavorable transformation. For example, in the solid state **1-P** is held in place which could potentially help to drive the [4+4] cyclization to occur by forcing distortion of the

porphyrin core due to its constrained conditions. Whereas in solution, the anthraceno moieties of **1-P** are not held in place or constrained and would much rather repel each other than undergo such a sterically demanding and energetically unfavorable transformation.

Literature shows many examples of porphyrin cores being distorted to an extreme extent, giving credence to the idea that the distortion of the **1-P** core needed for a [4+4] cycloaddition between the anthraceno moieties of **1-P** is possible. Finding out if this is possible might necessitate **1-P** being confined in a way to make distortion of the porphyrin core energetically favorable upon [4+4] cycloaddition of the anthraceno moieties, which means continued experimentation of its polymerization using the crystal and LB trough approaches.

5.7. Conclusion

Monomers **1-P** and **1-PZn** have been synthesized and efforts towards their polymerization via the single crystal and LB-tough methods have been attempted. Crystallization conditions for the single crystal method continue to be explored and polymerization of **1-PZn**, anchored by hydrophilic ligand **20**, using the LB trough approach has potential, and the project should be continued.

5.8. Experimental

Synthesis of anthraceno porphyrin (1-P). To a 1 L round bottom is added argon-purged, ethanol stabilized, chloroform (1 L) dried by 4 Å molecular sieves, freshly distilled pyrrole (0.679 mL, 10 mmol), and 9-anthraldehyde (2.06 g, 10 mmol). To the stirring solution, being bubbled with argon, $\text{BF}_3 \cdot \text{OEt}_2$ (1.8 mL, 30 mmol) is added to the foil covered round bottom at room temperature. One minute after the addition of $\text{BF}_3 \cdot \text{OEt}_2$, a stoichiometric equivalent of DDQ (2.27 g, 10 mmol) suspended in benzene (5 mL) is added to the stirring solution and let

to stir overnight. The reaction mixture is run through a pad of silica gel to eliminate polymeric tar. The filtrate is collected and evaporated under reduced pressure, followed by a second pad using 20% hexane/ CHCl₃, which allows separation of **1-P** and anthraldehyde, giving the target porphyrin at 3% yield. Mass and ¹H NMR matched previously reported results.⁷⁹ ¹H NMR (400 MHz, CDCl₃) δ -1.73 (s, 2H), 6.99 – 7.06 (m, 2H), 7.13 – 7.19 (d, *J* = 8.9 Hz, 2H), 7.36 – 7.44 (m, 2H), 8.06 – 8.11 (s, 2H), 8.18 – 8.24 (d, *J* = 8.6 Hz, 2H), 8.81 – 8.85 (s, 1H).

Synthesis of Zn anthraceno porphyrin (1-PZn): In a 100 mL round bottom, porphyrin **1-P** (36 mg, 0.035 mmol) was dissolved in a 1:4 mixture of methanol and CHCl₃ (20 mL) to which Zn(OAc)₂ (128 mg, 0.7 mmol) was added. The solution was let to reflux overnight under nitrogen in the dark. The reaction was brought to room temperature and evaporated under reduced pressure. Column chromatography using 20% hexanes/ CHCl₃ was performed on the crude mixture giving **1-PZn**, 65% yield.

Reference.

- (74) Moore, M. R. In *Tetrapyrroles*; Springer New York: New York, NY, 2009; pp 1–28.
- (75) Tanaka, T.; Osuka, A. *Chem Soc Rev* **2015**, *44* (4), 943.
- (76) Yoon, Z. S.; Osuka, A.; Kim, D. *Nat. Chem.* **2009**, *1* (2), 113.
- (77) Gust, D.; Moore, T. A.; Moore, A. L.; Leggett, L.; Lin, S.; DeGraziano, J. M.; Hermant, R. M.; Nicodem, D.; Craig, P. *J. Phys. Chem.* **1993**, *97* (30), 7926.
- (78) Kumar, A.; Maji, S.; Dubey, P.; Abhilash, G. J.; Pandey, S.; Sarkar, S. *Tetrahedron Lett.* **2007**, *48* (41), 7287.
- (79) Tohara, A.; Sato, M. *J. Porphyr. Phthalocyanines* **2007**, *11* (7), 513.
- (80) Michelsen, U.; Hunter, C. A. *Angew. Chem. Int. Ed.* **2000**, *39* (4), 764.
- (81) Hunter, C. A.; Sarson, L. D. *Angew. Chem.* **1994**, *106* (22), 2424.
- (82) Chi, X.; Guerin, A. J.; Haycock, R. A.; Hunter, C. A.; Sarson, L. D. *J. Chem. Soc. Chem. Commun.* **1995**, No. 24, 2567.
- (83) Zhang, J.-X.; Han, F.-M.; Liu, J.-C.; Li, R.-Z.; Jin, N.-Z. *Tetrahedron Lett.* **2016**, *57* (17), 1867.
- (84) Li, M.-J.; Kwok, W.-M.; Lam, W. H.; Tao, C.-H.; Yam, V. W.-W.; Phillips, D. L. *Organometallics* **2009**, *28* (6), 1620.
- (85) A. Shelnut, J.; Song, X.-Z.; Ma, J.-G.; Jia, S.-L.; Jentzen, W.; J. Medforth, C.; J. Medforth, C. *Chem. Soc. Rev.* **1998**, *27* (1), 31.
- (86) Fang, Y.; Bhyrappa, P.; Ou, Z.; Kadish, K. M. *Chem. - Eur. J.* **2014**, *20* (2), 524.

6. Antrip and Fantrip Co-crystallizations with Fullerenes Towards Single Crystal

Polymerizations.

6.1. Overview

Fantrip **1-F** and antrip **1-H** have been previously crystallized into hexagonally packed crystals and irradiated in the solid state to yield 2DPs with honey-comb lattices, Figure 6.1.

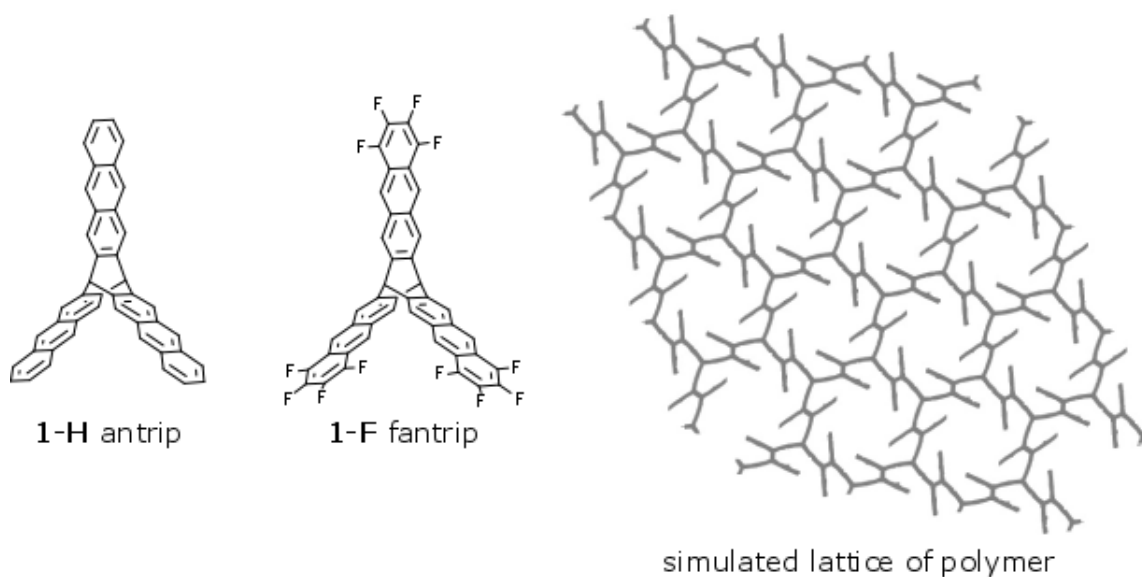


Figure 6.1. Structures of antrip **1-H** and fantrip **1-F** (left). Simulation representing the lattice of both polymers (right).

Poly antrip and poly fantrip are examples of polymers synthesized using the single crystal method of polymerization.^{9,23,19} With monomers **1-H** and **1-F** available, it made sense to use them together towards new 2DPs and continue advancement of the field.

Developing a co-crystal between antrip (**1-H**) or fantrip (**1-F**) and an appropriate guest molecule followed by its polymerization into a 2D copolymer would be a useful addition to the field of 2DPs.

A copolymer is a polymer consisting of two or more repeat units. The single crystal approach for a 2D copolymerization would utilize two different monomers that would be co-crystallized into a lattice that is capable of undergoing polymerization. The literature shows no evidence of a 2D copolymer being synthesized using the single crystal approach. The following describes my efforts towards co-crystallizations between fullerenes C_{60} and C_{70} and monomers **1-F** and **1-H** and the resulting co-crystals irradiations towards a copolymerization.

The simulated honeycomb lattice in Figure 6.1 represents both polyantrip and polyfantrip. The pore size of both polyantrip and polyfantrip is ~ 1 nm and the diameter of C_{60} and C_{70} are close to the same size. This motivated the co-crystallization of **1-F** and **1-H** each with both C_{60} and C_{70} in hopes for a packing motif that involves the anthraceno blades of **1-F** or **1-H** hugging the equator of a fullerene. The wanted packing of the co-crystal is a hexagonal packing of the monomer (either **1-H** or **1-F**) and the fullerene (either C_{60} or C_{70}) occupying the pores of the hexagonal units, Figure 6.2.

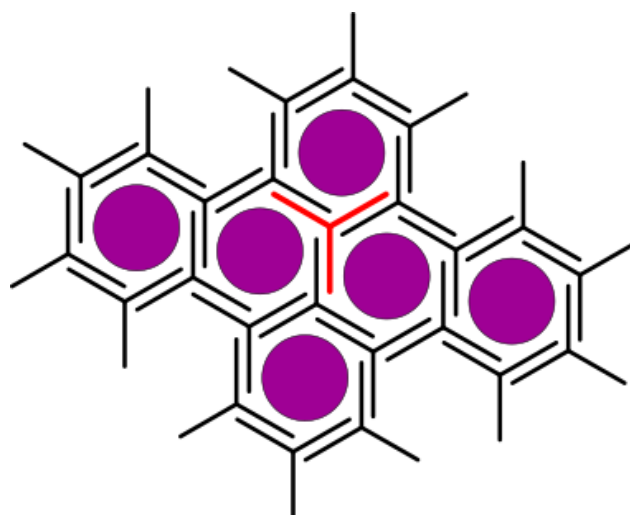


Figure 6.2. Illustration of an ideal packing between monomers **1-H** and **1-F** and either C_{60} or C_{70} . Monomers **1-H** and **1-F** are portrayed by the black “Y” shaped figures, one shown in red

for clarity. Fullerenes depicted by purple circles which occupy the hexagonal voids of the lattice.

The ideal result would be [4+4] cycloadditions between the anthracene blades of the monomers as well as cycloadditions between the monomers and the fullerenes. Polymerization would be accomplished by irradiation or possibly irradiation and heating of the co-crystals.

While cocrystallizations with both C_{60} and C_{70} were investigated, C_{70} was initially chosen to be co-crystallized with the above two monomers, due to its oblong geometry. The use of C_{70} would allow for more van der Waals contact between the anthracene blades and the fullerene due to the comparatively flat section of the C_{70} equator, Figure 6.3.

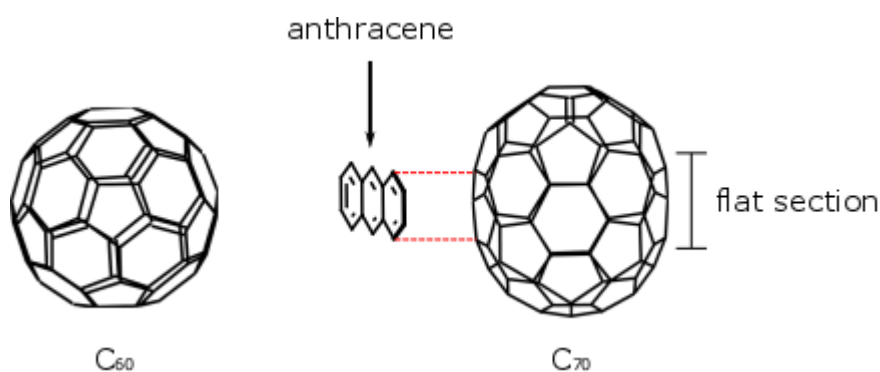


Figure 6.3. Geometry of C_{60} (left) and C_{70} (right). Illustration of the flat section of C_{70} that would allow for increased van der Waals contact between an acene (anthracene used in this example) in comparison to C_{60} .

Co-crystallizations involving fullerenes are extremely challenging, and obtaining X-ray quality single crystals with the appropriate packing necessary for 2D polymerization adds another level of difficulty. Typical host-guest co-crystallizations involving fullerenes make use of a host molecule that has a concave shape to act as a pocket for the fullerene, maximizing

van der Waals contact. Below is a crystal structure by Scott *et al.* of C_{60} and a concave corannulene molecule, Figure 6.4.⁸⁷

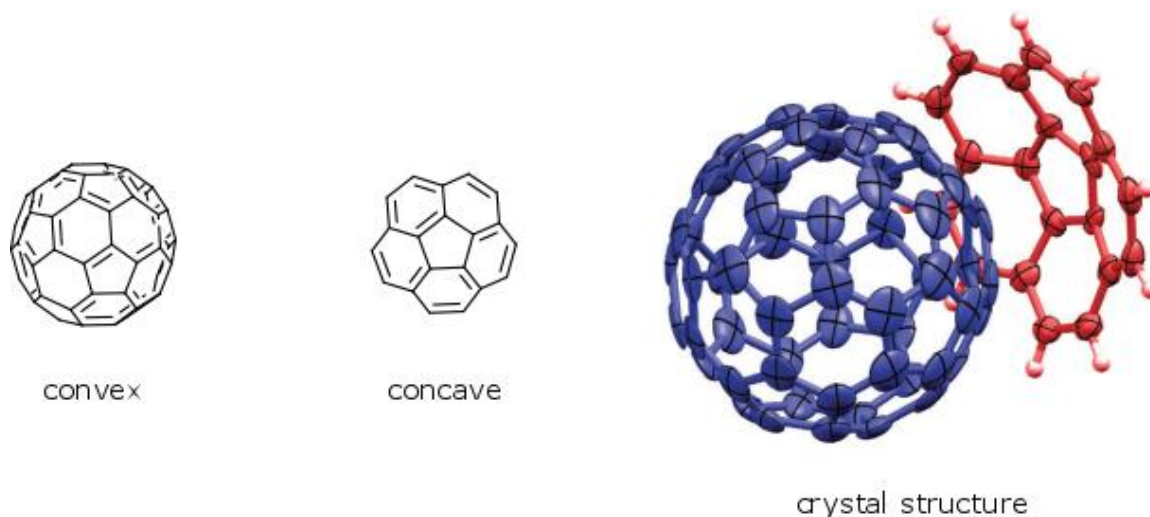


Figure 6.4. A 1:1 C_{60} :corannulene crystal structure by Scott *et al.*⁸⁷ The corannulene molecule acts as a concave host that can grip the fullerene.

Our monomers have very little ability to “cup” or act as a pocket during co-crystallization with a fullerene. An analogy of our system versus the above literature example would be, “trying to hold an egg with chop sticks” versus “trying to hold an egg with a spoon”. Nevertheless, conditions to allow co-crystallization of both monomers with fullerenes were sought out.

6.2. Co-crystallization

A high throughput screening of solvents for a co-crystallization between either monomer, **1-H** and **1-F**, and either C_{60} or C_{70} becomes difficult. Growing crystals using a microcrystalline approach with microscope well slides is not as useful because one is not able to easily determine if a given microcrystal is co-crystalline or not. One would need to use tweezers and accurately pick out microcrystals of a consistent shape and color, and analyze

them with an appropriate analytical technique such as NMR or mass spectra to determine if both compounds are present; during which, being 100% confident that contamination from crystals of a single compound were not included in the sample. This makes the screening of solvents and conditions for the above co-crystallizations limited to growing single crystals which can be analyzed by X-ray diffraction.

A major limitation of working with fullerenes such as C_{60} and C_{70} are their limited solubility. C_{60} and C_{70} are relatively large molecules that favor very few solvents.⁸⁸ Unlike **1-F** and **1-H**, which are soluble in most common solvents, performing a co-crystallization with fullerenes make the choice of solvents available much more limited. Working within the boundaries of limited solvent choices, one must find a creative approach through crystallization techniques and conditions that allows both components to crystallize together.

Fortunately C_{60} and C_{70} have similar solubility and there is a thorough list showing each solvents ability to dissolve C_{60} in mg/mL.⁸⁸ The list shows 22 solvents that are capable of dissolving at minimum 1 mg of C_{60} /mL of solvent. Out of these 22 solvents, we started with the solvents that were available in our lab. Seen below is a documentation of the different solvents used for the cocrystallization of the monomers **1-H** and **1-F** with fullerenes C_{60} and C_{70} , Table 6.1.

solvent	[C ₆₀], mg/ml
<i>trans</i> -decalin	1.3
1,1,2,2,-tetrachloroethane	5.3
tetrachloroethylene	1.2
benzene	1.7
toluene	2.8
xylenes	5.2
mesitylene	1.5
tetralin	16
bromobenzene	3.3
anisole	5.6
chlorobenzene	7
1,2-dichlorobenzene	27
1,2,4-trichlorobenzene	8.5
1-methylnaphthalene	33
carbon disulfide	7.9

Table 6.1. Solvents used for cocrystallizations between **1-H** or **1-F** and fullerenes and their ability to solvate C₆₀ in mg/ml.

Crystallization conditions, for each of the solvents, involved evaporation at room temperature, heating at 10-20 °C below the chosen solvents boiling point, or heating 120 °C for solvents with a boiling point exceeding 150 °C. A 3:1 ratio of **1-H** or **1-F** to fullerene was used for the cocrystallizations.

The co-crystallization attempts between monomers, **1-H** and **1-F**, and fullerenes, C₆₀ and C₇₀, resulted in only one partially solved crystal structure. A slow room temperature evaporation of a 3:1 mixture of **1-H** and C₇₀ resulted in, almost black, hexagonally shaped needles. Shown below in Figure 6.5 is a partially solved antrip/C₇₀ tetrachloroethylene solvate crystal structure from the tetragonal P crystal from, space group P4/n, a=b=18.96 Å, c=10.34 Å, $\alpha=\beta=\gamma=90^\circ$, and a volume of 3723 Å³.

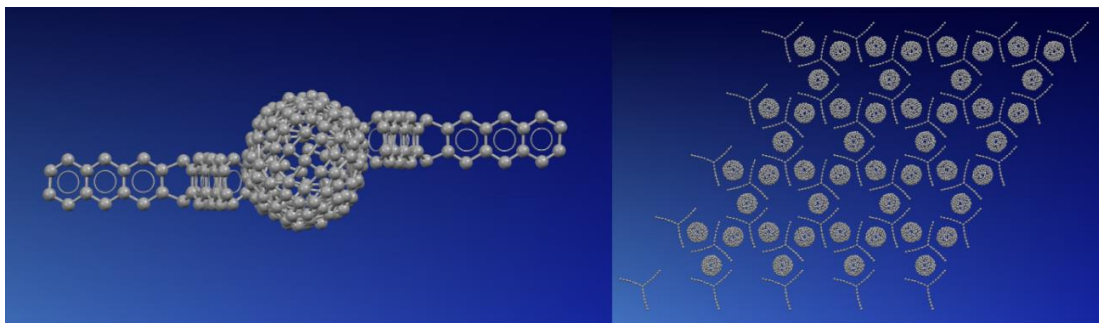


Figure 6.5. An edge on view of the antrip/ C_{70} tetrachloroethylene solvate crystal structure (left). A top down view of the antrip/ C_{70} tetrachloroethylene solvate showing hexagonally packed units.

As shown above in Figure 6.5, the packing of the monomers in the partially solved crystal structure were not the ideal packing illustrated in Figure 6.2. The anthraceno blades, however, were within van der Waals contact to C_{70} and had the potential to react. The crystal was irradiated while on the pin of the diffractometer at temperatures of 100K and 225K with 465nm and 365nm.

If a reaction occurs after irradiation of the crystal, the arrangement of the atoms within the unit cell will be re-oriented. A common way to monitor reactivity is to irradiate for an hour then run a matrix to see if the unit cell parameters have changed. Unfortunately, after multiple hours of irradiation at 465 and 365 nm at 100 K and 225 K, no reaction was detected.

Due to the fullerenes' lack of solubility compared to **1-H** or **1-F**, fullerene crystals would typically fall out of solution first when employing slow evaporation at high temperature and room temperature in various solvents, leaving either **1-H** or **1-F** in solution. Eventually **1-H** or **1-F** would crystallize, resulting in two very different colored and shaped crystals. When applicable, single crystal X-ray diffraction was used to determine that the darker colored crystals were in fact either a fullerene or a cocrystal. A **1-H** or **1-F** crystal will be light yellow,

making it quite obvious to screen for. The darker colored crystals indicate the presence of a fullerene. These were chosen for screening by X-ray diffraction because they had the potential to contain either just fullerene or both compounds. Unfortunately, all dark crystals, except the tetrachloroethylene solvate, turned out to be only C_{60} or C_{70} solvates.

Finally, mixed solvent systems using carbon disulfide and solvents such as chloroform or tetrahydrofuran were attempted. Carbon disulfide will dissolve C_{60} at 7mg/mL but is a poor solvent for **1-H** or **1-F**. This behavior contrasts with tetrahydrofuran and chloroform, which are great solvents for **1-H** and **1-F** but poor for both fullerenes. It was hoped that using a mixed solvent system such as carbon disulfide/tetrahydrofuran in a certain ratio would provide an environment that would allow saturation of both solvates at the same time, thus leading to a co-crystallization rather than the solvates separately crystallizing. Due to fullerenes limited solubility and the higher volatility of carbon disulfide, a slightly higher volume of carbon disulfide was used to keep the fullerene in solution and prevent it from prematurely crystallizing. Along with the presence of an ideal solvent for **1-H** or **1-F**, some control over the solubility of each component in solution was achieved. Unfortunately, none of the above solvent systems were successful and a perfect ratio was not found.

6.3. Conclusion

Neither **1-H** or **1-F** were synthetically designed to co-crystallize with fullerenes. With this limitation, one is at the mercy of crystallization conditions to acquire an X-ray quality co-crystal. Not only does one need conditions that result in a cocrystal but a cocrystal with an appropriate packing that allows a 2D polymerization. While acquiring a desired 2D lattice our monomers and a fullerene is a strenuous and time consuming task, it is worthy of continued research. Currently there are no fullerene containing 2DPs in the literature and accomplishing

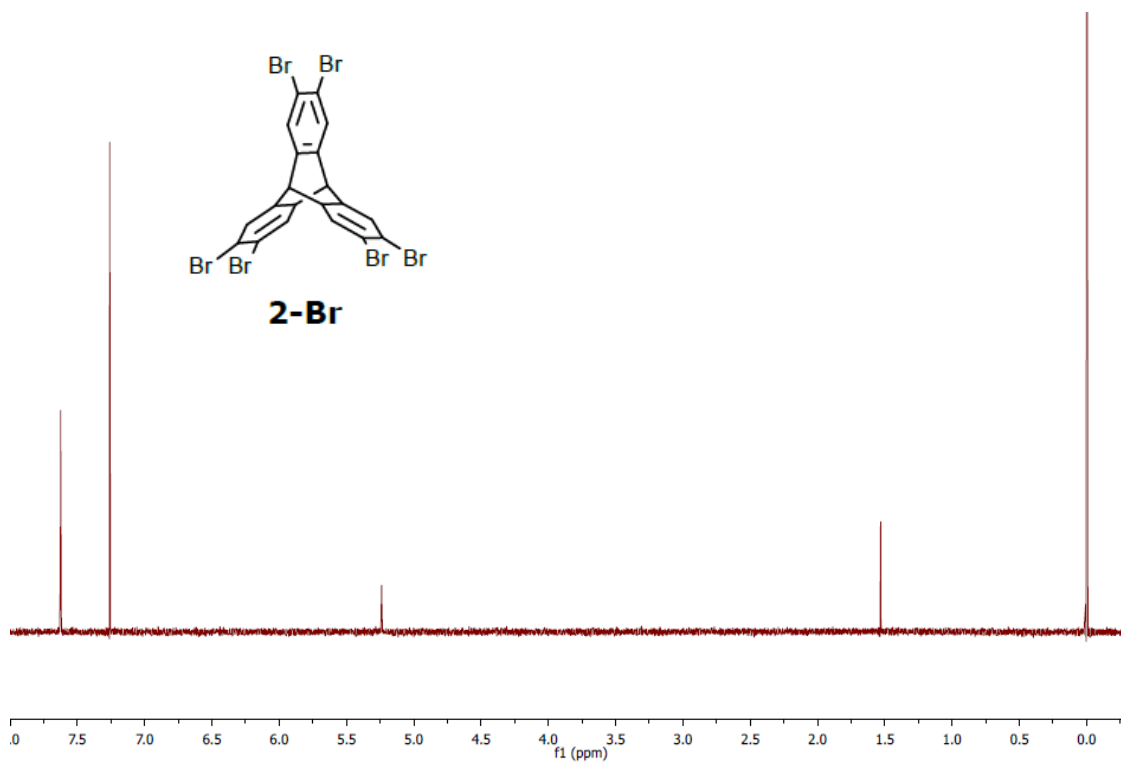
this would be a novel addition to the current library of 2DPs and perhaps inspire further research.

Reference.

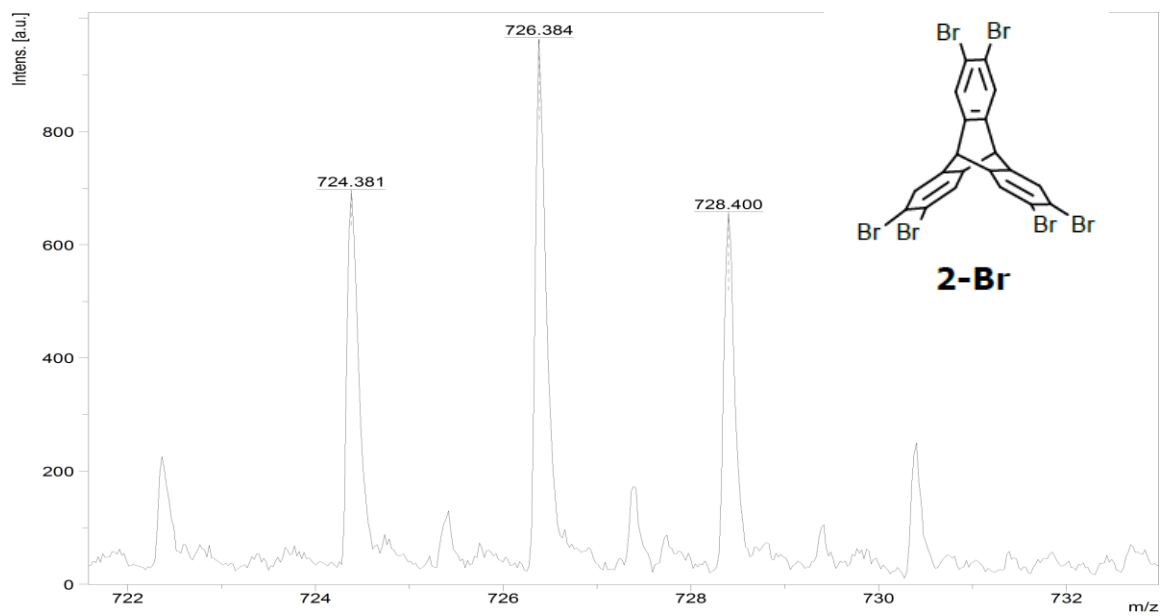
- (87) Dawe, L. N.; AlHujran, T. A.; Tran, H.-A.; Mercer, J. I.; Jackson, E. A.; Scott, L. T.; Georghiou, P. E. *Chem. Commun.* **2012**, 48 (45), 5563.
- (88) Ruoff, R. S.; Tse, D. S.; Malhotra, R.; Lorents, D. C. *J. Phys. Chem.* **1993**, 97 (13), 3379.

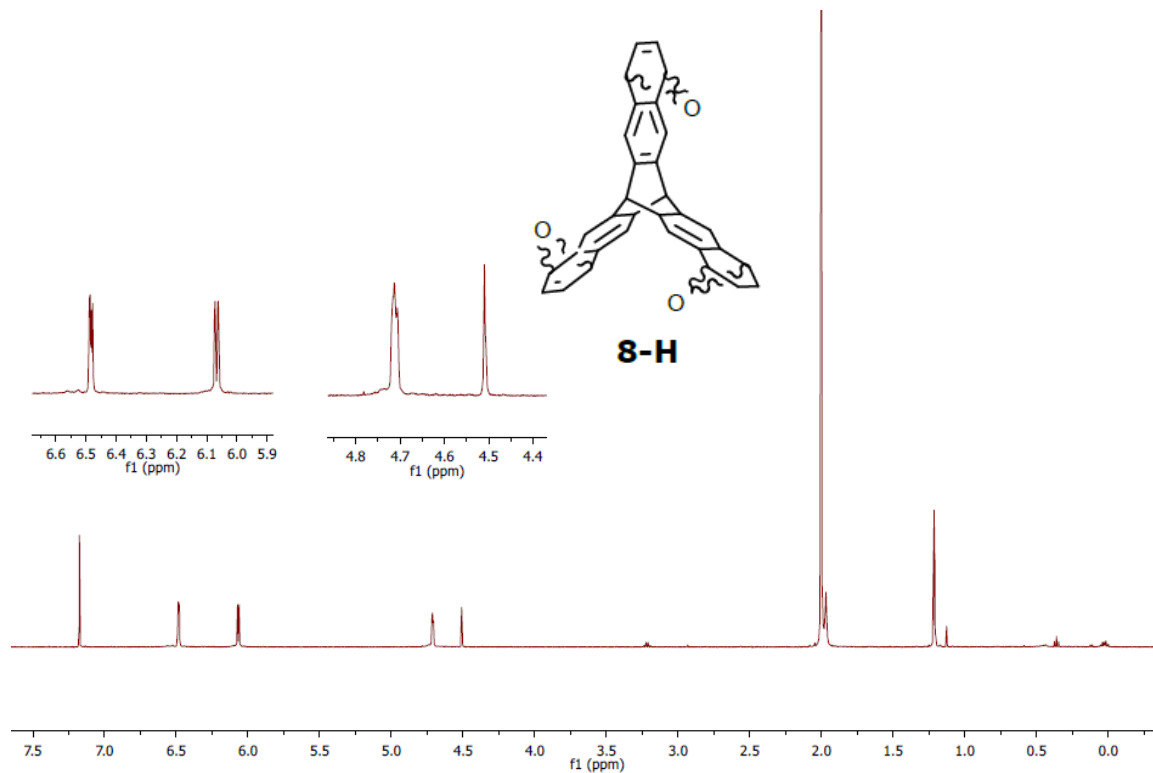
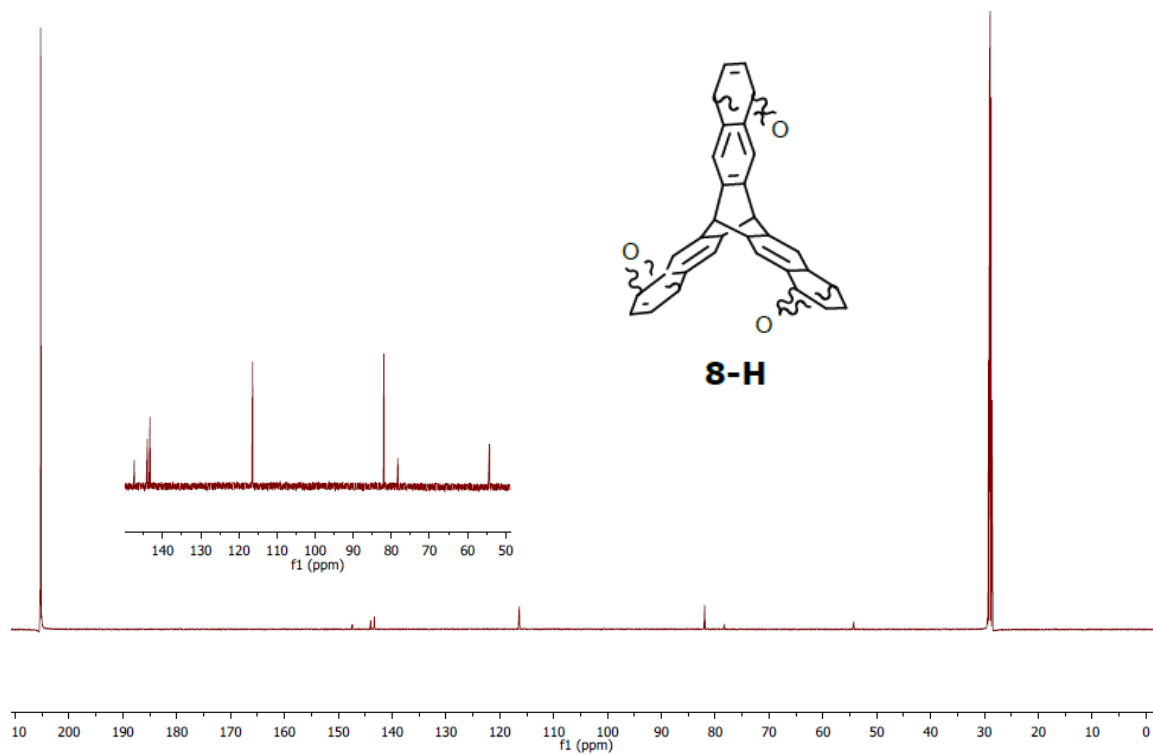
Appendix 1: Supplementary Information of Chapter 2
Synthetic routes towards Four Structurally Related Monomers

^1H NMR 2-H

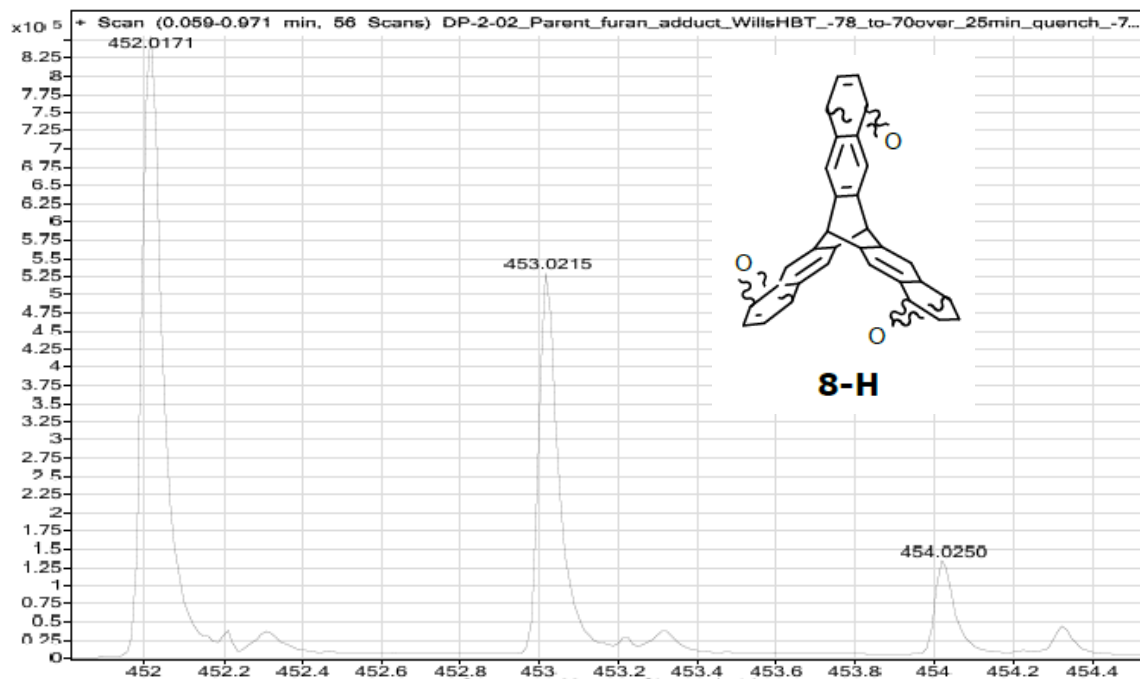


Maldi-TOF 2-H (DDQ matrix)

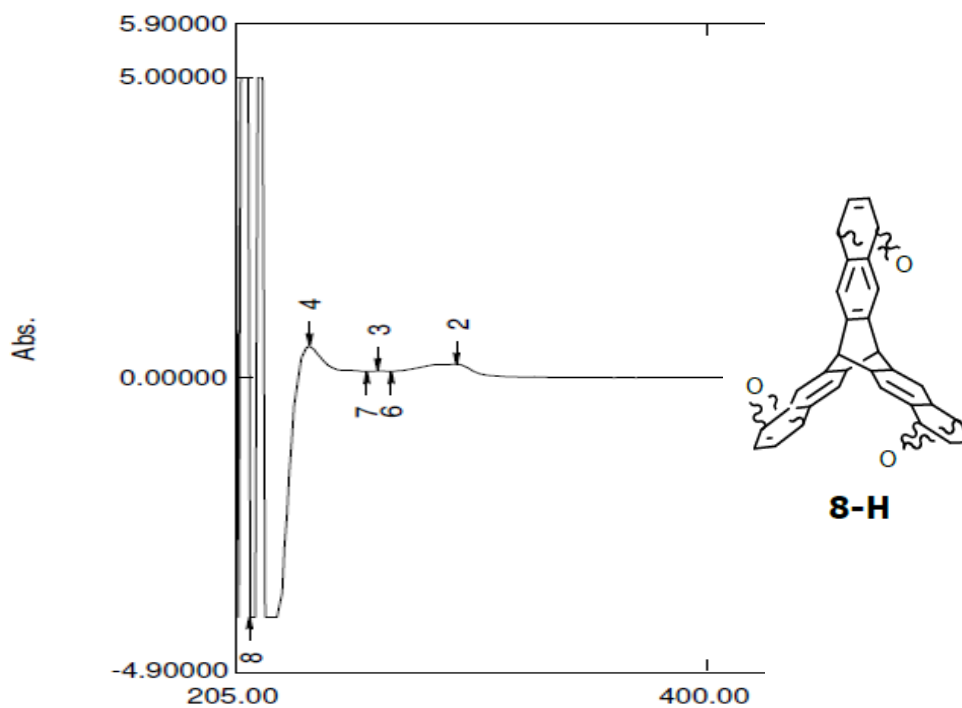


^1H NMR 8-H **^{13}C NMR 8-H**

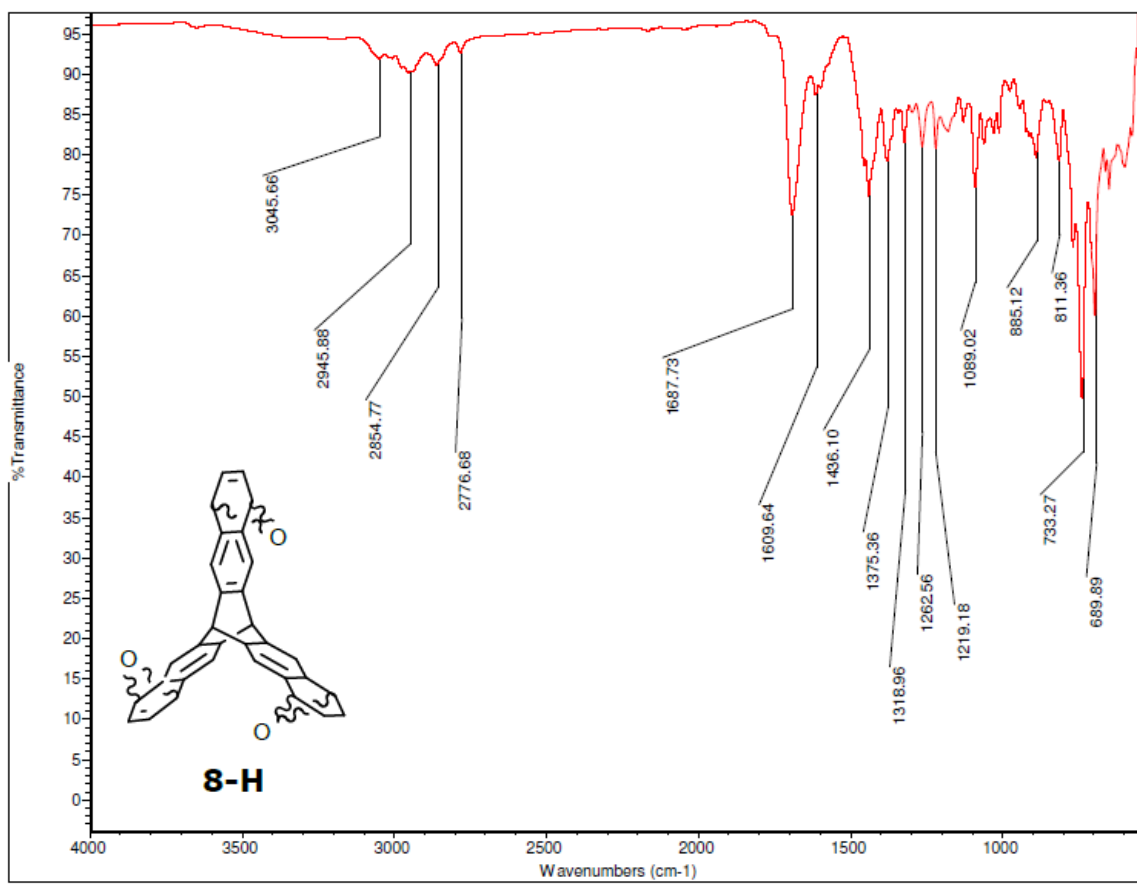
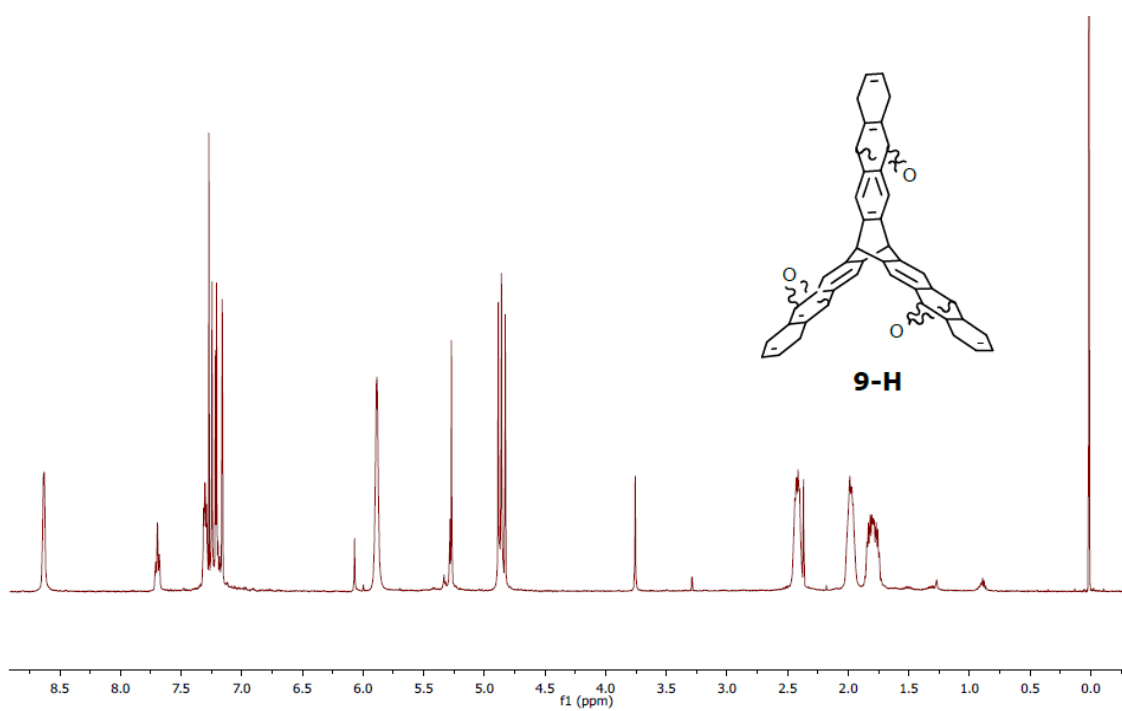
APPI-TOFMS 8-H

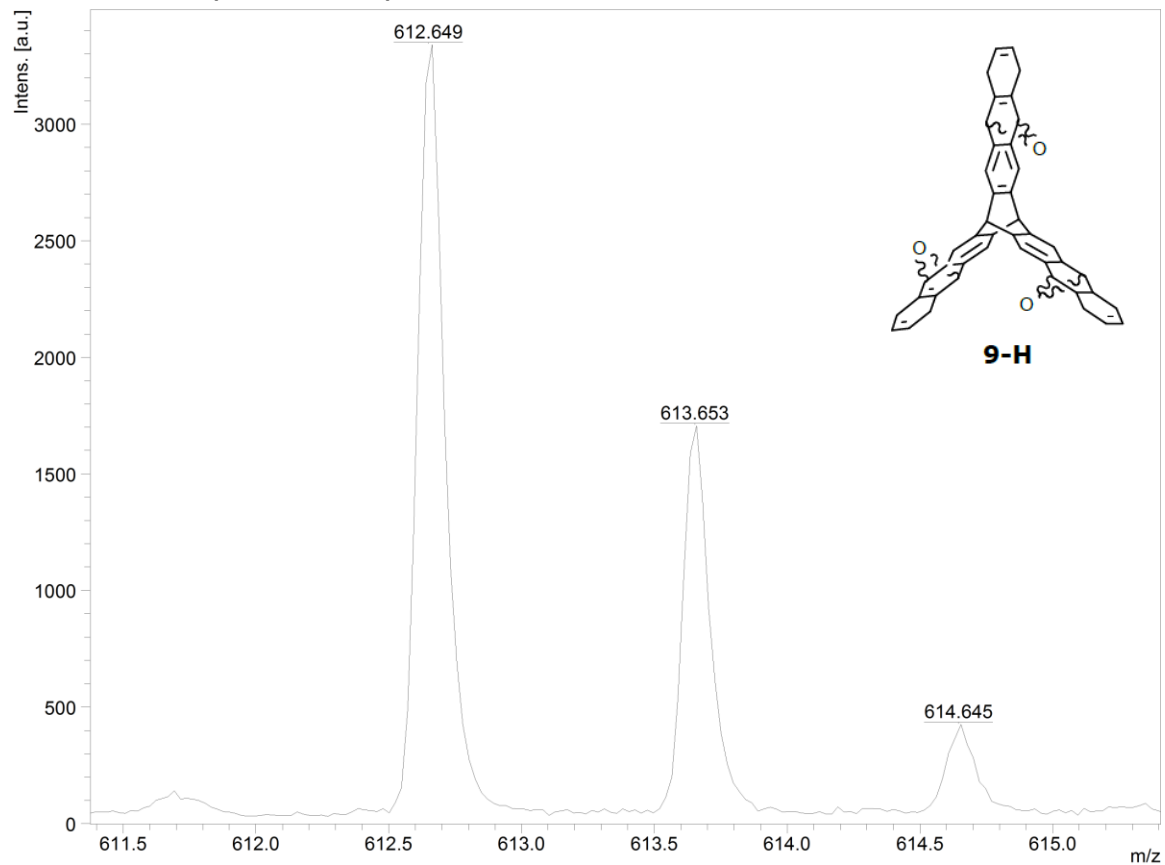
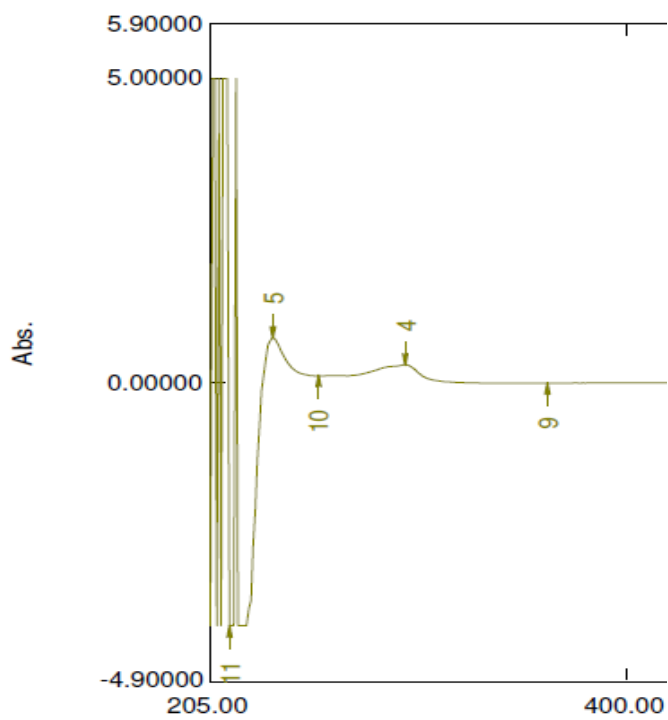


UV-vis 8-H

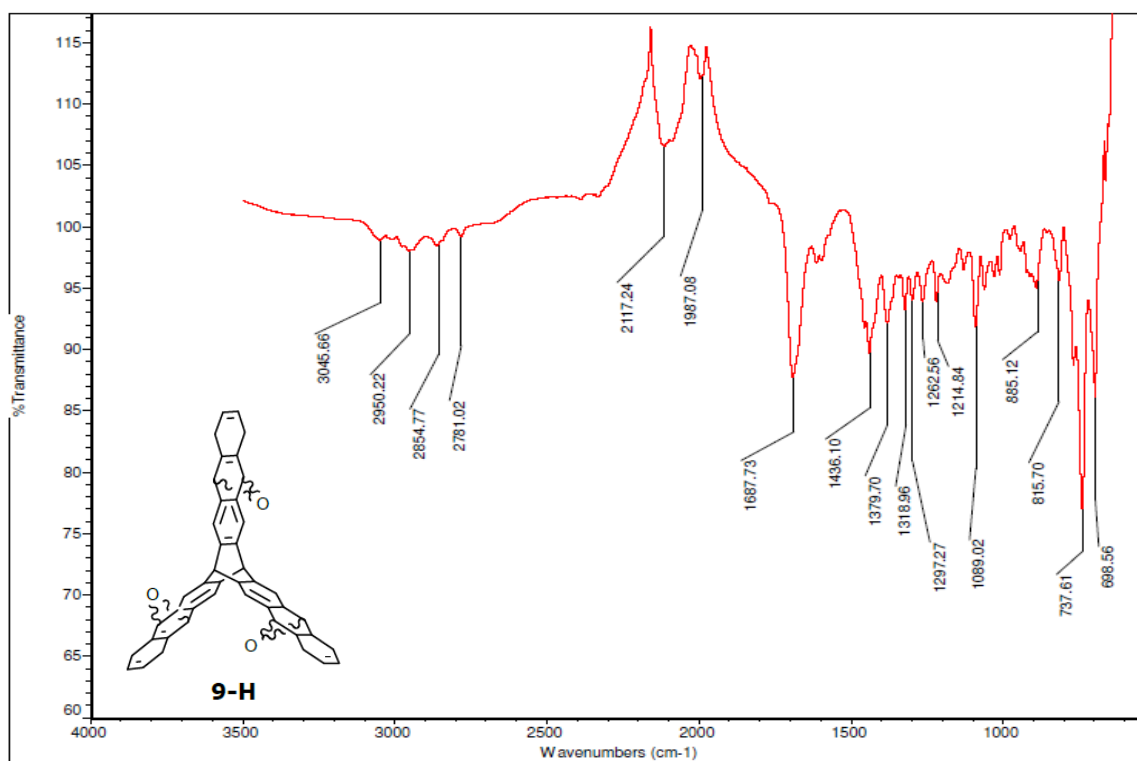
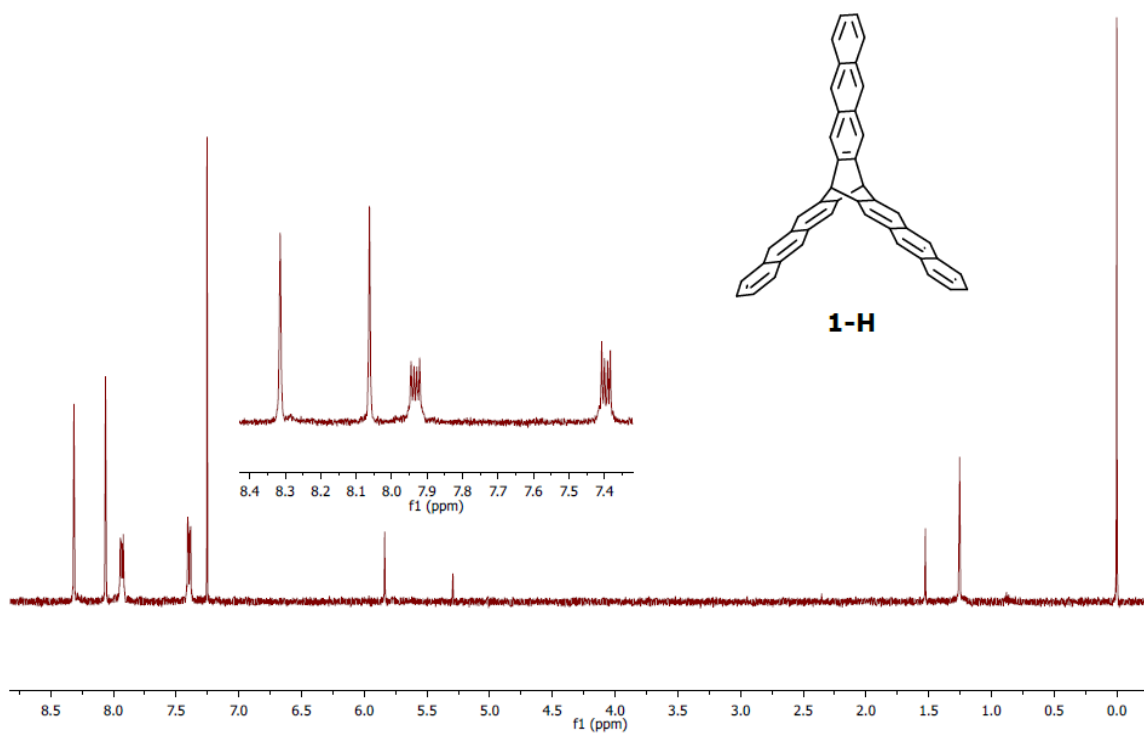


IR 8-H

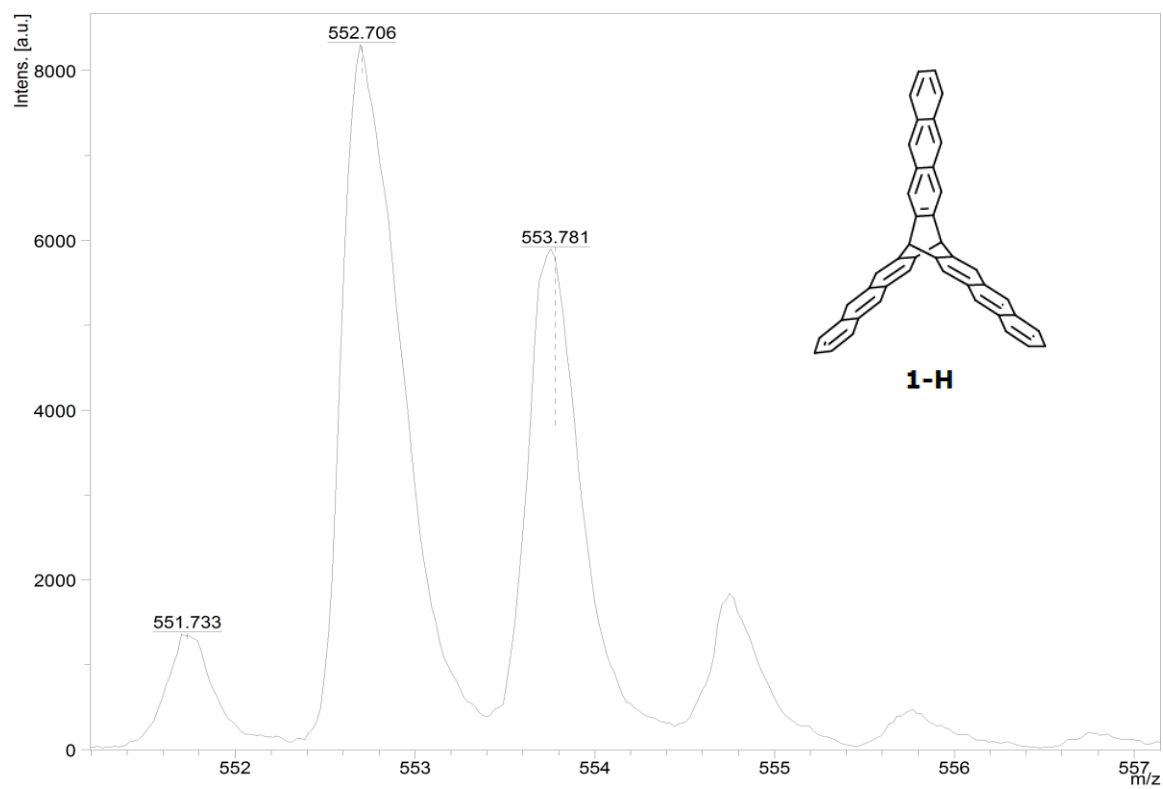
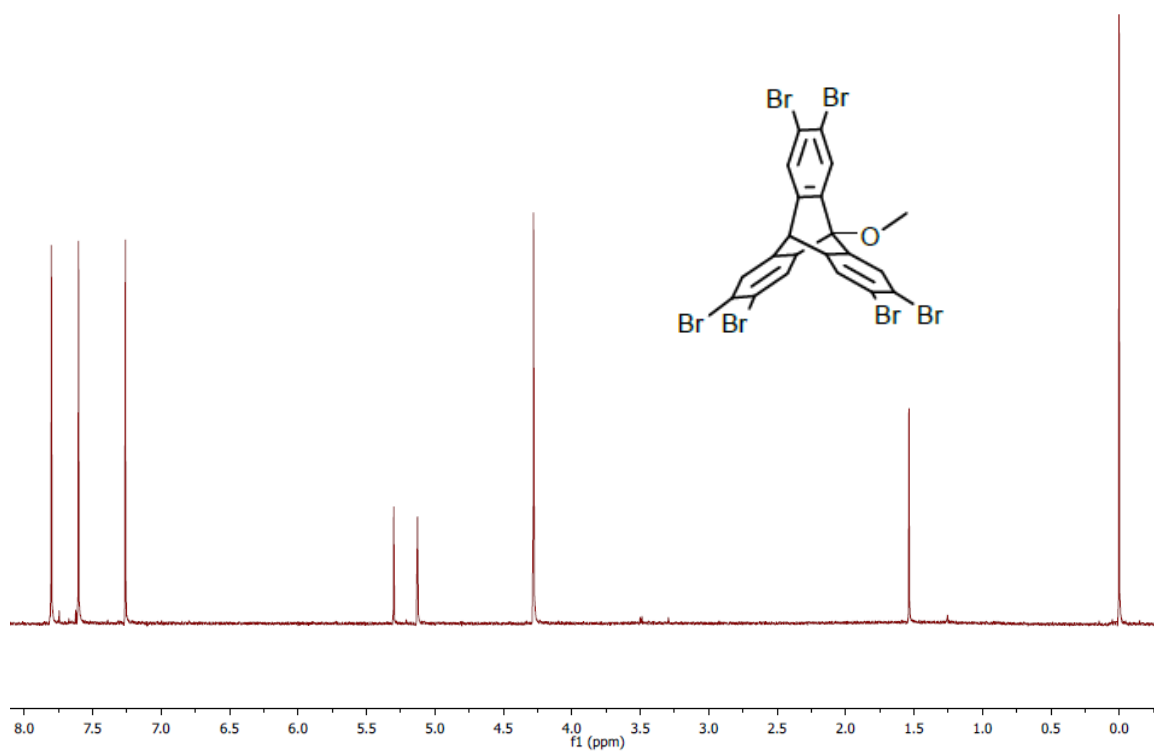
¹H-NMR 9-H

Maldi-TOF 9-H (DCTB matrix)**UV-vis 9-H**

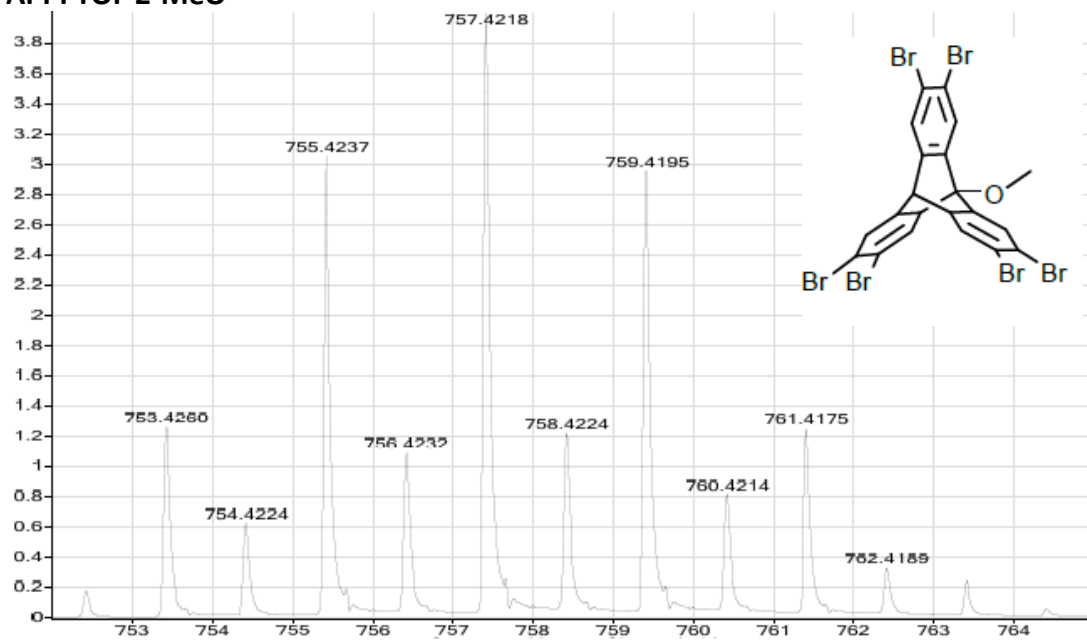
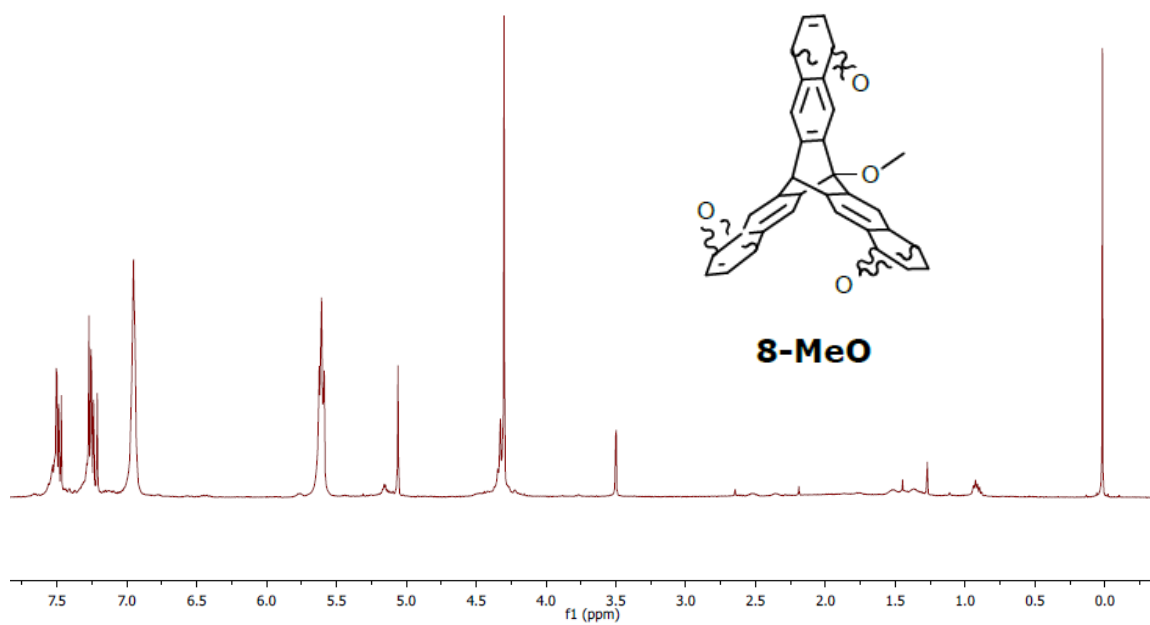
IR-9H

¹H NMR 1-H

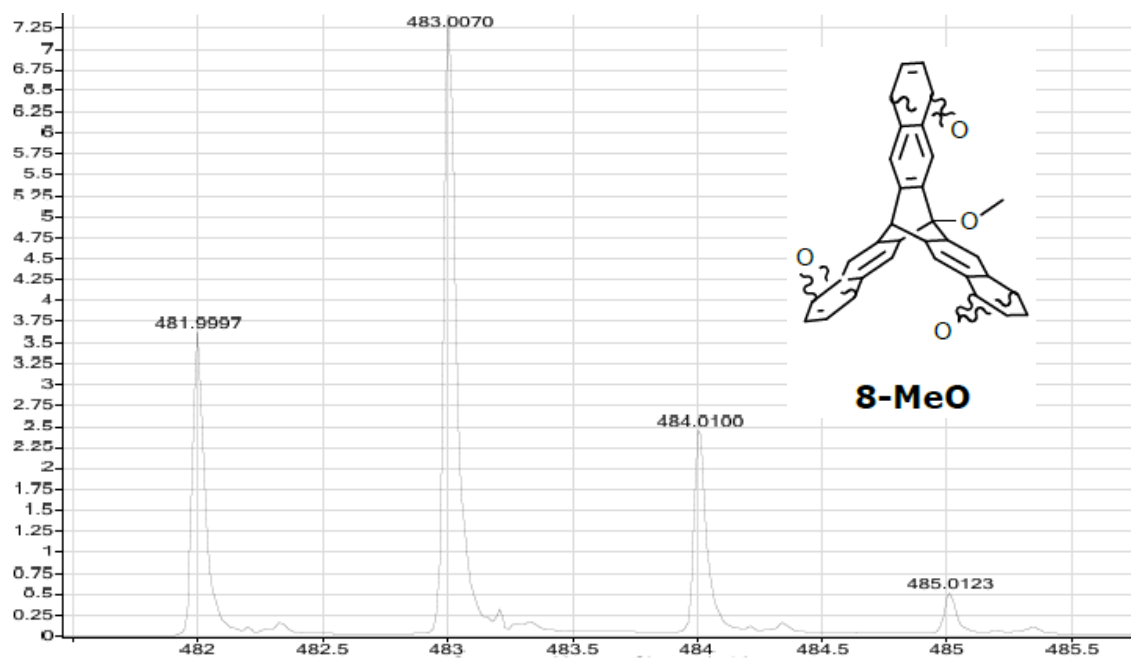
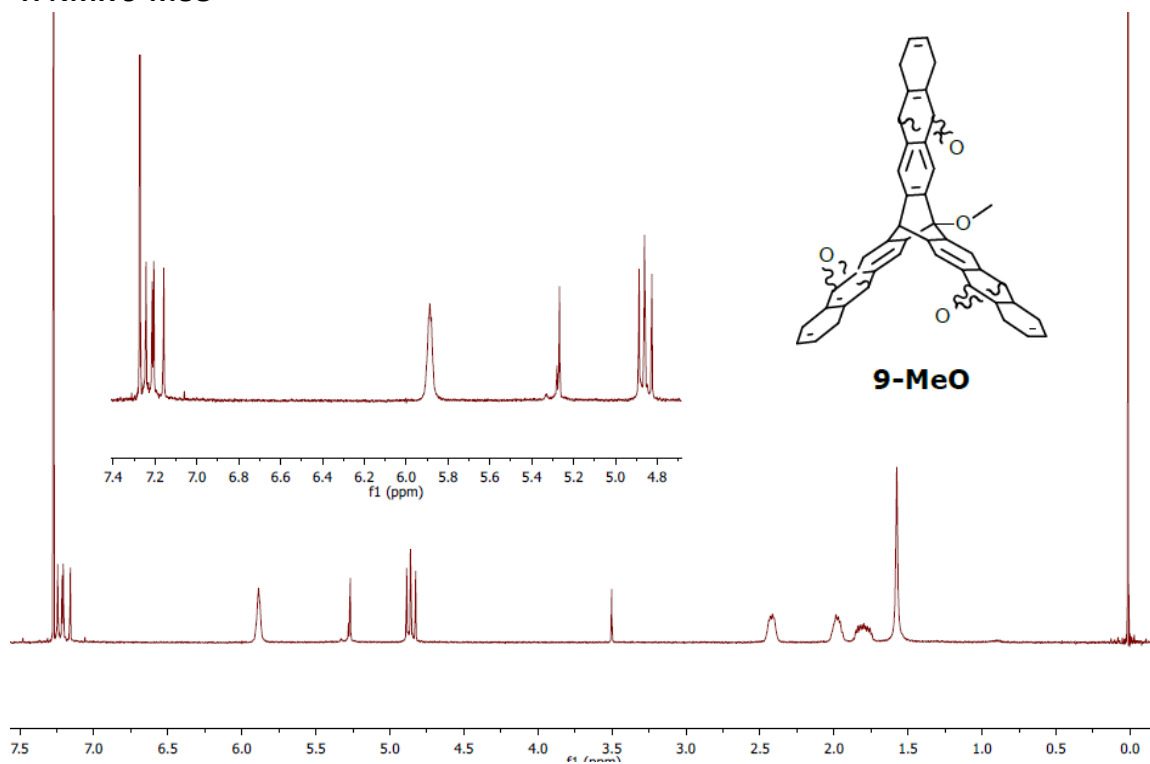
Maldi-TOF 1-H

 ^1H NMR 2-MeO

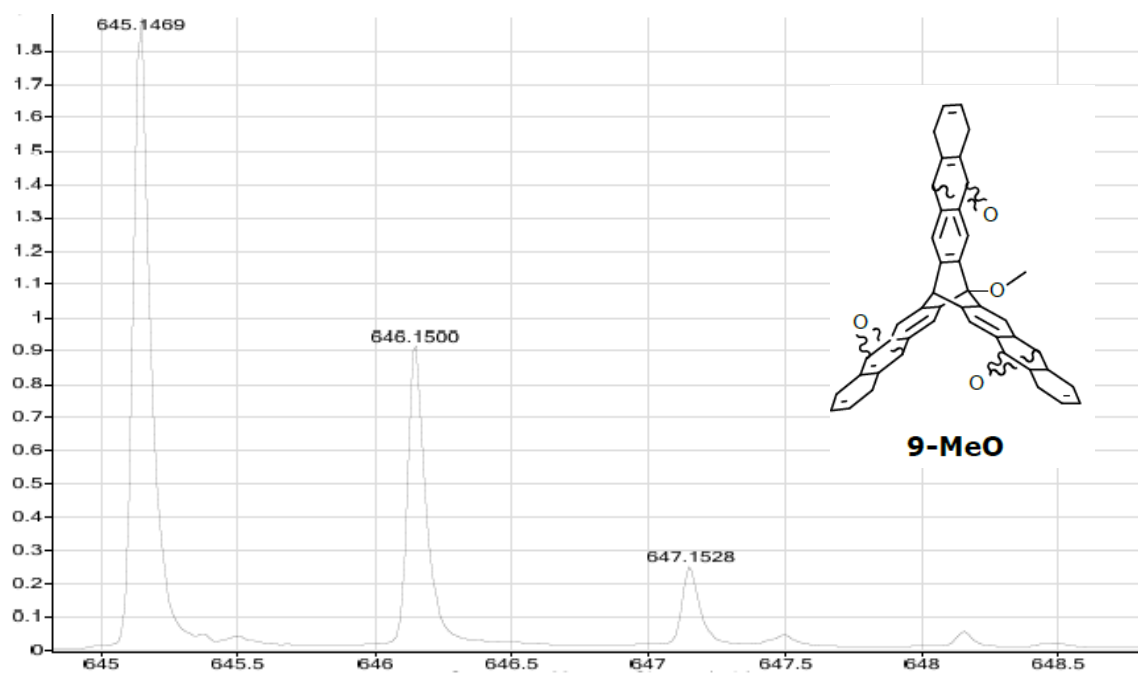
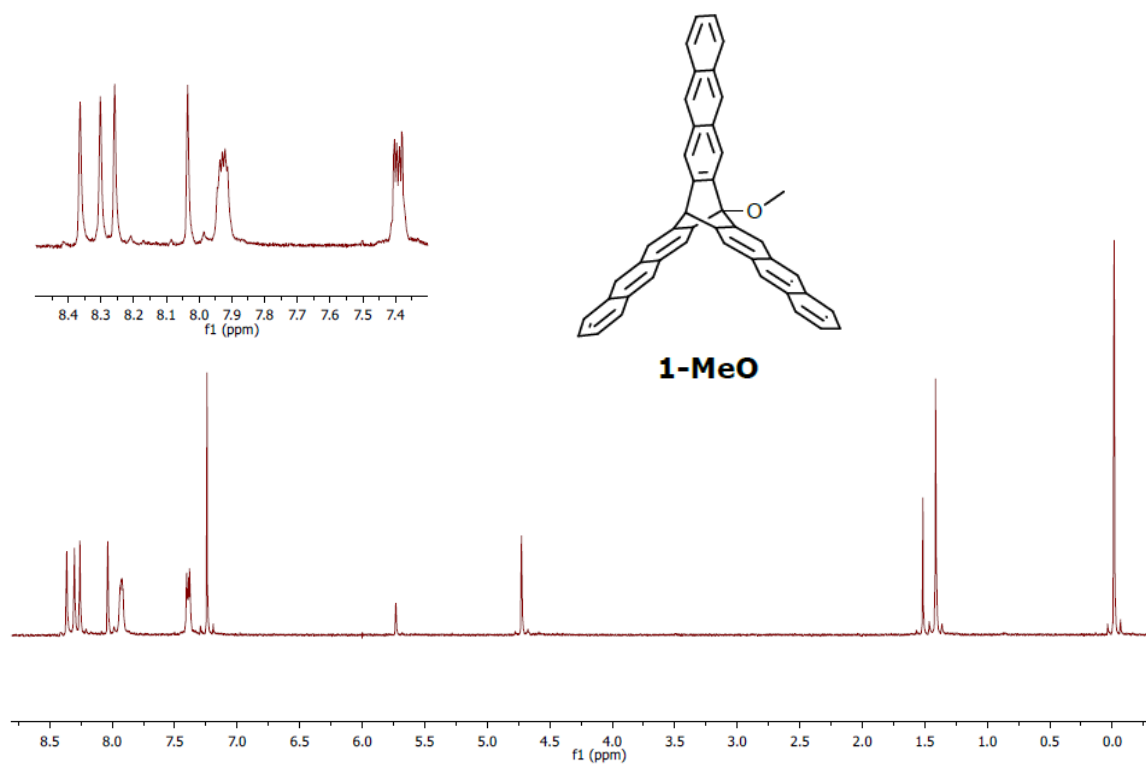
APPI TOF 2-MeO

 ^1H NMR 8-MeO

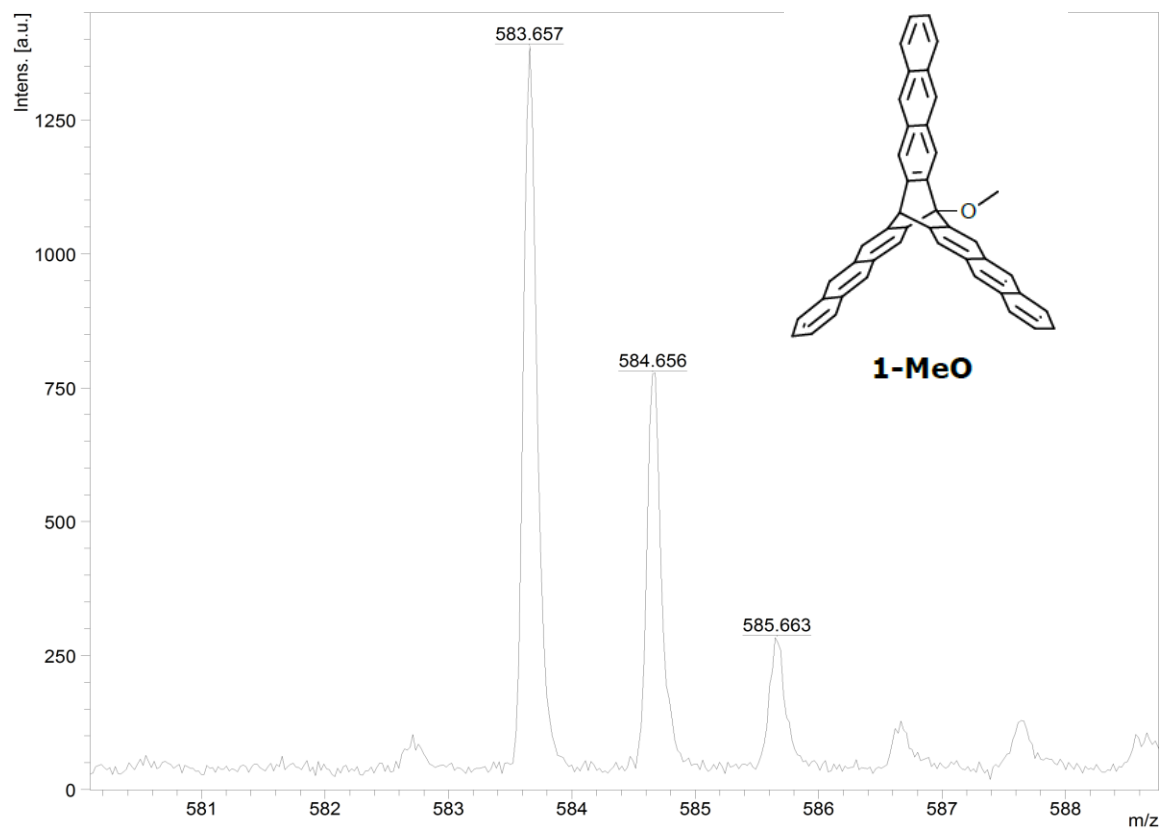
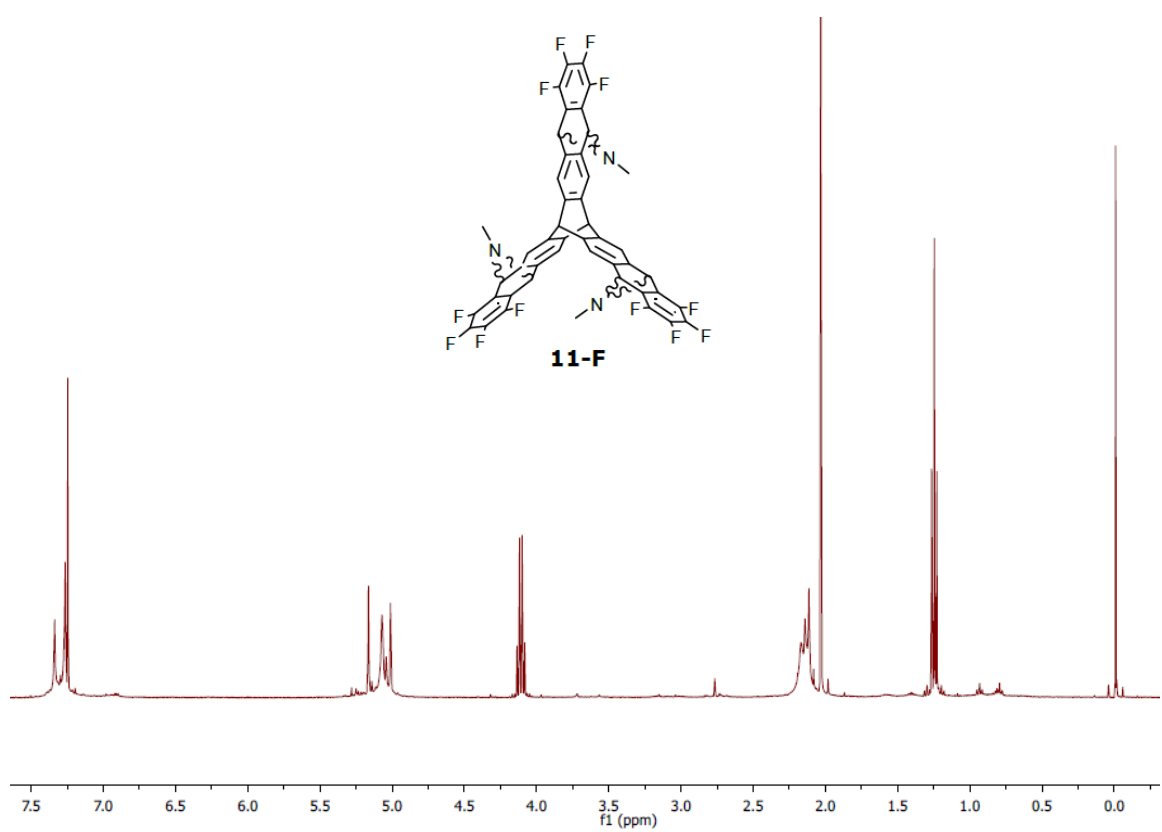
APPI TOF 8-MeO

 ^1H NMR 9-MeO

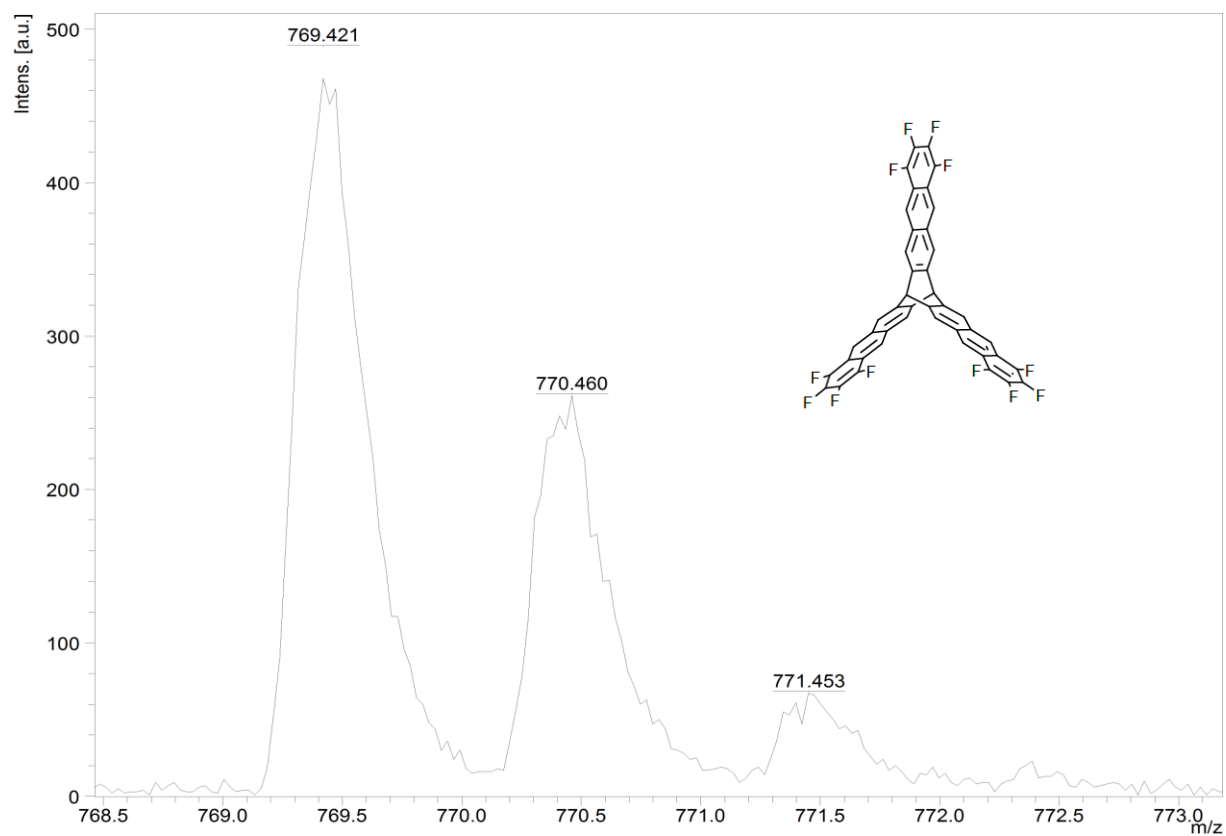
APPI TOF 9-MeO

 ^1H NMR 1-MeO (CDCl_3)

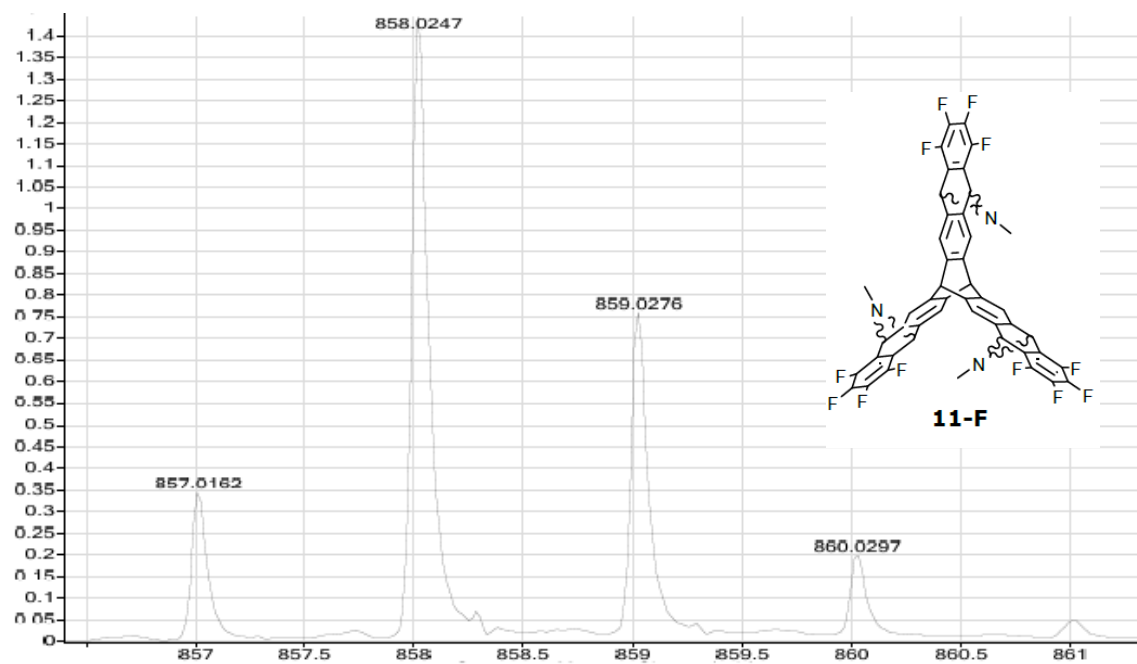
Maldi-TOF 1-MeO

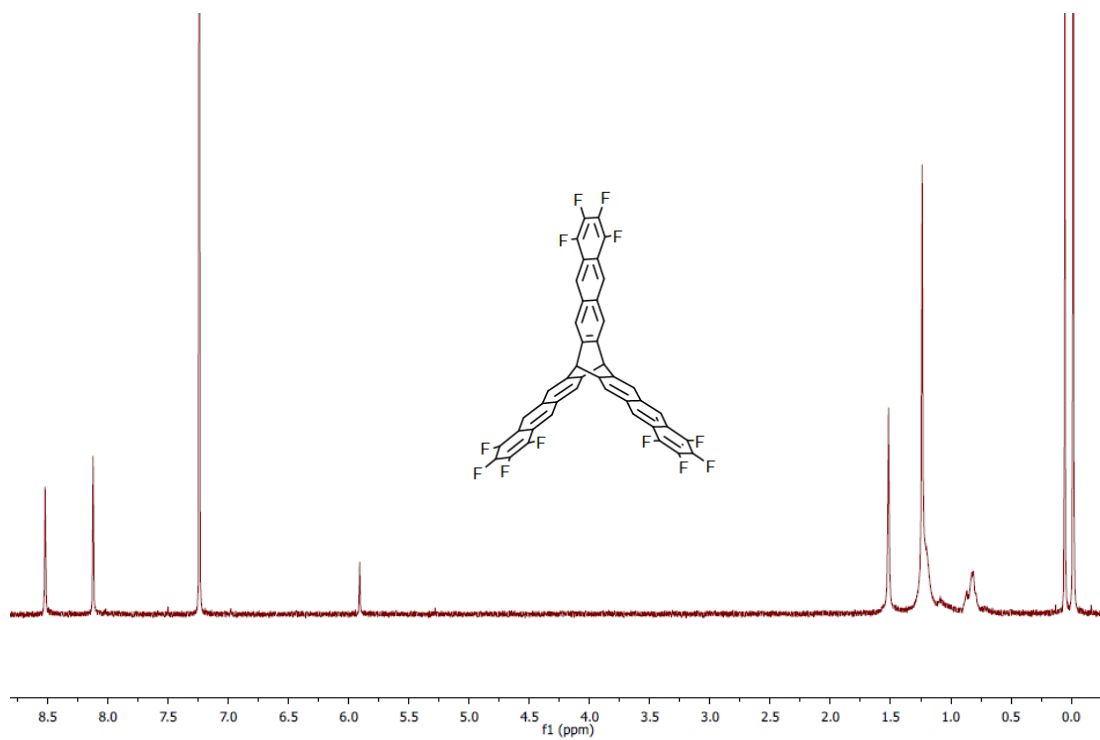
¹H NMR 11-F

APPI TOF 11-F



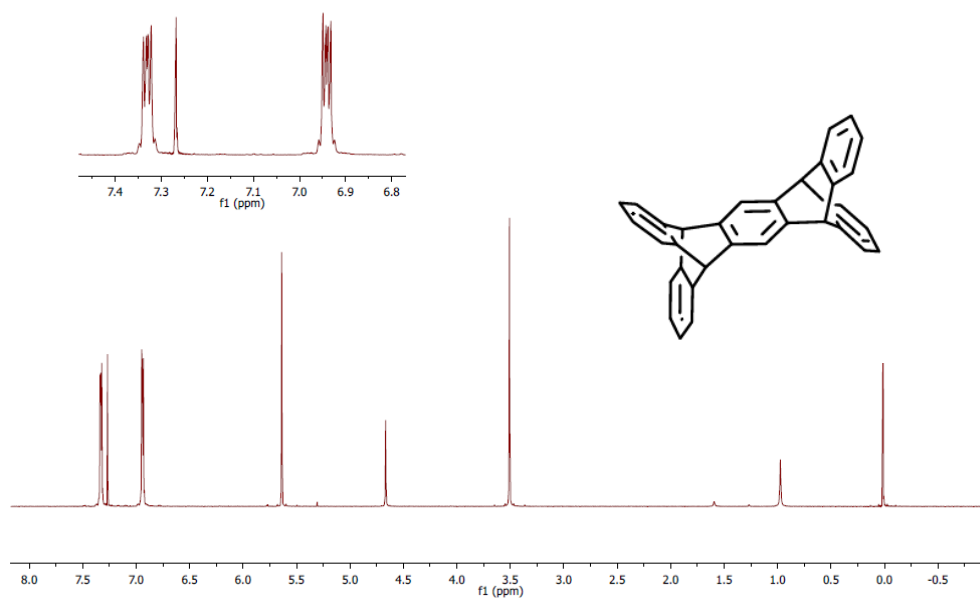
Maldi-TOF 1-F (DCTB matrix)



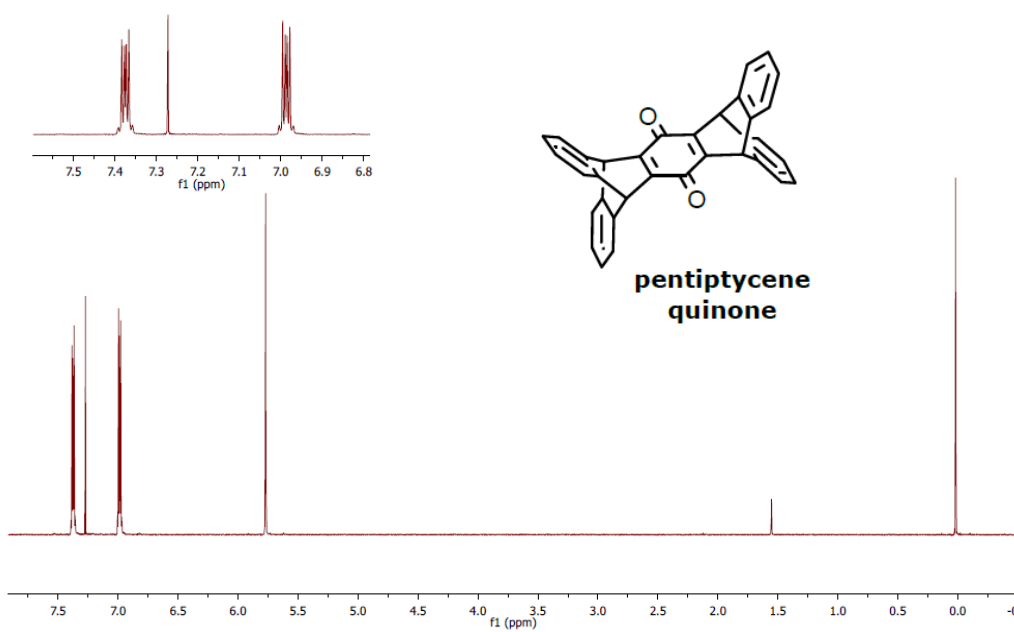
^1H NMR 1-F

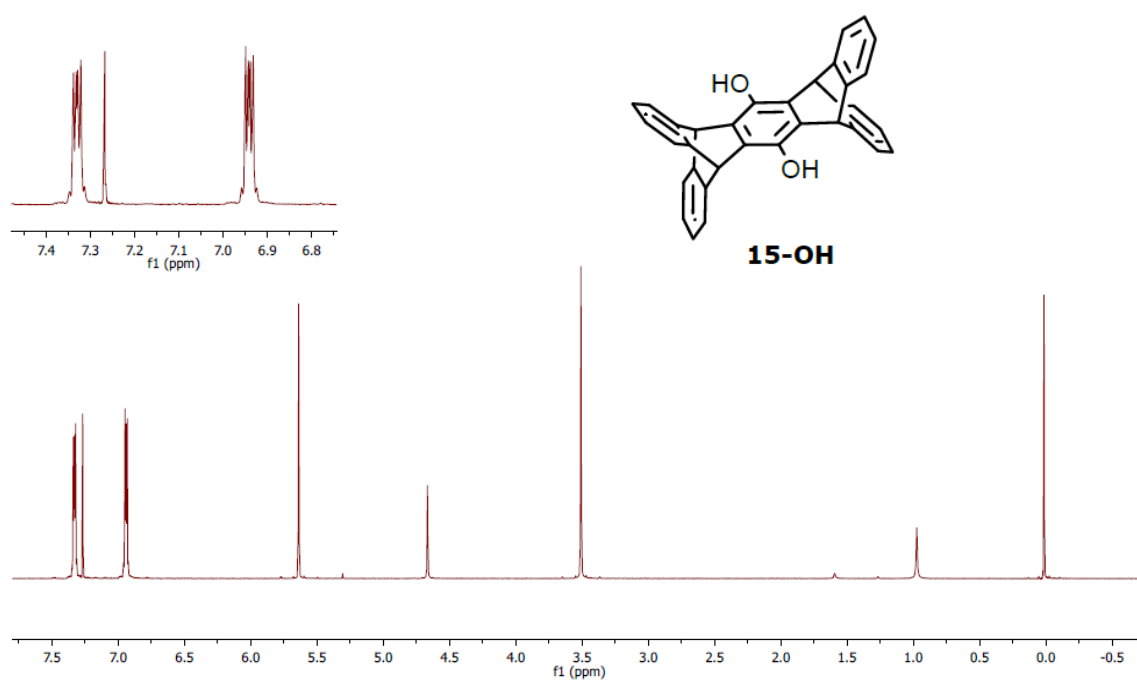
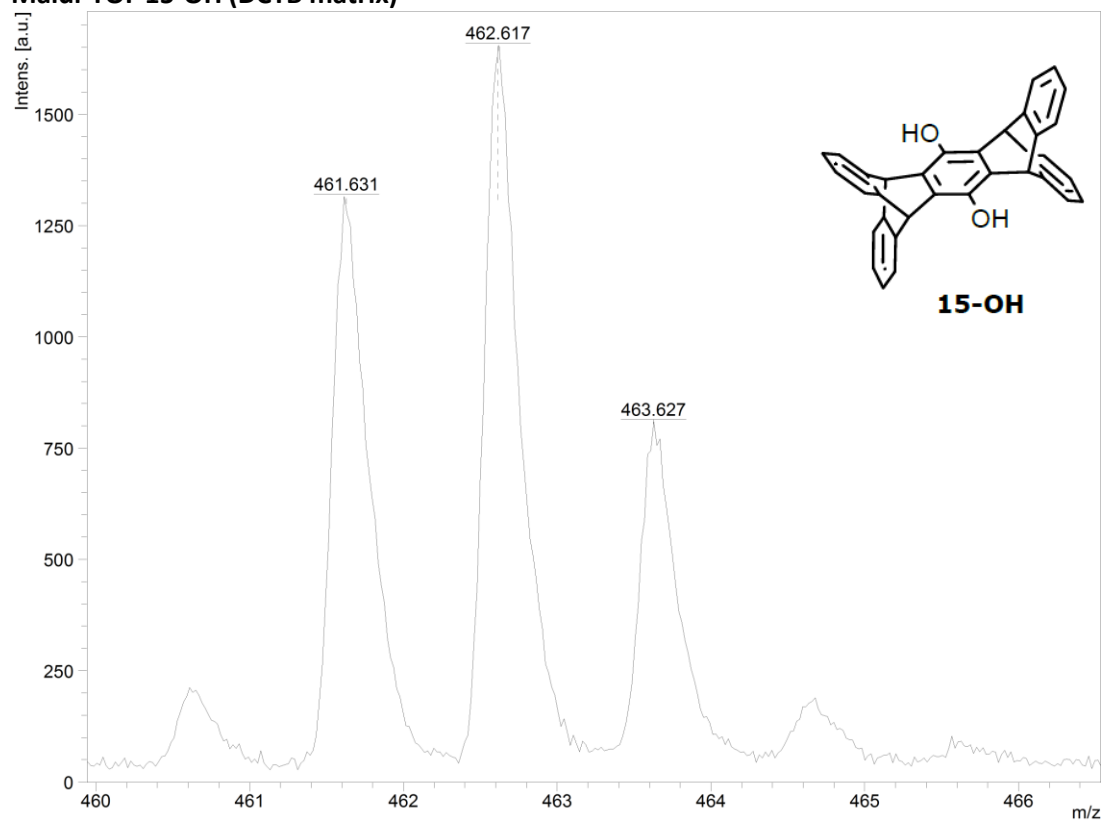
Appendix 2: Supplementary Information of Chapter 3
Synthetic Efforts Towards Pentiptycene based monomer

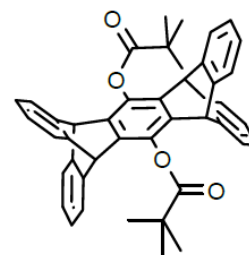
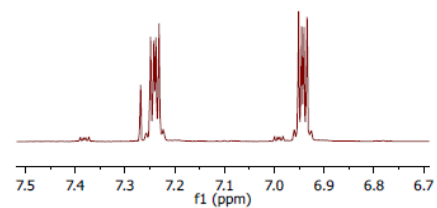
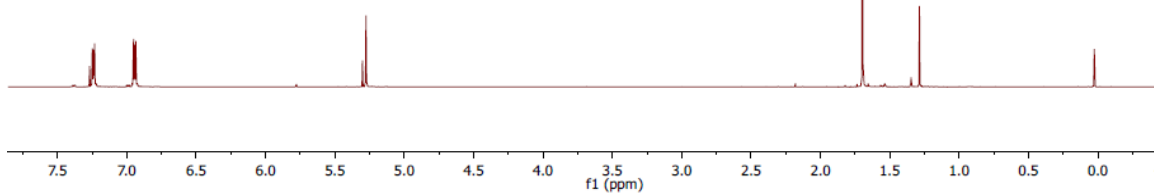
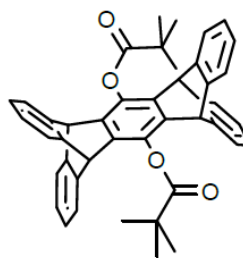
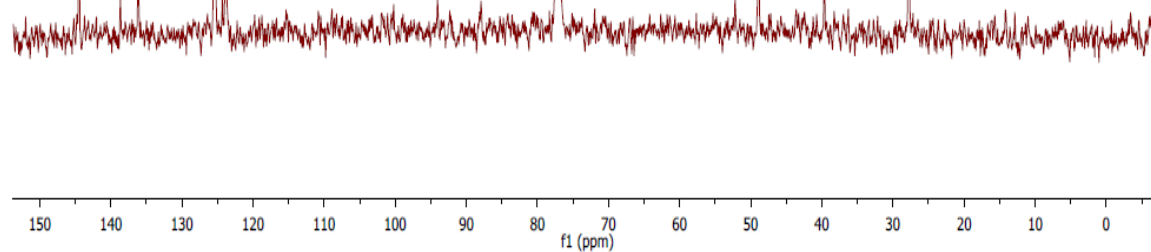
^1H NMR pentiptycene

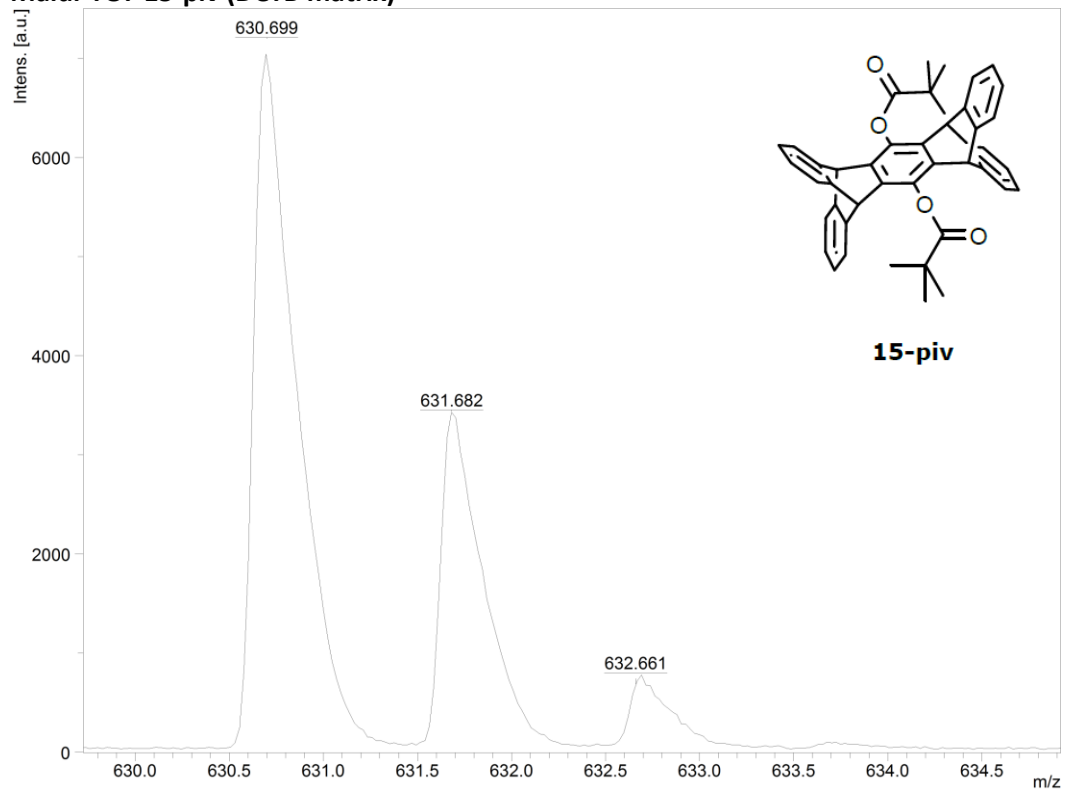
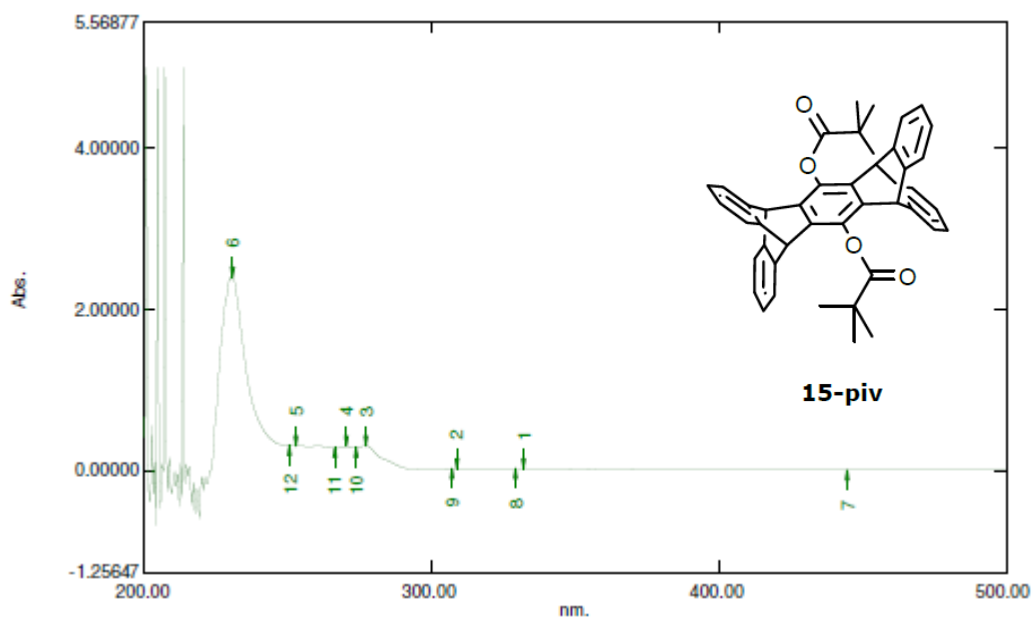


^1H NMR pentiptycene quinone

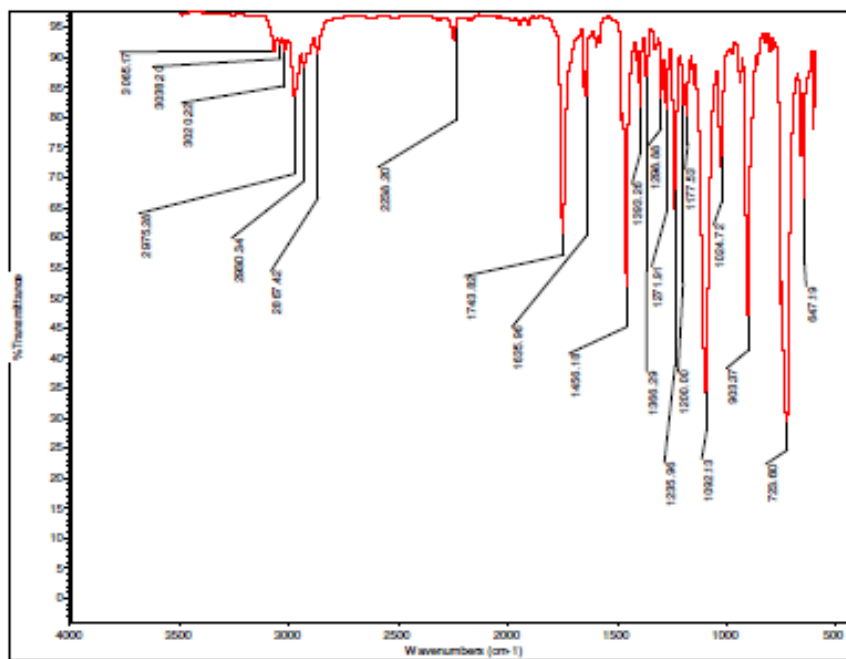


¹H NMR 15-OH**Maldi-TOF 15-OH (DCTB matrix)**

¹H NMR – 15-piv**15-piv****¹³C NMR 15-piv****15-piv**

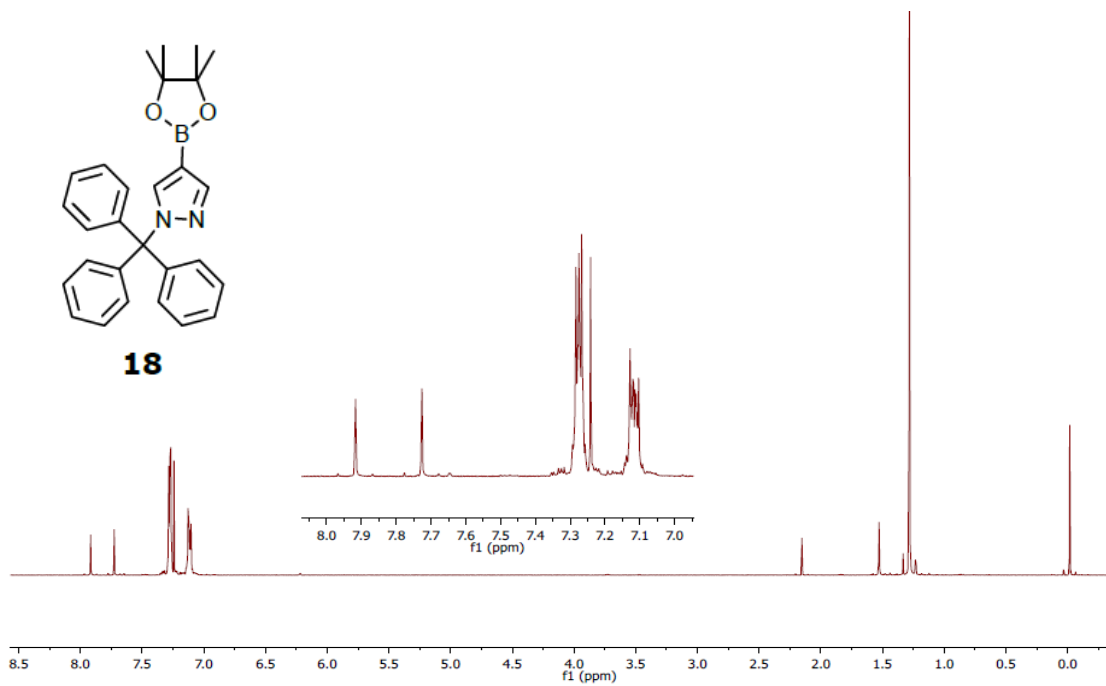
Maldi-TOF 15-piv (DCTB matrix)**UV-vis 15-piv**

IR 15-piv

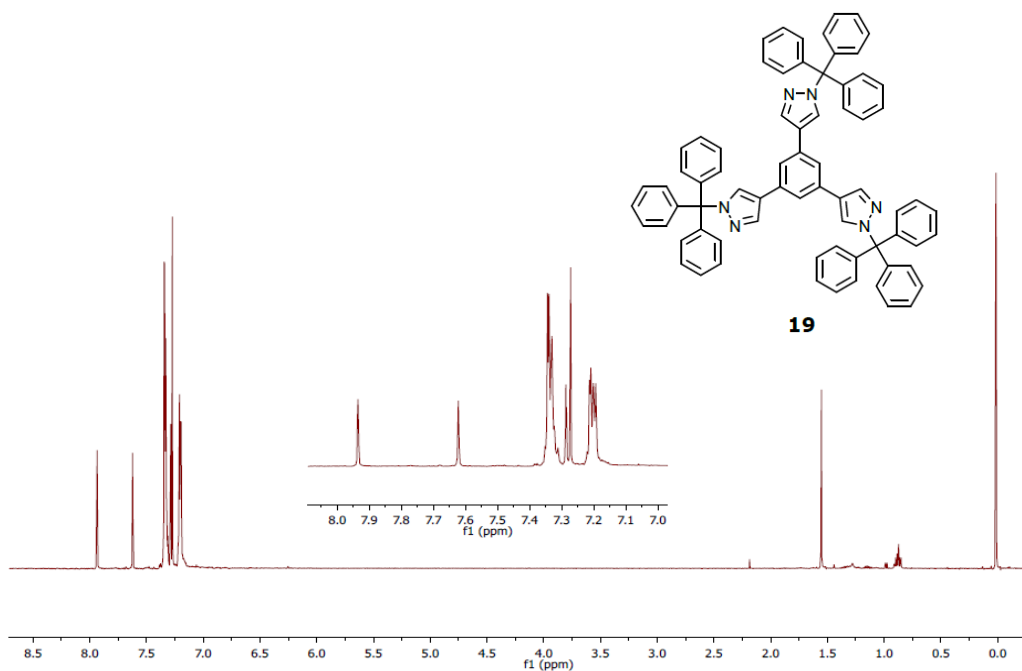


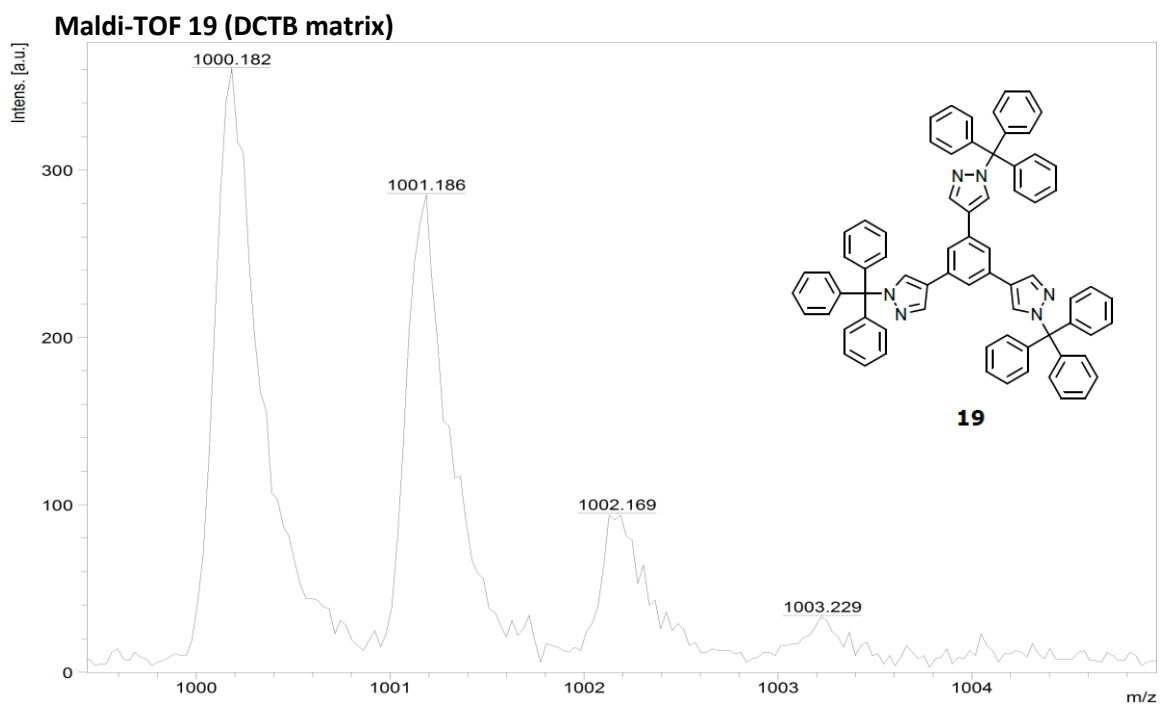
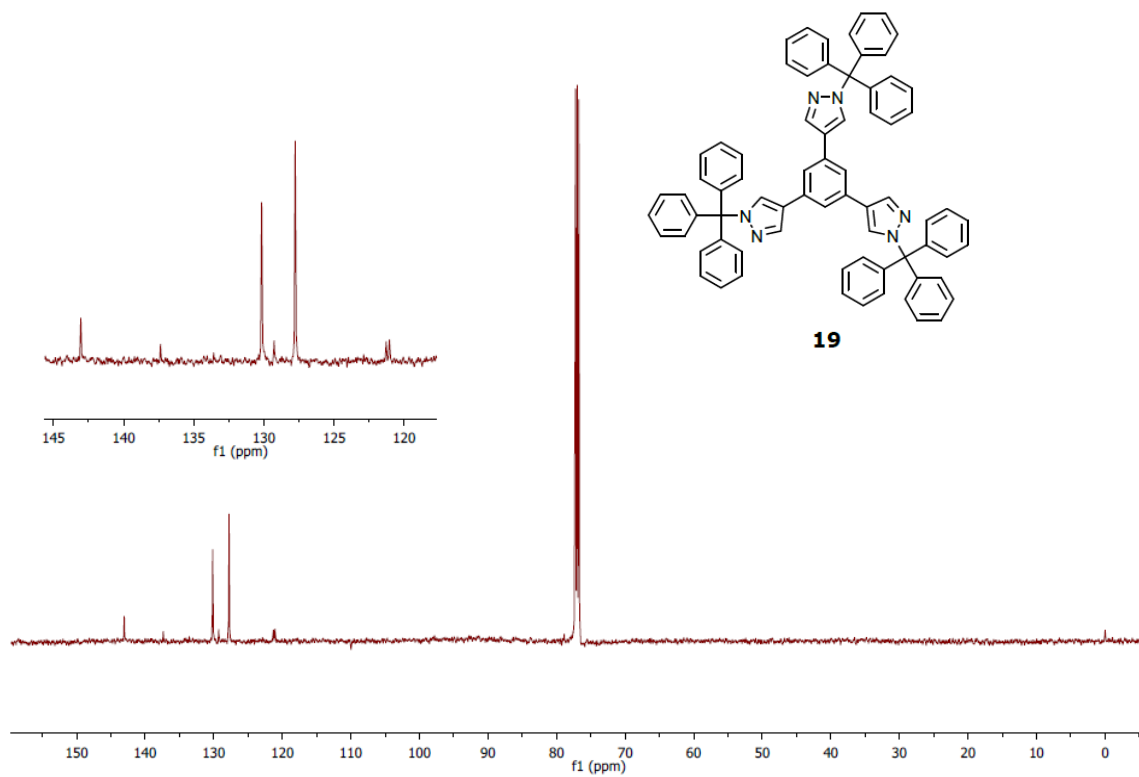
Appendix 3: Supplementary Information of Chapter 4
Synthetic Development of a 1,3,5-tripyrzole Benzene Monomer (1-pyz) and Efforts
Towards its 2D Polymerization

¹H NMR 18

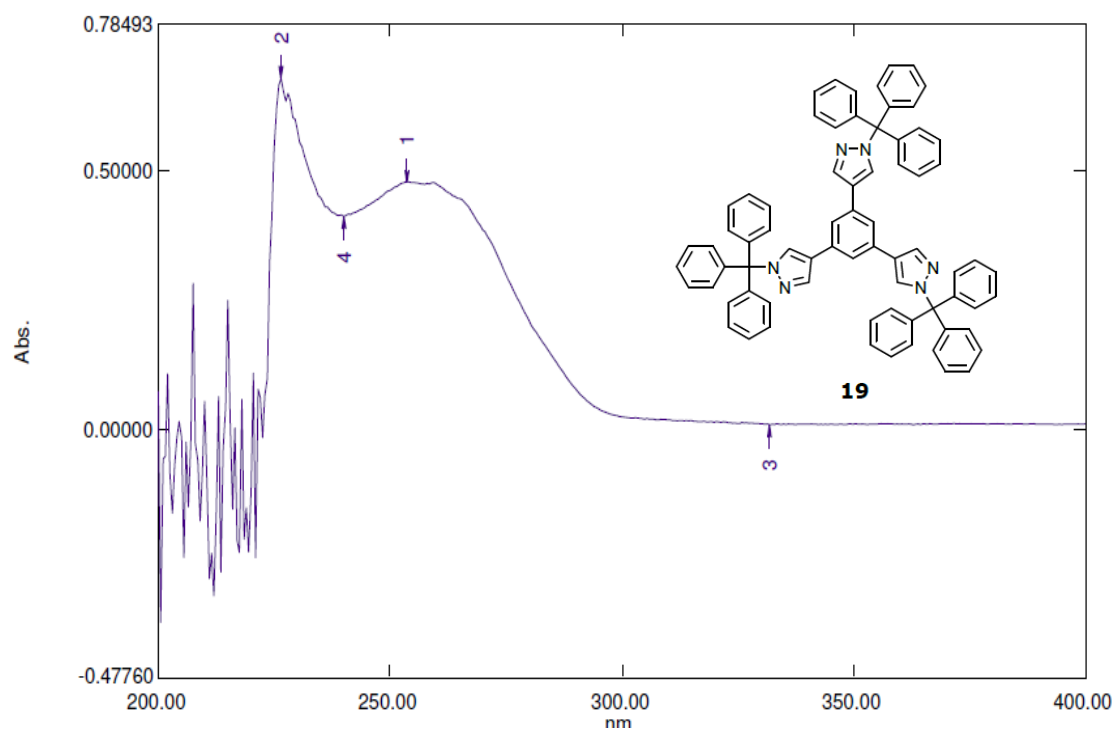


¹H NMR 19

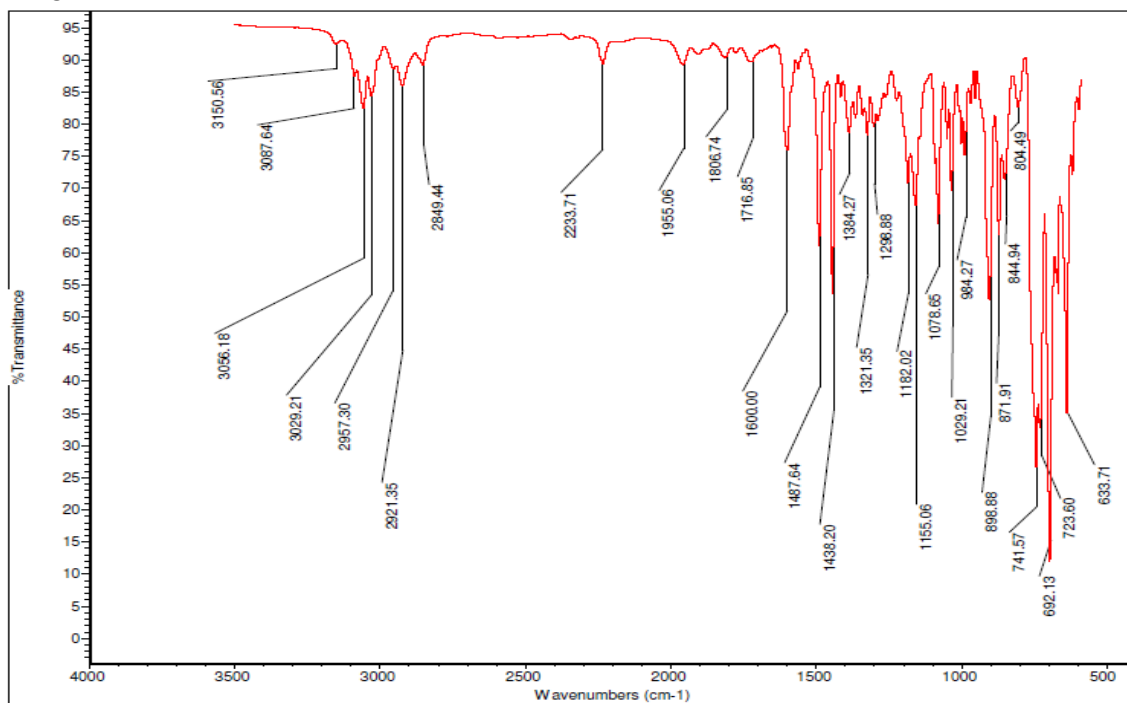


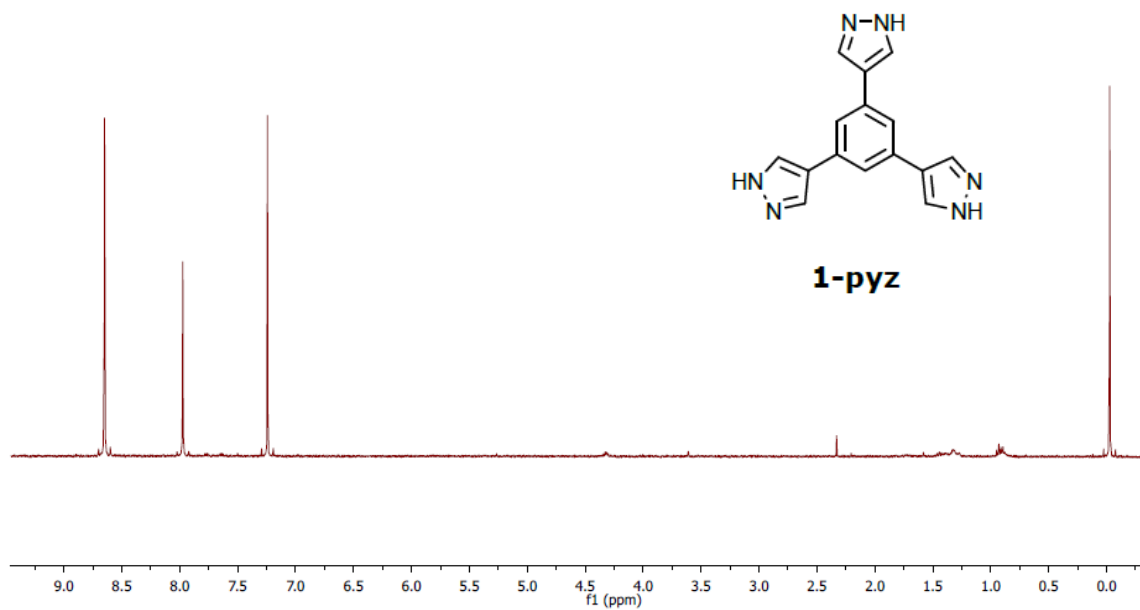
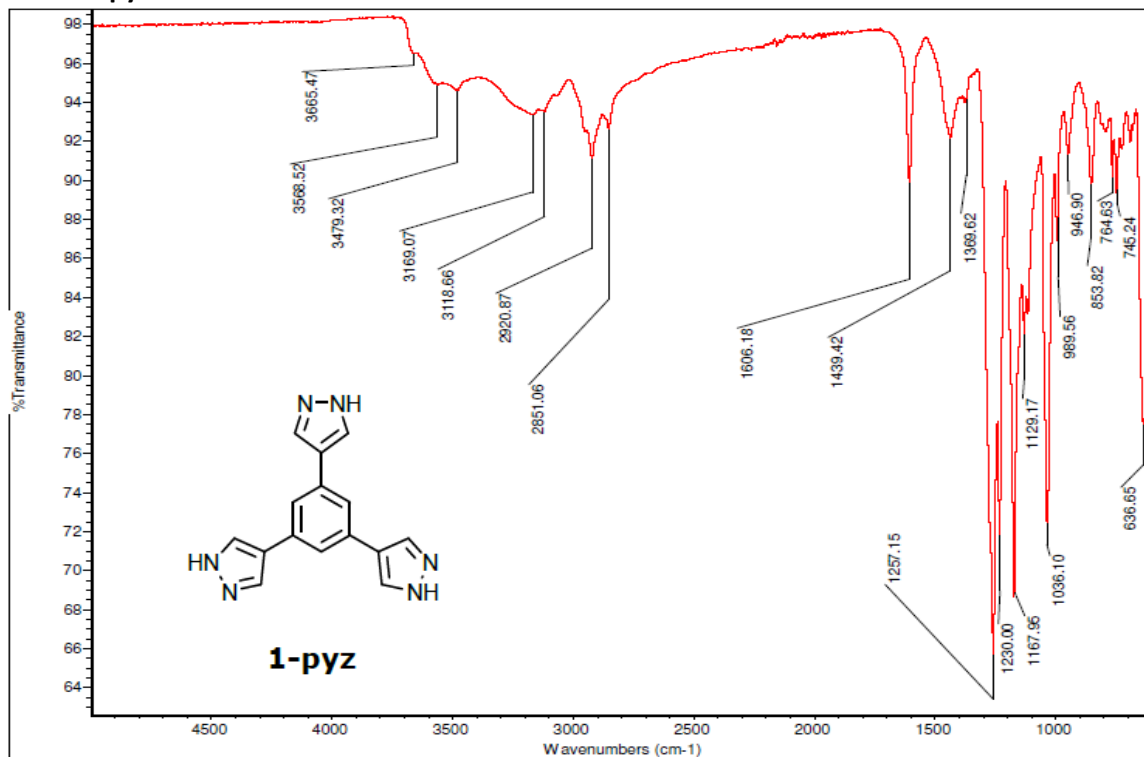
^{13}C NMR 19

UV-vis 19 (chloroform)



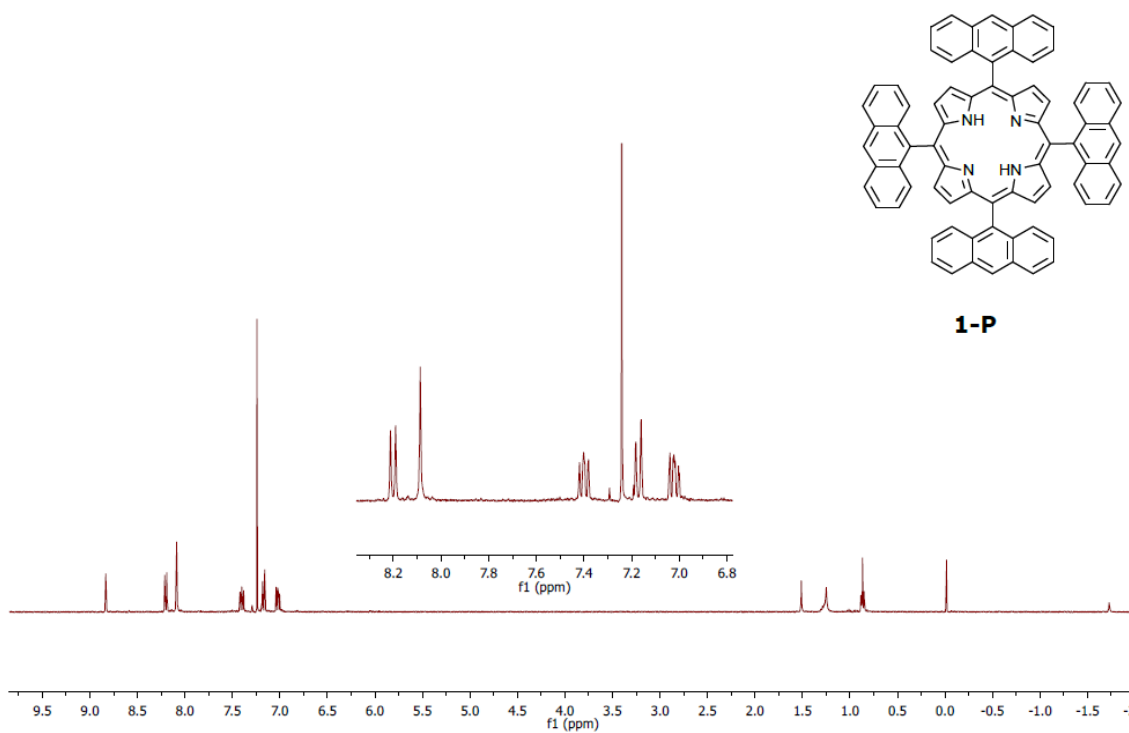
IR 19



¹H NMR 1-pyz (25% TFA/CDCl₃)**IR 1-pyz**

Appendix 4: Supplementary Information of Chapter 5
Efforts Towards the 2D Polymerization of a Porphyrin Based Monomer

^1H NMR 1-P



Malid-TOF 1-P (DCTB matrix)

